EQUILIBRIUM AND STABILITY PROPERTIES OF COLLISIONLESS CURRENT SHEET MODELS
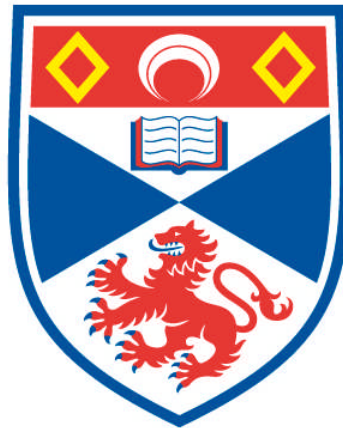
Fiona Wilson

A Thesis Submitted for the Degree of PhD
at the
University of St Andrews

2013

Equilibrium and Stability Properties of Collisionless Current Sheet Models

Fiona Wilson
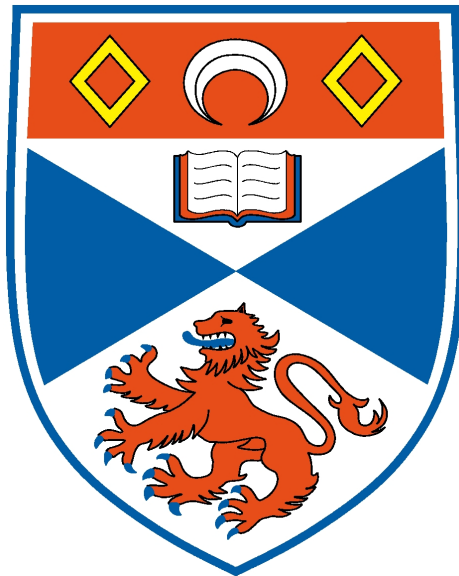
Thesis submitted for the degree of Doctor of Philosophy

of the University of St Andrews

18th December 2012

Abstract

The work in this thesis focuses primarily on equilibrium and stability properties of collisionless current sheet models, in particular of the force-free Harris sheet model.

A detailed investigation is carried out into the properties of the distribution function found by Harrison and Neukirch (2009b) for the force-free Harris sheet, which is so far the only known nonlinear force-free Vlasov-Maxwell equilibrium. Exact conditions on the parameters of the distribution function are found, which show when it can be single or multi-peaked in two of the velocity space directions. This is important because it may have implications for the stability of the equilibrium.

One major aim of this thesis is to find new force-free equilibrium distribution functions. By using a new method which is different from that of Harrison and Neukirch (2009b), it is possible to find a complete family of distribution functions for the force-free Harris sheet, which includes the Harrison and Neukirch (2009b) distribution function. Each member of this family has a different dependence on the particle energy, although the dependence on the canonical momenta remains the same. Three detailed analytical examples are presented. Other possibilities for finding further collisionless force-free equilibrium distribution functions have been explored, but were unsuccessful.

The first linear stability analysis of the Harrison and Neukirch (2009b) equilibrium distribution function is then carried out, concentrating on macroscopic instabilities, and considering two-dimensional perturbations only. The analysis is based on the technique of integration over unperturbed orbits. Similarly to the Harris sheet case (Harris, 1962), this is only possible by using approximations to the exact orbits, which are unknown. Furthermore, the approximations for the Harris sheet case cannot be used for the force-free Harris sheet, and so new techniques have to be developed in order to make analytical progress. Full analytical expressions for the perturbed current density are derived but, for the sake of simplicity, only the long wavelength limit is investigated. The dependence of the stability on various equilibrium parameters is investigated.

Declarations

I, Fiona Wilson, hereby certify that this thesis, which is approximately 29000 words in length, has been written by me, that it is the record of work carried out by me and that it has not been submitted in any previous application for a higher degree.

I was admitted as a research student in September 2008 and as a candidate for the degree of Doctor of Philosophy in September 2009; the higher study for which this is a record was carried out in the University of St Andrews between September 2008 and June 2012.

Date: _____ Signature of Candidate: _____.

I hereby certify that the candidate has fulfilled the conditions of the Resolution and Regulations appropriate for the degree of Doctor of Philosophy in the University of St Andrews and that the candidate is qualified to submit this thesis in application for that degree.

Date: _____ Signature of Supervisor: _____.

In submitting this thesis to the University of St Andrews we understand that we are giving permission for it to be made available for use in accordance with the regulations of the University Library for the time being in force, subject to any copyright vested in the work not being affected thereby. We also understand that the title and the abstract will be published, and that a copy of the work may be made and supplied to any bona fide library or research worker, that my thesis will be electronically accessible for personal or research use unless exempt by award of an embargo as requested below, and that the library has the right to migrate my thesis into new electronic forms as required to ensure continued access to the thesis. We have obtained any third-party copyright permissions that may be required in order to allow such access and migration, or have requested the appropriate embargo below.

The following is an agreed request by candidate and supervisor regarding the electronic publication of this thesis:

Embargo on all of electronic copy for the fixed period of two years on the following ground:

- publication would preclude future publication

Date: _____ Signature of Candidate: _____ Signature of Supervisor: _____ .

Publications

This thesis contains work which has been adapted from the following refereed publications:

1. **F. Wilson** & T. Neukirch, 'A Family of One-Dimensional Vlasov-Maxwell Equilibria for the Force-free Harris Sheet', Phys. Plasmas 18, 082108 (2011)

2. T. Neukirch, **F. Wilson** & M.G. Harrison, 'A Detailed Investigation of the Properties of a Vlasov-Maxwell Equilibrium for the Force-free Harris Sheet', Phys. Plasmas 16, 122102 (2009)

Acknowledgements

Contents

Chapter 1

Introduction

1.1 Background

Most of the matter on the Earth occurs in one of three states: solid, liquid, or gas. In the whole of the visible universe, however, it is estimated that over 99% of the matter takes the form of a 'fourth state of matter', known as plasma. Most plasmas can be described as ionised gases, formed when a neutral gas is heated to a sufficiently high temperature, such that the electrostatic forces binding electrons to atomic nuclei are overcome (Dendy, 1994), meaning that the electrons and positively charged ions can then move freely. Due to the ionisation, the behaviour of a plasma is strongly influenced by electromagnetic fields, and so it will exhibit different and more interesting behaviour than a neutral gas. As described by, for example, Krall and Trivelpiece (1973), the term 'fourth state of matter' comes from the fact that heating a solid results in a change of state into a liquid which, when heated further, changes state into a gas, and heating the gas further still results in an ionised gas, which can be classed as a plasma provided certain conditions are satisfied (e.g. Chen, 1995). This thesis will be concerned only with ionised gases, but it should also be noted that conducting fluids and even solids can be classified as plasmas, provided they contain enough free charged particles such that their behaviour is dominated by electromagnetic forces (Boyd and Sanderson, 1969).

Examples of naturally occurring plasmas visible from the Earth's surface are lightning and auroras. Such plasmas are relatively uncommon, however, due to the low temperature and high density of the Earth's atmosphere (Krall and Trivelpiece, 1973). Consequently, to study plasmas experimentally, they must be man-made in the laboratory, and much of laboratory research in plasma physics is concerned with controlled thermonuclear fusion as a possible source of renewable power for the future (e.g. Goedbloed and Poedts, 2004).

Although the natural occurrence of plasma on Earth is very rare, in the rest of the universe it occurs almost everywhere. Examples from our solar system include the Sun, solar wind, and planetary magnetospheres and ionospheres. Due to the abundance of plasma in the universe, a good understanding of the physics of plasmas is essential for an understanding of many astrophysical activity processes. It is generally believed that the magnetic field is the source of energy for many of these processes and, therefore, the storage of magnetic energy and its conversion into other forms of

energy (bulk flow, heat, non-thermal energy) is now one of the core parts of theoretical plasma astrophysics. Typical examples of activity processes in our solar system are magnetospheric substorms, solar flares, and coronal mass ejections.

A key process for magnetic energy release and conversion is magnetic reconnection - a process which changes the connectivity of field lines. This requires the plasma to be non-ideal. However, the high temperatures and low densities of many astrophysical plasmas imply that they should be very close to ideal, thus prohibiting the occurrence of magnetic reconnection. This apparent contradiction can be resolved by noticing that a plasma only needs to be non-ideal in a small region for magnetic reconnection to become possible. Of particular importance are so-called 'current sheets' - regions of large electric current density that are strongly localised in one spatial direction.

Due to their strong localisation, current sheets are very well described by one-dimensional equilibrium models. Using MHD, the task of finding such models is very simple. In many astrophysical plasmas, however, the length scales over which the current density is believed to vary are often microscopic. In such cases, it is more appropriate to use kinetic plasma equilibria. In tenuous, hot plasmas, collisions are very rare, and thus Vlasov-Maxwell theory has to be used.

Part of the work in this thesis, therefore, will focus on one-dimensional, non-relativistic, quasineutral Vlasov-Maxwell equilibria, that is equilibria depending on only one spatial coordinate (chosen here to be the z-coordinate). In such a set-up, the spatial invariance in the x- and y-directions means that the canonical momentum is conserved in both directions. The total particle energy (the Hamiltonian) must also be conserved, due to the time-independence of the problem. Thus, the distribution functions will depend on these three constants of motion. There are many examples of collisionless equilibria of this type (e.g. Tonks, 1959; Weibel, 1959; Grad, 1961; Morozov and Solov'ev, 1961; Hurley, 1961; Harris, 1962; Bertotti, 1963; Hurley, 1963; Nicholson, 1963; Sestero, 1964, 1966; Sestero and Zannetti, 1967; Lam, 1967; Parker, 1967; Lerche, 1967; Davies, 1968; Alpers, 1969; Su and Sonnerup, 1971; Kan, 1972; Lemaire and Burlaga, 1976; Roth, 1976; Mynick et al., 1979; Lee and Kan, 1979a,b; Greene, 1993; Roth et al., 1996; Attico and Pegoraro, 1999; Mottez, 2003, 2004; Fu and Hau, 2005; Yoon et al., 2006). There are also a small number of known examples of such equilibria for force-free fields (Sestero, 1967; Channell, 1976; Bobrova and Syrovatskiǐ, 1979; Bobrova et al., 2001; Harrison and Neukirch, 2009b), which are fields satisfying $\mathbf{j} \times \mathbf{B} = 0$, such that the magnetic field and current density are aligned with each other. Such fields can be used to model low-beta plasmas, such as that of the solar corona. Finding collisionless distribution functions for force-free field profiles is, however, a highly non-trivial task, which is reflected in the fact that relatively few examples are known. Of these known examples, only one is of the nonlinear force-free type, which was found by Harrison and Neukirch (2009b) for the force-free Harris sheet field profile, which is a force-free analogue of the well known Harris sheet model (Harris, 1962).

Knowledge of collisionless force-free equilibria is important for gaining a deeper understanding of both macroinstabilities, such as the collisionless tearing mode, from which collisionless reconnection can result (e.g. Schindler, 2007), and microinstabilities, which can result from a non-Maxwellian distribution function (e.g. Gary, 2005). An important microscopic plasma phenomenon is that of wave-particle interactions, such as Landau damping (e.g. Boyd and Sanderson, 2003; Gary, 2005), in which an exchange of energy can take place between plasma waves and particles that are moving with the same phase speed. In MHD models, the velocity space distribution of the particles is not taken into account, and so microscopic plasma phenomena cannot be studied. Although microinstabilities will not be considered in this thesis, it is important to note that kinetic models allow for investigations of a more diverse range of phenomena than MHD models.

Further discussion of the main points above will be given in the remainder of the present chapter. The definition of a plasma will be discussed in more detail in Section 1.2. The kinetic and MHD approaches for modelling plasmas will be described in Section 1.3. In Section 1.4, a discussion of both MHD and Vlasov-Maxwell equilibria will be given. It should be noted that, although the main focus of the work in this thesis is on Vlasov-Maxwell equilibrium theory, a discussion of MHD equilibria is given to illustrate the differences from Vlasov-Maxwell equilibria, and also because the MHD context is useful for introducing force-free magnetic fields. In the final section of the chapter, the main aims of this thesis will be given.

1.2 Definition of a Plasma

As stated in the previous section, most plasmas are ionised gases. It is wrong, however, to assume that all ionised gases can be described as plasmas, since all gases will be ionised to some degree, however small. Chen (1995) describes a plasma as 'a quasineutral gas of charged and neutral particles which exhibits collective behaviour'. This definition will be explained further in the remainder of the present section, and three criteria will be given, which must be satisfied to allow an ionised gas to be described as a plasma.

The term 'collective behaviour' refers to the fact that the motion of charged particles induces electromagnetic fields, which then have an effect on the motion of other charged particles in the plasma. This occurs over a long range, due to the fact that as the distance between two regions of plasma, r, is increased, the volume of plasma in one region that can affect the other increases as r^3, even though the Coulomb force between the two original regions decreases as $1/r^2$. Therefore, the long-range Coulomb force is important in determining the behaviour of a plasma, which means that it will exhibit different and more interesting behaviour than a neutral gas.

A quasineutral gas is one in which ions and electrons occur in roughly equal numbers, so that $n_i \approx n_e = n$, where n_i and n_e are the number densities of ions and electrons, respectively. This

will be true if $\lambda_D \ll L$, where L is a typical length scale of the problem, and λ_D is the Debye length, defined as

$$\lambda_D = \left(\frac{\epsilon_0 k_B T_e}{n_e e^2} \right)^{1/2}, \tag{1.1}$$

where ϵ_0 is the permittivity of free space, k_B is Boltzmann's constant, T_e is the temperature of the electrons and e is the charge of an ion. The Debye length is the distance over which any charge imbalance is shielded out from the rest of the plasma. If $\lambda_D \ll L$, therefore, then only a small volume is affected by a charge imbalance, in comparison to the length scale L, and so the electric fields which arise do not have an overall effect on the behaviour of the plasma. When any charge imbalance is introduced, the electrons quickly move to establish neutrality, which causes fluctuations about the equilibrium position (Boyd and Sanderson, 2003). These fluctuations oscillate at a frequency known as the electron plasma frequency, given by

$$\omega_{pe} = \left(\frac{n_e e^2}{\epsilon_0 m_e} \right)^{1/2}, \tag{1.2}$$

where $m_e = 9.1094 \times 10^{-31}$kg is the mass of an electron. An alternative expression for the Debye length in terms of this frequency is

$$\lambda_D = \frac{v_{th,e}}{\omega_{pe}}, \tag{1.3}$$

where $v_{th,e} = (k_B T_e / m_e)^{1/2}$ is the electron thermal velocity.

The number of electrons in a Debye sphere (a sphere of radius λ_D) is given by

$$\Lambda = \frac{4\pi}{3} n \lambda_D^3, \tag{1.4}$$

where Λ is known as the plasma parameter. The plasma will exhibit collective behaviour if $\Lambda \gg 1$.

A third criterion which a plasma satisfies is that the short-range binary collisions between charged particles and neutral atoms occur over a much longer time scale than that over which the oscillatory motion due to collective behaviour occurs. This is required to ensure that the majority of particles do not recombine into atoms, which would cause the ionised gas to behave as a neutral gas. Denoting the typical binary collision time scale as τ_b, and the typical time scale of the collective interactions as τ_c, the condition is $\tau_c \ll \tau_b$, which can also be written as $\omega_c \tau_b \gg 1$, where ω_c is the typical oscillation frequency ($= 1/\tau_c$).

To summarise, according to Chen (1995), a plasma is a type of ionised gas satisfying the following three conditions:

1. $\lambda_D \ll L$

2. $\Lambda \gg 1$

3. $\tau_c \ll \tau_b$.

1.3 Plasma Models

1.3.1 Kinetic (Microscopic) Description of a Plasma

The kinetic description of a plasma is centred around the assumption that, for each particle species s, with mass m_s and charge q_s, there exists a single particle distribution function $f_s(\mathbf{r}, \mathbf{v}, t)$, whose evolution is described by the general kinetic equation

$$\frac{\partial f_s}{\partial t} + \mathbf{v} \cdot \frac{\partial f_s}{\partial \mathbf{r}} + \frac{q_s}{m_s}(\mathbf{E} + \mathbf{v} \times \mathbf{B}) \cdot \frac{\partial f_s}{\partial \mathbf{v}} = \left(\frac{\partial f_s}{\partial t} \right)_c, \tag{1.5}$$

where $(\partial f_s / \partial t)_c$ is the rate of change of f_s with time due to collisions. The expression

$$f(\mathbf{r}, \mathbf{v}, t) d^3 r d^3 v \tag{1.6}$$

gives the number of particles of species s in the six-dimensional phase space volume $d^3 r d^3 v = dx dy dz dv_x dv_y dv_z$, centred at $(\mathbf{r}, \mathbf{v})$, at time t. Once the distribution function is known, a number of macroscopic quantities can be obtained from it by taking velocity moments, which involves multiplying by different powers of the velocity and then integrating over velocity space. The zeroth order velocity moment is obtained by multiplying by $\mathbf{v}^0$ and integrating, which defines the density of particle species s as

$$n_s = \int_{-\infty}^{\infty} f_s d^3 v, \tag{1.7}$$

where $d^3 v = dv_x dv_y dv_z$, and it is assumed that the distribution function has been normalised appropriately. The first order velocity moment, obtained by multiplying by $\mathbf{v}$ and integrating, defines the bulk flow velocity for species s as

$$\mathbf{u}_s = \frac{1}{n_s} \int_{-\infty}^{\infty} \mathbf{v} f_s d^3 v. \tag{1.8}$$

Another important quantity is the pressure tensor, with the (i, j) component given by

$$P_{ij} = \sum_s m_s \int_{-\infty}^{\infty} (v_i - u_{i,s})(v_j - u_{j,s}) f_s d^3 v$$

$$= \sum_s m_s \int_{-\infty}^{\infty} w_{i,s} w_{j,s} f_s d^3 v, \tag{1.9}$$

where $w_{i,s} = v_i - u_{i,s}$ is the deviation from the average velocity, v_i ($u_{i,s}$ is the drift velocity of species s in the i-direction).

The charge and current densities are defined in terms of n_s and $\mathbf{u}_s$ as

$$\sigma = \sum_s q_s n_s, \tag{1.10}$$

$$\mathbf{j} = \sum_s q_s n_s \mathbf{u}_s, \tag{1.11}$$

Knowledge of the distribution function is crucial, therefore, as it allows the charge and current densities to be calculated, from which the magnetic and electric field profiles can then be found via Maxwell's equations of electromagnetism (e.g. Fleisch, 2008). These consist of:

- Ampère's law,

$$\nabla \times \mathbf{B} = \mu_0 \mathbf{j} + \mu_0 \epsilon_0 \frac{\partial \mathbf{E}}{\partial t}, \tag{1.12}$$

  which states that an electric current, $\mathbf{j}$, and a time-varying electric field, $\partial \mathbf{E}/\partial t$, give rise to a circulating magnetic field, $\mathbf{B}$. The second term on the right-hand side of Equation (1.12) is known as the displacement current, and can be neglected if typical speeds are less than $c = 2.99792458 \times 10^8 \mathrm{ms}^{-1}$, the speed of light in a vacuum. The quantities $\mu_0 = 4 \times 10^7 \mathrm{Hm}^{-1}$ and $\epsilon_0 = 1/(\mu_0 c^2)$ are the permeability and permittivity of free space, respectively.

- The solenoidal condition,

$$\nabla \cdot \mathbf{B} = 0, \tag{1.13}$$

  which states that magnetic monopoles cannot exist.

- Faraday's law,

$$\nabla \times \mathbf{E} = -\frac{\partial \mathbf{B}}{\partial t}, \tag{1.14}$$

  which states that a time varying magnetic field, $\mathbf{B}$, induces a circulating electric field, $\mathbf{E}$.

- Gauss' law,

$$\nabla \cdot \mathbf{E} = \frac{\sigma}{\epsilon_0}, \tag{1.15}$$

	Photosphere	Corona
Number density n (m^{-3})	8×10^{22}	1×10^{15}
Temperature T (K)	6×10^{3}	2×10^{6}
Magnetic field strength B (T)	2×10^{-1}	1×10^{-2}
Debye length λ_D (m)	2×10^{-8}	3×10^{-3}
Plasma parameter Λ	2	1×10^{8}

Table 1.1: Typical parameter values for the solar corona (corresponding to an active region) and solar photosphere (corresponding to a sunspot). The values have been taken from Schindler (2007).

which states that the electric flux passing through a closed surface is proportional to the total charge within that surface.

The kinetic equation and Maxwell's equations form a self consistent system of equations, since the magnetic and electric fields depend on the distribution function through the charge and current densities, given by Equations (1.10) and (1.11), and the distribution function in turn depends on the fields through the kinetic equation (1.5).

The collision term on the right hand side of Equation (1.5) is, in general, a 'complicated, non linear, integral function of f' (Boyd and Sanderson, 1969). It is stated by Schindler (2007) that such a term is the result of Coulomb collisions between charged particles, which are 'based on electric fluctuations in the Debye sphere', a sphere with radius λ_D, where λ_D is the Debye length, given by Equation (1.1). It is also stated that the typical Coulomb collision terms scale as $\ln(\Lambda)/\Lambda$, where Λ is the plasma parameter given by Equation (1.4), which gives the number of electrons in a Debye sphere. Using the definition (1.1) of the Debye length, the plasma parameter can be written as

$$\Lambda = \frac{4\pi}{3} \left(\frac{\epsilon_0 k_B}{e^2} \right)^{3/2} \frac{T_e^{3/2}}{n_e^{1/2}}, \tag{1.16}$$

which clearly scales as $T_e^{3/2}/n_e^{1/2}$. Coulomb collisions can, therefore, be neglected for values of this ratio which make the plasma parameter very large, such that $\ln(\Lambda)/\Lambda$ is negligible. This is the case for plasmas with a sufficiently high temperature and low density. Such plasmas are described as collisionless, because the collision term in Equation (1.5) can be neglected completely. Table 1.1 shows typical parameter values for the solar corona, and solar photosphere (values from Schindler, 2007). This table shows that the plasma in the solar corona, for example, is approximately collisionless, due to typical temperatures being in the region of 2×10^6K, with the typical number density being in the region of 1×10^{15}m^{-3}, which gives $\Lambda = 1 \times 10^8$. The plasma of the solar photosphere, however, is an example of a plasma for which collision terms are significant, since typical temperatures are three orders of magnitude smaller than those of the corona (6×10^3K), and the plasma is much more dense (the number density is of the order 8×10^{22}m^{-3}),

giving a value of just 2 for the plasma parameter. It should be noted, however, that the photosphere contains a large amount of neutrals due to the lower temperature (only a small fraction of the gas is ionised) and, as such, much of the collisions occur between neutrals and protons, as opposed to collisions between charged particles.

In a collisionless plasma, the mean free path of collisions, λ_c, is much larger than the length scale, L, over which the macroscopic fields vary, so that

$$\lambda_c \gg L. \tag{1.17}$$

An alternative way to view this is that the collision frequency, Ω_c, is less than the characteristic frequency, ω, which describes the time rate of change of the macroscopic fields, so that

$$\Omega_c \ll \omega. \tag{1.18}$$

For a collisionless plasma, the evolution of the distribution function is described by the Vlasov equation,

$$\frac{\partial f_s}{\partial t} + \mathbf{v} \cdot \frac{\partial f_s}{\partial \mathbf{r}} + \frac{q_s}{m_s}(\mathbf{E} + \mathbf{v} \times \mathbf{B}) \cdot \frac{\partial f_s}{\partial \mathbf{v}} = 0, \tag{1.19}$$

and the above equation, together with Maxwell's equations (1.12)-(1.15), form the Vlasov-Maxwell system of equations. The left hand side of Equation (1.19) is the total time derivative of f_s, since

$$\frac{df_s(\mathbf{r}, \mathbf{v}, t)}{dt} = \frac{\partial f_s}{\partial t} + \frac{\partial f_s}{\partial \mathbf{r}} \cdot \frac{d\mathbf{r}}{dt} + \frac{\partial f_s}{\partial \mathbf{v}} \cdot \frac{d\mathbf{v}}{dt}, \tag{1.20}$$

where $d\mathbf{r}/dt$ and $d\mathbf{v}/dt$ are given by the equations of motion for a particle of mass m_s and charge q_s moving in an electromagnetic field:

$$\frac{d\mathbf{r}}{dt} = \mathbf{v}, \tag{1.21}$$

$$\frac{d\mathbf{v}}{dt} = \frac{q_s}{m_s}(\mathbf{E} + \mathbf{v} \times \mathbf{B}). \tag{1.22}$$

Equations (1.21) and (1.22) are the characteristic equations of the Vlasov equation, and thus the characteristic curves are simply the particle trajectories. The Vlasov equation, therefore, states that the distribution function must be constant along particle trajectories.

1.3.2 Fluid (Macroscopic) Description of a Plasma

As a plasma is electrically conducting, the governing equations on the macroscopic, or fluid, scale are the equations of magnetohydrodynamics (MHD), which consist of equations from fluid

mechanics together with Maxwell's equations of electromagnetism. In the fluid approach, all variables depend only on space and time, since the distribution function is assumed to be close to Maxwellian everywhere. The MHD equations can be derived from the kinetic equations, as described in a number of textbooks (e.g. Boyd and Sanderson, 1969; Bittencourt, 1986; Dendy, 1994; Schindler, 2007). The derivation will not be given here, however, since the primary focus of the work in this thesis is on Vlasov theory, and MHD will be discussed only briefly in order to highlight the differences from the Vlasov approach.

The resistive MHD equations are given by

$$\frac{\partial \rho}{\partial t} + \nabla \cdot (\rho \mathbf{v}) = 0, \tag{1.23}$$

$$\rho \left(\frac{\partial \mathbf{v}}{\partial t} + \mathbf{v} \cdot \nabla \mathbf{v} \right) = \mathbf{j} \times \mathbf{B} - \nabla p, \tag{1.24}$$

$$\left(\frac{\partial}{\partial t} + \mathbf{v} \cdot \nabla \right) \left(\frac{p}{\rho^\gamma} \right) = \frac{\gamma - 1}{\rho^\gamma} \eta j^2, \tag{1.25}$$

$$\nabla \times \mathbf{E} = -\frac{\partial \mathbf{B}}{\partial t}, \tag{1.26}$$

$$\nabla \cdot \mathbf{B} = 0, \tag{1.27}$$

$$\nabla \times \mathbf{B} = \mu_0 \mathbf{j}, \tag{1.28}$$

$$\mathbf{E} + \mathbf{v} \times \mathbf{B} = \eta \mathbf{j}, \tag{1.29}$$

where ρ is the density of the plasma, p the pressure, γ the polytropic index, and η the resistivity. Equation (1.23) is the mass continuity equation, Equation (1.24) is the equation of motion, Equation (1.25) is the energy equation, and Equations (1.26)-(1.28) are the remaining three Maxwell equations (Gauss' law is not needed since it is assumed that the plasma is quasineutral). Equation (1.29) is the resistive form of Ohm's law, which couples Maxwell's equations to the fluid equations through the plasma velocity, $\mathbf{v}$. It describes the motion of the plasma as it moves through a magnetic field, $\mathbf{B}$, and electric field, $\mathbf{E}$.

In ideal MHD (e.g. Schindler, 2007; Goedbloed and Poedts, 2004; Freidberg, 1987), it is assumed that the plasma is a perfect conductor, such that the resistivity, η, can be neglected. Ohm's law, given by Equation (1.29), then becomes the ideal Ohm's law

$$\mathbf{E} + \mathbf{v} \times \mathbf{B} = 0, \tag{1.30}$$

and the energy equation (1.25) becomes

$$\left(\frac{\partial}{\partial t} + \mathbf{v} \cdot \nabla \right) \left(\frac{p}{\rho^\gamma} \right) = 0. \tag{1.31}$$

These equations imply that magnetic field lines move with the plasma. so they are 'frozen' into the plasma (Alfvén, 1942). As mentioned in Section 1.1, many plasmas can be assumed to satisfy

the conditions of ideal MHD, which precludes the occurrence of non-ideal activity processes such as magnetic reconnection. This contradiction can, however, be explained by the fact that current sheets can form, where ideal MHD breaks down, and resistive MHD must then be used to model the plasma dynamics.

1.4 Plasma Equilibria

1.4.1 MHD Equilibria

In the present section, static equilibria of the MHD equations will be considered, for which $\partial/\partial t = 0$ and $\mathbf{v} = 0$ (e.g. Neukirch, 1998; Biskamp, 1993; Schindler, 2007). MHD equilibria are discussed here in order to a) explain some terminology that will later be used also for Vlasov-Maxwell equilibria, and b) to introduce some one-dimensional MHD equilibria whose Vlasov-Maxwell counterparts will be discussed later.

Setting $\partial/\partial t = 0$ and $\mathbf{v} = 0$ in the MHD equations (from Section 1.3.2) gives the equations of magnetohydrostatics (MHS) as

$$\mathbf{j} \times \mathbf{B} = \nabla p, \tag{1.32}$$

$$\nabla \times \mathbf{B} = \mu_0 \mathbf{j}, \tag{1.33}$$

$$\nabla \cdot \mathbf{B} = 0. \tag{1.34}$$

An equation of state or an energy equation is also required to complete the system of equations. Note also that the electric field can be written as $\mathbf{E} = \nabla\phi$, where ϕ is a scalar potential, since Faraday's law (1.26) gives $\nabla \times \mathbf{E} = 0$.

Equation (1.32) is the momentum equation, which now has the form of a force balance equation, and states that there must be a balance between the Lorentz force $\mathbf{j} \times \mathbf{B}$ and the pressure gradient ∇p. Equations (1.24) and (1.25) are Ampère's law and the solenoidal condition. Note also that the continuity equation (1.23) is automatically satisfied, and so, when neglecting gravity, the density does not appear in the equilibrium equations. It can, therefore, be chosen in line with the physics of the problem.

Using Ampère's law (1.33) to eliminate the current density $\mathbf{j}$ from the momentum equation (1.32), as well as using the vector identity

$$(\nabla \times \mathbf{B}) \times \mathbf{B} = (\mathbf{B} \cdot \nabla)\mathbf{B} - \frac{1}{2}\nabla(|\mathbf{B}|^2), \tag{1.35}$$

gives

$$
\begin{aligned}
\nabla p &= \frac{1}{\mu_0}(\nabla \times \mathbf{B}) \times \mathbf{B} \\
&= \frac{\mathbf{B} \cdot \nabla \mathbf{B}}{\mu_0} - \nabla \left(\frac{B^2}{2\mu_0} \right),
\end{aligned}
\tag{1.36}
$$

where $B = |\mathbf{B}|$. The first term in the second line of Equation (1.36) represents a magnetic tension force, and the second term is a magnetic pressure force.

For cases where the gradient of the plasma pressure, ∇p, can be neglected, the momentum (or force balance) equation (1.32) reduces to

$$
\mathbf{j} \times \mathbf{B} = 0,
\tag{1.37}
$$

which implies that the current arising from the magnetic field is parallel to the magnetic field,

$$
\mu_0 \mathbf{j} = \nabla \times \mathbf{B} = \alpha(\mathbf{r})\mathbf{B},
\tag{1.38}
$$

where $\mathbf{r} = (x, y, z)$. A magnetic field which satisfies Equations (1.37) and (1.38) is said to be a force-free field. Taking the divergence of Equation (1.38) gives

$$
\begin{aligned}
\nabla \cdot (\alpha \mathbf{B}) &= \nabla \cdot (\nabla \times \mathbf{B}), \\
\Rightarrow \alpha \nabla \cdot \mathbf{B} + \mathbf{B}.\nabla \alpha &= 0, \\
\Rightarrow \mathbf{B} \cdot \nabla \alpha &= 0,
\end{aligned}
\tag{1.39}
$$

where the solenoidal condition (1.27) has been used, together with the vector identities

$$
\begin{aligned}
\nabla \cdot (\nabla \times \mathbf{B}) &= 0, \tag{1.40} \\
\nabla \cdot (\alpha \mathbf{B}) &= \alpha \nabla \cdot \mathbf{B} + \mathbf{B} \cdot \nabla \alpha. \tag{1.41}
\end{aligned}
$$

Equation (1.39) states that the derivative of α in the direction of $\mathbf{B}$ vanishes, meaning that α must be constant along field lines. If α is constant with respect to $\mathbf{r}$, then $\mathbf{B}$ is said to be a linear force-free field. If α varies with $\mathbf{r}$, however, then $\mathbf{B}$ is said to be a nonlinear force-free field. In this case, α remains constant along a given field line, but varies from field line to field line. Note also that, if $\mathbf{j} = 0$, then $\mathbf{B}$ is said to be a potential field.

The plasma beta is defined as the ratio of the plasma pressure, p, to the magnetic pressure, $B^2/2\mu_0$:

$$
\beta = \frac{p}{(B^2/2\mu_0)},
\tag{1.42}
$$

where $B^2 = B_x^2 + B_y^2 + B_z^2$ in Cartesian coordinates. Force-free fields can be used to model low-beta plasmas, since the pressure gradient can be neglected if $\beta << 1$ (if the magnetic pressure is much greater than the plasma pressure). This situation arises in the solar corona, where the field can be treated as being approximately force-free. Figure 1.1 shows estimates of how the plasma beta varies for different regions on the Sun, from a model by Gary (2001). It shows that, for the most part, the plasma beta in the solar corona is less than one (this is also true for the chromosphere), but in the photosphere and solar wind, it is greater than one, meaning that the force-free description would not be appropriate for these plasmas, since the plasma pressure cannot be neglected.
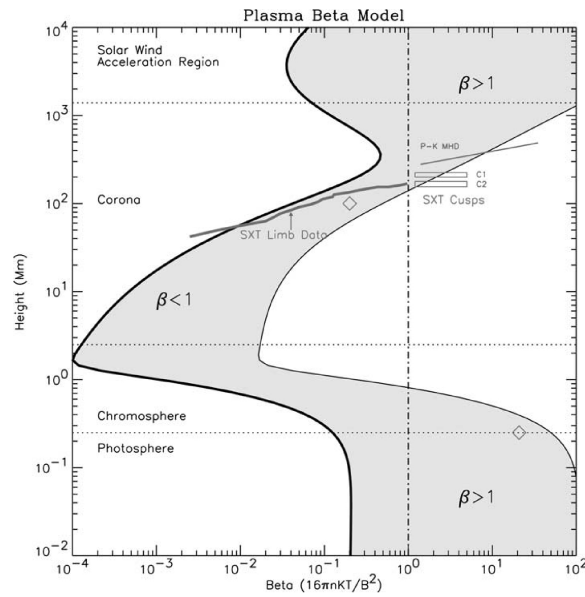
Figure 1.1: Plot showing how the plasma beta varies for the different regions on the Sun (shaded region). It is less than one throughout most of the solar corona and the chromosphere, and greater than one for the photosphere and solar wind. The boundaries of the shaded region come from two models: one of a plage, the other of the umbra of a sunspot. From Gary (2001).

The simplest solutions of the MHS equations are one-dimensional solutions. In a Cartesian coordinate system, assuming that the variation is in the z-direction, this type of solution is known as a sheet pinch, given by

$$\mathbf{B} = \mathbf{B}(z), \tag{1.43}$$

$$p = p(z). \tag{1.44}$$

For a one-dimensional equilibrium depending on z, the magnetic field must be of the form

$$\mathbf{B} = (B_x(z), B_y(z), 0), \tag{1.45}$$

since B_z must vanish in order to satisfy force balance. The field lines will, therefore, be straight lines in planes parallel to the x-y-plane, and hence there will be no magnetic tension force.

The momentum equation (1.36) gives the force balance equation for a one-dimensional equilibrium as

$$\frac{d}{dz}\left(p + \frac{B^2}{2\mu_0}\right) = 0, \tag{1.46}$$

where $B^2 = B_x^2 + B_y^2$. This implies that the sum of the plasma and magnetic pressures (the total pressure) is constant,

$$p + \frac{B^2}{2\mu_0} = p_{total} = \text{constant}. \tag{1.47}$$

1.4.1.1   The Harris Sheet

An example of a sheet pinch is the Harris sheet model (Harris, 1962). This is a well known model for a one-dimensional current sheet, and has been widely used in studies of plasma instabilities. Note that Harris (1962) actually found this as a Vlasov-Maxwell equilibrium. The MHD counterpart will first be introduced here, and the Vlasov-Maxwell case will be discussed later.

The magnetic field of the Harris sheet is given by

$$\mathbf{B}_{Harris} \quad = \quad B_0\left(\tanh(z/L), 0, 0\right), \tag{1.48}$$

where B_0 is a constant and L is a parameter which specifies the thickness of the sheet. The pressure is given by

$$P_{Harris} = \frac{B_0^2}{2\mu_0}\frac{1}{\cosh^2(z/L)} + P_b, \tag{1.49}$$

where P_b is a constant background pressure. Solving Ampère's law (1.33) gives the current density as

$$\mathbf{j}_{Harris} \quad = \quad \frac{B_0}{\mu_0 L}\left(0, \frac{1}{\cosh^2(z/L)}, 0\right). \tag{1.50}$$

$$\tag{1.51}$$

Figure 1.2 (from Harrison, 2009) shows a plot of normalised magnetic field, pressure and current density profiles for the Harris sheet, and a field-line plot is shown in Figure 1.3 (also from Harrison, 2009). Since there is no y-component of the magnetic field, the field lines are in the x-z-plane. As z gets larger in both the positive and negative directions, the field tends to a constant,
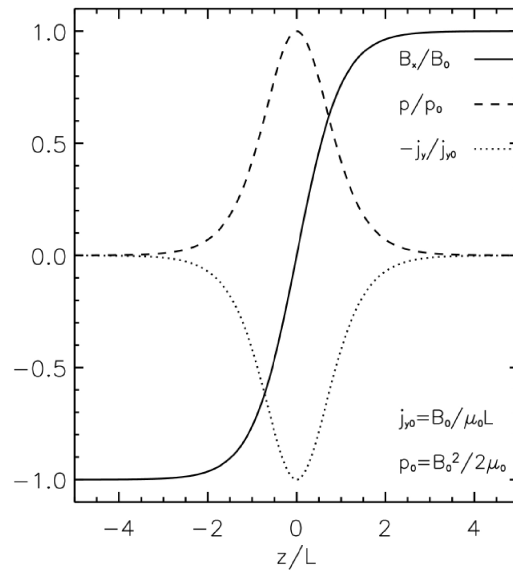
Figure 1.2: Plot of normalised magnetic field, current density and pressure profiles for the Harris sheet. Note that $-j_y$ has been plotted since j_y has the same profile as the pressure when normalised. From Harrison (2009).
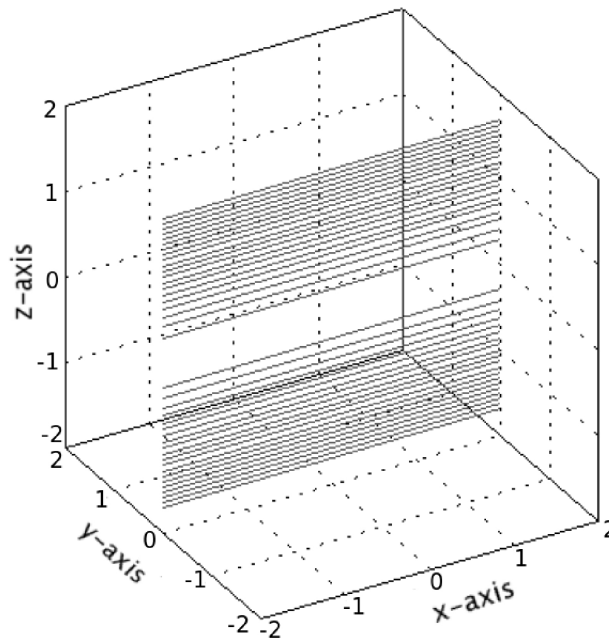
Figure 1.3: Field line plot for the Harris sheet (From Harrison, 2009).

$$\lim_{z \to \pm\infty} |\mathbf{B}_{Harris}| = B_0, \tag{1.52}$$

and so the field lines are equally spaced at higher values of z. The direction of the field lines are not shown in Figure 1.3 but, for positive values of z, they point in one direction and, for negative values of z, they point in the opposite direction.

1.4.1.2 The Force-Free Harris Sheet

A force-free analogue of the Harris sheet model is the force-free Harris sheet, which is a nonlinear force-free model for a one-dimensional current sheet. It consists of a magnetic field profile as follows,

$$\mathbf{B}_{ffhs} = B_0 \left(\tanh(z/L), \frac{1}{\cosh(z/L)}, 0 \right), \tag{1.53}$$

where B_0 is a constant and L is a parameter which specifies the thickness of the sheet. The x-component of the field is the same as that of the Harris sheet, and the addition of the shear field component in the y-direction makes the field force-free, since $B^2 = B_x^2 + B_y^2 = B_0^2$. Figure 1.4 (from Harrison, 2009) shows a plot of the field lines for the force-free Harris sheet. Using
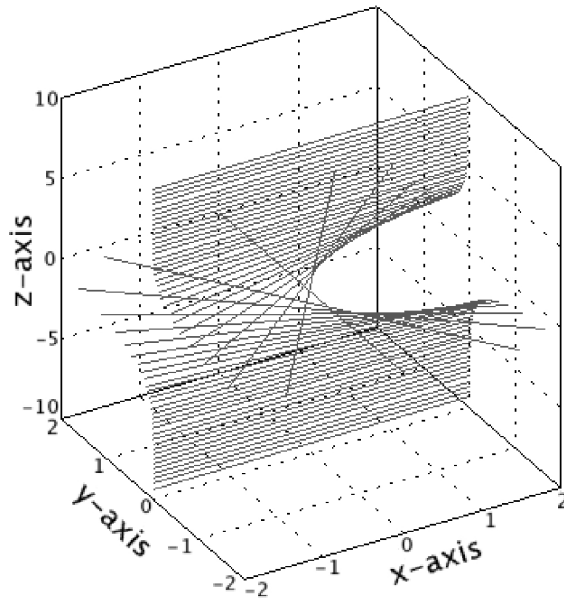
Figure 1.4: Field line plot for the force-free Harris sheet (from Harrison, 2009).

Ampère's law (Equation (1.33)), the current density is given by

$$\mathbf{j}_{ffhs} = \frac{B_0}{\mu_0 L} \frac{1}{\cosh(z/L)} \left(\tanh(z/L), \frac{1}{\cosh(z/L)}, 0 \right), \tag{1.54}$$

and so it can be seen that $\mathbf{j} \times \mathbf{B} = 0$, as is required for a force-free field. The magnetic pressure is given by

$$\frac{B^2}{2\mu_0} = \frac{B_x^2 + B_y^2}{2\mu_0} = \frac{B_0^2}{2\mu_0}, \tag{1.55}$$

which is constant, and so the plasma pressure is given by

$$P = P_{total} - P_{magnetic} = \text{constant.} \tag{1.56}$$

It is the y-component of the field, therefore, which maintains the force balance across the sheet, since both the plasma and magnetic pressure are constant, but the magnetic field itself varies with z. Figure 1.5 (from Harrison, 2009) shows normalised magnetic field and current density profiles for the force-free Harris sheet.

Figure 1.5: Plot of normalised magnetic field, current density and pressure profiles for the force-free Harris sheet (from Harrison, 2009).
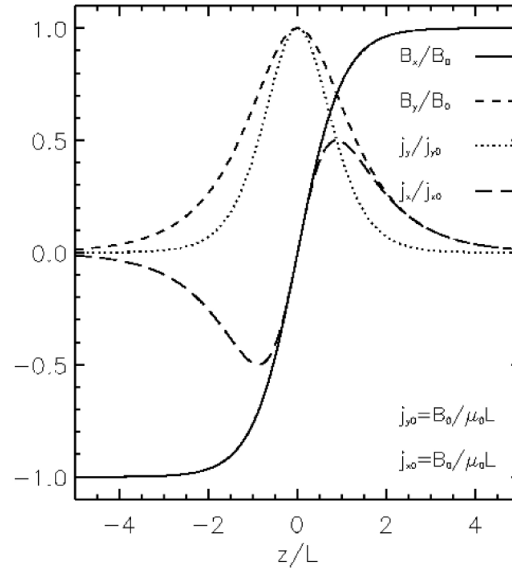
As the magnetic field (1.53) is force-free, the current density is parallel to the magnetic field,

$$\mathbf{j}_{ffhs} = \frac{\alpha(z)}{\mu_0} \mathbf{B}_{ffhs}, \tag{1.57}$$

with the force-free parameter $\alpha(z)$ given by

$$\alpha(z) = \frac{1}{L} \frac{1}{\cosh(z/L)}, \tag{1.58}$$

which varies with z, meaning that the force-free Harris sheet field is a nonlinear force-free field. As previously discussed, this means that α is constant along a given field line, but varies from field line to field line.

1.4.2 Vlasov-Maxwell Equilibria

Vlasov-Maxwell equilibria can be found by solving the steady-state Vlasov equation,

$$\mathbf{v} \cdot \frac{\partial f_s}{\partial \mathbf{r}} + \frac{q_s}{m_s}(\mathbf{E} + \mathbf{v} \times \mathbf{B}) \cdot \frac{\partial f_s}{\partial \mathbf{v}} = 0, \tag{1.59}$$

together with the steady-state Maxwell equations,

$$\nabla \cdot \mathbf{E} = \frac{\sigma}{\epsilon_0}, \tag{1.60}$$

$$\nabla \times \mathbf{E} = 0, \tag{1.61}$$

$$\nabla \times \mathbf{B} = \mu_0 \mathbf{j}, \tag{1.62}$$

$$\nabla \cdot \mathbf{B} = 0. \tag{1.63}$$

Throughout the work in this thesis, it is assumed that each equilibrium quantity varies only with the z-coordinate, so that there is spatial invariance with respect to the x- and y-coordinates. Furthermore, it is assumed that the magnetic field vanishes in the z-direction, and can be written as $\mathbf{B} = \nabla \times \mathbf{A}$, where $\mathbf{A} = (A_x, A_y, 0)$ is a vector potential whose z-component can be assumed to vanish without loss of generality. This assumption ensures that Equation (1.63) is automatically satisifed. The x- and y-components of $\mathbf{B}$ are then given by,

$$B_x = -\frac{dA_y}{dz}, \tag{1.64}$$

$$B_y = \frac{dA_x}{dz}, \tag{1.65}$$

It is also assumed that the electric field $\mathbf{E}$ can be written as $\mathbf{E} = -\nabla\phi$, where ϕ is a scalar potential, so that

$$E_z = -\frac{d\phi}{dz}, \tag{1.66}$$

which ensures that Equation (1.61) is satisfied. A further assumption is that the plasma consists of two particle species, ions and electrons, with charges $q_i = e$ and $q_e = -e$, respectively.

As discussed in Section 1.3.1, quasineutrality can be assumed if L, the typical length scale of the plasma, is much larger than the Debye length, λ_D. Note, however, that this does not imply that the electric field vanishes (Harrison and Neukirch, 2009a).

Due to the symmetries of the system. there are three constants of motion, namely the Hamiltonian H_s, arising from the time independence of the system, given by

$$H_s = \frac{1}{2}m_s(v_x^2 + v_y^2 + v_z^2) + q_s\phi, \tag{1.67}$$

the canonical momentum in the x-direction, arising from the spatial symmetry in the x-direction, given by

$$p_{xs} = m_s v_x + q_s A_x, \tag{1.68}$$

and the canonical momentum in the y-direction, arising from the spatial symmetry in the y-direction, given by

$$p_{ys} = m_s v_y + q_s A_y. \tag{1.69}$$

The steady-state Vlasov equation (1.59) is satisfied by positive functions (distribution functions) $f_s = f_s(H_s, p_{xs}, p_{ys})$, which depend only on the constants of motion.

The remaining two Maxwell equations to be solved are Gauss' law (Equation (1.60)) and Ampère's law (Equation (1.62)), the components of which can be expressed as

$$-\epsilon_0 \frac{d^2\phi}{dz^2} = \sigma, \tag{1.70}$$

$$-\frac{1}{\mu_0}\frac{d^2 A_x}{dz^2} = j_x, \tag{1.71}$$

$$-\frac{1}{\mu_0}\frac{d^2 A_y}{dz^2} = j_y, \tag{1.72}$$

where, as was discussed in Section 1.3.1, the charge density σ and the x- and y-components of the current density, j_x and j_y, can be expressed as moments of the distribution functions as follows,

$$\sigma(A_x, A_y, \phi) = \sum_s q_s \int_{-\infty}^{\infty} f_s(H_s, p_{xs}, p_{ys})d^3v, \tag{1.73}$$

$$j_x(A_x, A_y, \phi) = \sum_s q_s \int_{-\infty}^{\infty} v_x f_s(H_s, p_{xs}, p_{ys})d^3v, \tag{1.74}$$

$$j_y(A_x, A_y, \phi) = \sum_s q_s \int_{-\infty}^{\infty} v_y f_s(H_s, p_{xs}, p_{ys})d^3v. \tag{1.75}$$

It can be shown (e.g. Harrison and Neukirch, 2009a) that the components of the charge and current

densities satisfy the following relations

$$\frac{\partial \sigma}{\partial A_x} + \frac{\partial j_x}{\partial \phi} = 0, \tag{1.76}$$

$$\frac{\partial \sigma}{\partial A_y} + \frac{\partial j_y}{\partial \phi} = 0, \tag{1.77}$$

$$\frac{\partial j_x}{\partial A_y} - \frac{\partial j_y}{\partial A_x} = 0, \tag{1.78}$$

and also that, for a quasineutral plasma, the components of the current density can be expressed as

$$j_x(A_x, A_y, \phi) = \frac{\partial P_{zz}}{\partial A_x}, \tag{1.79}$$

$$j_y(A_x, A_y, \phi) = \frac{\partial P_{zz}}{\partial A_y}, \tag{1.80}$$

(see also Grad, 1961; Bertotti, 1963; Lerche, 1967; Channell, 1976; Mynick et al., 1979; Attico and Pegoraro, 1999). Additionally, the charge density σ can be written as

$$\sigma(A_x, A_y, \phi) = -\frac{\partial P_{zz}}{\partial \phi}, \tag{1.81}$$

(e.g. Bertotti, 1963; Lerche, 1967; Mynick et al., 1979). In Equations (1.79)-(1.81), P_{zz} is the zz-component of the pressure tensor, defined in terms of the distribution functions as

$$P_{zz} = \sum_s m_s \int v_z^2 f_s d^3 v. \tag{1.82}$$

Note that there is no drifting of particles in the z-direction, and so the above definition of P_{zz} is consistent with the general definition of the pressure tensor, given in Equation (1.9). Using Equations (1.79) and (1.80), Ampère's Law (Equations (1.71) and (1.72)) can then be written in terms of the vector potential, **A**, and the pressure, P_{zz}, which gives

$$\frac{d^2 A_x}{dz^2} = -\mu_0 \frac{\partial P_{zz}}{\partial A_x}, \tag{1.83}$$

$$\frac{d^2 A_y}{dz^2} = -\mu_0 \frac{\partial P_{zz}}{\partial A_y}. \tag{1.84}$$

The scalar potential ϕ can be determined from the quasineutrality condition $n_e = n_i$, which, to lowest order, corresponds to the condition

$$\frac{\partial P_{zz}}{\partial \phi} = 0, \tag{1.85}$$

(e.g. Harrison and Neukirch, 2009a), and so the equilibrium problem reduces to solving Equa-

Particle Motion	1D VM Equilibrium
time: t	coordinate: z
position: x, y	vector potential: A_x, A_y
potential: $V(x, y)$	pressure: $\mu_0 P_{zz}(A_x, A_y)$
energy: $m(v_x^2 + v_y^2)/2 + V(x, y)$	total pressure: $(B_x^2 + B_y^2)/2\mu_0 + P_{zz}$
equations of motion: $$\frac{d^2 x}{dt^2} = -\frac{\partial V}{\partial x}$$ $$\frac{d^2 y}{dt^2} = -\frac{\partial V}{\partial y}$$	Ampère's law: $$\frac{d^2 A_x}{dz^2} = -\mu_0 \frac{\partial P_{zz}}{\partial A_x}$$ $$\frac{d^2 A_y}{dz^2} = -\mu_0 \frac{\partial P_{zz}}{\partial A_y}$$

Table 1.2: The analogy between the one-dimensional Vlasov-Maxwell equilibrium problem and the problem of solving the equations of motion of a particle in a two-dimensional conservative potential.

tions (1.83) and (1.84) for the pressure P_{zz}, which can then be used to determine the distribution function (by using the definition (1.82) of P_{zz}).

Integrating Ampère's Law gives the force balance condition

$$\frac{B^2}{2\mu_0} + P_{zz} = P_T, \tag{1.86}$$

where P_T is a constant. This condition states that the sum of the plasma and magnetic pressures across the sheet must be constant. Note that other components of the pressure tensor could be calculated by taking different moments of the distribution function, but they are not important for the force balance and so will not be considered.

Solving Equations (1.83) and (1.84) for the pressure P_{zz} is analogous to solving the equations of motion of a particle in a two-dimensional conservative potential, as has been noticed by a number of authors (e.g. Grad, 1961; Sestero, 1966; Lam, 1967; Parker, 1967; Lerche, 1967; Alpers, 1969; Su and Sonnerup, 1971; Kan, 1972; Channell, 1976; Mynick et al., 1979; Lee and Kan, 1979b; Greene, 1993; Attico and Pegoraro, 1999; Harrison and Neukirch, 2009a), with z taking the role of time, A_x and A_y the coordinates of the particle and $\mu_0 P_{zz}$ the potential. Table 1.2 summarises this analogy, with the quantities and equations from the particle problem given on the left-hand side, and the equilibrium quantities and equations given on the right-hand side.

In the particle problem, the shape of the potential as a function of position can give insight into the nature of the particle trajectories. In analogy with this, the shape of the pressure P_{zz} can give information about the nature of the solutions of Equations (1.83) and (1.84). The force balance condition (1.86) corresponds to the condition of the total energy being constant in the particle problem. The particle analogy is particularly useful when considering force-free Vlasov-Maxwell equilibria, which will be discussed in Section 2.1.

1.4.2.1 Vlasov-Maxwell Equilibrium for the Harris Sheet

The Harris sheet model was discussed in Section 1.4.1.1 in the MHD context. It can also be represented in Vlasov theory, as described by Harris (1962). Listed again for reference, the magnetic field is given by

$$\mathbf{B}_{Harris} = B_0 \left(\tanh(z/L), 0, 0 \right), \tag{1.87}$$

where B_0 is a constant and L is a parameter which specifies the thickness of the sheet. The vector potential is given by

$$\mathbf{A}_{Harris} = B_0 L(0, -\ln[\cosh(z/L)], 0), \tag{1.88}$$

and solving Ampère's law (1.62) gives the current density as

$$\mathbf{j}_{Harris} = \frac{B_0}{\mu_0 L} \left(0, \frac{1}{\cosh^2(z/L)}, 0 \right). \tag{1.89}$$

The zz-component of the pressure tensor, $P_{zz,Harris}$, is given, as a function of z, by

$$P_{zz,Harris} = \frac{B_0^2}{2\mu_0} \frac{1}{\cosh^2(z/L)} + P_{b,zz}, \tag{1.90}$$

where $P_{b,zz}$ is a constant background pressure. This expression is the same as in the MHD context. Using the fact that $\cosh(z/L) = \exp(-A_y/B_0 L)$ (from equation (1.88)) gives the pressure in terms of A_x and A_y as

$$P_{zz}(A_x, A_y) = \frac{B_0^2}{2\mu_0} \exp\left(\frac{2A_y}{B_0 L} \right) + P_{b,zz}. \tag{1.91}$$

A solution of the steady-state Vlasov equation (1.59) for this magnetic field profile was obtained by Harris (1962), and is given by

$$f_{s,Harris} = \frac{n_{0s}}{(\sqrt{2\pi} v_{th,s})^3} \exp[-\beta_s(H_s - u_{ys} p_{ys})], \tag{1.92}$$

where u_{ys} is a constant average bulk flow velocity in the y-direction. Force balance across the sheet is maintained by a pressure gradient - since the magnetic pressure varies with z so must the plasma pressure in order to maintain force balance.

To illustrate that different distribution functions can give rise to the same magnetic field profile, it should be noted that another distribution function for the Harris sheet field profile was found by

Fu and Hau (2005), which is a kappa-type distribution function of the form

$$f_{s,fu} \quad = \quad \frac{n_0}{2\pi v_{th,s}^2} \frac{\Gamma(\kappa+1)}{\Gamma(\kappa-\frac{1}{2})\kappa^{3/2}} \left[1 + \frac{1}{2\kappa v_{th,s}^2} [c_{1s}^2 + (c_{2s} - u_s)^2 + c_{3s}^2] \right]^{-(\kappa+1)}, \qquad (1.93)$$

where Γ is the gamma function (e.g. Abramowitz and Stegun, 1964), and c_{1s}, c_{2s} and c_{3s} are the constants of motion, which are given by

$$c_{1s} \quad = \quad \left(v_z^2 - \frac{2q_s}{m_s} A_y v_y - \frac{q_s^2}{m_s^2} A_y^2 \right)^{1/2}, \qquad (1.94)$$

$$c_{2s} \quad = \quad v_y + \frac{q_s}{m_s} A_y = \frac{p_{ys}}{m_s}, \qquad (1.95)$$

$$c_{3s} \quad = \quad v_x = \frac{p_{xs}}{m_s}. \qquad (1.96)$$

It will be seen in Sections 2.7 and 2.8 that different distribution functions can also be found for the force-free Harris sheet, in addition to the known solution found by Harrison and Neukirch (2009b).

1.5 Aims and Outline of Thesis

The aims of this thesis can be summarised as follows:

1. Investigate in detail the properties of the known nonlinear one-dimensional force-free Vlasov-Maxwell equilibrium found by Harrison and Neukirch (2009b).

2. Find other one-dimensional force-free Vlasov-Maxwell equilibria.

3. Carry out a linear stability analysis of Harrison and Neukirch's equilibrium distribution function.

Aim 1 is motivated by the fact that the distribution function found by Harrison and Neukirch (2009b) can be multi-peaked in both the v_x- and v_y-directions. This is of interest, since such a distribution function may give rise to microinstabilities (e.g. Krall and Trivelpiece, 1973), in addition to macroscopic instabilities, such as the collisionless tearing mode (e.g. Schindler, 2007). Conditions on the parameters of the distribution function are given, which show when the distribution function can be single or multi-peaked. It should be noted, however, that an investigation into the microinstabilities themselves is beyond the scope of this thesis.

The motivation for aim 2 is the fact that force-free collisionless plasma equilibria are important in investigations of plasma activity processes. They can, for example, be used as initial conditions

for particle-in-cell (PIC) simulations of collisionless reconnection. At present, in order to mimic a force-free field, a constant guide field is added to the Harris sheet field (Harris, 1962). This approach gives a current density which is partially field aligned, but increasing the strength of the guide field does not change the strength of the current density, and so no free energy is added to the system. When starting with a proper force-free equilibrium, the strength of the current density and, hence, the available free energy, are coupled to the shear of the magnetic field. In addition, the plasma density and pressure are constant, which is not true in the guide field case. Harrison (2009) has carried out the first PIC simulations for the force-free Harris sheet, using the Harrison and Neukirch (2009b) distribution function as initial conditions. Although these simulations were preliminary, they hinted at possible significant differences to simulations using the Harris sheet plus guide field as initial conditions. PIC simulations will not be considered in this thesis, but it is important to note that finding further force-free distribution functions would give a bigger range of possible initial conditions, and thus may lead to a deeper understanding of the collisionless reconnection process in the future.

There are three separate parts which can all be categorised under aim 2. Firstly, a discussion will be given of attempts to use the method of Harrison and Neukirch (2009b) to look for equilibria for other nonlinear force-free field profiles. It will be shown, however, that even for seemingly simple field profiles, this method is unsuccessful. A new method was required, therefore, which led, secondly, to the discovery of a family of distribution functions for the force-free Harris sheet field profile, which includes the known solution found by Harrison and Neukirch (2009b). Thirdly, an attempt has been made to extend the theory of the one-dimensional equilibrium problem to cylindrical coordinates, and to find a distribution function for a one-dimensional flux tube, by considering the case where all quantities depend only upon the radial coordinate, r. This attempt, however, did not lead to a force-free equilibrium.

As stated above, the Harrison and Neukirch equilibrium may give rise to macroscopic instabilities, such as the collisionless tearing mode. This is the motivation for aim 3. A central difficulty in such a stability analysis, however, is that the Vlasov equation must be integrated over the unperturbed particle orbits, and so an expression for the orbits is required. This is, in general, not possible to do exactly analytically and so, in order to make analytical progress, it will be necessary to use an approximation for the force-free Harris sheet field profile, in addition to a number of other approximations.

The work in this thesis is laid out as follows: in Chapter 2, the focus is one-dimensional force-free Vlasov-Maxwell equilibria, with a detailed discussion of the properties of the Harrison and Neukirch (2009b) equilibrium given, together with a discussion of finding other distribution functions, for the force-free Harris sheet and other magnetic field profiles. In Chapter 3, the initial calculations for the stability analysis of Harrison and Neukirch's equilibrium are carried out. These calculations will set the scene for a numerical solution of Ampère's law, which is given in Chapter

4. Finally, Chapter 5 contains a summary and a discussion of potential future work.

Chapter 2

One-Dimensional Force-Free Vlasov-Maxwell Equilibria

Parts of the work in the present chapter have been adapted from Neukirch, Wilson, and Harrison (2009) and Wilson and Neukirch (2011).

2.1 Introduction

Investigations of plasma instabilities and plasma waves frequently start with a consideration of equilibrium solutions of the governing equations. In the MHD picture, as was discussed in Section 1.4.1, equilibria can be found by solving the equations of magnetohydrostatics (MHS) (e.g. Neukirch, 1998). When using kinetic theory, and assuming that the plasma is collisionless, the required equilibria can be found by solving the steady-state Vlasov-Maxwell equations (e.g. Krall and Trivelpiece, 1973). The general theory of one-dimensional Vlasov-Maxwell equilibria was discussed in Section 1.4.2.

The work in the present chapter will focus on one-dimensional force-free Vlasov-Maxwell equilibria. Force-free fields, for which $\mathbf{j} \times \mathbf{B} = 0$, such that the current density and magnetic field are parallel to each other, are useful for modelling low-beta plasmas such as that of the solar corona. Finding collisionless distribution functions for such field profiles is, however, a highly non-trivial task. This is reflected in the fact that there are relatively few known examples. Of these known examples, only one is of the nonlinear force-free type (Harrison and Neukirch, 2009b), with the rest being linear force-free (Sestero, 1967; Channell, 1976; Bobrova and Syrovatskiǐ, 1979; Bobrova et al., 2001).

Harrison and Neukirch (2009a) have discussed conditions for the existence of one-dimensional force-free solutions of the Vlasov-Maxwell equations. Using $\mathbf{j} = (\nabla \times \mathbf{B})/\mu_0$, the force-free condition for a one-dimensional model is given by

$$\frac{d}{dz}\left(\frac{B^2}{2\mu_0}\right) = 0, \tag{2.1}$$

which states that the magnetic pressure must be constant. The force-balance condition (1.86) then implies that the plasma pressure, P_{zz}, must also be constant. As discussed in Section 1.4.2, the x- and y- components of the current density can be written as partial derivatives of P_{zz} with respect to A_x and A_y (See Equations (1.79) and (1.80)). The force-balance condition would then appear to imply that the current density must also vanish for a force-free equilibrium. This condition, however, only implies that P_{zz} is constant as a function of z, and so it can still vary with respect to the vector potential. The condition gives

$$\frac{dP_{zz}}{dz} = \frac{\partial P_{zz}}{\partial A_x}\frac{dA_x}{dz} + \frac{\partial P_{zz}}{\partial A_y}\frac{dA_y}{dz} = 0, \tag{2.2}$$

and so it is clear that this condition can be satisfied even if the partial derivatives are non zero. This is an important property of one-dimensional force-free equilibria (Harrison and Neukirch, 2009a).

Returning to the particle analogy, which was discussed in Section 1.4.2, the condition (2.2) means that the pressure P_{zz} must have at least one contour which is also a particle trajectory in the A_x-A_y-plane, in order to allow a particle trajectory to be obtained that corresponds to a force-free field. As stated by Harrison and Neukirch (2009a), this is a necessary condition for the existence of a force-free Vlasov-Maxwell equilibrium. So, starting with a magnetic field profile, a first step is to calculate the vector potential **A**, then to use Ampère's law to find the pressure P_{zz}. A surface plot of P_{zz} in the A_x-A_y plane with the trajectory of **A** overplotted should then reveal that the trajectory is a contour of the pressure. This will be illustrated further in Sections 2.2 and 2.4, where the previously known force-free solutions will be discussed (Sestero, 1967; Channell, 1976; Bobrova and Syrovatskiĭ, 1979; Bobrova et al., 2001; Harrison and Neukirch, 2009b).

It is also noted by Harrison and Neukirch (2009a) that a well known family of potentials, attractive central potentials, allow trajectories which are contours of the potential. These potentials have circular contours, and allow circular particle trajectories. The known linear force-free solutions (Sestero, 1967; Channell, 1976; Bobrova and Syrovatskiĭ, 1979; Bobrova et al., 2001) give rise to such potentials, which will be discussed further in Section 2.2.

Once the pressure function P_{zz} is known, the solution to the Vlasov-Maxwell equations can be completed by finding a distribution function from P_{zz}. One way of doing this is to start with the definition (1.82) of the pressure and solve an integral equation for the distribution function. An illustration of this method has been given by Channell (1976), which will be discussed further in Section 2.3. Channell's method was used by Harrison and Neukirch (2009b) to find a distribution function for the force-free Harris sheet. This was the first non-linear force-free Vlasov-Maxwell equilibrium to be found, and has a number of interesting properties. In particular, the distribution function can be multi-peaked in both the v_x- and v_y-directions, meaning that the equilibrium may be unstable to microinstabilities. One of the main aims of the work in the present chapter is

to present a detailed discussion of the properties of this equilbrium, and to give conditions on the parameters which show when the distribution function can be single or multi-peaked. The derivation of the distribution function will be given in Section 2.4, and the conditions to ensure several maxima will be discussed in Section 2.5.

In Section 2.6, a discussion is given of attempts to use the method of Harrison and Neukirch (2009b) to find Vlasov-Maxwell equilibria for other magnetic field profiles. It will be shown that it is difficult to successfully use this method, even for seemingly simple magnetic field profiles. It seems, therefore, that the force-free Harris sheet is one of the few field profiles for which the method can be used successfully. Although these attempts were unsuccessful, another method was developed which allows a family of distribution functions to be found for the force-free Harris sheet, by using properties of the pressure P_{zz}. This method will be discussed in Sections 2.7 and 2.8.

It is also remarked by Channell (1976) that a straightforward extension of the one-dimensional force-free equilibrium problem to cylindrical coordinates is not possible. This will be discussed further in Section 2.9, and an example will be given of an attempt to find a linear force-free distribution function for one-dimensional flux tubes, by considering the case where all quantities depend only on the radial coordinate, r.

2.2   A Linear Force-Free Vlasov-Maxwell Equilibrium

As discussed by Harrison and Neukirch (2009a), the previously known linear force-free solutions (Sestero, 1967; Bobrova and Syrovatskiĭ, 1979; Bobrova et al., 2001) have a distribution function of the form

$$f_s = \frac{n_{0s}}{v_{th,s}^3} \exp\left[-\beta_s H_s - \frac{\beta_s a_s}{m_s}(p_{xs}^2 + p_{ys}^2)\right], \tag{2.3}$$

where it should be noted that the scalar potential ϕ vanishes as a result of the quasineutrality condition. The distribution function (2.3) gives rise to a pressure of the form

$$P_{zz} = P_0 \exp[-r(A_x^2 + A_y^2)], \tag{2.4}$$

where P_0 and r are constants (note that r must be negative so that the pressure P_{zz} given by Equation (2.4) represents an attractive central potential). Using Equations (1.79) and (1.80) gives Ampère's law (Equations (1.83) and (1.84)) as

$$\frac{d^2 A_x}{dz^2} = 2\mu_0 P_0 r A_x \exp[-r(A_x^2 + A_y^2)], \tag{2.5}$$

$$\frac{d^2 A_y}{dz^2} = 2\mu_0 P_0 r A_y \exp[-r(A_x^2 + A_y^2)], \tag{2.6}$$

which has solutions of the form

$$A_x = k \sin \alpha z, \tag{2.7}$$
$$A_y = k \cos \alpha z, \tag{2.8}$$

and so, using Equations (1.64) and (1.65), the magnetic field profile is given by

$$B_x = k\alpha \sin \alpha z, \tag{2.9}$$
$$B_y = k\alpha \cos \alpha z. \tag{2.10}$$

It is clear that $B_x^2 + B_y^2 = k^2 \alpha^2 = $ constant, and so the field is a linear force-free field. This can also be seen by looking at the current density, which has the form

$$j_x = -2P_0 r A_x \exp[-r(A_x^2 + A_y^2)], \tag{2.11}$$
$$j_y = -2P_0 r A_y \exp[-r(A_x^2 + A_y^2)], \tag{2.12}$$

which can be written as $\mathbf{j} = \alpha \mathbf{B}$, where

$$\alpha = \sqrt{(-2rP_0)} \exp\left(\frac{-rk^2}{2}\right), \tag{2.13}$$

which is constant with respect to z, as is required for a linear force-free field. Note that the square root in Equation (2.13) gives a real number, since $r < 0$. Figure 2.1 (from Harrison, 2009) shows a surface plot of the pressure (2.4) in the A_x-A_y-plane, with the solutions (2.7) and (2.8) plotted as a trajectory at the top. This figure reveals that the solution for $\mathbf{A}$ is clearly a contour of the potential, which illustrates the fact that this must be true for a linear force-free solution.

Another example of a distribution function that gives rise to the linear force-free magnetic field components (2.9) and (2.10) has been given by Channell (1976) and Attico and Pegoraro (1999) as

$$f_s(H_s, p_{xs}, p_{ys}) = \exp(-\beta_s H_s)(F_{0s} + F_{1s}(p_{xs}^2 + p_{ys}^2)), \tag{2.14}$$

where F_{0s} and F_{1s} are constants. This distribution function results from a P_{zz} of the form

$$P_{zz} = P_{00} + \frac{1}{2}P_{01}(A_x^2 + A_y^2), \tag{2.15}$$

where P_{00} and P_{01} are positive constants. Ampère's law consists of the following two decoupled
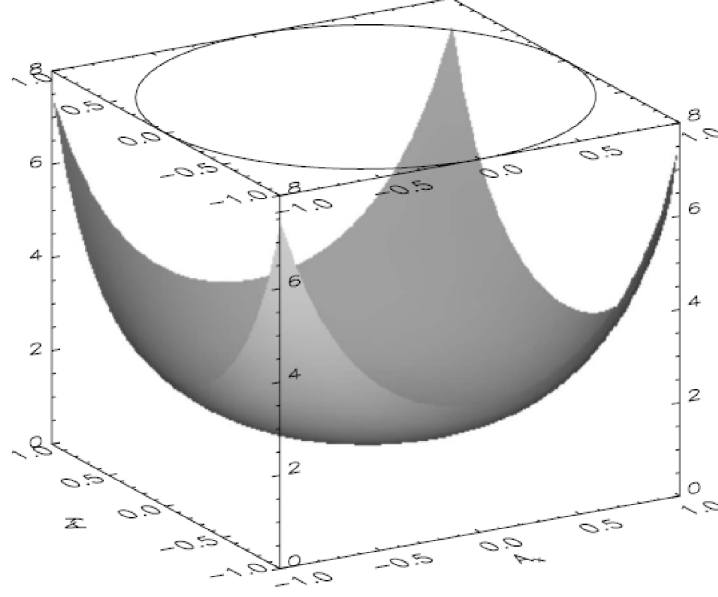
Figure 2.1: Surface plot of P_{zz} over the A_x-A_y-plane for the linear force-free solution described by Sestero (1967); Bobrova and Syrovatskiǐ (1979); Bobrova et al. (2001). The solutions (2.7) and (2.8) are plotted as a trajectory at the top of the plot, showing that **A** is a contour of the pressure (from Harrison, 2009).

second order ODEs,

$$-\frac{d^2 A_x}{dz^2} = P_{01} A_x, \tag{2.16}$$

$$-\frac{d^2 A_y}{dz^2} = P_{01} A_y, \tag{2.17}$$

which can be solved to give the components of the vector potential as

$$A_x = A_{x0} \sin(\sqrt{P_{01}} z + \delta_x), \tag{2.18}$$

$$A_y = A_{y0} \sin(\sqrt{P_{01}} z + \delta_y). \tag{2.19}$$

As noted by Harrison and Neukirch (2009a), choosing $A_{x0} = A_{y0} = k$, $\delta_x = 0$, $\delta_y = \pi/2$ and $\sqrt{P_{01}} = \alpha$ gives the solutions (2.7) and (2.8).

It has also been shown by Harrison and Neukirch (2009a) that all distribution functions of the form

$$f_s = f_s(H_s, p_s^2), \tag{2.20}$$

where $p_s^2 = p_{xs}^2 + p_{ys}^2$, give rise to a P_{zz} which corresponds to a central potential. Therefore, all distribution functions of this form which give rise to an attractive central potential will give rise to

the linear force-free field components (2.9) and (2.10).

For nonlinear force-free solutions, the potential cannot be an attractive central potential, but must still have a contour which is also a particle trajectory (Harrison and Neukirch, 2009b). This will be discussed further in Section 2.4.

2.3   Channell's Method for Finding Force-Free Vlasov-Maxwell Equilibria

For a known distribution function, the zz-component of the pressure tensor, P_{zz}, can be calculated directly through the definition (1.82). Ampère's law in the form given by Equations (1.71) and (1.72) can then be used to determine the magnetic field profile. If the aim is to find a distribution function corresponding to a given magnetic field profile, however, then the problem must be solved in the inverse direction. This is a natural way to solve the problem for force-free fields, since the magnetic field is restricted by the condition $\mathbf{j} \times \mathbf{B} = 0$.

Such a method for finding force-free Vlasov-Maxwell equilibria has been suggested by Channell (1976). It is assumed, firstly, that the distribution functions have the form

$$f_s = \frac{n_{0s}}{(\sqrt{2\pi}v_{th,s})^3} \exp(-\beta_s H_s)g_s(p_{xs}, p_{ys}), \tag{2.21}$$

where g_s is an arbitrary function of the canonical momenta and $\beta_s = 1/(k_B T_s)$, with k_B equal to the Boltzmann constant. The pressure, P_{zz}, resulting from this arbitrary distribution function is given, using the definition (1.82), by

$$P_{zz} = \sum_s \frac{1}{\beta_s} \exp(-\beta_s q_s \phi) N_s(A_x, A_y), \tag{2.22}$$

where N_s is given by

$$N_s(A_x, A_y) = \frac{n_{0s}}{2\pi v_{th,s}^2} \int_{-\infty}^{\infty} \int_{-\infty}^{\infty} \exp\left[-\frac{\beta_s m_s}{2}(v_x^2 + v_y^2)\right] \\ \times g_s(p_{xs}, p_{ys})dv_x dv_y. \tag{2.23}$$

The quasineutrality condition means, to lowest order, that the charge density, $\sigma = -\partial P_{zz}/\partial \phi$, vanishes, which gives

$$\sigma(A_x, A_y, \phi) = \sum_s q_s \exp(-\beta_s q_s \phi) N_s(A_x, A_y) = 0, \tag{2.24}$$

Summing over particle species (ions and electrons) and solving for the quasineutral electric potential, ϕ_{qn}, then gives

$$\phi_{qn} = \frac{1}{e(\beta_e + \beta_i)} \ln\left(\frac{N_i}{N_e}\right). \tag{2.25}$$

It can be seen that setting $N_e = N_i = N$ gives $\phi_{qn} = 0$. This corresponds to strict charge neutrality, since setting $\phi = 0$ in Equation (2.22) means that N_s gives the number density of species s. In order to satisfy the condition of strict charge neutrality, certain conditions will have to be imposed on the various parameters in the distribution function, which can be determined once the full expression is known.

Substituting the quasineutral electric potential (2.25) into Equation (2.22) gives the quasineutral pressure, $P_{zz,qn}$, as

$$P_{zz,qn}(A_x, A_y) = \frac{\beta_e + \beta_i}{\beta_e \beta_i} N(A_x, A_y), \tag{2.26}$$

and Equation (2.23) can then be rewritten as

$$\frac{n_{0s}}{2\pi m_s^2 v_{th,s}^2} \int_{-\infty}^{\infty} \int_{-\infty}^{\infty} \exp\left[-\frac{\beta_s}{2m_s}[(p_{xs} - q_s A_x)^2 + (p_{ys} - q_s A_y)^2]\right]$$
$$\times g_s(p_{xs}, p_{ys})dp_{xs}dp_{ys} = \frac{\beta_e \beta_i}{\beta_e + \beta_i} P_{zz,qn}(A_x, A_y), \tag{2.27}$$

where the integration has been written over the canonical momenta instead of v_x and v_y. Equation (2.27) is a Fredholm integral equation of the first type (e.g. Moiseiwitsch, 1977), which must be solved for the function g_s. This integral equation has the kernel

$$K(p_{xs}, p_{ys}; q_s A_x, q_s A_y) \propto \exp\left(-\frac{\beta_s}{2m_s}\left[(p_{xs} - q_s A_x)^2 + (p_{ys} - q_s A_y)^2\right]\right), \tag{2.28}$$

which depends only on the difference of its arguments, and so the double integral in Equation (2.27) is of convolution type. Such an integral equation can be solved by using Fourier transforms, as suggested by Channell (1976). This is useful, as it allows the double integral to be dealt with without actually doing the integration directly.

Channell's method works for the Force-Free Harris sheet model (Harrison and Neukirch, 2009a; Neukirch, Wilson, and Harrison, 2009), but for other pressure profiles, resulting from seemingly simple nonlinear force-free magnetic fields, it does not work (see Section 2.6 for a further discussion of this point). In order for the method to work, the Fourier transform of P_{zz} must exist, and the inverse Fourier transform of the resulting function must also exist, from which the function g_s would then be obtained. The second of these conditions can be difficult to satisfy, since the Fourier transform introduces an exponential function with a positive quadratic argument (the in-

verse of the exponential term in the double integral of Equation (2.27)). It seems, therefore, that Channell's Fourier transform method will only work for a few specially selected magnetic field profiles. Channell does, however, discuss other examples for which the Fourier transform method does not work.

In the next section, a derivation of the Harrison and Neukirch distribution function for the force-free Harris sheet will be given (Harrison and Neukirch, 2009a; Neukirch, Wilson, and Harrison, 2009). Although Fourier transforms do work for this particular field profile, they will not be used in the derivation, since they are of limited applicability, as will be demonstrated further in Section 2.6.

2.4 Force-Free Harris Sheet - Harrison and Neukirch Equilibrium

The force-free Harris sheet equilibrium is straightforward in MHD, as demonstrated in Section 1.4.1.2. In Vlasov theory, however, finding distribution functions from the magnetic field profile is a non-trivial task. In the present section, a derivation will be given of the distribution function found by Harrison and Neukirch (Harrison and Neukirch, 2009b; Neukirch, Wilson, and Harrison, 2009).

The magnetic field of the force-free Harris sheet is given by

$$
\begin{align}
B_{x,ffhs} &= B_0 \tanh(z/L), \tag{2.29} \\
B_{y,ffhs} &= \frac{B_0}{\cosh(z/L)}, \tag{2.30}
\end{align}
$$

with $B_{z,ffhs} = 0$. Using Equations (1.64) and (1.65) gives the non-vanishing components of the vector potential as

$$
\begin{align}
A_{x,ffhs} &= 2B_0 L \tan^{-1}(e^{z/L}), \tag{2.31} \\
A_{y,ffhs} &= -B_0 L \ln \cosh(z/L). \tag{2.32}
\end{align}
$$

The non-vanishing components of the current density are given by

$$
\begin{align}
j_{x,ffhs} &= \frac{B_0}{\mu_0 L} \frac{\sinh(z/L)}{\cosh^2(z/L)}, \tag{2.33} \\
j_{y,ffhs} &= \frac{B_0}{\mu_0 L} \frac{1}{\cosh^2(z/L)}. \tag{2.34}
\end{align}
$$

As explained in Section 2.3, in order to calculate a distribution function, the pressure P_{zz} must

first be calculated from Ampère's law, which can be written in the form

$$\frac{d^2 A_x}{dz^2} = -\mu_0 \frac{\partial P_{zz}}{\partial A_x}, \tag{2.35}$$

$$\frac{d^2 A_y}{dz^2} = -\mu_0 \frac{\partial P_{zz}}{\partial A_y}. \tag{2.36}$$

To do this analytically for the force-free Harris sheet, Harrison and Neukirch (2009b) assumed that the pressure is a sum of two individual functions, one of A_x and one of A_y, given by

$$P_{zz,ffhs}(A_x, A_y) = P_1(A_x) + P_2(A_y). \tag{2.37}$$

Multiplying Equation (2.35) by dA_x/dz, rearranging, and using the fact that

$$\frac{\partial P_{zz}}{\partial A_x} = \frac{dP_1}{dA_x}, \tag{2.38}$$

gives

$$\frac{dA_x}{dz} \frac{d^2 A_x}{dz^2} + \mu_0 \frac{dA_x}{dz} \frac{dP_1}{dA_x} = 0, \tag{2.39}$$

so that

$$\frac{d}{dz}\left[\frac{1}{2}\left(\frac{dA_x}{dz}\right)^2 + \mu_0 P_1(A_x)\right] = 0, \tag{2.40}$$

which, finally, gives the condition

$$\left(\frac{dA_x}{dz}\right)^2 + 2\mu_0 P_1(A_x) = 2\mu_0 P_{01}, \tag{2.41}$$

where the quantity $\mu_0 P_{01}$ has been chosen as the constant of integration. A similar condition for the function $P_2(A_y)$ is given by

$$\left(\frac{dA_y}{dz}\right)^2 + 2\mu_0 P_2(A_y) = 2\mu_0 P_{02}, \tag{2.42}$$

which can be obtained by multiplying Equation (2.36) by dA_y/dz, and using the fact that

$$\frac{\partial P_{zz}}{\partial A_y} = \frac{dP_2}{dA_y}. \tag{2.43}$$

The function $P_1(A_x)$ can be calculated by firstly using the definition (2.31) of A_x in Equation

(2.41), which gives P_1 as

$$P_1(A_x) = P_{01} - \frac{B_0^2}{2\mu_0} \frac{1}{\cosh^2(z(A_x)/L)}, \tag{2.44}$$

where it has been stated explicitly that z depends on A_x (since A_x depends on z), and so P_1 is a function of A_x, which can also be written as

$$P_1(A_x) = P_{01} - \frac{B_0^2}{\mu_0} \frac{2}{[\exp(z/L) + \exp(-z/L)]^2}. \tag{2.45}$$

The definition (2.31) of A_x can then be rearranged to give

$$\exp\left(\frac{z}{L}\right) = \tan\left(\frac{A_x}{2B_0 L}\right), \tag{2.46}$$

which can be substituted into Equation (2.45) to give P_1, explicitly in terms of A_x, as

$$P_1(A_x) = P_{01} - \frac{B_0^2}{4\mu_0}\left(1 - \cos\left(\frac{2A_x}{B_0 L}\right)\right), \tag{2.47}$$

by using standard trigonometric identities.

The function $P_2(A_y)$ can be calculated by firstly using the definition (2.32) of A_y in Equation (2.42), which gives

$$P_2(A_y) = P_{02} - \frac{B_0^2}{2\mu_0}\left(1 - \frac{1}{\cosh^2(z(A_y)/L)}\right), \tag{2.48}$$

where this time an expression for z in terms of A_y is needed to give P_2 as a function of A_y. From the definition (2.32) of A_y, $\cosh(z/L) = \exp\left(-A_y/B_0 L\right)$, which gives P_2, explicitly in terms of A_y, as

$$P_2(A_y) = P_{02} - \frac{B_0^2}{2\mu_0}\left(1 - \exp\left(\frac{2A_y}{B_0 L}\right)\right), \tag{2.49}$$

which is clearly of the same form as $P_{zz,Harris}$, given by Equation (1.91) for the Harris sheet. This is of course true, since $B_{x,ffhs} = B_{x,Harris} = B_0 \tanh(z/L)$.

Finally, combining the functions $P_1(A_x)$ and $P_2(A_y)$ gives P_{zz} as

$$P_{zz}(A_x, A_y) = \frac{B_0^2}{2\mu_0}\left[\frac{1}{2}\cos\left(\frac{2A_x}{B_0 L}\right) + \exp\left(\frac{2A_y}{B_0 L}\right)\right] + P_b, \tag{2.50}$$

where

$$P_b = P_{01} + P_{02} - \frac{3B_0^2}{4\mu_0}, \tag{2.51}$$

is a constant background pressure. Note that a solution of Equations (2.35) and (2.36) in the form of (2.37) is unique up to a constant. Figure (2.2) shows a surface plot of P_{zz} over the A_x-A_y-plane, with the vector potential for the force-free Harris sheet shown as a trajectory at the top of the plot. This trajectory is identical to a contour of P_{zz}, as is required for a force-free equilibrium (Harrison and Neukirch, 2009a).
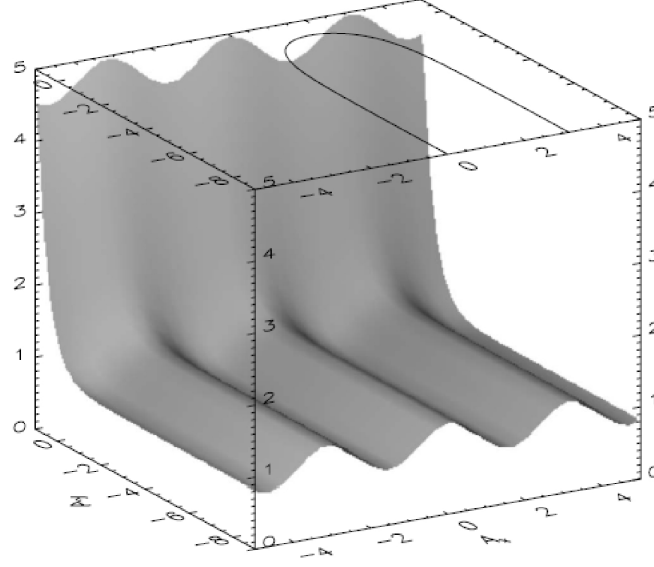

Figure 2.2: Surface plot of P_{zz} over the A_x-A_y-plane for the force-free Harris sheet. The vector potential of the force-free Harris sheet traces out a trajectory identical to a contour of P_{zz}, which is shown at the top of the plot.

Referring now to the method by Channell (1976) (see Section 2.3), the expression (2.50) for P_{zz} can now be substituted into the integral equation (2.27), to allow the unknown function g_s, and hence the distribution function, to be calculated. Since P_{zz} was assumed to be of the form (2.37), the function g_s must also be a sum of two separate functions, as follows

$$g_s(p_{xs}, p_{ys}) = g_{1s}(p_{xs}) + g_{2s}(p_{ys}), \tag{2.52}$$

and so the integral equation (2.27) can be split into the following two equations for $g_{1s}(p_{xs})$ and $g_{2s}(p_{ys})$,

$$n_{0s}\sqrt{\frac{\beta_s}{2\pi m_s}} \int_{-\infty}^{\infty} \exp\left[-\frac{\beta_s}{2m_s}(p_{xs} - q_s A_x)^2\right] g_{1s}(p_{xs})dp_{xs}$$
$$= \frac{\beta_e \beta_i}{\beta_e + \beta_i} P_1(A_x), \tag{2.53}$$
$$n_{0s}\sqrt{\frac{\beta_s}{2\pi m_s}} \int_{-\infty}^{\infty} \exp\left[-\frac{\beta_s}{2m_s}(p_{ys} - q_s A_y)^2\right] g_{2s}(p_{ys})dp_{ys}$$

$$= \frac{\beta_e \beta_i}{\beta_e + \beta_i} P_2(A_y). \tag{2.54}$$

It was stated in Section 1.4.2.1 that a distribution function for the Harris sheet model (Harris, 1962) is given by

$$f_{s,Harris} = \frac{n_{0s}}{(\sqrt{2\pi} v_{th,s})^3} \exp[-\beta_s(H_s - u_{ys} p_{ys})]. \tag{2.55}$$

Since the function $P_2(A_y)$ for the force-free Harris sheet is identical to $P_{zz,Harris}$, given by Equation (1.91), the function $g_{2s}(p_{ys})$ in Equation (2.54) must be proportional to $\exp(\beta_s u_{ys} p_{ys})$, and so the part of the force-free Harris sheet distribution function depending on p_{ys} is identical to the Harris sheet distribution function (2.55).

The function $g_{1s}(p_{xs})$ can be found from Equation (2.53) by using Fourier transforms, but it can also be solved in a more straightforward way, by firstly rewriting Equation (2.53) as an integral over v_x instead of p_{xs}, to give

$$\frac{n_{0s}}{\sqrt{2\pi} v_{th,s}} \int_{-\infty}^{\infty} \exp\left(-\frac{\beta_s m_s}{2} v_x^2\right) g_{1s}(p_{xs}) dv_x = \frac{\beta_e \beta_i}{\beta_e + \beta_i} \tag{2.56}$$
$$\times \left[P_{01} - \frac{B_0^2}{4\mu_0} \left(1 - \cos\left(\frac{2A_x}{B_0 L}\right) \right) \right],$$

and then by using the the integral (e.g. Gradshteyn and Ryzhik, 1966)

$$\int_{-\infty}^{\infty} \exp(-ax^2) \cos[b(x+c)] dx = \sqrt{\frac{\pi}{a}} \exp\left(-\frac{b^2}{4a}\right) \cos bc. \tag{2.57}$$

It is clear that a $P_1(A_x) \propto \cos(\beta_s u_{xs} q_s A_x)$ arises from a function

$$g_{1s} \propto \cos(\beta_s u_{xs} p_{xs}) = \cos(\beta_s u_{xs}(m_s v_x + q_s A_x)), \tag{2.58}$$

where the parameter u_{xs} must have the dimension of a velocity to ensure that the argument of the cosine function is dimensionless. Note, also, that the functions $P_1(A_x)$ and $P_2(A_y)$ contain constants, which will simply give rise to a constant part of g_s, and hence a Gaussian part of the distribution function.

Putting everything together, the Harrison and Neukirch distribution function for the force-free Harris sheet is given by

$$f_s = \frac{n_{0s}}{(\sqrt{2\pi} v_{th,s})^3} \exp(-\beta_s H_s) \left[\exp(\beta_s u_{ys} p_{ys}) + a_s \cos(\beta_s u_{xs} p_{xs}) + b_s \right], \tag{2.59}$$

where a_s, b_s, u_{xs}, u_{ys}, n_{0s} and β_s are constant parameters. Note that it is assumed that $b_s >$

$|a_s| \geq 0$, to ensure that $f_s \geq 0$. The assumption of strict charge neutrality (Channell, 1976) leads to conditions on the parameters of the distribution function. These can be obtained by calculating P_{zz} from the distribution function (2.59), which has the form given in Equation (2.22), with the number density $N_s(A_x, A_y)$ given by

$$
\begin{aligned}
N_s(A_x, A_y) = {} & n_{0s} \exp\left(\frac{\beta_s m_s}{2} u_{ys}^2\right) \\
& \times \left[a_s \exp\left(-\frac{\beta_s m_s}{2}(u_{xs}^2 + u_{ys}^2)\right) \cos(\beta_s u_{xs} q_s A_x) \right. \\
& \left. + \exp(\beta_s u_{ys} q_s A_y) + b_s \exp\left(-\frac{\beta_s m_s}{2} u_{ys}^2\right) \right].
\end{aligned}
\tag{2.60}
$$

The strict neutrality assumption, $N_e(A_x, A_y) = N_i(A_x, A_y)$, then gives

$$
n_{0e} \exp\left(\frac{\beta_e m_e}{2} u_{ye}^2\right) = n_{0i} \exp\left(\frac{\beta_i m_i}{2} u_{yi}^2\right) = n_0,
\tag{2.61}
$$

$$
a_e \exp\left[-\frac{\beta_e m_e}{2}(u_{xe}^2 + u_{ye}^2)\right] = a_i \exp\left[-\frac{\beta_i m_i}{2}(u_{xi}^2 + u_{yi}^2)\right] = a,
\tag{2.62}
$$

$$
b_e \exp\left(-\frac{\beta_e m_e}{2} u_{ye}^2\right) = b_i \exp\left(-\frac{\beta_i m_i}{2} u_{yi}^2\right) = b,
\tag{2.63}
$$

$$
\beta_e |u_{xe}| = \beta_i |u_{xi}|,
\tag{2.64}
$$

$$
-\beta_e u_{ye} = \beta_i u_{yi}.
\tag{2.65}
$$

The relation (2.64) has been obtained by noting that $\cos(\beta_s u_{xs} q_s A_x)$ must be equal for ions and electrons, and so the moduli of the arguments must be equal (since cosine is an even function). The relation (2.65) has been obtained by noting that $\exp(\beta_s u_{ys} q_s A_y)$ must be equal for both species, and so the arguments of the exponentials must be equal. The other three relations ((2.61)-(2.63)) have been obtained by equating the respective parts of N_s for both species.

Using the relations (2.61)-(2.65) gives the general expression for $P_{zz,ffhs}$ as

$$
P_{zz,ffhs}(A_x, A_y) = \frac{\beta_e + \beta_i}{\beta_e \beta_i} n_0 [a \cos(e\beta_e u_{xe} A_x) + \exp(-e\beta_e u_{ye} A_y) + b],
\tag{2.66}
$$

where only the electron parameters have been used.

The microscopic parameters β_s, u_{xs}, u_{ys}, a_s and b_s of the distribution function can be related to the macroscopic parameters B_0 and L of the equilibrium by comparing Equation (2.66) with Equation (2.50), which gives

$$
\frac{B_0^2}{2\mu_0} = \frac{\beta_e + \beta_i}{\beta_e \beta_i} n_0,
\tag{2.67}
$$

$$
\frac{1}{2} = a,
\tag{2.68}
$$

$$P_b = \frac{\beta_e + \beta_i}{\beta_e \beta_i} n_0 b, \tag{2.69}$$

$$\frac{2}{|B_0|L} = e\beta_e |u_{xe}| = e\beta_i |u_{xi}|, \tag{2.70}$$

$$\frac{2}{B_0 L} = -e\beta_e u_{ye} = e\beta_i u_{yi}, \tag{2.71}$$

where it is assumed that $L > 0$, but B_0 is allowed to be positive or negative. Note that condition (2.68) means that $b_s > 1/2$, to ensure that the distribution function is always positive. Using Equations (2.70) and (2.71) gives the following relation between u_{xs} and u_{ys},

$$|u_{xs}| = |u_{ys}|. \tag{2.72}$$

Note that, in the work throughout this thesis, it will be assumed that $u_{xs} = u_{ys}$. Equations (2.67) and (2.71) can be used to derive an expression for the macroscopic length scale L, in terms of the microscopic parameters. This is given by

$$L = \left[\frac{2(\beta_e + \beta_i)}{\mu_0 e^2 \beta_e \beta_i n_0 (u_{yi} - u_{ye})^2} \right]^{1/2}, \tag{2.73}$$

which is symmetric in the electron and ion parameters. It is also possible, if required, to calculate expressions for L using only electron or ion parameters. An expression for the number density $N(A_x, A_y)$, which is symmetric in electron and ion parameters, can be obtained by using Equations (2.61)-(2.63), (2.67) and (2.71), and is given by

$$N(A_x, A_y) = n_0 \left[a \cos\left(\frac{2A_x}{A_0} \right) + \exp\left(\frac{2A_y}{A_0} \right) + b \right], \tag{2.74}$$

where

$$A_0 = \frac{2(\beta_e + \beta_i)}{e\beta_e \beta_i |u_{yi} - u_{ye}|}. \tag{2.75}$$

An expression for $P_{zz,ffhs}$, which is also symmetric in electron and ion parameters, is given by substituting Equation (2.74) into Equation (2.26) to give

$$P_{zz} = n_0 \frac{\beta_e + \beta_i}{\beta_e \beta_i} \left[a \cos\left(\frac{2A_x}{A_0} \right) + \exp\left(\frac{2A_y}{A_0} \right) + b \right]. \tag{2.76}$$

The density, n_s, of species s, and the components of the bulk flow velocity $\langle \mathbf{v}_s \rangle$, can be calculated from the distribution function (2.59) through the definitions (1.7) and (1.8), and are given by

$$n_s = n_0 \left(\frac{1}{2} + b \right), \tag{2.77}$$

$$\langle v_{xs}\rangle \;\; = \;\; \frac{u_{ys}}{(\frac{1}{2}+b)}\frac{\sinh(z/L)}{\cosh^2(z/L)}, \tag{2.78}$$

$$\langle v_{ys}\rangle \;\; = \;\; \frac{u_{ys}}{(\frac{1}{2}+b)}\frac{1}{\cosh^2(z/L)}, \tag{2.79}$$

where the identities

$$\cos[4\tan^{-1}(e^{z/L})] \;\; = \;\; 1 - \frac{2}{\cosh^2(z/L)}, \tag{2.80}$$

$$\sin[4\tan^{-1}(e^{z/L})] \;\; = \;\; -2\frac{\sinh(z/L)}{\cosh^2(z/L)}, \tag{2.81}$$

have been used (see Appendix A), together with Equation (2.61). The x- and y-components of the current density can then be calculated by using Equation (1.11), and are given by

$$j_x \;\; = \;\; en_0(u_{yi}-u_{ye})\frac{\sinh(z/L)}{\cosh^2(z/L)}, \tag{2.82}$$

$$j_y \;\; = \;\; en_0(u_{yi}-u_{ye})\frac{1}{\cosh^2(z/L)}. \tag{2.83}$$

It is straightforward to show, by using the conditions (2.67) and (2.73), that these expressions for the current density components are equivalent to the expressions (2.33) and (2.34), which were obtained from the magnetic field.

The force-free parameter $\alpha(z)$, given by Equation (1.58), can also be expressed in terms of the microscopic parameters, by using Equation (2.73), which gives,

$$\alpha(z) \;\; = \;\; \left(\frac{\mu_0 e^2\beta_e\beta_i n_0(u_{yi}-u_{ye})^2}{2(\beta_e+\beta_i)}\right)^{1/2}$$
$$\times \left(\cosh\left[\left(\frac{\mu_0 e^2\beta_e\beta_i n_0(u_{yi}-u_{ye})^2}{2(\beta_e+\beta_i)}\right)^{1/2}z\right]\right)^{-1}. \tag{2.84}$$

2.5 Properties of the Harrison and Neukirch Equilibrium

The distribution function (2.59) can be written explicitly in terms of the velocity components as

$$f_s \;\; = \;\; \frac{1}{2}\frac{n_{0s}}{(\sqrt{2\pi}v_{th,s})^3}\exp\left(\beta_s m_s u_{xs}^2 - \frac{\beta_s m_s}{2}(v_x^2+v_y^2+v_z^2)\right)$$
$$\times \left[\frac{2}{C(z)}\exp(\beta_s m_s u_{xs}(v_y-u_{xs})) + \cos(\beta_s m_s u_{xs}v_x + T(z)) + \bar{b}_s\right], \tag{2.85}$$

where

$$C(z) \;\; = \;\; \cosh^2(z/L), \tag{2.86}$$

$$T(z) = 4\tan^{-1}(e^{z/L}), \tag{2.87}$$

$$\bar{b}_s = 2b\exp\left(-\frac{\beta_s m_s}{2}u_{xs}^2\right). \tag{2.88}$$

Due to the cosine dependence on v_x, it is suspected that this distribution function will exhibit more interesting properties than that of the Harris sheet (Harris, 1962), which is a drifting Maxwellian. The cosine term arises from the introduction of the shear field component B_y, which makes the field force-free. Plots of the distribution function in the v_x- and v_y-directions show that there are regions of parameter space in which the distribution function is multi-peaked. This will be discussed in more detail in Sections 2.5.1 and 2.5.2. The multi-peaked behaviour of the distribution function is important to investigate, because it may give rise to microinstabilities, which may then have an overall effect on the macroscopic stability of the plasma. In the present section, it will be shown that conditions on the parameters exist, which show when the distribution function can be single or multi-peaked.

2.5.1 The v_x-Direction

Figure (2.3) shows the distribution function (2.59) plotted in the v_x-direction, for the parameter values $u_{ys} = v_{th,s}$, $b_s = 2.85$, $L = 1$ and $v_y = v_z = 0$. In this case, the distribution function has a single maximum regardless of the value of z/L. Heuristically, this can be explained by the fact that, for the set of parameters used, the exponential parts of the distribution function must dominate over the cosine part, which means that there are no oscillations. It can also be seen that on going from $z = 0$ to $z = 2$, the peak of the distribution function has shifted slightly to the right, and then on increasing z it returns to the centre of the sheet. This behaviour is due to the fact that the x-component of the current density, given in Equation (1.54) and plotted in Figure 1.5, has a maximum value at $z/L \approx 1$. For values of z/L around this value, there are more particles moving with a higher drift speed, and so the maximum of the distribution function shifts to the right.

Figure (2.4) shows a case where there are two maxima in the v_x-direction close to $z = 0$ (the centre of the sheet), but a single maximum as z is increased. The parameter values used are $u_{ys} = v_{th,s}$, $b_s = 1.43$, $L = 1$ and $v_y = v_z = 0$. The behaviour at the centre of the sheet can be explained by the fact that the cosine term is more prominent for this value of z, then as z is increased, the exponential parts of the distribution function begin to dominate and so the oscillation is smoothed out.

Figure (2.5) shows a case where there are several maxima in the v_x-direction for a wider range of values of z, for the parameter values $u_{ys} = 2v_{th,s}$, $b_s = 28.66$, $L = 1$ and $v_y = v_z = 0$. The multiple maxima in the v_x-direction arise because, for these parameter values, the cosine part of the distribution function dominates over the other parts, giving rise to large oscillations.
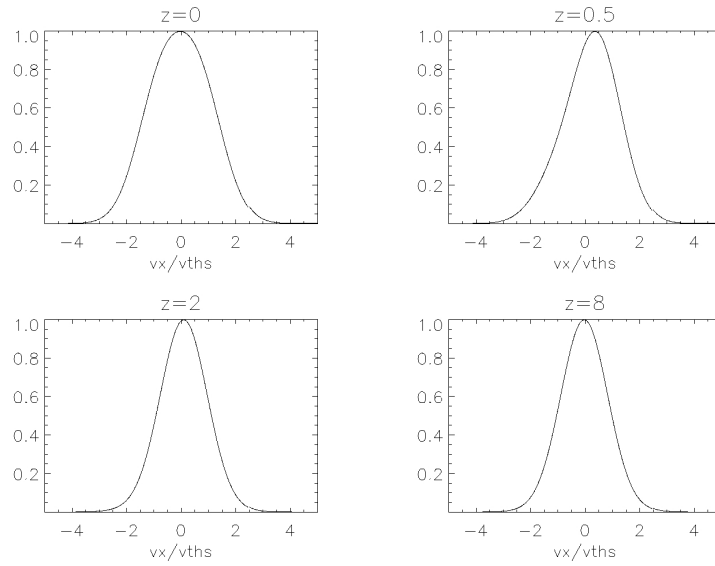
Figure 2.3: Plots of the distribution function (2.59) in the v_x-direction for $u_{ys} = v_{th,s}$, $b_s = 2.85$, $L = 1$ and $v_y = v_z = 0$ for various values of z. This shows a case where the distribution function has a single maximum for all values of z.
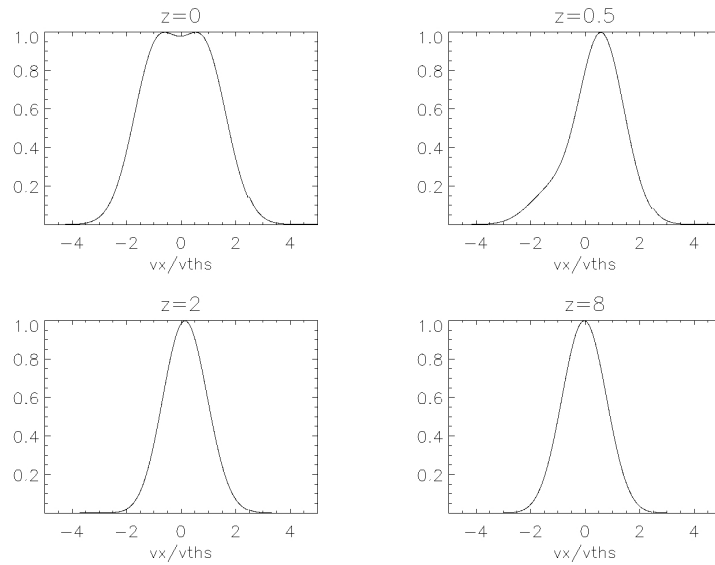

Figure 2.4: Plots of the distribution function (2.59) in the v_x-direction for $u_{ys} = v_{th,s}$, $b_s = 1.43$, $L = 1$ and $v_y = v_z = 0$, for various values of z. This shows a case where the distribution function has two maxima close to the centre of the sheet, but only one maximum as z is increased.
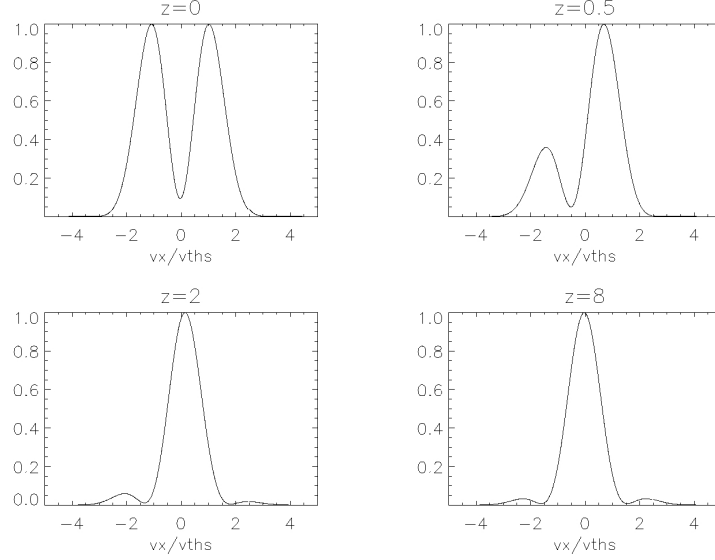
Figure 2.5: Plots of the distribution function (2.59) in the v_x-direction for $u_{ys} = 2v_{th,s}$, $b_s = 28.66$, $L = 1$ and $v_y = v_z = 0$, for various values of z. This shows a case where there is more than one maximum for a wider range of z values than in Figure (2.4).

It can be shown that a necessary and sufficient condition for having only one maximum in the v_x-direction is

$$b_s > \frac{1}{2}\left(\frac{u_{ys}^2}{v_{th,s}^2} + 1\right)\exp\left(\frac{u_{ys}^2}{v_{th,s}^2}\right), \tag{2.89}$$

although it should be noted that violating this condition does not guarantee more than one maximum. A further explanation of this point, together with a proof of the condition (2.89), will be given in the remainder of the present section.

The distribution function (2.59) can be written as a function of the canonical momenta in the x-, y- and z-directions, which gives

$$\begin{aligned}
f_s(p_{xs}, p_{ys}, p_{zs}, z) &= \frac{n_{0s}}{(\sqrt{2\pi}v_{th,s})^3}\exp\left(-\frac{\beta_s}{2m_s}\left[(p_{xs} - q_s A_x)^2 + (p_{ys} - q_s A_y)^2 + p_{zs}^2\right]\right)\\
&\times [a_s\cos(\beta_s u_{xs}p_{xs}) + \exp(\beta_s u_{ys}p_{ys}) + b_s].
\end{aligned} \tag{2.90}$$

The dependence on p_{zs} can be integrated out, since it will have no effect on the calculation. This then gives the reduced distribution function

$$\begin{aligned}
F_s(p_{xs}, p_{ys}, z) &= \frac{1}{m_s^3}\int_{-\infty}^{\infty} f_s(p_{xs}, p_{ys}, p_{zs})dp_{zs}\\
&= \frac{n_{0s}}{2\pi v_{th,s}^2 m_s^2}\exp\left(-\frac{\beta_s}{2m_s}[(p_{xs} - q_s A_x)^2 + (p_{ys} - q_s A_y)^2]\right)
\end{aligned}$$

$$\times [a_s \cos(\beta_s u_{xs} p_{xs}) + \exp(\beta_s u_{ys} p_{ys}) + b_s], \tag{2.91}$$

which can be written in terms of normalised quantities as

$$\begin{aligned}
\bar{F}_s(\bar{p}_{xs}, \bar{p}_{ys}, \bar{z}) &= \exp\left(-\frac{1}{2\bar{u}_{ys}^2}[(\bar{p}_{xs} - \bar{A}_x)^2 + (\bar{p}_{ys} - \bar{A}_y)^2]\right) \\
&\quad \times [a_s \cos(\bar{p}_{xs}) + \exp(\bar{p}_{ys}) + b_s],
\end{aligned} \tag{2.92}$$

where

$$\bar{F}_s = \frac{2\pi}{n_{0s}}(m_s v_{th,s})^2 F_s, \tag{2.93}$$

$$\bar{z} = \frac{z}{L}, \tag{2.94}$$

$$\bar{u}_{ys} = \frac{u_{ys}}{v_{th,s}}, \tag{2.95}$$

$$\bar{p}_{xs} = \beta_s u_{ys} p_{xs}, \tag{2.96}$$

$$\bar{p}_{ys} = \beta_s u_{ys} p_{ys}, \tag{2.97}$$

$$\bar{A}_x = q_s \beta_s u_{ys} A_x = \frac{2A_x}{B_0 L}, \tag{2.98}$$

$$\bar{A}_y = q_s \beta_s u_{ys} A_y = \frac{2A_y}{B_0 L}. \tag{2.99}$$

Note that in Equation (2.91) a factor of $1/m_s^3$ was added in front of the integral to keep the dimensions correct.

A maximum or minimum of $\bar{F}_s$ in the $\bar{p}_{xs}$-direction (analogous to the v_x-direction) occurs when the partial derivative

$$\begin{aligned}
\frac{\partial \bar{F}_s}{\partial \bar{p}_{xs}} &= -\exp\left(-\frac{1}{2\bar{u}_{ys}^2}[(\bar{p}_{xs} - \bar{A}_x)^2 + (\bar{p}_{ys} - \bar{A}_y)^2]\right) \\
&\quad \times \left(a_s \sin(\bar{p}_{xs}) + \frac{1}{\bar{u}_{ys}^2}(\bar{p}_{xs} - \bar{A}_x)\right. \\
&\quad \left. \times [a_s \cos(\bar{p}_{xs}) + \exp(\bar{p}_{ys}) + b_s]\right),
\end{aligned} \tag{2.100}$$

equals zero, which gives

$$\bar{p}_{xs} - \bar{A}_x = -\frac{a_s \bar{u}_{ys}^2 \sin(\bar{p}_{xs})}{a_s \cos(\bar{p}_{xs}) + \exp(\bar{p}_{ys}) + b_s}. \tag{2.101}$$

Equation (2.101) can be written as

$$\bar{p}_{xs} - \bar{A}_x = R(\bar{p}_{xs}), \tag{2.102}$$

where $R(\bar{p}_{xs})$ is a bounded periodic function of $\bar{p}_{xs}$, given by

$$R(\bar{p}_{xs}) = -\frac{C \sin \bar{p}_{xs}}{\cos(\bar{p}_{xs}) + D}, \tag{2.103}$$

with

$$C = \bar{u}_{ys}^2, \tag{2.104}$$
$$D = [b_s + \exp(\bar{p}_{ys})]/a_s. \tag{2.105}$$

Note that $C > 0$ and $D > 1$ since $b_s > a_s$. There will be multiple maxima of the distribution function when there is more than one value of $\bar{p}_{xs}$ which satisfies Equation (2.101). The function $\bar{A}_x(z)$ is given by $\bar{A}_x(z) = 4 \tan^{-1} e^{\bar{z}}$, which takes the range of values $0 < \bar{A}_x < 2\pi$, and so $R(\bar{p}_{xs})$ must cross the $\bar{p}_{xs}$ axis between $p_{xs} = 0$ and $p_{xs} = 2\pi$, as can be seen from Equation (2.102). The slope of $R(\bar{p}_{xs})$ is given by

$$\frac{dR}{d\bar{p}_{xs}} = -C \frac{D \cos(\bar{p}_{xs}) + 1}{(\cos(\bar{p}_{xs}) + D)^2}. \tag{2.106}$$

It can be seen from Equation (2.106) that the slope is positive if $\cos(\bar{p}_{xs}) < -1/D$. This is always true for some value of $\bar{p}_{xs}$ in the interval $0 \leq \bar{p}_{xs} \leq 2\pi$ (note, however, that it is not true for all of the values in this interval). The left hand side of Equation (2.101) is a linear function of $\bar{p}_{xs}$ with a slope of one and so, if $R(\bar{p}_{xs})$ is to intersect the function $\bar{p}_{xs} - \bar{A}_x$ more than once, then it must have a maximum slope which is greater than one. This is illustrated in Figure 2.6, which shows plots of $R(\bar{p}_{xs})$ (the solid lines) against $\bar{p}_{xs}$, with the straight line $\bar{p}_{xs} - \pi$ overplotted (the dashed lines). In the top left panel, the maximum slope of R is greater than one, giving three intersections, which corresponds to three solutions of Equation (2.101), and hence two maxima of the distribution function (plus a minimum). In the top right panel, the maximum slope of R is less than one, giving only one intersection, and hence this corresponds to a single maximum case. The bottom left panel shows the case when the maximum slope of R is equal to one. This is where the transition occurs between having one and two maxima.

The required condition, therefore, for the distribution function to have multiple maxima in the $\bar{p}_{xs}$ (and hence v_x-) direction is

$$\left(\frac{dR}{d\bar{p}_{xs}} \right)_{max} > 1. \tag{2.107}$$

The values of $\bar{p}_{xs}$ which give a maximum or minimum slope of $R(\bar{p}_{xs})$ can be calculated by solving the equation

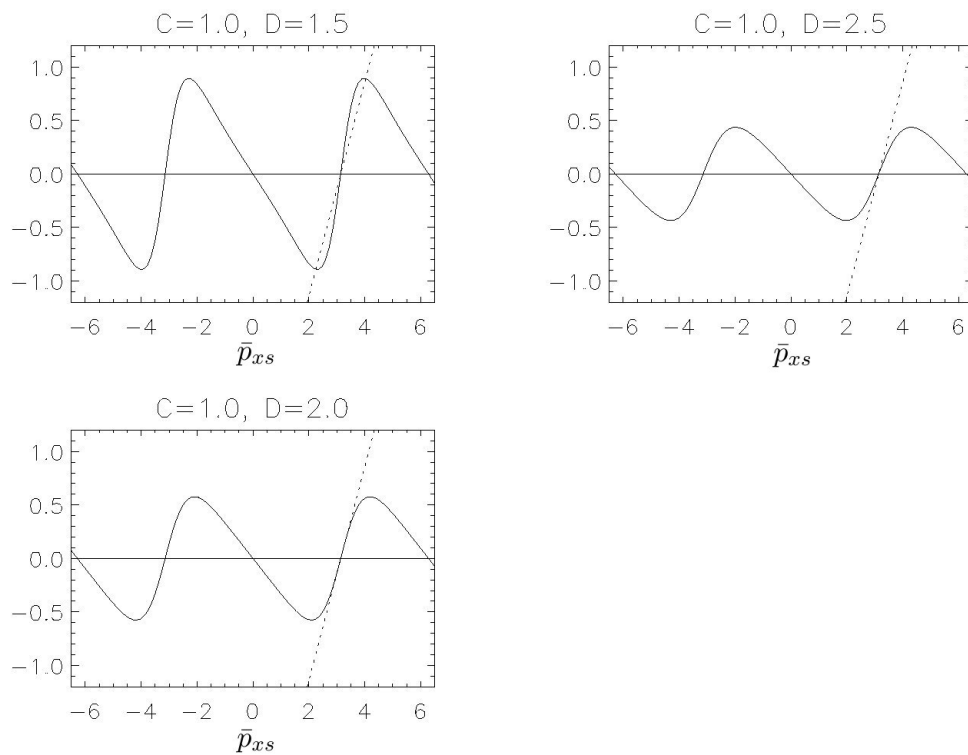$$\frac{d^2 R}{d\bar{p}_{xs}^2} = 0. \tag{2.108}$$

Figure 2.6: Plots of $R(\bar{p}_{xs})$ (solid line) and $\bar{p}_{xs}$ (dashed line) against $\bar{p}_{xs}$ for different parameter values. In the top left panel, the maximum slope of $R(\bar{p}_{xs})$ is greater than one, in the top right panel it is greater than one, and in the bottom left panel it is equal to one.

The second derivative of R is given by

$$\frac{d^2R}{d\bar{p}_{xs}^2} = C\sin(\bar{p}_{xs})\frac{D^2 - D\cos(\bar{p}_{xs}) - 2}{(D + \cos(\bar{p}_{xs}))^3},$$ (2.109)

and so Equation (2.108) has a solution when either $\bar{p}_{xs} = n\pi$ ($\sin(\bar{p}_{xs}) = 0$, $\cos(\bar{p}_{xs}) = (-1)^n$) or when $D^2 - D\cos(\bar{p}_{xs}) - 2 = 0$. For $\bar{p}_{xs} = n\pi$, the slope is given by

$$\left.\frac{dR}{d\bar{p}_{xs}}\right|_{\bar{p}_{xs}=n\pi} = -C\frac{D(-1)^n + 1}{((-1)^n + D)^2} = \begin{cases} -C/(1+D), & \text{for } n \text{ even} \\ C/(D-1), & \text{for } n \text{ odd} \end{cases},$$ (2.110)

which shows that $R(\bar{p}_{xs})$ has a positive slope when n is an odd integer (this is the maximum slope - even values of n give the minimum slope, which is negative). When $\cos(\bar{p}_{xs}) = (D^2 - 2)/D$ ($D^2 - D\cos(\bar{p}_{xs}) - 2 = 0$), the slope is given by

$$\left.\frac{dR}{d\bar{p}_{xs}}\right|_{\cos(\bar{p}_{xs})=(D^2-2)/D} = -\frac{CD^2}{4(D^2-1)},$$ (2.111)

which is always negative since $C > 0$ and $D > 1$, and so there is no need to consider these solutions, since they cannot give rise to a slope which is greater than one, and so cannot give rise to multiple maxima of the distribution function. From Equation (2.110), therefore, the condition (2.107) for having multiple maxima in the v_x- direction becomes

$$C > D - 1.$$ (2.112)

Substituting in the definitions (2.104) and (2.105) of C and D into the above condition gives

$$\bar{u}_{ys}^2 > \frac{b_s + \exp(\bar{p}_{ys})}{a_s} - 1$$ (2.113)

$$> \frac{b_s}{a_s} - 1,$$ (2.114)

where the second line follows since $\exp(\bar{p}_{ys}) \to 0$ as $\bar{p}_{ys} \to -\infty$. Finally, using Equations (2.62) and (2.68) for a_s in the above inequality, and writing $\bar{u}_{ys}$ in its dimensional form (see Equation (2.95)) gives the condition for the distribution function to have only one maximum in the v_x-direction as

$$b_s > \frac{1}{2}\exp\left(\frac{u_{ys}^2}{v_{th,s}^2}\right)\left(\frac{u_{ys}^2}{v_{th,s}^2} + 1\right),$$ (2.115)

where it is assumed, in line with the previous discussion, that $u_{xe} = u_{ye}$. Note that a violation of the condition (2.115) does not necessarily mean that there will be multiple maxima, as this depends also on the values of v_y and z through the condition (2.113). It simply means that there

will be at least one set of parameters for which the distribution function is multi-peaked.

The parameter b_s is present in the purely Gaussian part of the distribution function, and so it is clear that, if b_s is increased beyond a certain value, then the Gaussian part of the distribution function will dominate over the cosine dependent part, and so the distribution function can have only one maximum, as illustrated in Figure 2.3. As illustrated in Figure 2.4, a violation of this condition does not guarantee that there will be more than one maximum for all z and v_y, it only means that there is at least one combination of parameter values for which the distribution function is multi-peaked. Note that, as $u_{ys}/v_{th,s} \to 0$, $b_s \to 1/2$, which is consistent with the condition $b_s > 1/2$ mentioned previously in Section 2.4.

2.5.2   The v_y-Direction

The distribution function (2.85) can be written as

$$
\begin{aligned}
f_s &= \frac{1}{2}\frac{n_{0s}}{(\sqrt{2\pi}v_{th,s})^3}\exp(\beta_s m_s u_{xs}^2) \\
&\quad \times \left[\frac{2}{C(z)}\exp\left(-\frac{\beta_s m_s}{2}\left(v_x^2 + (v_y - u_{ys})^2 + v_z^2 + u_{ys}^2\right)\right) \right. \\
&\quad \left. + \exp\left(-\frac{\beta_s m_s}{2}\left(v_x^2 + v_y^2 + v_z^2\right)\right)\left(\cos(\beta_s m_s u_{xs}v_x + T(z)) + \bar{b}_s\right) \right],
\end{aligned}
\tag{2.116}
$$

where the assumption $u_{xs} = u_{ys}$ should again be noted. In the v_y-direction, this consists partly of a Maxwellian drifting with velocity u_{ys} (the Harris sheet part), and also of a part which is a Maxwellian at rest (if regarded purely as a function of v_y). It is intuitively clear that an increase in the drift velocity, u_{ys}, will lead to the drifting part and the non-drifting part becoming further and further apart, so that at some stage the distribution function will have two peaks in the v_y-direction. Changing the parameter b_s, however, also has an impact on the number of maxima. This is illustrated in Figures 2.7-2.9.

Figure 2.7 shows a case where there is a single maximum for all values of z, for the parameter values $u_{ys} = 3v_{th,s}$, $b_s = 4.659 \times 10^3$, $L = 1$ and $v_x = v_z = 0$. Note that, at $z = 0$, there is a slight wiggle in the distribution function, caused by the drifting Maxwellian part. This is, however, dominated by the non-drifting Maxwellian part, and so does not have an effect on the number of maxima, since it has not drifted very far from the centre of the sheet.

Figure 2.8 shows the point where a transition occurs between having a single maximum and having two maxima, for the parameter values $u_{ys} = 3v_{th,s}$, $b_s = 4.227 \times 10^3$, $L = 1$ and $v_x = v_z = 0$. Again, there is a wiggle at $z = 0$, which is more pronounced than before. This is because the drifting Maxwellian part of the distribution has become more predominant than in Figure 2.7, as
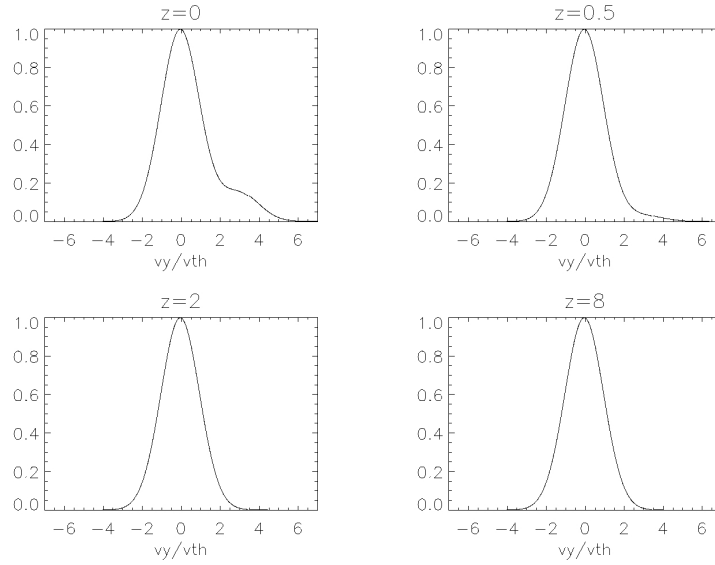
Figure 2.7: Plots of the distribution function (2.59) in the v_y-direction for $u_{ys} = 3v_{th,s}$, $b_s = 4.659 \times 10^3$, $L = 1$ and $v_x = v_z = 0$, for various values of z. This shows a case where the distribution function has one maximum for all values of z.

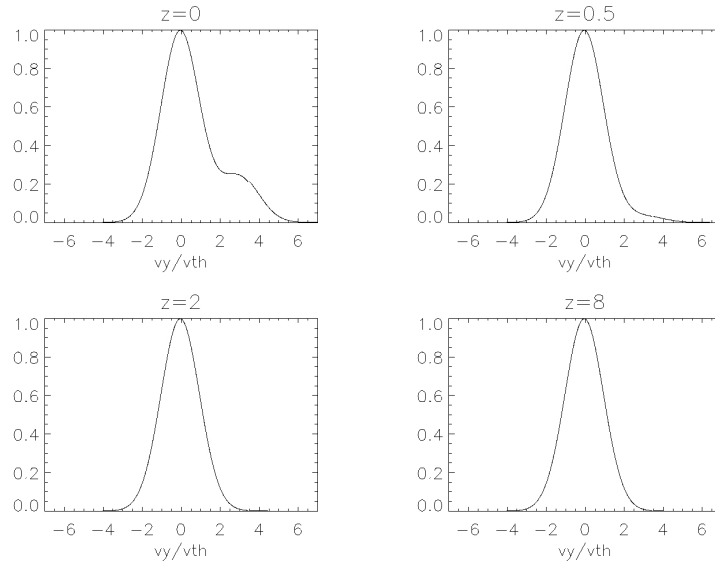it has moved further away from the non-drifting Maxwellian part.

Figure 2.8: Plots of the distribution function (2.59) in the v_y-direction for $u_{ys} = 3v_{th,s}$, $b_s = 4.227 \times 10^3$, $L = 1$ and $v_x = v_z = 0$, for various values of z. This shows a case where the transition between having one and two maxima occurs (at $z = 0$).

Figure 2.9 shows a case where there are two maxima at the centre of the sheet ($z = 0$), but just a single maximum as z is increased. The parameter values in this case are $u_{ys} = 3v_{th,s}$,

$b_s = 4.254 \times 10^3$, $L = 1$ and $v_x = v_z = 0$. At $z = 0$, the drifting Maxwellian part has now moved even further away from the non-drifting part, and so a second peak has developed.
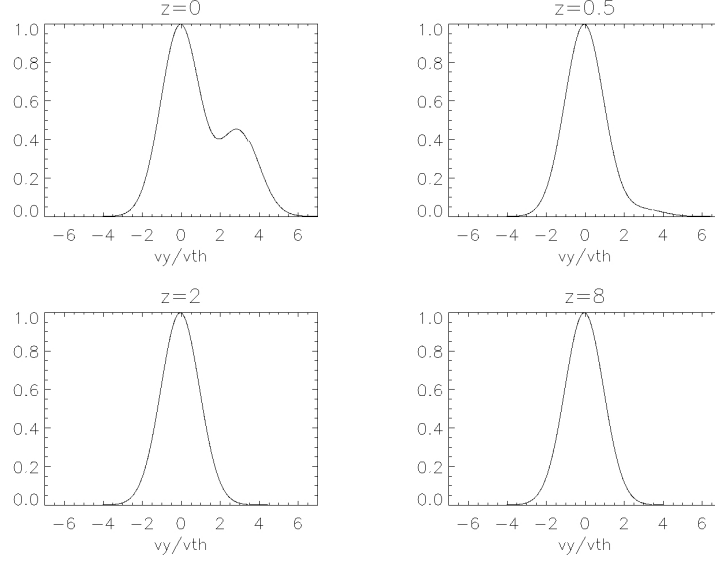

Figure 2.9: Plots of the distribution function (2.59) in the v_y-direction for $u_{ys} = 3v_{th,s}$, $b_s = 4.254 \times 10^3$, $L = 1$ and $v_x = v_z = 0$, for various values of z. This shows a case where the distribution function has two maxima for $z = 0$, but only one maximum for the other values of z shown.

Note that in each of the Figures 2.7-2.9, the interesting behaviour occurs only at $z = 0$. For larger values of z, there are no wiggles and the distribution function has only one maximum. The z-dependence comes from $p_{ys} = m_s v_y + q_s A_y(z)$, in the form of $1/\cosh^2(z)$, which multiplies the drifting Maxwellian part. This function has its maximum value at $z = 0$ and so the drifting Maxwellian part will be more predominant for $z = 0$. As z increases, the function $1/\cosh^2(z)$ decreases and so the drifting Maxwellian part becomes increasingly less important.

It can be shown that the distribution function (2.59) will be multi-peaked in the v_y-direction, for some value of z, if the following two conditions are satisfied,

$$|u_{ys}| \;>\; 2v_{th,s}, \tag{2.117}$$

$$
b_s \;<\; \frac{1}{2}\exp\left(\frac{u_{ys}^2}{v_{th,s}^2}\right) + \frac{1}{2v_{th,s}^2}(u_{ys}^2 - 2v_{th,s}^2 - |u_{ys}|\sqrt{u_{ys}^2 - 4v_{th,s}^2})
$$
$$
\times \exp\left(\frac{2u_{ys}^2}{u_{ys}^2 - |u_{ys}|\sqrt{u_{ys}^2 - 4v_{th,s}^2}}\right), \tag{2.118}
$$

The proofs of the above two conditions will be discussed in the remainder of the present section. They follow a very similar procedure to that discussed in the Section 2.5.1 for the v_x-direction.

A maximum or minimum of $\bar{F}_s$ (given by Equation (2.92)) in the $\bar{p}_{ys}$-direction (analogous to the v_y-direction) occurs when the partial derivative

$$
\begin{aligned}
\frac{\partial \bar{F}_s}{\partial \bar{p}_{ys}} = \ & \exp\left(-\frac{1}{2\bar{u}_{ys}^2}[(\bar{p}_{xs} - \bar{A}_x)^2 + (\bar{p}_{ys} - \bar{A}_y)^2]\right) \\
& \times \left(\exp(\bar{p}_{ys}) - \frac{1}{\bar{u}_{ys}^2}(\bar{p}_{ys} - \bar{A}_y) \right. \\
& \left. \times [a_s \cos(\bar{p}_{xs}) + \exp(\bar{p}_{ys}) + b_s]\right)
\end{aligned}
\tag{2.119}
$$

vanishes, which gives

$$
\bar{p}_{ys} - \bar{A}_y = \frac{\bar{u}_{ys}^2 \exp(\bar{p}_{ys})}{a_s \cos(\bar{p}_{xs}) + \exp(\bar{p}_{ys}) + b_s}.
\tag{2.120}
$$

Note that the right hand side of this expression contains no singularities, since $b_s > a_s \geq 0$. Equation (2.120) can be written as

$$
\bar{p}_{ys} - \bar{A}_y = S(\bar{p}_{ys}),
\tag{2.121}
$$

where $S(\bar{p}_{ys})$ is a positive monotonically increasing function given by,

$$
S(\bar{p}_{ys}) = \frac{A}{1 + B\exp(-\bar{p}_{ys})},
\tag{2.122}
$$

where.

$$
A = \bar{u}_{ys}^2 > 0,
\tag{2.123}
$$

$$
B = a_s \cos(\bar{p}_{xs}) + b_s > 0.
\tag{2.124}
$$

Note also that the function $S(\bar{p}_{ys})$ is bounded between 0 and A.

There will be more than one maximum of the distribution function when there is more than one value of $\bar{p}_{ys}$ which satisfies Equation (2.121). The function $\bar{A}_y(z)$ is given by $\bar{A}_y(z) = -2\ln\cosh(\bar{z})$, which takes the range of values $-\infty < \bar{A}_y \leq 0$, and so $S(\bar{p}_{ys})$ must cross the $\bar{p}_{ys}$ axis for some negative value of $\bar{p}_{ys}$ (or when $\bar{p}_{ys} = 0$). The slope of $S(\bar{p}_{ys})$ is given by

$$
\frac{dS}{d\bar{p}_{ys}} = \frac{AB\exp(-\bar{p}_{ys})}{(1 + B\exp(-\bar{p}_{ys}))^2},
\tag{2.125}
$$

which is of course always positive since $S(\bar{p}_{ys})$ is a monotonically increasing function. The left-hand side of Equation (2.121) is a linear function of $\bar{p}_{ys}$ with a slope of one, and so if the function $S(\bar{p}_{ys})$ is to intersect this linear function of $\bar{p}_{ys}$ more than once, then it must have a maximum slope

which is greater than one. This is illustrated in Figure 2.10, which shows plots of $S(\bar{p}_{ys})$ (solid line) against $\bar{p}_{ys}$ for different parameter values, together with a plot (dashed line) of the straight line of slope one which passes through the point $(\ln B, A/2)$, which is the point of maximum slope of $S(\bar{p}_{ys})$. The top left panel shows a case where the maximum slope of S is less than
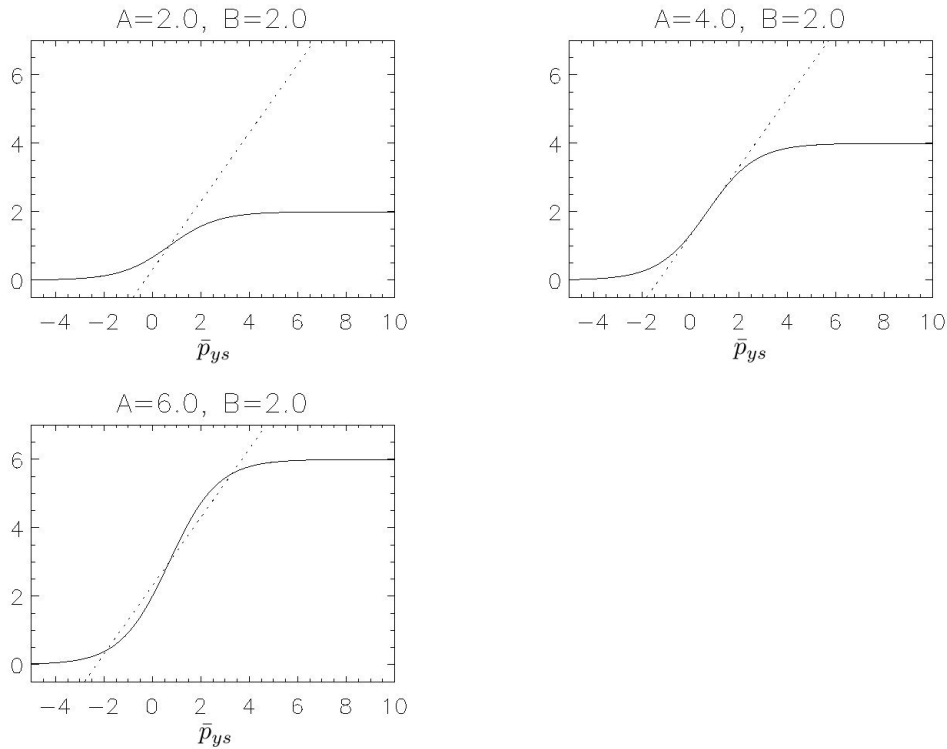

Figure 2.10: Plots of $S(\bar{p}_{ys})$ (solid line) against $\bar{p}_{ys}$ for different parameter values. Over plotted (dashed line) is the straight line $\bar{p}_{ys} - \bar{A}_y$ that passes through the point of maximum slope of $S(\bar{p}_{ys})$ (the point $(\ln B, A/2)$). In the top left panel, the maximum slope of $S(\bar{p}_{ys})$ is less than one, in the top right panel it is equal to one, and in the bottom left panel it is greater than one.

one, and there is one intersection, which corresponds to there being only one solution of Equation (2.121) and, hence, only one maximum of the distribution function. The top right panel shows the case where the maximum slope of S is equal to one. In this case, the straight line is tangent to the curve at the point of maximum slope. This is where the transition occurs between having one and two maxima of the distribution function. The bottom left panel shows a case where the maximum slope of S is greater then one, for which there are three intersections, corresponding to three solutions of Equation (2.121) and, hence, two maxima of the distribution function (plus a minimum).

A necessary condition, therefore, for having multiple maxima in the p_{ys}- (and hence v_y-) direction

is

$$\left(\frac{dS}{d\bar{p}_{ys}}\right)_{max} > 1. \tag{2.126}$$

Values of $\bar{p}_{ys}$ which give a maximum or minimum slope of S can be found by solving the equation

$$\frac{d^2S}{d\bar{p}_{ys}^2} = 0. \tag{2.127}$$

The second derivative of S is given by

$$\frac{d^2S}{d\bar{p}_{ys}^2} = -AB\exp(-\bar{p}_{ys})\left[\frac{1 - B\exp(-\bar{p}_{ys})}{(1 + B\exp(-\bar{p}_{ys}))^3}\right], \tag{2.128}$$

and so it is clear that Equation (2.127) has a solution when $\bar{p}_{ys} = \ln B$, from which the maximum slope is given through Equation (2.125) as $A/4$. This is clearly the maximum value of the slope, not the minimum, since the minimum slope is zero, which will occur in the limit $\bar{p}_{ys} \to \infty$ (this is also a solution of Equation (2.127)).

The necessary condition for the distribution function to have more than one maximum is then given by (using the definition (2.123) of A)

$$\frac{A}{4} > 1, \tag{2.129}$$

$$\Rightarrow \quad \frac{\bar{u}_{ys}^2}{4} > 1,$$

$$\Rightarrow \quad \frac{u_{ys}^2}{4v_{th,s}} > 1,$$

$$\Rightarrow \quad |u_{ys}| > 2v_{th,s}. \tag{2.130}$$

Although this is a necessary condition for having more than one maximum of the distribution function in the v_y-direction, it is not a sufficient condition, since even if it is satisfied, there is still the possibility that $S(\bar{p}_{ys})$ only intersects the linear function $\bar{p}_{ys} - \bar{A}_y$ once, which can happen if the value of B is sufficiently large. This is because the maximum slope of $S(\bar{p}_{ys})$ occurs at $\bar{p}_{ys} = \ln B$ and, as previously discussed, the function $\bar{p}_{ys} - \bar{A}_y$ is a straight line of gradient one which must cross the $\bar{p}_{ys}$ axis for $\bar{p}_{ys} \le 0$. Thus, if B is large enough, there will be only one intersection of the two functions. This is illustrated in Figure (2.11). In this figure, the maximum slope of S is greater than one, but the 'large' value of B ensures that there is only one intersection, which means that there will be only one maximum of the distribution function.

A second condition is therefore needed, which will guarantee that there are two intersections and, hence, two maxima of the distribution function in the v_y-direction, for some set of parameter
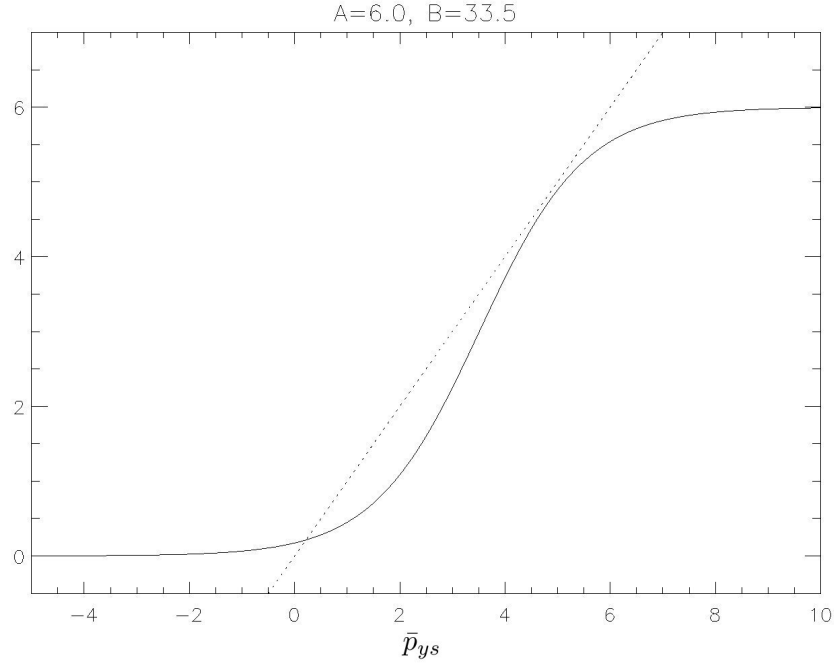
Figure 2.11: Plot of $S(\bar{p}_{ys})$ (solid line) and $\bar{p}_{ys} - \bar{A}_y$ (dashed line) against $\bar{p}_{ys}$, for a case where the maximum slope of $S(\bar{p}_{ys})$ is greater than one, but also where the value of B is sufficiently large so that only one intersection occurs. The straight line shown passes through the origin.

values. The transition between three intersections and only one intersection will occur when the straight line $\bar{p}_{ys} - \bar{A}_y$ passing through the origin ($\bar{A}_y = 0$) just touches the curve $S(\bar{p}_{ys})$ at the point where it has slope one (equal to the slope of the straight line). There are two values of $\bar{p}_{ys}$ for which $S(\bar{p}_{ys})$ has a slope of one. The larger root is the one to consider here, since this is where the transition will occur between one and two intersections (this can be seen more clearly from Figure (2.11)). The root can be calculated from Equation (2.125), and is given by

$$\bar{p}_{ys1} = \ln(2B) - \ln(A - 2 - \sqrt{A(A - 4)}). \tag{2.131}$$

A further requirement coming from this calculation is that $A > 4$ for $\bar{p}_{ys1}$ to be real. This is consistent with the necessary condition (2.129) for the distribution function to have more than one maximum.

The value of B for which the transition between three intersections and one intersection occurs, B_t, can be determined by solving the equation

$$\bar{p}_{ys1} = S(\bar{p}_{ys1}), \tag{2.132}$$

which gives

$$B_t = \frac{1}{2}(A - 2 - \sqrt{A(A-4)}) \exp\left(\frac{2A}{A - \sqrt{A(A-4)}}\right). \tag{2.133}$$

The second condition for there to be more than one intersection and, hence, more than one maximum of the distribution function in the v_y-direction is, therefore,

$$B < B_t, \tag{2.134}$$
$$\Rightarrow \quad a_s \cos(\bar{p}_{xs}) + b_s < B_t, \tag{2.135}$$
$$\Rightarrow \quad b_s - a_s < B_t, \tag{2.136}$$

where in the last step the cosine term has been replaced by the minimum value it can take. Finally, using the definitions (2.62) and (2.123) for a_s and A gives the condition as,

$$\begin{aligned}
b_s \quad < \quad & \frac{1}{2}\exp\left(\frac{u_{ys}^2}{v_{th,s}^2}\right) + \frac{1}{2v_{th,s}^2}(u_{ys}^2 - 2v_{th,s}^2 - |u_{ys}|\sqrt{u_{ys}^2 - 4v_{th,s}^2}) \\
& \times \exp\left(\frac{2u_{ys}^2}{u_{ys}^2 - |u_{ys}|\sqrt{u_{ys}^2 - 4v_{th,s}^2}}\right).
\end{aligned} \tag{2.137}$$

It has been shown, therefore, that the two conditions for having multiple peaks in the v_y-direction are

$$|u_{ys}| \quad > \quad 2v_{th,s}, \tag{2.138}$$
$$\begin{aligned}
b_s \quad < \quad & \frac{1}{2}\exp\left(\frac{u_{ys}^2}{v_{th,s}^2}\right) + \frac{1}{2v_{th,s}^2}(u_{ys}^2 - 2v_{th,s}^2 - |u_{ys}|\sqrt{u_{ys}^2 - 4v_{th,s}^2}) \\
& \times \exp\left(\frac{2u_{ys}^2}{u_{ys}^2 - |u_{ys}|\sqrt{u_{ys}^2 - 4v_{th,s}^2}}\right).
\end{aligned} \tag{2.139}$$

As previously stated, when this condition is satisfied together with the condition (2.130), then there will be more than one maximum in the v_y-direction for some value of z. The first condition (2.138) states that the drift velocity must be greater than twice the thermal velocity. The second condition (2.139) states that, if b_s is increased beyond a certain limiting value, then the part of $f_{s,vy}$ which is at rest will dominate over the drifting part, and so a second maximum cannot develop, even if condition (2.138) is satisfied. Note, however, that the upper limit on b_s grows exponentially with $u_{ys}^2/v_{th,s}^2$, and so the condition (2.139) is not very restrictive. In Figures (2.7) to (2.9), it can be seen that the transition between two maxima and one maximum occurs at very large values of b_s, which illustrates this fact. As in the v_x-direction, a violation of the conditions (2.138) and (2.139) does not mean that the distribution function will always have more than one maximum -

it only means that there is at least one set of parameter values which gives rise to more than one maximum.

Further insight can be gained into the physical meaning of the conditions discussed above by expressing the ratio $u_{ys}/v_{th,s}$ in terms of the current sheet thickness, L. This can be done by using Equation (2.71), and gives,

$$\frac{u_{ys}^2}{v_{th,s}^2} = 4\frac{r_{g,s}^2}{L^2},\tag{2.140}$$

where $r_{g,s} = m_s v_{th,s}/eB_0$ is the thermal gyroradius of species s. Fixing all the parameters except u_{ys} and L in the above expression, it can be seen that if the current sheet thickness is decreased beyond a certain point, then there will eventually be multiple maxima in the distribution function, firstly in the v_x-direction by violating condition (2.89), and then also in the v_y-direction.

2.6 Attempts to Find Vlasov-Maxwell Equilibria for other Force-Free Magnetic Field Profiles

In the present section, examples will be given of attempts to use the method of Harrison and Neukirch (2009b) to find equilibria for nonlinear force-free magnetic field profiles other than that of the force-free Harris sheet. The method can be broken down into the following steps:

1. An x-component of the magnetic field is chosen arbitrarily (although it makes sense to choose a function which is bounded).

2. The y-component of the magnetic field can then be calculated from the from the force free constraint $B_x^2 + B_y^2 = B_0^2$, where B_0 is a positive constant.

3. The x- and y-components of the vector potential **A** can then be calculated as functions of z ($A_x(z)$ and $A_y(z)$) by using Equations (1.64) and (1.65).

4. These expressions must then be inverted to give two expressions for z, one as a function of A_y, the other as a function of A_x ($z(A_x)$ and $z(A_y)$).

5. The zz-component of the pressure tensor, P_{zz}, can then be calculated by using Ampère's law (in the form of Equations (2.41) and (2.42)).

6. Assume that the distribution functions have the form given in Equation (2.21), and use the Fourier transform method suggested by Channell (1976) to find the unknown function $g_s(p_{xs}, p_{ys})$.

This method is, in theory, a systematic way of finding distribution functions analytically for given magnetic field profiles.

Consider, as a first example, the following magnetic field profile,

$$B_x = B_0 \frac{z}{L}, \tag{2.141}$$

$$B_y = \pm B_0 \sqrt{1 - \frac{z^2}{L^2}}, \tag{2.142}$$

where $z \leq L$. Note, however, that this is not a bounded magnetic field profile. The x- and y-components of the vector potential arising from this magnetic field are given by

$$A_x = \frac{B_0}{2} \left(z\sqrt{1 - \frac{z^2}{L^2}} + L\sin^{-1}\left(\frac{z}{L}\right) \right), \tag{2.143}$$

$$A_y = -\frac{B_0}{2L} z^2. \tag{2.144}$$

Clearly, there is no obvious way to invert the expression for $A_x(z)$ to obtain $z(A_x)$, and so for this simple magnetic field profile, it is not possible to calculate a pressure P_{zz} analytically by Channell's method.

As a second example, consider the magnetic field profile given by

$$B_x = -\frac{B_0}{L} \sqrt{z}, \tag{2.145}$$

$$B_y = \pm B_0 \sqrt{1 - \frac{z}{L^2}}, \tag{2.146}$$

where $0 \leq z \leq L^2$. This gives the components of the vector potential as

$$A_x = \frac{2}{3} B_0 L^2 \left(1 - \frac{z}{L^2}\right)^{3/2}, \tag{2.147}$$

$$A_y = \frac{2}{3} \frac{B_0}{L} z^{3/2}. \tag{2.148}$$

Inverting Equations (2.147) and (2.148) to express them as functions of z gives

$$z(A_x) = L^2 \left[1 - \left(\frac{3A_x}{2B_0 L^2}\right)^{2/3} \right], \tag{2.149}$$

$$z(A_y) = \left(\frac{3LA_y}{2B_0}\right)^{2/3}, \tag{2.150}$$

and P_{zz} is then given by

$$P_{zz}(A_x, A_y) = P_{03} - \frac{3^{\frac{2}{3}}}{2^{\frac{5}{3}} \mu_0} \left(\frac{B_0}{L}\right)^{\frac{4}{3}} \left(A_x^{\frac{2}{3}} + A_y^{\frac{2}{3}} \right). \tag{2.151}$$

In this case, it is the final step of the method which causes problems, as the Fourier transform cannot be carried out due to the fractional powers of A_x and A_y in Equation (2.151).

For the final example, consider the magnetic field profile

$$B_x = \frac{B_0 z}{\sqrt{z^2 + a^2}}, \tag{2.152}$$

$$B_y = \pm\frac{B_0 a}{\sqrt{z^2 + a^2}}, \tag{2.153}$$

where a is a constant. This gives the components of the vector potential as

$$A_x = B_0 a \sinh^{-1}\left(\frac{z}{a}\right), \tag{2.154}$$

$$A_y = -B_0 \sqrt{z^2 + a^2}. \tag{2.155}$$

Inverting Equations (2.154) and (2.155) to express them as functions of z gives

$$z(A_x) = a \sinh\left(\frac{A_x}{B_0 a}\right), \tag{2.156}$$

$$z(A_y) = \sqrt{\left(\frac{A_y}{B_0}\right)^2 - a^2}, \tag{2.157}$$

and P_{zz} is then given by

$$P_{zz}(A_x, A_y) = P_{03} - \frac{B_0^2}{2\mu_0}\left(\text{sech}^2\left(\frac{A_x}{B_0 a}\right) - \left(\frac{B_0 a}{A_y}\right)^2 + 1\right). \tag{2.158}$$

Once again, it is the Fourier transform step which causes problems, due to the negative power of A_y in Equation (2.158).

The examples discussed in the present section further illustrate that, even for apparently simple force-free magnetic field profiles, finding Vlasov-Maxwell equilibria analytically is a non-trivial task. Channell (1976) has discussed another method for finding distribution functions, as an alternative to the Fourier transform method. This method involves the use of Hermite polynomials, and could possibly be used to find other Vlasov-Maxwell equilibria analytically. This is beyond the scope of the work in this thesis, but would be interesting to investigate in future work.

2.7 Finding a Family of Distribution Functions for the Force-Free Harris Sheet

In the present section, a method will be discussed for calculating a family of distribution functions for the force-free Harris sheet, which includes the previously known solution (Harrison and Neukirch, 2009b). The method involves assuming a distribution function of the same form as that found by Harrison and Neukirch (2009b), but with a different dependence on the particle energy H_s. The idea of finding new distribution functions for a given magnetic field profile by changing the dependence on H_s has been used before, but only for cases depending on the particle energy and a single component of the canonical momentum. Fu and Hau (2005), for example, showed that kappa type distribution functions can be used for the Harris sheet magnetic field profile (Harris, 1962), as previously discussed in Section 1.4.2.1. More recently, Kocharovsky et al. (2010) discussed distribution functions with an arbitrary dependence on the particle energy and a fixed dependence on one component of the canonical momentum for the relativistic case. It must, however, be emphasized that, for finding force-free Vlasov-Maxwell equilibria, it is crucial that the distribution functions depend on two components of the canonical momentum, and that the magnetic field has more than one non-zero component (Sestero, 1967; Channell, 1976; Bobrova and Syrovatskiǐ, 1979; Bobrova et al., 2001; Harrison and Neukirch, 2009a,b; Neukirch et al., 2009).

Consider a distribution function of the general form

$$f_{s,g} = \frac{m_s^3}{q_s^4} f_0 h\left(\frac{m_s H_s}{q_s^2}\right) [a_s \cos(\beta_s u_{xs} p_{xs}) + \exp(\beta_s u_{ys} p_{ys}) + b_s], \tag{2.159}$$

where h is an arbitrary function of $(m_s H_s)/q_s^2$ and f_0 is a positive constant. Note that H_s must contain a multiplying factor in order to make the argument of the function h dimensionless. The distribution function (2.159) is of the same form as the distribution function found by Harrison and Neukirch (2009b), given by Equation (2.59), but it has a different dependence on the particle energy.

It will be shown that, when calculating velocity moments of distribution functions of the form

$$f_{s,g} = \frac{m_s^3}{q_s^4} F\left(\frac{m_s H_s}{q_s^2}, \frac{p_{xs}}{q_s}, \frac{p_{ys}}{q_s}\right), \tag{2.160}$$

it is possible to make the resulting integrals independent of the particle species s whenever $\phi = 0$, that is, whenever strict charge neutrality is assumed. This has been shown before for distribution functions depending only on energy and one component of the canonical momentum (Schmid-Burgk, 1965), and can be used to show that distribution functions of the form (2.159) are solutions

of the Vlasov-Maxwell equations for the force-free Harris sheet, provided certain conditions on the parameters are satisfied. Note that the assumption of strict charge neutrality, although restrictive, is made for calculational purposes. In reality, a plasma would likely be only quasineutral, satisfying the condition

$$\frac{n_e - n_i}{n_e + n_i} \ll 1. \tag{2.161}$$

The density, $n_{s,g}$, can be calculated from the distribution function (2.159) by using the definition

$$n_{s,g}(A_x, A_y, \phi) = \int f_{s,g} d^3 v \tag{2.162}$$

$$= \frac{1}{m_s^3} \int f_{s,g} d^3 p, \tag{2.163}$$

where $d^3 v = dv_x dv_y dv_z$ and $d^3 p = dp_{xs} dp_{ys} dp_{zs}$. This gives

$$
\begin{aligned}
n_{s,g}(A_x, A_y, \phi) &= \frac{f_0}{q_s^4} \int_{-\infty}^{\infty} \int_{-\infty}^{\infty} \int_{-\infty}^{\infty} h\left(\frac{m_s H_s}{q_s^2}\right) \\
&\quad \times [a_s \cos(\beta_s u_{xs} p_{xs}) + \exp(\beta_s u_{ys} p_{ys}) + b_s] dp_{xs} dp_{ys} dp_{zs} \tag{2.164} \\
&= \frac{2 f_0}{q_s^4} \int_{-\infty}^{\infty} \int_{-\infty}^{\infty} \int_0^{\infty} h\left(\frac{m_s H_s}{q_s^2}\right) \\
&\quad \times [a_s \cos(\beta_s u_{xs} p_{xs}) + \exp(\beta_s u_{ys} p_{ys}) + b_s] dp_{zs} dp_{xs} dp_{ys}, \tag{2.165}
\end{aligned}
$$

with the second line coming from the fact that the integrand is even in p_{zs}. Changing the p_{zs}-integration to an integration over H_s by using the following

$$H_s = \frac{1}{2m_s}[(p_{xs} - q_s A_x)^2 + (p_{ys} - q_s A_y)^2 + p_{zs}^2] + q_s \phi, \tag{2.166}$$

$$\frac{dp_{zs}}{dH_s} = m_s[2m_s(H_s - q_s \phi) - (p_{xs} - q_s A_x)^2 - (p_{ys} - q_s A_y)^2]^{-1/2}, \tag{2.167}$$

then gives

$$
\begin{aligned}
n_{s,g}(A_x, A_y, \phi) &= \frac{2 m_s f_0}{q_s^4} \int_{-\infty}^{\infty} \int_{-\infty}^{\infty} \int_{H_{min}}^{\infty} dH_s dp_{xs} dp_{ys} h\left(\frac{m_s H_s}{q_s^2}\right) \\
&\quad \times [a_s \cos(\beta_s u_{xs} p_{xs}) + \exp(\beta_s u_{ys} p_{ys}) + b_s] \\
&\quad \times [2m_s(H_s - q_s \phi) - (p_{xs} - q_s A_x)^2 - (p_{ys} - q_s A_y)^2]^{-1/2}, \tag{2.168}
\end{aligned}
$$

where

$$H_{min} = \frac{1}{2m_s}[(p_{xs} - q_s A_x)^2 + (p_{ys} - q_s A_y)^2] + q_s \phi. \tag{2.169}$$

Defining three new variables, E, P and Q as

$$E = \frac{m_s H_s}{q_s^2}, \tag{2.170}$$

$$P = \frac{p_{xs}}{q_s}, \tag{2.171}$$

$$Q = \frac{p_{ys}}{q_s}, \tag{2.172}$$

and using these as integration variables, gives

$$
\begin{aligned}
n_{s,g}(A_x, A_y, \phi) &= \frac{2f_0}{|q_s|} \int_{-\infty}^{\infty} \int_{-\infty}^{\infty} \int_{E_{min}}^{\infty} h(E)[a_s \cos(\beta_s u_{xs} q_s P) + \exp(\beta_s u_{ys} q_s Q) + b_s] \\
&\quad \times [2E - \frac{2m_s \phi}{q_s} - (P - A_x)^2 - (Q - A_y)^2]^{-1/2} dE\,dP\,dQ,
\end{aligned} \tag{2.173}
$$

where

$$E_{min} = \frac{1}{2}[(P - A_x)^2 + (Q - A_y)^2] + \frac{m_s \phi}{q_s}. \tag{2.174}$$

The zz-component of the pressure tensor, $P_{zz,g}$, can be written as

$$P_{zz,g}(A_x, A_y, \phi) = \sum_s \frac{1}{m_s^4} \int p_{zs}^2 f_{s,g} d^3 p, \tag{2.175}$$

and is given by, using the integration variables defined in Equations (2.170)-(2.172),

$$
\begin{aligned}
P_{zz,g}(A_x, A_y, \phi) &= 2f_0 \sum_s \frac{|q_s|}{m_s} \\
&\quad \times \int_{-\infty}^{\infty} \int_{-\infty}^{\infty} \int_{E_{min}}^{\infty} h(E)[a_s \cos(\beta_s u_{xs} q_s P) + \exp(\beta_s u_{ys} q_s Q) + b_s] \\
&\quad \times \left[2E - \frac{2m_s \phi}{q_s} - (P - A_x)^2 - (Q - A_y)^2\right]^{1/2} dE\,dP\,dQ.
\end{aligned} \tag{2.176}
$$

Note that, at this point, the dependence of $n_{s,g}$ and $P_{zz,g}$ on ϕ is still stated explicitly. It will later be assumed, however, that $\phi = 0$. The charge density, σ_g, can be calculated from $P_{zz,g}$ by using the definition in Equation (1.81), or from $n_{s,g}$ by using Equation (1.10), and is given by

$$
\begin{aligned}
\sigma_g(A_x, A_y, \phi) &= 2f_0 \sum_s \frac{|q_s|}{q_s} \\
&\quad \times \int_{-\infty}^{\infty} \int_{-\infty}^{\infty} \int_{E_{min}}^{\infty} h(E)[a_s \cos(\beta_s u_{xs} q_s P) + \exp(\beta_s u_{ys} q_s Q) + b_s] \\
&\quad \times \left[2E - \frac{2m_s \phi}{q_s} - (P - A_x)^2 - (Q - A_y)^2\right]^{-1/2} dE\,dP\,dQ.
\end{aligned} \tag{2.177}
$$

It can be seen that the terms inside the integration in Equation (2.177) will all be independent of s, that is they will not depend upon the particle species, if the following three conditions are satisfied,

$$\phi = 0, \tag{2.178}$$

$$e\beta_e|u_{xe}| = e\beta_i|u_{xi}| = \alpha, \tag{2.179}$$

$$-e\beta_e u_{ye} = e\beta_i u_{yi} = \gamma. \tag{2.180}$$

The above conditions are consistent with those discussed in Section 2.4. Due to the modulus signs in Equation (2.179), the parameter α is always positive, and so u_{xe} and u_{xi} from the distribution function (2.159) can be positive or negative, and can have the same or opposite sign from each other. The neutrality condition $\sigma = 0$ gives

$$\sum_s \text{sign}(q_s)(a_s I_1 + I_2 + b_s I_3) = 0, \tag{2.181}$$

where

$$I_1 = \int_{-\infty}^{\infty} \int_{-\infty}^{\infty} \int_{E_{min,0}}^{\infty} h(E)\cos(\alpha P)$$

$$\times \left[2E - (P - A_x)^2 - (Q - A_y)^2\right]^{-1/2} dE dP dQ, \tag{2.182}$$

$$I_2 = \int_{-\infty}^{\infty} \int_{-\infty}^{\infty} \int_{E_{min,0}}^{\infty} h(E)\exp(\gamma Q) \tag{2.183}$$

$$\times \left[2E - (P - A_x)^2 - (Q - A_y)^2\right]^{-1/2} dE dP dQ, \tag{2.184}$$

$$I_3 = \int_{-\infty}^{\infty} \int_{-\infty}^{\infty} \int_{E_{min,0}}^{\infty} h(E)$$

$$\times \left[2E - (P - A_x)^2 - (Q - A_y)^2\right]^{-1/2} dE dP dQ,$$

where $E_{min,0}$ is the value of E_{min} when $\phi = 0$, given by

$$E_{min,0} = \frac{1}{2}[(P - A_x)^2 + (Q - A_y)^2]. \tag{2.185}$$

This then gives

$$(a_i - a_e)I_1 + (b_i - b_e)I_3 = 0, \tag{2.186}$$

which will of course be satisified if

$$a_e = a_i = A_g, \tag{2.187}$$

$$b_e = b_i = B_g. \tag{2.188}$$

Note that the condition $b_s > a_s$ mentioned in Section 2.4 leads to the condition $B_g > A_g$, which must be satisfied to ensure that the distribution functions are positive. When the conditions (2.178)-(2.180), (2.187) and (2.188) are satisifed, the pressure $P_{zz.g}$, given by Equation (2.176), can be rewritten as

$$P_{zz,g}(A_x, A_y) = 2f_0 \frac{(m_e + m_i)e}{m_e m_i} [A_g H_1 \cos(\alpha A_x) + H_2 \exp(\gamma A_y) + B_g H_3], \qquad (2.189)$$

where

$$H_1 = \int_{-\infty}^{\infty} \int_{-\infty}^{\infty} \int_{E_{min,0}}^{\infty} h(E) \left[2E - S^2 - T^2 \right]^{1/2} \cos(\alpha S) dE dS dT, \qquad (2.190)$$

$$H_2 = \int_{-\infty}^{\infty} \int_{-\infty}^{\infty} \int_{E_{min,0}}^{\infty} h(E) \left[2E - S^2 - T^2 \right]^{1/2} \exp(\gamma T) dE dS dT, \qquad (2.191)$$

$$H_3 = \int_{-\infty}^{\infty} \int_{-\infty}^{\infty} \int_{E_{min,0}}^{\infty} h(E) \left[2E - S^2 - T^2 \right]^{1/2} dE dS dT, \qquad (2.192)$$

with $S = P - A_x$ and $T = Q - A_y$. Note also that, after this change of variable,

$$E_{min,0} = \frac{1}{2}(S^2 + T^2). \qquad (2.193)$$

It can be seen that the general pressure given by Equation (2.189) will be equal to the pressure (2.66) if the following additional conditions are satisfied,

$$\frac{2(m_e + m_i)e}{m_e m_i} f_0 H_2 = \frac{\beta_e + \beta_i}{\beta_e \beta_i} n_0, \qquad (2.194)$$

$$\frac{A_g H_1}{H_2} = \frac{1}{2}, \qquad (2.195)$$

$$\frac{B_g H_3}{H_2} = b. \qquad (2.196)$$

When these conditions are satisfied, in addition to conditions (2.178)-(2.180), (2.187) and (2.188), Ampère's law in the form given by Equations (1.83) and (1.84) is satisfied for the set of general distribution functions (2.159) and, therefore, they form a family of equilibrium solutions of the Vlasov-Maxwell equations for the force-free Harris sheet, in addition to the known distribution function (Harrison and Neukirch, 2009b). In Section 2.8, three explicit examples are given, which show possible choices of the function $h(m_s H_s/q_s^2) = h(E)$. The validity of the conditions (2.194)-(2.196) will of course depend on the choice of the function $h(E)$, and this will be discussed in each of the three examples.

2.8 Examples of New Distribution Functions for the Force-Free Harris Sheet

The following three examples in this section illustrate the use of the method discussed in Section 2.7, for various choices of the function $h(m_s H_s/q_s^2) = h(E)$.

2.8.1 Delta Function

Consider a distribution function of the form (2.159), with the function $h(m_s H_s/q_s^2) = h(E)$ given by a delta function,

$$h(E) = \delta(E - E_0), \tag{2.197}$$

where $E_0 > E_{min,0}$. This corresponds to a case where the distribution function is zero everywhere except for one particular value of the energy ($E = E_0$), and so all particles are assumed to have the same energy. Carrying out the E-integration first gives $P_{zz,g}$ as

$$
\begin{aligned}
P_{zz,g}(A_x, A_y) &= 2f_0 \sum_s \frac{|q_s|}{m_s} \Bigg[A_g \cos(\alpha A_x) \int_{-\infty}^{\infty} \int_{-\infty}^{\infty} (2E_0 - S^2 - T^2)^{1/2} \cos(\alpha S) dS dT \\
&\quad + \exp(\gamma A_y) \int_{-\infty}^{\infty} \int_{-\infty}^{\infty} (2E_0 - S^2 - T^2)^{1/2} \exp(\gamma T) dS dT \\
&\quad + B_g \int_{-\infty}^{\infty} \int_{-\infty}^{\infty} (2E_0 - S^2 - T^2)^{1/2} dS dT \Bigg].
\end{aligned}
\tag{2.198}
$$

Using cylindrical coordinates (r,θ), with

$$
\begin{aligned}
S^2 + T^2 &= 2E_0 r^2, & (2.199) \\
S &= \sqrt{2E_0} r \cos\theta, & (2.200) \\
T &= \sqrt{2E_0} r \sin\theta, & (2.201)
\end{aligned}
$$

then gives

$$
\begin{aligned}
P_{zz,g}(A_x, A_y) &= 2\sqrt{8E_0^3} f_0 \frac{(m_e + m_i)e}{m_e m_i} \\
&\quad \times \Bigg[A_g \cos(\alpha A_x) \int_0^{2\pi} \int_0^1 r(1 - r^2)^{1/2} \cos(\alpha' r \cos\theta) dr d\theta \\
&\quad + \exp(\gamma A_y) \int_0^{2\pi} \int_0^1 r(1 - r^2)^{1/2} \exp(\gamma' r \sin\theta) dr d\theta + \frac{2\pi B_g}{3} \Bigg],
\end{aligned}
\tag{2.202}
$$

where

$$\alpha' = \sqrt{2E_0}\alpha, \tag{2.203}$$

$$\gamma' = \sqrt{2E_0}\gamma. \tag{2.204}$$

The remaining integrations can then be carried out by using the formulae in Appendix B, which gives $P_{zz,g}$ as

$$
\begin{aligned}
P_{zz,g}(A_x, A_y) &= 4\pi\sqrt{8E_0^3}f_0\frac{(m_e + m_i)e}{m_e m_i}\Bigg[A_g\sqrt{\frac{\pi}{2\alpha'^3}}J_{3/2}(\alpha')\cos(\alpha A_x) \\
&\quad + \sqrt{\frac{\pi i}{2\gamma'^3}}J_{3/2}(i\gamma')\exp(\gamma A_y) + \frac{B_g}{3}\Bigg].
\end{aligned}
\tag{2.205}
$$

The Bessel functions $J_{3/2}$ in Equation (2.205), which are of fractional order, can be written in terms of spherical Bessel functions j_1 (of integer order) through the identity

$$j_n(z) = \sqrt{\frac{\pi}{2z}}J_{n+1/2}(z), \tag{2.206}$$

which gives,

$$J_{3/2}(z) = \sqrt{\frac{2z}{\pi}}j_1(z), \tag{2.207}$$

where

$$j_1(z) = \frac{\sin z}{z^2} - \frac{\cos z}{z}. \tag{2.208}$$

This gives $P_{zz,g}$ as

$$
\begin{aligned}
P_{zz,g}(A_x, A_y) &= 4\pi f_0\frac{(m_e + m_i)e}{m_e m_i}\frac{\sqrt{8E_0^3}}{\gamma'^3}\left(\gamma'\cosh\gamma' - \sinh\gamma'\right) \\
&\quad \times \Bigg[A_g\cos(\alpha A_x)\frac{\gamma'^3}{\alpha'^3}\left(\frac{\sin\alpha' - \alpha'\cos\alpha'}{\gamma'\cosh\gamma' - \sinh\gamma'}\right) \\
&\quad + \exp(\gamma A_y) + \frac{B_g}{3}\left(\frac{\gamma'^3}{\gamma'\cosh\gamma' - \sinh\gamma'}\right)\Bigg].
\end{aligned}
\tag{2.209}
$$

The conditions (2.194)-(2.196) for the pressure (2.209) to be equal to the pressure (2.50) are then given by

$$\frac{\beta_e + \beta_i}{\beta_e\beta_i}n_0 = 4\pi f_0\frac{(m_e + m_i)e}{m_e m_i}\frac{\sqrt{8E_0^3}}{\gamma'^3}\left(\gamma'\cosh\gamma' - \sinh\gamma'\right), \tag{2.210}$$

$$\frac{1}{2} = A_g \frac{\gamma'^3}{\alpha'^3} \left(\frac{\sin \alpha' - \alpha' \cos \alpha'}{\gamma' \cosh \gamma' - \sinh \gamma'} \right), \tag{2.211}$$

$$b = \frac{B_g}{3} \left(\frac{\gamma'^3}{\gamma' \cosh \gamma' - \sinh \gamma'} \right), \tag{2.212}$$

and the condition $B_g > A_g$ gives rise to the following condition on b:

$$b > \frac{1}{6} \left(\frac{\alpha'^3}{\sin \alpha' - \alpha' \cos \alpha'} \right). \tag{2.213}$$

The right-hand side of condition (2.210) is always positive since the γ'-dependent function, $(\gamma' \cosh \gamma' - \sinh \gamma')/\gamma'^3$, is always positive, regardless of the value of γ'. Note also that $m_s, e, E_0, f_0 > 0$. Condition (2.210) is, therefore, a valid condition since its left-hand side is also always positive ($\beta_s, n_0 > 0$). The constant A_g in condition (2.211) is positive, and the γ'-dependent part is the same as in condition (2.210) which, as discussed, is always positive for any value of γ'. The α'-dependent part is given by

$$\frac{\sin \alpha' - \alpha' \cos \alpha'}{\alpha'^3} = \frac{j_1(\alpha')}{\alpha'}, \tag{2.214}$$

which can be positive or negative due to the spherical Bessel function $j_1(\alpha')$, shown in Figure 2.12. Condition (2.211) is, therefore, only valid in the regions where $j_1(\alpha') > 0$. It can be seen from Figure 2.12 that it is valid for small values of α'. Condition (2.212) is also a valid condition, since both the left- and right-hand sides are positive (B_g is positive and the γ'-dependent part is positive). The fact that γ' can be positive or negative means that the parameters u_{ye} and u_{yi} from the distribution function (2.159) (with the function $h(m_s H_s/q_s^2) = h(E)$ given by Equation (2.197)) can be positive or negative, but must have opposite signs from each other through the definition (2.180) of $\gamma = \gamma'/\sqrt{2E_0}$.
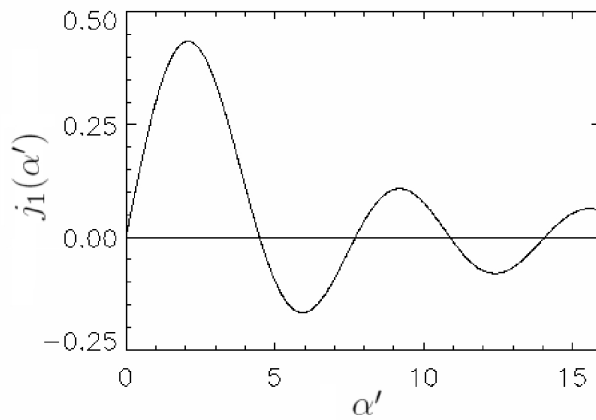

Figure 2.12: The spherical Bessel function $j_1(\alpha')$

2.8.2 Step Function

Consider a distribution function of the form (2.159), with the function $h(m_s H_s/q_s^2) = h(E)$ given by a step function,

$$h(E) = \Theta(E_0 - E) = \begin{cases} 1, & E \leq E_0 \\ 0, & E_0 < E \end{cases}.$$ (2.215)

The lower bound for the energy integration is $E_{min,0}$, given by Equation (2.193). The E-integral is the same for each part of $P_{zz,g}$, and is given by

$$\int_{E_{min,0}}^{\infty} \Theta(E_0 - E)(2E - S^2 - T^2)^{1/2} dE = \int_{E_{min,0}}^{E_0} (2E - S^2 - T^2)^{1/2} dE$$ (2.216)

$$= \frac{1}{3}(2E_0 - S^2 - T^2)^{3/2}.$$ (2.217)

Using a cylindrical coordinate system (r, θ) as in the first example (see Equations (2.199)-(2.201)), the resulting integrals can then be evaluated in a similar way to the previous example (see Appendix B for details). Then, using Equation (2.206) as in the previous example, the resulting Bessel functions (of order $5/2$) can be expressed in terms of the spherical Bessel function j_2, where

$$j_2(z) = \left(\frac{3}{z^3} - \frac{1}{z}\right) \sin z - \frac{3}{z^2} \cos z.$$ (2.218)

The pressure is then given by

$$\begin{aligned} P_{zz,g}(A_x, A_y) &= 4\pi f_0 \frac{(m_e + m_i)e}{m_e m_i} \frac{\sqrt{32E_0^5}}{\gamma'^5} \left[(3 + \gamma'^2) \sinh \gamma' - 3\gamma' \cosh \gamma'\right] \\ &\quad \times \left[A_g \cos(\alpha A_x) \frac{\gamma'^5}{\alpha'^5} \frac{(3 - \alpha'^2) \sin \alpha' - 3\alpha' \cos \alpha'}{(3 + \gamma'^2) \sinh \gamma' - 3\gamma' \cosh \gamma'} \right. \\ &\quad \left. + \exp(\gamma A_y) + \frac{B_g}{15} \frac{\gamma'^5}{(3 + \gamma'^2) \sinh \gamma' - 3\gamma' \cosh \gamma'} \right], \end{aligned}$$ (2.219)

where α' and γ' are given by Equations (2.203) and (2.204). The conditions (2.194)-(2.196) for the pressure (2.219) to be equal to the pressure (2.50) are then given by

$$\frac{\beta_e + \beta_i}{\beta_e \beta_i} n_0 = 4\pi f_0 \frac{(m_e + m_i)e}{m_e m_i} \frac{\sqrt{32E_0^5}}{\gamma'^5} \left[(3 + \gamma'^2) \sinh \gamma' - 3\gamma' \cosh \gamma'\right],$$ (2.220)

$$\frac{1}{2} = A_g \frac{\gamma'^5}{\alpha'^5} \frac{(3 - \alpha'^2) \sin \alpha' - 3\alpha' \cos \alpha'}{(3 + \gamma'^2) \sinh \gamma' - 3\gamma' \cosh \gamma'},$$ (2.221)

$$b = \frac{B_g}{15} \frac{\gamma'^5}{(3 + \gamma'^2) \sinh \gamma' - 3\gamma' \cosh \gamma'},$$ (2.222)

and the condition $B_g > A_g$ gives the following condition on b:

$$b > \frac{1}{30} \frac{\alpha'^5}{(3 - \alpha'^2) \sin \alpha' - 3\alpha' \cos \alpha'}. \tag{2.223}$$

The right-hand side of condition (2.220) is always positive since the γ'-dependent function, $((3 + \gamma'^2) \sinh \gamma' - 3\gamma' \cosh \gamma')/\gamma'^5$, is always positive, regardless of the value of γ'. Note also that $m_s, e, E_0, f_0 > 0$. Condition (2.220) is, therefore, a valid condition since its left-hand side is also always positive ($\beta_s, n_0 > 0$). The constant A_g in condition (2.221) is positive, and the γ'-dependent part is the same as in condition (2.220) which, as discussed, is always positive for any value of γ'. The α'-dependent part is given by

$$\frac{(3 - \alpha'^2) \sin \alpha' - 3\alpha' \cos \alpha'}{\alpha'^5} = \frac{j_2(\alpha')}{\alpha'^2}, \tag{2.224}$$

which can be positive or negative due to the spherical Bessel function $j_2(\alpha')$, which has a similar profile (qualitatively) to that of the spherical Bessel function $j_1(\alpha')$, shown in Figure 2.12. Condition (2.221) is, therefore, only valid in the regions where $j_2(\alpha') > 0$. Condition (2.222) is also a valid condition, since both the left- and right-hand sides are positive (B_g is positive and the γ'-dependent part is positive). The fact that γ' can be positive or negative means that the parameters u_{ye} and u_{yi} from the distribution function (2.159) (with the function $h(m_s H_s/q_s^2) = h(E)$ given by (2.215)) can be positive or negative, but must have opposite signs from each other through the definition (2.180) of $\gamma = \gamma'/\sqrt{2E_0}$.

2.8.3 Power of $E_0 - E$

Consider a distribution function of the form (2.159), with the function $h(m_s H_s/q_s^2) = h(E)$ given by

$$h(E) = \begin{cases} (E_0 - E)^\chi, & E < E_0 \\ 0, & E_0 \leq E \end{cases}, \tag{2.225}$$

where $\chi > -1$ and the lower bound for the energy integration is $E_{min,0}$, given by Equation (2.193). When calculating $P_{zz,g}$ using Equation (2.189), the E-integration is the same in each triple integral, and is given by

$$\int_{E_{min,0}}^{E_0} (E_0 - E)^\chi [2(E - E_{min,0})]^{1/2} dE, \tag{2.226}$$

which can be written as

$$\sqrt{2} \int_0^{\psi_0} \psi^\chi (\psi_0 - \psi)^{1/2} d\psi, \tag{2.227}$$

where $\psi = E_0 - E$ and $\psi_0 = E_0 - E_{min,0}$. The integral (2.227) can be evaluated by using the formula

$$\int_0^z t^{\nu-1}(z-t)^{\mu-1}dt = z^{\mu+\nu-1}B(\mu,\nu), \tag{2.228}$$

where $B(\mu,\nu)$ is a beta function defined by

$$B(\mu,\nu) = \frac{\Gamma(\mu)\Gamma(\nu)}{\Gamma(\mu+\nu)}, \tag{2.229}$$

and $\Re\mu > 0$, $\Re\nu > 0$ (which gives $\chi > -1$). The integral (2.226) is then given by

$$\int_{E_{min,0}}^{E_0} (E_0 - E)^\chi [2(E - E_{min,0})]^{1/2}dE$$
$$= \frac{\sqrt{\pi}}{4.2^\chi}\frac{\Gamma(\chi+1)}{\Gamma(\chi+5/2)}(2E_0 - S^2 - T^2)^{3/2+\chi}, \tag{2.230}$$

where $E_{min,0} = (1/2)(S^2 + T^2)$. Using a cylindrical coordinate system as before (see Equations (2.199)-(2.201)) gives $P_{zz,g}$ as

$$\begin{aligned}P_{zz,g}(A_x, A_y) &= \frac{f_0(m_e + m_i)e}{m_e m_i}\frac{\sqrt{\pi}}{2^{\chi+1}}\frac{\Gamma(\chi+1)}{\Gamma(\chi+5/2)}(2E_0)^{\chi+5/2}\\
&\times\left[A_g\cos(\alpha A_x)\int_0^{2\pi}\int_0^1 r(1-r^2)^{3/2+\chi}\cos(\alpha'r\cos\theta)drd\theta\right.\\
&\left.+\exp(\gamma A_y)\int_0^{2\pi}\int_0^1 r(1-r^2)^{3/2+\chi}\exp(\gamma'r\sin\theta)drd\theta + \frac{\pi B_g}{\chi+5/2}\right],\end{aligned} \tag{2.231}$$

where α' and γ' are given by Equations (2.203) and (2.204). As in the previous two examples, the remaining integrations can be carried out by using the formulae in Appendix B. The pressure $P_{zz,g}$ is then given by

$$\begin{aligned}P_{zz,g}(A_x, A_y) &= (2\pi)^{3/2}\frac{f_0(m_e + m_i)e}{m_e m_i}\Gamma(\chi+1)(2E_0)^{\chi+5/2}\frac{J_{\chi+5/2}(i\gamma')}{(i\gamma')^{\chi+5/2}}\\
&\times\left[A_g\left(\frac{i\gamma'}{\alpha'}\right)^{\chi+5/2}\frac{J_{\chi+5/2}(\alpha')}{J_{\chi+5/2}(i\gamma')}\cos(\alpha A_x) + \exp(\gamma A_y)\right.\\
&\left.+\frac{B_g(i\gamma')^{\chi+5/2}}{2^{\chi+5/2}\Gamma(\chi+7/2)J_{\chi+5/2}(i\gamma')}\right].\end{aligned} \tag{2.232}$$

The conditions (2.194)-(2.196) for the pressure (2.232) to be equal to (2.50) are then given by,

$$\frac{\beta_e + \beta_i}{\beta_e\beta_i}n_0 = (2\pi)^{3/2}\frac{f_0(m_e + m_i)e}{m_e m_i}\Gamma(\chi+1)(2E_0)^{\chi+5/2}$$

$$\times \frac{J_{\chi+5/2}(i\gamma')}{(i\gamma')^{\chi+5/2}}, \tag{2.233}$$

$$\frac{1}{2} = A_g \left(\frac{i\gamma'}{\alpha'} \right)^{\chi+5/2} \frac{J_{\chi+5/2}(\alpha')}{J_{\chi+5/2}(i\gamma')}, \tag{2.234}$$

$$b = \frac{B_g (i\gamma')^{\chi+5/2}}{2^{\chi+5/2}\Gamma(\chi+7/2)J_{\chi+5/2}(i\gamma')}. \tag{2.235}$$

Conditions (2.233) to (2.235) reduce to the two conditions

$$\frac{J_{\chi+5/2}(\gamma')}{\gamma'^{\chi+5/2}} > 0, \tag{2.236}$$

$$\frac{J_{\chi+5/2}(\alpha')}{\alpha'^{\chi+5/2}} > 0, \tag{2.237}$$

on removing known positive quantities from the inequalities and using the fact that $J_\nu(iz) = i^\nu J_\nu(z)$. The condition $B_g > A_g$ gives the following condition on b

$$b > \frac{(\alpha')^{\chi+5/2}}{2^{\chi+7/2}\Gamma(\chi+7/2)J_{\chi+5/2}(\alpha')}. \tag{2.238}$$

The condition (2.236) contains a root of γ' meaning that, in general, γ' must be positive, and so the conditions (2.236) and (2.237) are satisfied in the regions where $J_{\chi+5/2}(\alpha')$ and $J_{\chi+5/2}(\gamma')$ are positive (note again that $\alpha' = \sqrt{2E_0}\alpha > 0$ through the definition (2.179)). Note that, when χ is an integer, the identity (2.206) can be used to express the Bessel functions $J_{n+1/2}$ in terms of spherical Bessel functions j_n. This was done in the previous example (which corresponds to $\chi = 0$). In that example, the conditions (2.233) to (2.235) were expressed in terms of $\sin\alpha'$, $\cos\alpha'$, $\sinh\gamma'$ and $\cosh\gamma'$ (from the spherical Bessel function j_1 given by (2.208)) and it was observed that γ' could be positive or negative without violating the conditions on the parameters (the fractional part of the power of γ' cancelled out).

The method of Section 2.7, together with the examples given in the present section, have further illustrated that different distribution functions can give rise to the same magnetic field profile. As previously discussed, the force-free Harris sheet is the only magnetic field profile for which nonlinear force-free Vlasov-Maxwell equilibria are known. If an equilibrium solution were discovered for another field profile, however, then this method could potentially be used to extend the known solution to a family of solutions.

2.9 Looking for Force-Free Vlasov-Maxwell Equilibria Using Cylindrical Coordinates

An interesting extension to the force-free Vlasov-Maxwell equilibrium problem involves trying to find equilibria using a cylindrical coordinate system (r, θ, z). As mentioned by Channell (1976), it is not obvious how to extend the general theory in order to find distribution functions for a given magnetic field profile. It is, of course, possible to solve the problem in the opposite direction, by starting with a certain form of distribution function, and investigating whether or not this gives rise to a force-free equilibrium. An attempt to solve the problem in such a way will be discussed in the present section. Before this, however, some preliminary details will be discussed, to illustrate why the general theory cannot be extended in an obvious way.

Assuming that all quantities depend only upon the radial coordinate r, the three constants of motion in the model are the Hamiltonian, arising from the time-independence of the system, given by

$$H_s = \frac{1}{2} m_s (v_r^2 + v_\theta^2 + v_z^2) + q_s \phi, \tag{2.239}$$

the canonical momentum in the θ- (azimuthal-) direction, arising from the assumed invariance in this direction, given by

$$p_{\theta s} = r(m_s v_\theta + q_s A_\theta), \tag{2.240}$$

and the canonical momentum in the z-direction, arising from the invariance in this direction, given by

$$p_{zs} = m_s v_z + q_s A_z, \tag{2.241}$$

where $v_r = \dot{r}$, $v_\theta = r\dot{\theta}$ and $v_z = \dot{z}$ are the velocities in the r- θ- and z-directions, respectively.

It is shown in Appendix C that the following relations hold

$$\frac{\partial \sigma}{\partial A_\theta} + \frac{\partial j_\theta}{\partial \phi} = 0, \tag{2.242}$$

$$\frac{\partial \sigma}{\partial A_z} + \frac{\partial j_z}{\partial \phi} = 0, \tag{2.243}$$

$$\frac{\partial j_\theta}{\partial A_z} - \frac{\partial j_z}{\partial A_\theta} = 0, \tag{2.244}$$

$$\tag{2.245}$$

and also that the θ- and z-components of the current density can be written as

$$j_\theta = \frac{\partial P_{rr}}{\partial A_\theta}, \tag{2.246}$$

$$j_z = \frac{\partial P_{rr}}{\partial A_z}, \tag{2.247}$$

and the charge density as

$$\frac{\partial P_{rr}}{\partial \phi} = -\sigma, \tag{2.248}$$

where P_{rr} is the rr-component of the pressure tensor (the component which is important for force-balance), given by

$$P_{rr} = \sum_s m_s \int_{-\infty}^{\infty} v_r^2 f_s d^3v. \tag{2.249}$$

Note that, alternatively, the current density components could be calculated directly from a known distribution function through the following definitions,

$$j_\theta = \sum_s q_s \int_{-\infty}^{\infty} v_\theta f_s d^3v, \tag{2.250}$$

$$j_z = \sum_s q_s \int_{-\infty}^{\infty} v_z f_s d^3v. \tag{2.251}$$

It is assumed that the magnetic field vanishes in the r-direction, and that $\mathbf{B} = \nabla \times \mathbf{A}$, where now $\mathbf{A} = (0, A_\theta, A_z)$. The magnetic field can be written as

$$\mathbf{B} = \nabla \times \mathbf{A} = \left(0, -\frac{dA_z}{dr}, \frac{1}{r}\frac{d}{dr}(rA_\theta)\right). \tag{2.252}$$

The non-zero components of Ampère's law, $\nabla \times \mathbf{B} = \mu_0 \mathbf{j}$, are then given by

$$\mu_0 j_\theta = -\frac{d}{dr}\left(\frac{1}{r}\frac{d}{dr}(rA_\theta)\right), \tag{2.253}$$

$$\mu_0 j_z = -\frac{1}{r}\frac{d}{dr}\left(r\frac{dA_z}{dr}\right), \tag{2.254}$$

which can be written in terms of derivatives of P_{rr} as

$$\frac{\partial P_{rr}}{\partial A_\theta} = -\frac{1}{\mu_0}\frac{d}{dr}\left(\frac{1}{r}\frac{d}{dr}(rA_\theta)\right), \tag{2.255}$$

$$\frac{\partial P_{rr}}{\partial A_z} = -\frac{1}{\mu_0 r}\frac{d}{dr}\left(r\frac{dA_z}{dr}\right), \tag{2.256}$$

A solution of these equations would result in a P_{rr} with an explicit dependence on the radial

coordinate, r. This is different from the Cartesian case, in which the pressure function, P_{zz}, does not depend explicitly on z (the coordinate on which all quantities depend). It should be noted that such a dependence on r does not imply that the total time derivative, dP_{rr}/dr, is non-zero - it only implies that $\partial P_{rr}/\partial r \neq 0$, and so it may be possible to find a force-free equilibrium solution.

In the remainder of the present section, an example will be given of an attempt to find a force-free equilibrium in cylindrical coordinates. Firstly, it is assumed that the distribution functions have the form

$$f_s = f_{s0} \exp(-\beta_s H_s) \left(a_s + b_{s\theta} p_{\theta s}^2 + b_{sz} p_{zs}^2 \right), \tag{2.257}$$

where f_{s0}, a_s and b_s are constants, and $\beta_s = 1/(k_B T_s)$, with k_B equal to the Boltzmann constant and T_s the temperature of particle species s. A distribution function of this form was chosen since it is known to give rise to a force-free equilibrium in Cartesian coordinates (Channell, 1976; Attico and Pegoraro, 1999). The rr-component of the pressure tensor can be calculated by substituting Equation (2.257) into the definition (2.249), which, after carrying out the integration, gives

$$P_{rr} = \sum_s \sqrt{8\pi^3} v_{th,s}^5 f_{s0} m_s \exp(-\beta_s q_s \phi)$$
$$\times \left(a_s + b_{s\theta} r^2 \left(\frac{m_s}{\beta_s} + (q_s A_\theta)^2 \right) + b_{sz} \left(\frac{m_s}{\beta_s} + (q_s A_z)^2 \right) \right). \tag{2.258}$$

Using Equations (2.246) and (2.247) then gives the θ- and z-components of the current density as

$$j_\theta = D_\theta r^2 A_\theta, \tag{2.259}$$
$$j_z = D_z A_z, \tag{2.260}$$

where

$$D_\theta = 2\sqrt{8\pi^3} \sum_s v_{th,s}^5 m_s f_{s0} q_s^2 \exp(-\beta_s q_s \phi) b_{s\theta}, \tag{2.261}$$
$$D_z = 2\sqrt{8\pi^3} \sum_s v_{th,s}^5 m_s f_{s0} q_s^2 \exp(-\beta_s q_s \phi) b_{sz}. \tag{2.262}$$

Substituting Equations (2.259) and (2.260) into Ampère's law (Equations (2.253) and (2.254)) gives the following two ordinary differential equations

$$-\frac{1}{\mu_0} \frac{d}{dr} \left(\frac{1}{r} \frac{d}{dr} (r A_\theta) \right) = D_\theta r^2 A_\theta, \tag{2.263}$$
$$-\frac{1}{\mu_0 r} \frac{d}{dr} \left(r \frac{dA_z}{dr} \right) = D_z A_z, \tag{2.264}$$

which can be solved for A_θ and A_z, which will then give the magnetic field profile. Equation

(2.263) can be rewritten as

$$-\frac{1}{\mu_0}\frac{d}{du}\left(\frac{d\psi}{du}\right) = D_\theta\psi, \tag{2.265}$$

where $\psi = rA_\theta$ and $u = \frac{1}{2}r^2$. This equation has the solution

$$rA_\theta = A\sin\left(\frac{\sqrt{\mu_0 D_\theta}}{2}r^2\right) + B\cos\left(\frac{\sqrt{\mu_0 D_\theta}}{2}r^2\right), \tag{2.266}$$

where A and B are constants. Then, using the fact that $rA_\theta = 0$ when $r = 0$ gives $B = 0$, so that the azimuthal component of $\mathbf{A}$ is given by

$$A_\theta = \frac{A}{r}\sin\left(\frac{\sqrt{\mu_0 D_\theta}}{2}r^2\right). \tag{2.267}$$

This can then be substituted into Equation (2.252), which gives the z-component of the magnetic field as

$$B_z = A\sqrt{\mu_0 D_\theta}\cos\left(\frac{\sqrt{\mu_0 D_\theta}}{2}r^2\right). \tag{2.268}$$

Equation (2.264) can be expanded to give

$$r^2\frac{d^2 A_z}{dr^2} + r\frac{dA_z}{dr} + (r\sqrt{\mu_0 D_z})^2 A_z = 0, \tag{2.269}$$

which, by letting $R = \sqrt{\mu_0 D_z}\,r$, can be written as

$$\frac{d^2 A_z}{dR^2} + \frac{1}{R}\frac{dA_z}{dR} + A_z = 0. \tag{2.270}$$

Equation (2.270) is Bessel's equation with solution

$$A_z = J_0(R) = J_0(\sqrt{\mu_0 D_z}\,r), \tag{2.271}$$

where J_0 is a Bessel function of the first kind (e.g. Abramowitz and Stegun, 1964). The θ-component of the magnetic field can then be calculated from Equation (2.252), and is given by

$$B_\theta = \sqrt{\mu_0 D_z}J_1(\sqrt{\mu_0 D_z}\,r), \tag{2.272}$$

by using the relation $J_0'(\sqrt{\mu_0 D_z}\,r) = -\sqrt{\mu_0 D_z}J_1(\sqrt{\mu_0 D_z}\,r)$.

To summarise, the magnetic field profile arising from the distribution function (2.257) is given by

$$B_\theta = \sqrt{\mu_0 D_z}J_1(\sqrt{\mu_0 D_z}\,r), \tag{2.273}$$

$$B_z = A\sqrt{\mu_0 D_\theta} \cos\left(\frac{\sqrt{\mu_0 D_\theta}}{2} r^2\right), \tag{2.274}$$

which gives rise to a current density

$$j_\theta = AD_\theta r \sin\left(\frac{\sqrt{\mu_0 D_\theta}}{2} r^2\right), \tag{2.275}$$

$$j_z = D_z J_0(\sqrt{\mu_0 D_z} r). \tag{2.276}$$

Figure 2.13 shows a plot of the magnetic field lines. By looking at the expressions (2.275) and (2.276) for the current density components, it is clear that the magnetic field is not force-free, since $\mathbf{j} \neq \alpha \mathbf{B}$. Thus, the equilibrium given by the magnetic field profile (2.273), (2.274) and distribution function (2.257) is not a force-free equilibrium, illustrating that the approach used here has not been successful. It would be more desirable to have a theory which allows distribution functions to be calculated from a given linear (or non-linear) force-free field.
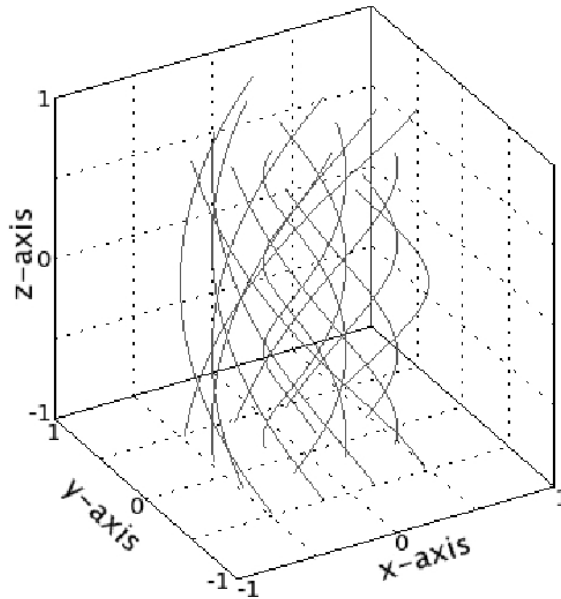
Figure 2.13: Plot of the helical field lines for $\mu_0 D_z = 50$, $\mu_0 D_\theta = 25$ and $A = 1$.

For completeness, the parallel current, quasineutral electric potential, and quasineutral pressure function for this equilibrium are given below. The parallel current, $j_\parallel$, which is the component of the current density parallel to the magnetic field, can be calculated by using the formula

$$j_\parallel = \frac{\mathbf{j} \cdot \mathbf{B}}{|\mathbf{B}|}. \tag{2.277}$$

Using Equations (2.273)-(2.276) for the magnetic field and current density components gives the

parallel current as

$$
\begin{aligned}
j_{\parallel} &= \left[AD_\theta \sqrt{\mu_0 D_z} \, r \sin\left(\frac{\sqrt{\mu_0 D_\theta}}{2} r^2 \right) J_1(\sqrt{\mu_0 D_z} r) \right. \\
&\quad \left. + AD_z \sqrt{\mu_0 D_\theta} \cos\left(\frac{\sqrt{\mu_0 D_\theta}}{2} r^2 \right) J_0(\sqrt{\mu_0 D_z} r) \right] \\
&\quad \times \left[\mu_0 D_z \left[J_1(\sqrt{\mu_0 D_z} r) \right]^2 + A^2 \mu_0 D_\theta \cos^2\left(\frac{\sqrt{\mu_0 D_\theta}}{2} r^2 \right) \right]^{-1/2}.
\end{aligned}
\tag{2.278}
$$

Finding an equilibrium involves solving Ampère's law for the magnetic field, as well as Gauss' law for the electric potential, and hence the electric field. Throughout this work it is assumed that the plasma is quasineutral which, to lowest order, corresponds to the condition

$$
\sigma = -\frac{\partial P_{rr}}{\partial \phi} = 0.
\tag{2.279}
$$

Substituting Equation (2.258) for P_{rr} into the Equation (2.279), summing over ions and electrons, and solving for the quasineutral electric potential ϕ_{qn} gives,

$$
\phi_{qn} = \frac{1}{e(\beta_e + \beta_i)} \ln[f(r)],
\tag{2.280}
$$

where,

$$
f(r) = \frac{\beta_i}{\beta_e} \frac{N_i(A_\theta, A_z, r)}{N_e(A_\theta, A_z, r)},
\tag{2.281}
$$

with the function N_s (for species s) defined by,

$$
\begin{aligned}
N_s &= \sqrt{8\pi^3} v_{th,s}^5 m_s f_{s0} \left[a_s + b_{s\theta} r^2 \left(\frac{m_s}{\beta_s} + q_s^2 A_\theta^2 \right) \right. \\
&\quad \left. + b_{sz} \left(\frac{m_s}{\beta_s} + q_s^2 A_z^2 \right) \right].
\end{aligned}
\tag{2.282}
$$

The quasineutral electric potential (2.280) can then be substituted back into the Equation (2.258) for P_{rr}, to give an expression for the quasineutral pressure, $P_{rr,qn}$, which, after some algebra, is given by

$$
P_{rr,qn} = \left[\left(\frac{\beta_i}{\beta_e} \right)^{\beta_e/(\beta_e+\beta_i)} + \left(\frac{\beta_e}{\beta_i} \right)^{\beta_i/(\beta_e+\beta_i)} \right] N_e^{\beta_i/(\beta_e+\beta_i)} N_i^{\beta_e/(\beta_e+\beta_i)}.
\tag{2.283}
$$

2.10   Summary

The work in this chapter has focused on one-dimensional force-free Vlasov-Maxwell equilibria. Properties of the previously known nonlinear force-free solution found by Harrison and Neukirch (2009b) have been discussed in detail. In particular, conditions have been given on the parameters of the distribution function, which show when it can be single or multi-peaked. This is of interest, since a multi-peaked distribution function may give rise to microinstabilities. A study of the microinstabilities themselves is, however, beyond the scope of this thesis.

A discussion has been given of attempts to find distribution functions for nonlinear force-free magnetic field profiles, other than that of the force-free Harris sheet, by using the method of Harrison and Neukirch (2009b). These attempts were unsuccessful, however, which has highlighted the fact that finding Vlasov-Maxwell equilibria analytically is not straightforward.

A method has been discussed which allows a family of distribution functions to be calculated for the force-free Harris sheet. This family includes the Harrison and Neukirch (2009b) solution, in addition to distribution functions with a different dependence on the particle energy. Three examples of distrbution functions from the family have been given, in order to illustrate the use of the general method. Although there are no other nonlinear force-free magnetic field profiles for which Vlasov-Maxwell equilibria are known, if another solution was found, then this method could potentially be used to extend that solution to a family of solutions.

An attempt has also been made to reformulate the force-free Vlasov-maxwell equilibrium problem in cylindrical coordinates, by considering the case where all quantities depend only on the radial coordinate, r. It has been illustrated that, in general, this is not straightforward, in agreement with Channell (1976). An example has been given, which involves assuming a distribution function of a similar form to that previously discussed by Channell (1976) and Attico and Pegoraro (1999) in Cartesian coordinates, which gives rise to a linear force-free magnetic field. It was found, however, that in cylindrical coordinates, such a distribution function does not give rise to a linear force-free magnetic field.

As stated above, the equilibrium distribution function found by Harrison and Neukirch (2009b) may be unstable to microinstabilities. In addition, there is the possibility that macroscopic instabilities may occur. In the next two chapters, therefore, a linear stability analysis will be carried out, in order to investigate the occurrence of the collisionless tearing mode.

Chapter 3

Vlasov Stability

3.1 Introduction

A large part of the work in Chapter 2 focused on the Harrison and Neukirch (2009b) equilibrium for the force-free Harris sheet. Conditions on the parameters of the distribution function were given which show when it can be single or multi-peaked in two of the velocity space directions. This may have implications for the stability of the equilibrium. As stated previously, an investigation into occurrence of microinstabilities is beyond the scope of this thesis, but there is also the possibility that the equilibrium is unstable to macroscopic instabilities, such as the collisionless tearing mode (e.g. Schindler, 2007), which can give rise to collisionless reconnection. The main aim of the present chapter, therefore, is to carry out the initial calculations required for a linear stability analysis of Harrison and Neukirch's equilibrium, in order to investigate the occurrence of such an instability.

Many authors (Dobrowolny, 1968; Hoh, 1966; Yamanaka, 1978; Lapenta and Brackbill, 1997; Daughton, 1998, 1999; Silin et al., 2002; Camporeale et al., 2006) have investigated the Vlasov stability of the Harris sheet equilibrium (Harris, 1962). The first step in such a stability analysis is to linearise the Vlasov-Maxwell equations, by considering small perturbations to the equilibrium. This will be discussed in Section 3.2, and then a review of previous work on the stability of the Harris sheet will be given in Section 3.3.

In Section 3.4, the initial calculations of the stability analysis for Harrison and Neukirch's equilibrium are carried out. The analysis follows a similar procedure to that used by a number of authors (e.g. Dobrowolny, 1968; Lapenta and Brackbill, 1997; Silin et al., 2002) for the Harris sheet. After linearising the Vlasov-Maxwell equations, the linearised Vlasov equation must be integrated to obtain the perturbed distribution function. The integration is carried out over the unperturbed particle orbits, since these are the characteristic curves of the Vlasov equation (see Section 1.3.1). The calculation of the particle orbits is a central difficulty in any Vlasov stability analysis and, in general, cannot be carried out analytically without an approximation. It is necessary, therefore, to use an approximation for the force-free Harris sheet field, in order to calculate approximate particle orbits. These expressions are then used alongside the perturbed distribution function to calculate the perturbed density and current density, by taking velocity moments of the distribution

function and carrying out the time integrations. Note that the perturbed density expression is not needed for the stability analysis, but it is calculated for completeness, and because its calculation serves as a useful exercise to prepare for the longer calculation of the perturbed current density, which is crucial to the stability analysis. The perturbed current density can be substituted into the linearised Ampère's law, which can be solved to give various dispersion plots for the instability. An approximate numerical solution of Ampère's law will be discussed in Chapter 4.

3.2 Linearised Vlasov-Maxwell Equations

The first step in the linear Vlasov stability analysis involves linearising the Vlasov-Maxwell equations

$$\frac{\partial f_s}{\partial t} + \mathbf{v} \cdot \frac{\partial f_s}{\partial \mathbf{r}} + \frac{q_s}{m_s}(\mathbf{E} + \mathbf{v} \times \mathbf{B}) \cdot \frac{\partial f_s}{\partial \mathbf{v}} = 0, \tag{3.1}$$

$$\nabla \times \mathbf{B} = \mu_0 \mathbf{j}, \tag{3.2}$$

$$\nabla \times \mathbf{E} = -\frac{\partial \mathbf{B}}{\partial t}, \tag{3.3}$$

$$\nabla \cdot \mathbf{B} = 0, \tag{3.4}$$

$$\nabla \cdot \mathbf{E} = \frac{\sigma}{\epsilon_0}. \tag{3.5}$$

It is also assumed that typical speeds are much less than the speed of light, c, so that the displacement current term in Ampère's law can be neglected. The set of Equations (3.1)-(3.3) can be linearised by writing each quantity as the sum of an equilibrium quantity, with subscript 0, plus a small perturbed quantity, with subscript 1,

$$f_s = f_{0s} + f_{1s}, \tag{3.6}$$

$$\mathbf{E} = \mathbf{E}_1, \tag{3.7}$$

$$\mathbf{B} = \mathbf{B}_0 + \mathbf{B}_1, \tag{3.8}$$

$$\mathbf{j} = \mathbf{j}_0 + \mathbf{j}_1, \tag{3.9}$$

$$\sigma = \sigma_0 + \sigma_1, \tag{3.10}$$

where $E_0 = 0$, and squares and products of the perturbed quantites are assumed to be much less than one, such that they can be neglected. Starting with the Vlasov equation (3.1), using Equations (3.6)-(3.8) gives

$$\frac{\partial f_{0s}}{\partial t} + \frac{\partial f_{1s}}{\partial t} + \mathbf{v} \cdot \frac{\partial f_{0s}}{\partial \mathbf{r}} + \mathbf{v} \cdot \frac{\partial f_{1s}}{\partial \mathbf{r}} + \frac{q_s}{m_s} \left[\mathbf{E}_1 + \mathbf{v} \times (\mathbf{B}_0 + \mathbf{B}_1) \right] \cdot \frac{\partial f_{0s}}{\partial \mathbf{v}}$$
$$+ \frac{q_s}{m_s} \left[\mathbf{E}_1 + \mathbf{v} \times (\mathbf{B}_0 + \mathbf{B}_1) \right] \cdot \frac{\partial f_{1s}}{\partial \mathbf{v}} = 0, \tag{3.11}$$

and then multiplying out the brackets gives

$$
\frac{\partial f_{0s}}{\partial t} + \frac{\partial f_{1s}}{\partial t} + \mathbf{v} \cdot \frac{\partial f_{0s}}{\partial \mathbf{r}} + \mathbf{v} \cdot \frac{\partial f_{1s}}{\partial \mathbf{r}} + \frac{q_s}{m_s} \left[\mathbf{v} \times \mathbf{B}_0 \right] \cdot \frac{\partial f_{0s}}{\partial \mathbf{v}}
$$
$$
+ \frac{q_s}{m_s} \left[\mathbf{v} \times \mathbf{B}_0 \right] \cdot \frac{\partial f_{1s}}{\partial \mathbf{v}} + \frac{q_s}{m_s} \left[\mathbf{E}_1 + \mathbf{v} \times \mathbf{B}_1 \right] \cdot \frac{\partial f_{0s}}{\partial \mathbf{v}}
$$
$$
+ \frac{q_s}{m_s} \left[\mathbf{E}_1 + \mathbf{v} \times \mathbf{B}_1 \right] \cdot \frac{\partial f_{1s}}{\partial \mathbf{v}} \quad = \quad 0. \tag{3.12}
$$

Neglecting squares and products of perturbed quantities, and using the equilibrium Vlasov equation (1.59) to cancel terms, then gives

$$
\frac{\partial f_{1s}}{\partial t} + \mathbf{v} \cdot \frac{\partial f_{1s}}{\partial \mathbf{r}} + \frac{q_s}{m_s} \left[\mathbf{v} \times \mathbf{B}_0 \right] \cdot \frac{\partial f_{1s}}{\partial \mathbf{v}} + \frac{q_s}{m_s} \left[\mathbf{E}_1 + \mathbf{v} \times \mathbf{B}_1 \right] \cdot \frac{\partial f_{0s}}{\partial \mathbf{v}} = 0. \tag{3.13}
$$

The total time derivative of $f_{1s}(\mathbf{r}, \mathbf{v}, t)$ can be expressed, using the chain rule, as

$$
\frac{df_{1s}}{dt} \quad = \quad \frac{\partial f_{1s}}{\partial t} + v_x \frac{\partial f_{1s}}{\partial x} + v_y \frac{\partial f_{1s}}{\partial y} + v_z \frac{\partial f_{1s}}{\partial z} + \frac{\partial f_{1s}}{\partial v_x} \frac{dv_x}{dt} + \frac{\partial f_{1s}}{\partial v_y} \frac{dv_y}{dt} + \frac{\partial f_{1s}}{\partial v_z} \frac{dv_z}{dt} \tag{3.14}
$$
$$
= \quad \frac{\partial f_{1s}}{\partial t} + \mathbf{v} \cdot \frac{\partial f_{1s}}{\partial \mathbf{r}} + \mathbf{a} \cdot \frac{\partial f_{1s}}{\partial \mathbf{v}} \tag{3.15}
$$
$$
= \quad \frac{\partial f_{1s}}{\partial t} + \mathbf{v} \cdot \frac{\partial f_{1s}}{\partial \mathbf{r}} + \frac{q_s}{m_s} (\mathbf{v} \times \mathbf{B}_0) \cdot \frac{\partial f_{1s}}{\partial \mathbf{v}}, \tag{3.16}
$$

where

$$
\mathbf{a} \quad = \quad \frac{d\mathbf{v}}{dt} \tag{3.17}
$$
$$
= \quad \frac{q_s}{m_s} (\mathbf{v} \times \mathbf{B}_0), \tag{3.18}
$$

is the acceleration of a particle due to the equilibrium magnetic field $\mathbf{B}_0$ (the equilibrium electric field is assumed to vanish). This means that the linearised Vlasov equation can be written, in general, as

$$
\frac{df_{1s}}{dt} = -\frac{q_s}{m_s} \left[\mathbf{E}_1 + \mathbf{v} \times \mathbf{B}_1 \right] \cdot \frac{\partial f_{0s}}{\partial \mathbf{v}}. \tag{3.19}
$$

Linearising Equations (3.2)-(3.5) then gives the set of linearised Vlasov-Maxwell equations as

$$
\frac{df_{1s}}{dt} \quad = \quad -\frac{q_s}{m_s} \left[\mathbf{E}_1 + \mathbf{v} \times \mathbf{B}_1 \right] \cdot \frac{\partial f_{0s}}{\partial \mathbf{v}}, \tag{3.20}
$$
$$
\nabla \times \mathbf{B}_1 \quad = \quad \mu_0 \mathbf{j}_1, \tag{3.21}
$$
$$
\nabla \times \mathbf{E}_1 \quad = \quad -\frac{\partial \mathbf{B}_1}{\partial t}, \tag{3.22}
$$
$$
\nabla \cdot \mathbf{B}_1 \quad = \quad 0, \tag{3.23}
$$
$$
\nabla \cdot \mathbf{E}_1 \quad = \quad \frac{\sigma_1}{\epsilon_0}. \tag{3.24}
$$

Assuming that $\mathbf{B}_1 = \nabla \times \mathbf{A}_1$, so that Equation (3.23) is satisfied, gives the linearised form of Ampère's law (Equation (3.21)) as

$$\nabla^2 \mathbf{A}_1 = -\mu_0 \mathbf{j}_1, \tag{3.25}$$

by using the vector identity

$$\nabla \times (\nabla \times \mathbf{A}) = \nabla(\nabla \cdot \mathbf{A}) - \nabla^2 \mathbf{A}, \tag{3.26}$$

and the gauge condition $\nabla \cdot \mathbf{A}_1 = 0$.

The linearised form of Faraday's law (Equation (3.22)) can be written as

$$\nabla \times \mathbf{E}_1 = -\frac{\partial}{\partial t}(\nabla \times \mathbf{A}_1), \tag{3.27}$$

$$= -\nabla \times \left(\frac{\partial \mathbf{A}_1}{\partial t}\right), \tag{3.28}$$

and removing the curl operator gives the perturbed electric field as

$$\mathbf{E}_1 = -\frac{\partial \mathbf{A}_1}{\partial t} - \nabla \phi_1, \tag{3.29}$$

where ϕ_1 is a scalar potential.

The linearised Vlasov-Maxwell equations then reduce to the following set of equations:

$$\frac{df_{1s}}{dt} = -\frac{q_s}{m_s}\left[-\frac{\partial \mathbf{A}_1}{\partial t} - \nabla \phi_1 + \mathbf{v} \times (\nabla \times \mathbf{A}_1)\right] \cdot \frac{\partial f_{0s}}{\partial \mathbf{v}}, \tag{3.30}$$

$$\nabla^2 \mathbf{A}_1 = -\mu_0 \mathbf{j}_1, \tag{3.31}$$

$$\nabla^2 \phi_1 = -\frac{\sigma_1}{\epsilon_0}, \tag{3.32}$$

where the perturbed current density, $\mathbf{j}_1$, is given in terms of the perturbed distribution function, f_{1s}, as

$$\mathbf{j}_1 = \sum_s q_s \int \mathbf{v} f_{1s} d^3 v, \tag{3.33}$$

and the perturbed charge density, σ_1, is given by

$$\sigma_1 = \sum_s q_s \int f_{1s} d^3 v. \tag{3.34}$$

3.3   Vlasov Stability - Harris Sheet

The Vlasov stability of the Harris sheet equilibrium (1.92) has been investigated by a number of authors. This equilibrium can give rise to the collisionless tearing mode, for example, which, as described by Schindler (2007), can be obtained for perturbations which are independent of the y-coordinate (the direction of the equilibrium current density), and for a symmetric perturbed vector potential, $\mathbf{A}_1$. A central difficulty in any Vlasov stability analysis is the calculation of the particle orbits, which, in general, cannot be carried out analytically without an approximation. Coppi et al. (1966) proposed an approximation in which the orbits are assumed to be straight lines for the region inside the current sheet, where the field is inhomogeneous, and helical orbits in the region outside the current sheet, where the field is approximately constant. Hoh (1966) approximated the Harris sheet field by a linear function, which gives rise to elliptic functions in the particle orbit expressions. Dobrowolny (1968) used the straight line approximation of Coppi et al. (1966), and calculated a dispersion relation for the instability, which agrees with the one calculated by Hoh (1966).

Yamanaka (1978) considered perturbations independent of the direction along the magnetic field, with the particle orbits given in terms of elliptic functions (using a similar approach to Hoh, 1966). A wave equation was solved, and a discussion given of the possible existence of a low frequency wave propagating in the direction of the equilibrium current density, which was found to depend critically on the thickness of the current sheet. Analytical and numerical estimates were given of the growth rate of the plasma wave. Instability was found to occur for an electron-ion temperature ratio of greater than 0.75.

The straight line orbit approximation used by Coppi et al. (1966) and Dobrowolny (1968) has also been used by Lapenta and Brackbill (1997) in an investigation of the drift-kink instability, which is described as 'a long wavelength, electromagnetic instability of a magnetic neutral sheet with a wave vector aligned along the direction of current flow', which may be important for magnetic reconnection in the Earth's magnetotail. As in the work by Dobrowolny (1968), two-dimensional perturbations were considered, but were chosen to be independent of the magnetic field direction, in order to pick out the required instability. It was found that the maximum growth rate decreases with the ion-electron temperature ratio, T_i/T_e, and also with the drift velocity. However, instability still occurs for high values of T_i/T_e and moderate drift velocities, conditions which correspond to those in the magnetotail. The obtained growth rates agree to an extent with previous simulation results, although at the realistic mass ratio $m_i/m_e = 1836$, a sausage mode structure was found, which does not agree with the kink mode type structure found in simulations for smaller mass ratios. The analysis by Lapenta and Brackbill (1997) is similar in some sense to that of Yamanaka (1978), but the instability was found to occur for magnetotail conditions, which was not found by Yamanaka (1978).

A study of the drift-kink instability has also been carried out by Daughton (1998), in which it is remarked that a number of the analytical approximations made by Lapenta and Brackbill (1997), which are appropriate for the collisionless tearing mode, are not valid for the drift-kink instability, due to the time scales involved. In this approach, therefore, the particle orbits were calculated numerically, by taking advantage of their periodicity. Electrostatic effects were also considered, which were not taken into account by Lapenta and Brackbill (1997). The resulting differential equations were solved by using a second order central differencing scheme. The trend of decreasing growth rate with increasing ion-electron temperature ratio was also found in this work, in agreement with Lapenta and Brackbill (1997). The simulations were only carried out for non-physical mass ratios, however, due to numerical restrictions.

In another paper by Daughton (1999), the drift-kink instability has again been discussed, in addition to the collisionless tearing mode for the Harris sheet. The exact particle orbits were calculated numerically using the same method as Daughton (1998), but in this case, a more efficient method for solving the differential equations was used, which involves expressing the unknowns (A_1 and ϕ) in terms of sums of Hermite functions (e.g. Morse and Feshbach, 1953). This method allows results to be obtained for a physical mass ratio, unlike the central differencing method used in the earlier paper (Daughton, 1998). For the collisionless tearing mode, it was found that the results agree with previous analytical results, and the same conclusion applies to the drift-kink instability, although this method shows a reduced growth rate with increasing mass ratio, contradicting what was found in the earlier paper (Daughton, 1998).

Silin et al. (2002) considered general three-dimensional perturbations, and solved Ampère's law by assuming the perturbation wavelength to be large compared with the current sheet thickness, such that the current density can be approximated by a delta function. This approach allows Ampère's law to be written as a set of algebraic equations instead of differential equaions, which can be solved numerically for the eigenvalues ω. Three different modes were then discussed, depending on the choice of perturbation - the collisionless tearing mode, sausage modes, and obliquely propagating modes. For the collisionless tearing mode, it was found that the growth rate increases as the sheet thickness is increased.

Camporeale et al. (2006) have discussed a method for solving the Vlasov stability problem for the Harris sheet equilibrium. In this method, the velocity dependence of the distribution functions are given in terms of series of Hermite polynomials. While beyond the scope of the work in this thesis, it would be interesting to investigate the use of this method for the force-free Harris sheet in future work, as it would potentially allow for an investigation into the types of microinstabilities which may occur from the multi-peaked distribution function (Harrison and Neukirch, 2009b; Neukirch, Wilson, and Harrison, 2009).

In order to illustrate the type of calculation which will be used in the next section (and in Chapter

4) to investigate the stability of the Harrison and Neukirch (2009b) equilibrium, the calculations by Lapenta and Brackbill (1997) and Silin et al. (2002) will now be discussed in more detail. Although this will not exactly match the calculation for the force-free Harris sheet (slightly different approximations will be used), much of the procedure will be the same.

Following the analysis by Lapenta and Brackbill (1997), consider firstly the Harris sheet distribution function (1.92), which can be written in terms of velocity as

$$f_{s,Harris} = \frac{\bar{n}_{0s}(z)}{\left(\sqrt{2\pi}v_{th,s}\right)^3} \exp\left[-\frac{\beta_s m_s}{2}\left(v_x^2 + (v_y - u_{ys})^2 + v_z^2\right)\right], \tag{3.35}$$

where u_{ys} is a constant drift velocity in the y-direction, and

$$\bar{n}_{0s}(z) = n_{0s}\exp\left(-\frac{\beta_s m_s}{2}u_{ys}^2 + \beta_s u_{ys} q_s A_y(z)\right), \tag{3.36}$$

with $A_y(z)$ given by the y-component of Equation (1.88). Note that Lapenta and Brackbill (1997) use x as the independent variable instead of z, but z will be used here since it has been used in the calculations throughout this thesis. The gradient of f_{0s} with respect to the velocity, $\mathbf{v}$, is given by

$$\frac{\partial f_{0s}}{\partial \mathbf{v}} = \beta_s m_s \left(-\mathbf{v} + u_{ys}\hat{\mathbf{e}}_y\right) f_{0s}, \tag{3.37}$$

where $\hat{\mathbf{e}}_y$ is a unit vector in the y-direction. This expression can then be substituted into the general linearised Vlasov equation (3.30) to give

$$\frac{df_{1s}}{dt} = -q_s\beta_s\left[-\frac{\partial \mathbf{A}_1}{\partial t} + \mathbf{v} \times (\nabla \times \mathbf{A}_1)\right] \cdot \left[-\mathbf{v} + u_{ys}\hat{\mathbf{e}}_y\right] f_{0s}, \tag{3.38}$$

where it is assumed that $\mathbf{A}_1 = (0, A_{1y}, A_{1z})$ and $\phi_1 = 0$. Equation (3.38) can then be integrated to give

$$f_{1s} = q_s\beta_s f_{0s}\left[u_{ys}A_{1y} - \int_{-\infty}^t \left(v_y'\frac{\partial A_{1y}}{\partial t'} + u_{ys}v_y'\frac{\partial A_{1y}}{\partial y'}\right)dt'\right], \tag{3.39}$$

where the integration is carried out over the unperturbed particle orbits. In Equation (3.39), the primed quantities are quantities which depend on the unperturbed orbit. Considering two-dimensional perturbations only, and assuming the following harmonic dependence,

$$A_{1y}(y, z, t) = \bar{A}_{1y}(z)\exp\left(-i\omega t + iky\right), \tag{3.40}$$

$$f_{1s}(y, z, t, \mathbf{v}) = \bar{f}_{1s}(z, \mathbf{v})\exp\left(-i\omega t + iky\right), \tag{3.41}$$

gives an expression for the z-dependent part of the perturbed distribution function as

$$
\bar{f}_{1s}(z, \mathbf{v}) = q_s \beta_s f_{0s} \left[u_{ys} \bar{A}_{1y} \right.
$$
$$
\left. + i(\omega - k u_{ys}) \int_{-\infty}^{t} v_y' \bar{A}_{1y}(z') \exp \left[-i\omega(t' - t) + ik(y' - y) \right] dt' \right]. \quad (3.42)
$$

At this point, it is assumed that $\bar{A}_{1y}(z')$ remains constant along the particle orbits, so that it can be taken outside of the orbit integral. It is argued by Daughton (1998) that this is an invalid assumption to make for the drift-kink instability, due to the time scales involved, though it is valid for the collisionless tearing mode. This then gives $\bar{f}_{1s}$ as

$$
\bar{f}_{1s}(z, \mathbf{v}) = q_s \beta_s f_{0s} \left[u_{ys} \bar{A}_{1y} \right.
$$
$$
\left. + i(\omega - k u_{ys}) \bar{A}_{1y} \int_{-\infty}^{t} v_y' \exp \left[-i\omega(t' - t) + ik(y' - y) \right] dt' \right]. \quad (3.43)
$$

It should also be noted that, in Section 3.4, two-dimensional perturbations independent of y will be considered (in a similar way to the analysis of Dobrowolny, 1968), which is different from that just described, but this calculation has been included only to give an illustration of the analytical method which will be used, with less attention being devoted to the physical meaning of the results.

For the next stage of the analysis, an expression for the particle orbits is required. In order to make analytical progress, Lapenta and Brackbill (1997) approximated the particle orbits by straight lines, as suggested by Coppi et al. (1966) and used by Dobrowolny (1968), as well as, for example, Silin et al. (2002). According to Dobrowolny (1968), the assumption of straight line orbits gives good results if it is assumed that the time integral in Equation (3.43) vanishes when $z > \sqrt{r_s L}$, where r_s is the gyroradius of particle species s (see also Coppi et al., 1966). Alternatively, the exact orbits could be calculated numerically (e.g. Daughton, 1998, 1999), or by using elliptic integrals (e.g. Hoh, 1966; Yamanaka, 1978).

Lapenta and Brackbill (1997) assume that

$$
y' - y = v_y(t' - t), \quad (3.44)
$$

where the velocity in the y-direction, v_y, is assumed to be constant. Equation (3.44) is just the equation of straight line motion at a constant velocity. The time integral in Equation (3.43) can be evaluated by introducing the integration variable $\tau = t' - t$, which gives the final expression for

the perturbed distribution function as

$$\bar{f}_{1s} = q_s \beta_s f_{0s} \left(u_{ys} - v_y \frac{\omega - k u_{ys}}{\omega - k v_y} \right) \bar{A}_{1y}. \tag{3.45}$$

The perturbed current density, $\mathbf{j}_1$, can be calculated from the perturbed distribution function (3.43) through the definition

$$\mathbf{j}_1 = \sum_s q_s \int \mathbf{v} \bar{f}_{1s} d^3 v. \tag{3.46}$$

The y-component, j_{1y}, is given by

$$j_{1y} = \begin{cases} j_{1y,adi} + J_{1y} & \text{if } z \leq \sqrt{r_s L}, \\ j_{1y,adi} & \text{if } z > \sqrt{r_s L}, \end{cases} \tag{3.47}$$

where $j_{1y,adi}$ is the adiabatic perturbed current density, which is the part of the perturbed current density that does not depend on the time integral in Equation (3.43). Note that, in the geometry considered here, the method used by Lapenta and Brackbill (1997) would involve assuming that j_{1x} vanishes, and then that j_{1z} can be calculated by integrating the Lorentz gauge condition,

$$\frac{\partial j_{1y}}{\partial y} + \frac{\partial j_{1z}}{\partial z} = 0, \tag{3.48}$$

once j_{1y} is known. The adiabatic part of j_{1y} is given by

$$j_{1y,adi} = \frac{2}{\mu_0 L^2} \frac{\bar{A}_{1y}}{\cosh^2(z/L)}. \tag{3.49}$$

Inside the current sheet, the time integral in Equation (3.43) contributes to j_{1y}, and this is reflected in the term J_{1y}, given by

$$J_{1y} = -\bar{A}_{1y} \sum_s q_s^2 \beta_s (\omega - k u_{ys}) \int \frac{v_y^2 f_{0s}}{\omega - k v_y} d^3 v. \tag{3.50}$$

The v_x- and v_z- integrations in Equation (3.50) are straightforward, and carrying these out gives J_{1y} as

$$J_{1y} = \sum_s \frac{\bar{A}_{1y} \bar{n}_{0s}(z)}{\sqrt{2\pi} v_{th,s}} q_s^2 \beta_s \left(\frac{\omega - k u_{ys}}{k} \right)$$
$$\times \int_{-\infty}^{\infty} \frac{v_y^2}{v_y - \frac{\omega}{k}} \exp\left[-\frac{\beta_s m_s}{2} (v_y - u_{ys})^2 \right] dv_y. \tag{3.51}$$

The remaining integral contains a singularity at $v_y = \omega/k$, which can be dealt with by using the

plasma dispersion function (see Appendix D). Using the substitution

$$\bar{v}_y = \frac{v_y - u_{ys}}{\sqrt{2}v_{th,s}},$$
(3.52)

and Equations (D.8) and (D.9) from Appendix D, gives J_{1y} as

$$
\begin{aligned}
J_{1y} &= -\frac{\bar{A}_{1y}}{2} \sum_s \bar{n}_{0s}(z) q_s^2 \beta_s \left(\frac{\omega - k u_{ys}}{k} \right) \\
&\quad \times \left[\left(\frac{\omega - k u_{ys}}{k} + 2u_{ys} \right) Z' \left(\frac{\omega - k u_{ys}}{\sqrt{2}k v_{th,s}} \right) - \frac{\sqrt{2}u_{ys}^2}{v_{th,s}} Z \left(\frac{\omega - k u_{ys}}{\sqrt{2}k v_{th,s}} \right) \right].
\end{aligned}
$$
(3.53)

The next stage in the calculation is to substitute the perturbed current density into Ampère's law, which gives the following second order ODE for $\bar{A}_{1y}$,

$$
\frac{d^2 \bar{A}_{1y}}{dz^2} - k^2 \bar{A}_{1y} = \begin{cases} j_{1y,adi} + J_{1y} & \text{if } z \leq \sqrt{r_s L}, \\ j_{1y,adi} & \text{if } z > \sqrt{r_s L}, \end{cases}
$$
(3.54)

where $j_{1y,adi}$ and J_{1y} are given by Equations (3.49) and (3.53), respectively. This ODE is an eigenvalue problem in $\bar{A}_{1y}$, where ω is the eigenvalue, which can be complex. J_{1y} depends on ω in a nonlinear fashion, and so this equation must be solved numerically. This can be done using a shooting method (Press et al., 1992). Note that, for the force-free Harris sheet, the perturbed current density will have both an x- and y- component, arising from the two components of the equilibrium current density, given by Equation (1.54). This means that Ampère's law will take the form of two coupled second order ODEs.

A useful approximation for evaluating the stability, which has already been described briefly, is one which has been used by Silin et al. (2002). It is assumed that the perturbation wavelength is large compared to the sheet thickness, such that the current density can be approximated by a delta function. Ampère's law takes the form of a second order ODE in $\mathbf{A}_1$, which is similar to that found by Lapenta and Brackbill (1997), and there is also another second order ODE to be solved, for the perturbed electrostatic potential, ϕ_1, which is assumed to be non-zero.

Following the analysis by Silin et al. (2002), the long wavelength assumption means that Ampère's law can be written as

$$
\left(\frac{d^2}{dz^2} - k^2 \right) \bar{A} = U(z)\delta(z),
$$
(3.55)

where $\bar{A}$ represents either $\bar{A}_{1x}$, $\bar{A}_{1y}$ or ϕ_1, and $U(z)$ represents the right-hand sides of Ampère's law, which it is not necessary to show. Integrating Equation (3.55) across a layer of thickness 2ϵ

then gives

$$\int_{-\epsilon}^{\epsilon} \frac{d^2 \bar{A}}{dz^2} dz - k^2 \int_{-\epsilon}^{\epsilon} \bar{A} dz = \int_{-\epsilon}^{\epsilon} U(z)\delta(z) dz. \tag{3.56}$$

Since $\bar{A}$ is continuous, the second integral on the left-hand side vanishes as $\epsilon \to 0$. The first integral gives the jump in the first derivative across the layer, and the integral on the right-hand side is just equal to the function U evaluated at $z = 0$. Equation (3.56) then becomes

$$\left. \frac{d\bar{A}}{dz} \right|_+ - \left. \frac{d\bar{A}}{dz} \right|_- = U(0). \tag{3.57}$$

Equation (3.55) has solutions of the form

$$\bar{A}(z) = -\frac{U(0)}{2k} e^{-k|z|}, \tag{3.58}$$

and so Equation (3.57) can be written as

$$\left. \frac{d\bar{A}}{dz} \right|_+ - \left. \frac{d\bar{A}}{dz} \right|_- = -2k\bar{A}(0), \tag{3.59}$$

This method, therefore, allows Ampère's law to be transformed into a set of algebraic equations, which can then be solved numerically by using a root finding algorithm such as the Newton Raphson method (e.g. Press et al., 1992).

3.4   Vlasov Stability - Force-Free Harris Sheet

In the present section, a stability analysis of the (Harrison and Neukirch, 2009b) equilibrium for the force-free Harris sheet will be discussed. The same general procedure as used by, for example, Lapenta and Brackbill (1997) (discussed in Section 3.3) will be used. Note, however, that due to the different nature of the equilibria, different approximations will need to be used, since the straight-line orbit approximation is not valid for the force-free Harris sheet, due to the presence of the shear field in the y-direction.

3.4.1   The Perturbed Distribution Function

The distribution function (2.59) found by Harrison and Neukirch (2009b) can be written in terms of the velocity components as

$$f_s = \frac{1}{2} \frac{n_{0s}}{\left(\sqrt{2\pi} v_{th,s}\right)^3} \exp\left[-\frac{\beta_s m_s}{2}(v_x^2 + v_y^2 + v_z^2) + \beta_s m_s u_{xs}^2\right]$$

$$\times \left[\frac{2}{C(z)} \exp\left[\beta_s m_s u_{xs}(v_y - u_{xs})\right] + \cos(\beta_s m_s u_{xs} v_x + T(z)) + \bar{b}_s \right], \tag{3.60}$$

where

$$C(z) = \cosh^2(z/L), \tag{3.61}$$

$$T(z) = 4 \tan^{-1}(e^{z/L}), \tag{3.62}$$

$$\bar{b}_s = 2b \exp\left(-\frac{\beta_s m_s}{2} u_{xs}^2\right), \tag{3.63}$$

and, as before, it is assumed that $u_{xs} = u_{ys}$.

The first stage in the stability analysis, as with the Harris sheet case, is to calculate the perturbed distribution function from the linearised Vlasov equation (3.30). Throughout the calculations in the present chapter, it will be assumed that the scalar potential ϕ_1 vanishes.

For the force-free Harris sheet, the components of $\partial f_{0s}/\partial \mathbf{v}$ are given by

$$\frac{\partial f_{0s}}{\partial v_x} = -\beta_s m_s v_x f_{0s} - \frac{1}{2}\beta_s m_s u_{xs} \frac{n_{0s}}{(\sqrt{2\pi}v_{th,s})^3} \exp\left(\beta_s m_s u_{xs}^2\right) \tag{3.64}$$

$$\times \exp\left[-\frac{\beta_s m_s}{2}(v_x^2 + v_y^2 + v_z^2)\right] \sin(\beta_s m_s u_{xs} v_x + T),$$

$$\frac{\partial f_{0s}}{\partial v_y} = -\beta_s m_s v_y f_{0s} + \frac{1}{C}\beta_s m_s u_{xs} \frac{n_{0s}}{(\sqrt{2\pi}v_{th,s})^3} \tag{3.65}$$

$$\times \exp\left[-\frac{\beta_s m_s}{2}(v_x^2 + v_y^2 + v_z^2) + \beta_s m_s u_{xs} v_y\right],$$

$$\frac{\partial f_{0s}}{\partial v_z} = -\beta_s m_s v_z f_{0s}, \tag{3.66}$$

which can be written in vector notation as

$$\frac{\partial f_{0s}}{\partial \mathbf{v}} = -\beta_s m_s \mathbf{v} f_{0s} + \beta_s m_s u_{xs} \frac{n_{0s}}{(\sqrt{2\pi}v_{th,s})^3} \exp\left[-\frac{\beta_s m_s}{2}(v_x^2 + v_y^2 + v_z^2)\right]\mathbf{V}, \tag{3.67}$$

where

$$\mathbf{V} = \left[-\frac{1}{2}\exp(\beta_s m_s u_{xs}^2)\sin(\beta_s m_s u_{xs} v_x + T), \frac{1}{C}\exp(\beta_s m_s u_{xs} v_y), 0\right]. \tag{3.68}$$

The x- and y- components of the expression

$$-\frac{\partial \mathbf{A}_1}{\partial t} + \mathbf{v} \times (\nabla \times \mathbf{A}_1), \tag{3.69}$$

from Equation (3.30), can be written as

$$
\begin{aligned}
\left[-\frac{\partial \mathbf{A}_1}{\partial t} + \mathbf{v} \times (\nabla \times \mathbf{A}_1) \right]_x &= -\frac{\partial A_{1x}}{\partial t} + v_y \frac{\partial A_{1y}}{\partial x} - v_y \frac{\partial A_{1x}}{\partial y} - v_z \frac{\partial A_{1x}}{\partial z} \\
&= -\left(\frac{\partial A_{1x}}{\partial t} + v_y \frac{\partial A_{1x}}{\partial y} + v_z \frac{\partial A_{1x}}{\partial z} + v_x \frac{\partial A_{1x}}{\partial x} \right) \\
&\quad + v_y \frac{\partial A_{1y}}{\partial x} + v_x \frac{\partial A_{1x}}{\partial x}, \\
&= -\left(\frac{\partial}{\partial t} + \mathbf{v} \cdot \nabla \right) A_{1x} + \mathbf{v} \cdot \frac{\partial \mathbf{A}_1}{\partial x},
\end{aligned}
\tag{3.70}
$$

and

$$
\begin{aligned}
\left[-\frac{\partial \mathbf{A}_1}{\partial t} + \mathbf{v} \times (\nabla \times \mathbf{A}_1) \right]_y &= -\frac{\partial A_{1y}}{\partial t} - v_z \frac{\partial A_{1y}}{\partial z} - v_x \frac{\partial A_{1y}}{\partial x} + v_x \frac{\partial A_{1x}}{\partial y} \\
&= -\left(\frac{\partial A_{1y}}{\partial t} + v_x \frac{\partial A_{1y}}{\partial x} + v_z \frac{\partial A_{1y}}{\partial z} + v_y \frac{\partial A_{1y}}{\partial y} \right) \\
&\quad + v_y \frac{\partial A_{1y}}{\partial y} + v_x \frac{\partial A_{1x}}{\partial y} \\
&= -\left(\frac{\partial}{\partial t} + \mathbf{v} \cdot \nabla \right) A_{1y} + \mathbf{v} \cdot \frac{\partial \mathbf{A}_1}{\partial y}.
\end{aligned}
\tag{3.71}
$$

Using Equations (3.68), (3.70) and (3.71) in Equation (3.30) gives the linearised Vlasov equation for the distribution function (3.60) as

$$
\begin{aligned}
\frac{df_{1s}}{dt} =\ & -q_s \beta_s \Bigg[\left(\mathbf{v} \cdot \frac{\partial \mathbf{A}_1}{\partial t} \right) f_{0s} \\
& -\frac{1}{2} \frac{u_{xs} n_{0s}}{(\sqrt{2\pi} v_{th,s})^3} \exp\left[-\frac{\beta_s m_s}{2}(v_x^2 + v_y^2 + v_z^2) + \beta_s m_s u_{xs}^2 \right] \\
& \times \sin(\beta_s m_s u_{xs} v_x + T) \left[-\left(\frac{\partial}{\partial t} + \mathbf{v} \cdot \nabla \right) A_{1x} + \mathbf{v} \cdot \frac{\partial \mathbf{A}_1}{\partial x} \right] \\
& +\frac{1}{C} \frac{u_{xs} n_{0s}}{(\sqrt{2\pi} v_{th,s})^3} \exp\left[-\frac{\beta_s m_s}{2}(v_x^2 + v_y^2 + v_z^2) + \beta_s m_s u_{xs} v_y \right] \\
& \times \left[-\left(\frac{\partial}{\partial t} + \mathbf{v} \cdot \nabla \right) A_{1y} + \mathbf{v} \cdot \frac{\partial \mathbf{A}_1}{\partial y} \right] \Bigg].
\end{aligned}
\tag{3.72}
$$

To find the perturbed distribution function, f_{1s}, Equation (3.72) must be integrated over the unperturbed particle orbits, since they are the characteristic curves of the Vlasov equation (see Section 1.3.1). They can be calculated from the equilibrium magnetic field profile, which is not straightforward to do analytically without an approximation. In Section 3.4.2, such an approximation will be discussed, and approximate particle orbits will be calculated.

Integrating Equation (3.72) in such a way, without expressing the particle orbits explicitly yet,

gives

$$
\begin{aligned}
f_{1s} \;=\; & -q_s\beta_s\Bigg[f_{0s}\int_{-\infty}^{t}\left(\mathbf{v}'\cdot\frac{\partial\mathbf{A}_1}{\partial t'}\right)dt' \\
& -\frac{1}{2}\frac{u_{xs}n_{0s}}{(\sqrt{2\pi}v_{th,s})^3}\exp(\beta_s m_s u_{xs}^2)\exp\left[-\frac{\beta_s m_s}{2}(v_x^2+v_y^2+v_z^2)\right] \\
& \times\sin(\beta_s m_s u_{xs}v_x+T)\int_{-\infty}^{t}\left[-\left(\frac{\partial}{\partial t'}+\mathbf{v}'\cdot\nabla\right)A_{1x}+\mathbf{v}'\cdot\frac{\partial\mathbf{A}_1}{\partial x'}\right]dt' \\
& +\frac{u_{xs}n_{0s}}{(\sqrt{2\pi}v_{th,s})^3}\frac{\exp(\beta_s m_s u_{xs}v_y)}{C}\exp\left[-\frac{\beta_s m_s}{2}(v_x^2+v_y^2+v_z^2)\right] \\
& \times\int_{-\infty}^{t}\left[-\left(\frac{\partial}{\partial t'}+\mathbf{v}'\cdot\nabla\right)A_{1y}+\mathbf{v}'\cdot\frac{\partial\mathbf{A}_1}{\partial y'}\right]dt'\Bigg],
\end{aligned}
\tag{3.73}
$$

where the primes refer to quantities which are time dependent (they depend on the unperturbed particle orbits). Note that the exponential and sine terms (which contain velocities) depend only on constants of motion (either the particle energy, H_s, the x-component of the canonical momentum, p_{xs}, or the y-component of the canonical momentum, p_{ys}) and so can be taken outside of the time integral. Then, using the fact that

$$
\frac{\partial}{\partial t'}+\mathbf{v}'\cdot\nabla=\frac{d}{dt'},
\tag{3.74}
$$

gives

$$
\int_{-\infty}^{t}\left[-\left(\frac{\partial}{\partial t'}+\mathbf{v}'\cdot\nabla\right)A_{1x}+\mathbf{v}'\cdot\frac{\partial\mathbf{A}_1}{\partial x'}\right]dt'=-A_{1x}+\int_{-\infty}^{t}\mathbf{v}'\cdot\frac{\partial\mathbf{A}_1}{\partial x'}dt',
\tag{3.75}
$$

and

$$
\int_{-\infty}^{t}\left[-\left(\frac{\partial}{\partial t'}+\mathbf{v}'\cdot\nabla\right)A_{1y}+\mathbf{v}'\cdot\frac{\partial\mathbf{A}_1}{\partial y'}\right]dt'=-A_{1y}+\int_{-\infty}^{t}\mathbf{v}'\cdot\frac{\partial\mathbf{A}_1}{\partial y'}dt',
\tag{3.76}
$$

which then gives the perturbed distribution function as

$$
\begin{aligned}
f_{1s} \;=\; & -q_s\beta_s\Bigg[f_{0s}\int_{-\infty}^{t}\left(\mathbf{v}'\cdot\frac{\partial\mathbf{A}_1}{\partial t'}\right)dt' \\
& -\frac{1}{2}\frac{u_{xs}n_{0s}}{(\sqrt{2\pi}v_{th,s})^3}\exp(\beta_s m_s u_{xs}^2)\exp\left[-\frac{\beta_s m_s}{2}(v_x^2+v_y^2+v_z^2)\right] \\
& \times\sin(\beta_s m_s u_{xs}v_x+T)\int_{-\infty}^{t}\mathbf{v}'\cdot\frac{\partial\mathbf{A}_1}{\partial x'}dt' \\
& +\frac{u_{xs}n_{0s}}{(\sqrt{2\pi}v_{th,s})^3}\frac{\exp(\beta_s m_s u_{xs}v_y)}{C}\exp\left[-\frac{\beta_s m_s}{2}(v_x^2+v_y^2+v_z^2)\right] \\
& \times\int_{-\infty}^{t}\mathbf{v}'\cdot\frac{\partial\mathbf{A}_1}{\partial y'}dt'
\end{aligned}
$$

$$+\frac{1}{2}\frac{u_{xs}n_{0s}}{(\sqrt{2\pi}v_{th,s})^3}\exp(\beta_s m_s u_{xs}^2)\exp\left[-\frac{\beta_s m_s}{2}(v_x^2+v_y^2+v_z^2)\right]$$

$$\times\sin(\beta_s m_s u_{xs}v_x+T)A_{1x}$$

$$-\frac{u_{xs}n_{0s}}{(\sqrt{2\pi}v_{th,s})^3}\frac{\exp(\beta_s m_s u_{xs}v_y)}{C}\times\exp\left[-\frac{\beta_s m_s}{2}(v_x^2+v_y^2+v_z^2)\right]A_{1y}\Bigg]. \qquad (3.77)$$

It will now be assumed that the perturbed quantities are two-dimensional, and depend only on x and z. Then, since the equilibrium depends only on z, it can be assumed that the perturbed quantities have a harmonic dependence on x and t, which gives $\mathbf{A}_1$ and f_{1s} as

$$\mathbf{A}_1(x,z,t) = \bar{\mathbf{A}}_1(z)\exp(-i\omega t+ikx), \qquad (3.78)$$

$$f_{1s}(x,z,t,\mathbf{v}) = \bar{f}_{1s}(z,\mathbf{v})\exp(-i\omega t+ikx). \qquad (3.79)$$

The derivatives from Equation (3.77) are then given by

$$\frac{\partial\mathbf{A}_1}{\partial t'} = -i\omega\mathbf{A}_1, \qquad (3.80)$$

$$\frac{\partial\mathbf{A}_1}{\partial x'} = ik\mathbf{A}_1, \qquad (3.81)$$

$$\frac{\partial\mathbf{A}_1}{\partial y'} = 0, \qquad (3.82)$$

which gives the perturbed distribution function as

$$\bar{f}_{1s}\exp(-i\omega t+ikx) = -q_s\beta_s\Bigg[\left(-i\omega f_{0s}-\frac{ik}{2}\frac{u_{xs}n_{0s}}{(\sqrt{2\pi}v_{th,s})^3}\exp(\beta_s m_s u_{xs}^2)\right.$$

$$\times\exp\left[-\frac{\beta_s m_s}{2}(v_x^2+v_y^2+v_z^2)\right]\sin(\beta_s m_s u_{xs}v_x+T)\Bigg)$$

$$\times\int_{-\infty}^{t}(\mathbf{v}'\cdot\bar{\mathbf{A}}_1)\exp(-i\omega t'+ikx')dt'$$

$$+\frac{1}{2}\frac{u_{xs}n_{0s}}{(\sqrt{2\pi}v_{th,s})^3}\exp\left[-\frac{\beta_s m_s}{2}(v_x^2+v_y^2+v_z^2)+\beta_s m_s u_{xs}^2\right]$$

$$\times\sin(\beta_s m_s u_{xs}v_x+T)\bar{A}_{1x}\exp(-i\omega t+ikx)$$

$$-\frac{u_{xs}n_{0s}}{(\sqrt{2\pi}v_{th,s})^3}\frac{\bar{A}_{1y}}{C}\exp(-i\omega t+ikx)$$

$$\times\exp\left[-\frac{\beta_s m_s}{2}(v_x^2+v_y^2+v_z^2)+\beta_s m_s u_{xs}v_y\right]\Bigg].$$

$$(3.83)$$

The exponential factor in Equation (3.83) can be taken over to the right-hand side, and then the

time integral in the equation becomes

$$\int_{-\infty}^{t} (\mathbf{v}' \cdot \bar{\mathbf{A}}_1) \exp(-i\omega(t' - t) + ik(x' - x))dt'. \tag{3.84}$$

At this stage, it is convenient to introduce a new integration variable, $\tau = t' - t$, which satisfies the initial conditions

$$\left.\begin{array}{c} x' \to x \\ y' \to y \\ z' \to z \end{array}\right\} \quad \text{as } \tau \to 0 \; (t' \to t). \tag{3.85}$$

The time integral (3.84) then becomes

$$\int_{-\infty}^{0} (\mathbf{v}' \cdot \bar{\mathbf{A}}_1) \exp(-i\omega\tau + ikx'(\tau))d\tau, \tag{3.86}$$

where $x'(\tau) = x' - x$. Finally, this gives the z-dependent part of the perturbed distribution function as

$$\begin{aligned}
\bar{f}_{1s} &= -q_s\beta_s\Bigg[\bigg(-i\omega f_{0s} - \frac{ik}{2}\frac{u_{xs}n_{0s}}{(\sqrt{2\pi}v_{th,s})^3}\exp\bigg[-\frac{\beta_s m_s}{2}(v_x^2 + v_y^2 + v_z^2) + \beta_s m_s u_{xs}^2\bigg] \\
&\quad \times \sin(\beta_s m_s u_{xs}v_x + T)\bigg)\int_{-\infty}^{0}(\mathbf{v}'\cdot\bar{\mathbf{A}}_1)\exp(-i\omega\tau + ikx'(\tau))d\tau \\
&\quad +\frac{1}{2}\frac{u_{xs}n_{0s}}{(\sqrt{2\pi}v_{th,s})^3}\exp\bigg[-\frac{\beta_s m_s}{2}(v_x^2 + v_y^2 + v_z^2) + \beta_s m_s u_{xs}^2\bigg] \\
&\quad \times \sin(\beta_s m_s u_{xs}v_x + T)\bar{A}_{1x} \tag{3.87} \\
&\quad -\frac{u_{xs}n_{0s}}{(\sqrt{2\pi}v_{th,s})^3}\frac{1}{C}\exp\bigg[-\frac{\beta_s m_s}{2}(v_x^2 + v_y^2 + v_z^2) + \beta_s m_s u_{xs}v_y\bigg]\bar{A}_{1y}\Bigg].
\end{aligned}$$

Once the form of the particle orbits are known, the time integral in Equation (3.87) can be evaluated, which will give the final expression for the perturbed distribution function. It should be noted, however, that the perturbed distribution function does not reveal anything about the macroinstability by itself - such information can only be achieved by taking velocity moments, and therefore it will only be necessary to use the orbit expressions when calculating the perturbed density and perturbed current density.

3.4.2 Approximate Particle Orbits

In the present section, approximate particle orbits will be calculated for the force-free Harris sheet, which can then be used in the perturbed distribution function (3.87) to calculate the perturbed density and perturbed current density. In the previous work on the Vlasov stability of the Harris sheet, a number of authors (e.g. Dobrowolny, 1968; Lapenta and Brackbill, 1997; Silin et al., 2002) have used a straight line approximation for the particle orbits, since it is not possible to obtain exact analytical expressions. Such an approximation is, however, not valid for the force-free Harris sheet, due to the presence of the shear field in the y-direction. Hence, an alternative approximation is required. Using the fact that, for increasing z in either direction, $B_{y,ffhs} \to 0$, and for decreasing z in either direction, $B_{x,ffhs} \to 0$, a reasonable approximation for the force-free Harris sheet field is a field of the form

$$\mathbf{B}_{approx} = \begin{cases} (0, B_{y0}, 0), & \text{if } |z| \leq L \text{ (inside sheet)} \\ (\text{sign}(z)B_{x0}, 0, 0), & \text{if } |z| > L \text{ (outside sheet).} \end{cases} \tag{3.88}$$

where B_{x0} and B_{y0} are constants. Figure 3.1 shows the x-component of $\mathbf{B}_{approx}$ and $B_{x,ffhs}$ plotted against $\bar{z} = z/L$, for $B_{x0} = 1$, and Figure 3.2 shows the y-component of $\mathbf{B}_{approx}$ and $B_{y,ffhs}$ plotted against $\bar{z} = z/L$, for $B_{y0} = 1$.
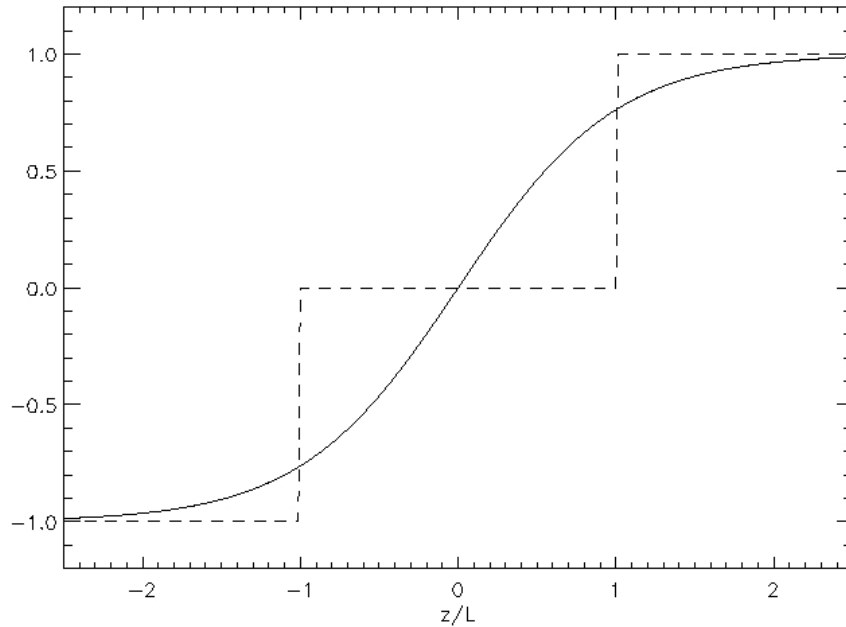
Figure 3.1: Plot of the x-component of $\mathbf{B}_{approx}$ (dashed line) and $B_{x,ffhs}$ (solid line) against $z/L = \bar{z}$, for $B_0 = B_{x0} = 1$.

Such an approximation is useful, as it allows the particle orbits to be calculated in a straightforward
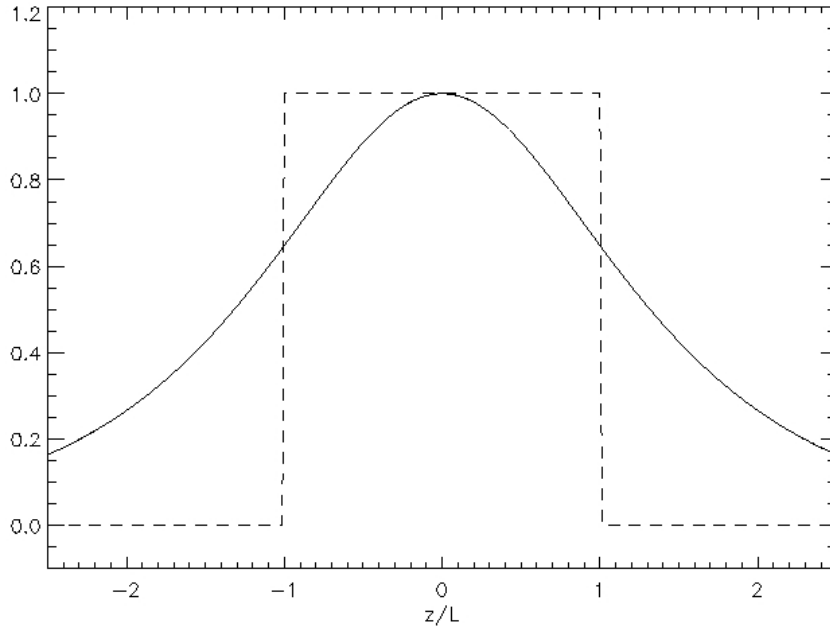
Figure 3.2: Plot of the y-component of $\mathbf{B}_{approx}$ (dashed line) and $B_{y,ffhs}$ (solid line) against $z/L = \bar{z}$, for $B_0 = B_{y0} = 1$.

way (e.g. Boyd and Sanderson, 2003) for a constant magnetic field in one coordinate direction.

The equation of motion for a particle moving in the magnetic field $\mathbf{B}_{approx}$ is given by (using τ as the time variable)

$$\frac{d\mathbf{v}}{d\tau} = \frac{q_s}{m_s}(\mathbf{v} \times \mathbf{B}). \tag{3.89}$$

For the region $z \leq L$ inside the sheet, the components of Equation (3.89) are given by

$$\frac{dv_x}{d\tau} = -\Omega_{ys}v_z, \tag{3.90}$$

$$\frac{dv_y}{d\tau} = 0, \tag{3.91}$$

$$\frac{dv_z}{d\tau} = \Omega_{ys}v_x, \tag{3.92}$$

where $\Omega_{ys} = q_s B_{y0}/m_s$ is the gyrofrequency of particle species s, resulting from the constant magnetic field B_{y0}.

Integrating Equation (3.91) gives

$$v_y = v_{||}, \tag{3.93}$$

where $v_{||}$ is the velocity parallel to the direction of the magnetic field, which is constant. Integrating Equation (3.93) then gives

$$y = v_{||}\tau + y_0, \tag{3.94}$$

where y_0 is a constant.

Equations (3.90) and (3.92) can be dealt with by defining $\chi = z + ix$ such that

$$\frac{d^2\chi}{d\tau^2} + i\Omega_{ys}\frac{d\chi}{d\tau} = 0. \tag{3.95}$$

This is a first order linear ordinary differential equation in $\dot{\chi} = d\chi/d\tau$, and the solution is

$$\dot{\chi} = \dot{\chi}(0)\exp(-i\Omega_{ys}\tau). \tag{3.96}$$

Assuming $\dot{\chi}(0) = v_\perp \exp(-i\theta)$ gives

$$\begin{aligned}
\frac{d\chi}{d\tau} &= v_\perp \exp[-i(\Omega_{ys}\tau + \theta)] \\
&= v_\perp \cos(\Omega_{ys}\tau + \theta) - iv_\perp \sin(\Omega_{ys}\tau + \theta),
\end{aligned} \tag{3.97}$$

and using the definition $\chi = z + ix$ gives

$$\begin{aligned}
v_x &= -v_\perp \sin(\Omega_{ys}\tau + \theta), \\
v_z &= v_\perp \cos(\Omega_{ys}\tau + \theta).
\end{aligned} \tag{3.98}$$

The particle orbits are, hence, given by

$$\begin{aligned}
x' &= \frac{v_\perp}{\Omega_{ys}}\cos(\Omega_{ys}\tau + \theta) + x_0', \\
y' &= v_{||}\tau + y_0', \\
z' &= \frac{v_\perp}{\Omega_{ys}}\sin(\Omega_{ys}\tau + \theta) + z_0',
\end{aligned} \tag{3.99}$$

and the velocities by

$$\begin{aligned}
v_x' &= -v_\perp \sin(\Omega_{ys}\tau + \theta), \\
v_y' &= v_{||}, \\
v_z' &= v_\perp \cos(\Omega_{ys}\tau + \theta).
\end{aligned} \tag{3.100}$$

The values of the constants of integration, x_0', y_0' and z_0' in Equations (3.99) can be found by

applying the initial conditions given in Equation (3.85). This gives

$$
\begin{aligned}
x_0' &= x - \frac{v_\perp}{\Omega_{ys}} \cos\theta, \\
y_0' &= y, \\
z_0' &= z - \frac{v_\perp}{\Omega_{ys}} \sin\theta,
\end{aligned}
\tag{3.101}
$$

which then gives the particle orbits as

$$
\begin{aligned}
x' &= \frac{v_\perp}{\Omega_{ys}} \cos(\Omega_{ys}\tau + \theta) - \frac{v_\perp}{\Omega_{ys}} \cos\theta + x, \\
y' &= v_\parallel \tau + y, \\
z' &= \frac{v_\perp}{\Omega_{ys}} \sin(\Omega_{ys}\tau + \theta) - \frac{v_\perp}{\Omega_{ys}} \sin\theta + z.
\end{aligned}
\tag{3.102}
$$

The following initial conditions on the velocities are assumed,

$$
\begin{aligned}
v_x'(0) &= v_x, \\
v_y'(0) &= v_y, \\
v_z'(0) &= v_z,
\end{aligned}
\tag{3.103}
$$

so that $v_x = -v_\perp \sin\theta, v_y = v_\parallel$ and $v_z = v_\perp \cos\theta$. The velocities (3.100) can then be expressed as

$$
\begin{aligned}
v_x' &= -v_z \sin\Omega_{ys}\tau + v_x \cos\Omega_{ys}\tau, \\
v_y' &= v_y, \\
v_z' &= v_z \cos\Omega_{ys}\tau + v_x \sin\Omega_{ys}\tau,
\end{aligned}
\tag{3.104}
$$

and so $x'(\tau)$ in the time integral (3.86) is given, for the region inside the sheet, by

$$
\begin{aligned}
x'(\tau) &= \frac{v_\perp}{\Omega_{ys}} \cos(\Omega_{ys}\tau + \theta) - \frac{v_\perp}{\Omega_{ys}} \cos\theta \\
&= \frac{v_z'}{\Omega_{ys}} - \frac{v_z}{\Omega_{ys}} \\
&= \frac{v_z}{\Omega_{ys}} \cos\Omega_{ys}\tau + \frac{v_x}{\Omega_{ys}} \sin\Omega_{ys}\tau - \frac{v_z}{\Omega_{ys}} \\
&= \frac{v_z}{\Omega_{ys}} (\cos\Omega_{ys}\tau - 1) + \frac{v_x}{\Omega_{ys}} \sin\Omega_{ys}\tau.
\end{aligned}
\tag{3.105}
$$

For the region $z > L$ outside the sheet, the components of the equation of motion (3.89) are

$$
\frac{dv_x}{d\tau} = 0,
\tag{3.106}
$$

$$
\frac{dv_y}{d\tau} = \Omega_{xs} v_z,
\tag{3.107}
$$

$$\frac{dv_z}{d\tau} = -\Omega_{xs}v_y, \tag{3.108}$$

where $\Omega_{xs} = q_s B_{x0}/m_s$ is the gyrofrequency of particle species s, resulting from the constant magnetic field B_{x0}. Equation (3.106) can be integrated to give $v_x = v_{||}$, and Equations (3.107) and (3.108) can be dealt with by this time defining $\chi = y + iz$ such that

$$\frac{d^2\chi}{d\tau^2} + i\Omega_{xs}\frac{d\chi}{d\tau} = 0. \tag{3.109}$$

Using a similar procedure as for the inner region, the particle orbits for the outer region are given by

$$\begin{aligned}
x'(\tau) &= v_x\tau, \\
v_x' &= v_{||} = v_x, \\
v_y' &= v_y\cos\Omega_{xs}\tau + v_z\sin\Omega_{xs}\tau, \\
v_z' &= -v_y\sin\Omega_{xs}\tau + v_z\cos\Omega_{xs}\tau.
\end{aligned} \tag{3.110}$$

It can be seen that the function $x'(\tau)$ is considerably simpler for the outer region than for the inner region, which means that the calculations of the perturbed density and current density outside the sheet will be simpler than those for inside the sheet. This will be illustrated in Sections 3.4.3 and 3.4.5.

3.4.3 The Perturbed Density

Knowledge of the perturbed distribution function, $\bar{f}_{1s}$, calculated in Section 3.4.1, is useful, since it can be used to calculate macroscopic perturbed quantities such as the perturbed density and perturbed current density, by taking velocity moments. Although knowledge of the perturbed density is not essential for the stability analysis, it is calculated in the present section for illustrative purposes. In addition, the calculation serves as a good exercise to prepare for the longer calculation of the perturbed current density, since some of the integrals will be needed also for this calculation.

The perturbed density, n_{1s}, is defined in terms of the perturbed distribution function, $\bar{f}_{1s}$, as

$$n_{1s} = \int \bar{f}_{1s}d^3v, \tag{3.111}$$

and can be calculated by using the appropriate values of $\mathbf{v}'$ and $x'(\tau)$ (given by Equations (3.104) and (3.105) for the region inside the sheet, and Equations (3.110) for the region outside the sheet).

The adiabatic part of the perturbed density, $n_{1s,a}$, is the part of the perturbed density which does

not contain the time integral (3.86), and is given by

$$
\begin{aligned}
n_{1s,a} &= -\frac{1}{2}q_s\beta_s\frac{u_{xs}n_{0s}}{(\sqrt{2\pi}v_{th,s})^3}\left[\exp(\beta_s m_s u_{xs}^2)\bar{A}_{1x}\int \exp\left[-\frac{\beta_s m_s}{2}(v_x^2+v_y^2+v_z^2)\right]\right. \\
&\quad \times \sin(\beta_s m_s u_{xs}v_x + T(z))d^3v \\
&\quad \left. -\frac{2\bar{A}_{1y}}{C(z)}\int \exp\left[-\frac{\beta_s m_s}{2}(v_x^2+v_y^2+v_z^2)\right]\exp(\beta_s m_s u_{xs}v_y)d^3v\right] \\
&= \frac{q_s\beta_s u_{xs}n_{0s}}{C(z)}\exp\left(\frac{\beta_s m_s}{2}u_{xs}^2\right)[\sinh(z/L)\bar{A}_{1x}+\bar{A}_{1y}],
\end{aligned}
\tag{3.112}
$$

where the identity

$$
\sin(T(z)) = -2\frac{\sinh(z/L)}{\cosh^2(z/L)},
\tag{3.113}
$$

has been used (see Appendix A for the derivation), and the velocity integrals used are detailed in Appendix E. The expression (3.112) is, of course, the same for inside and outside of the sheet, since it does not depend upon the particle orbits.

3.4.3.1 Perturbed Density Inside the Sheet

To calculate the perturbed density for the region inside the sheet, $n_{1s,in}$, the relevant equations for the particle orbits (Equations (3.104) and (3.105)) can be substituted into the time integral (3.86), which becomes

$$
\int_{-\infty}^0 (-v_z\bar{A}_{1x}\sin\Omega_{ys}\tau + v_x\bar{A}_{1x}\cos\Omega_{ys}\tau + v_y\bar{A}_{1y})\exp[X(v_x,v_z,\tau)]d\tau,
\tag{3.114}
$$

where

$$
X(v_x,v_z,\tau) = -i\omega\tau + \frac{ik}{\Omega_{ys}}(\cos\Omega_{ys}\tau - 1)v_z + \frac{ikv_x}{\Omega_{ys}}\sin\Omega_{ys}\tau.
\tag{3.115}
$$

This gives the perturbed density inside the sheet as,

$$
\begin{aligned}
n_{1s,in} &= n_{1s,a} + q_s\beta_s\left[i\omega\int f_{0s}d^3v\right. \\
&\quad \times \int_{-\infty}^0 (-v_z\bar{A}_{1x}\sin\Omega_{ys}\tau + v_x\bar{A}_{1x}\cos\Omega_{ys}\tau + v_y\bar{A}_{1y})\exp[X(v_x,v_z,\tau)]d\tau \\
&\quad + \frac{ik}{2}\frac{u_{xs}n_{0s}}{(\sqrt{2\pi}v_{th,s})^3}\exp(\beta_s m_s u_{xs}^2) \\
&\quad \times \int \exp\left[-\frac{\beta_s m_s}{2}(v_x^2+v_y^2+v_z^2)\right]\sin(\beta_s m_s u_{xs}v_x + T)d^3v
\end{aligned}
$$

$$\times \int_{-\infty}^{0} (-v_z \sin \Omega_{ys} \tau \bar{A}_{1x} + v_x \cos \Omega_{ys} \tau \bar{A}_{1x} + v_y \bar{A}_{1y})$$

$$\times \exp[X(v_x, v_z, \tau)]d\tau \Bigg], \tag{3.116}$$

where $n_{1s,a}$ is the adiabatic part of the perturbed density, given by Equation (3.112). The time and velocity integrations in Equation (3.116) can be interchanged, for convenience, since v_x, v_y and v_z do not depend on time (they are the initial values of v'_x, v'_y and v'_z, as given by Equation (3.103)). The expression for $n_{1s,in}$ then becomes

$$\begin{aligned}
n_{1s,in} = \ & n_{1s,a} + q_s \beta_s \Bigg[-i\omega \bar{A}_{1x} \int_{-\infty}^{0} \sin \Omega_{ys} \tau d\tau \int v_z f_{0s} \exp(X(v_x, v_z, \tau)) d^3v \\
& +i\omega \bar{A}_{1x} \int_{-\infty}^{0} \cos \Omega_{ys} \tau d\tau \int v_x f_{0s} \exp(X(v_x, v_z, \tau)) d^3v \\
& +i\omega \bar{A}_{1y} \int_{-\infty}^{0} d\tau \int v_y f_{0s} \exp(X(v_x, v_z, \tau)) d^3v \\
& -\frac{ik}{2} \frac{u_{xs} n_{0s}}{(\sqrt{2\pi} v_{th,s})^3} \exp(\beta_s m_s u_{xs}^2) \bar{A}_{1x} \int_{-\infty}^{0} \sin \Omega_{ys} \tau d\tau \\
& \times \int v_z \exp\left[-\frac{\beta_s m_s}{2}(v_x^2 + v_y^2 + v_z^2) \right] \\
& \times \sin(\beta_s m_s u_{xs} v_x + T) \exp(X(v_x, v_z, \tau)) d^3v \\
& +\frac{ik}{2} \frac{u_{xs} n_{0s}}{(\sqrt{2\pi} v_{th,s})^3} \exp(\beta_s m_s u_{xs}^2) \bar{A}_{1x} \int_{-\infty}^{0} \cos \Omega_{ys} \tau d\tau \\
& \times \int v_x \exp\left[-\frac{\beta_s m_s}{2}(v_x^2 + v_y^2 + v_z^2) \right] \\
& \times \sin(\beta_s m_s u_{xs} v_x + T(z)) \exp(X(v_x, v_z, \tau)) d^3v, \tag{3.117}
\end{aligned}$$

where it should be noted that the integral

$$\int_{-\infty}^{\infty} \exp\left[-\frac{\beta_s m_s}{2}(v_x^2 + v_y^2 + v_z^2) \right] \sin(\beta_s m_s u_{xs} v_x + T) d^3v$$

$$\times \int_{-\infty}^{0} v_y \bar{A}_{1y} \exp[X(v_x, v_z, \tau)] d\tau, \tag{3.118}$$

in Equation (3.116) vanishes due to the v_y-integration (the integrand is odd in v_y and the integration is carried out from $-\infty$ to ∞). At this stage, it has been assumed that the perturbed vector potential remains constant along particle orbits, and so can be taken outside of the integration. This assumption will be used throughout the calculations in the remainder of the present chapter.

The expression for $n_{1s,in}$ can also be simplified further, by writing

$$-\frac{1}{2\beta_s m_s}\frac{k^2}{\Omega_{ys}^2}(\cos\Omega_{ys}\tau - 1)^2 - \frac{1}{2\beta_s m_s}\frac{k^2}{\Omega_{ys}^2}\sin^2\Omega_{ys}\tau = K_s(\cos\Omega_{ys}\tau - 1), \tag{3.119}$$

and

$$-\frac{1}{2\beta_s m_s}\frac{k^2}{\Omega_{ys}^2}(\cos\Omega_{ys}\tau - 1)^2 - \frac{1}{2\beta_s m_s}\left(\frac{k}{\Omega_{ys}}\sin\Omega_{ys}\tau \mp \beta_s m_s u_{xs}\right)^2$$

$$= -K_s - \frac{\beta_s m_s}{2}u_{xs}^2 + K_s\cos\Omega_{ys}\tau \pm \frac{k}{\Omega_{ys}}u_{xs}\sin\Omega\tau$$

$$= -K_s - \frac{\beta_s m_s}{2}u_{xs}^2 + A_s\cos(\Omega_{ys}\tau \pm \alpha), \tag{3.120}$$

where

$$K_s = \frac{1}{\beta_s m_s}\frac{k^2}{\Omega_{ys}^2}, \tag{3.121}$$

$$A_s = \pm\frac{k}{\Omega_{ys}}\sqrt{u_{xs}^2 + \frac{K_s}{\beta_s m_s}}, \tag{3.122}$$

$$\alpha_s = \tan^{-1}\left[-\frac{1}{\beta_s m_s u_{xs}}\frac{k}{\Omega_{ys}}\right]. \tag{3.123}$$

The velocity integrations can be carried out by using some of the integrals listed in Appendix E. The expression obtained is lengthy, but a number of terms cancel with each other. Equation (3.117) contains six separate terms. After carrying out the velocity integrations, the first and second terms both contain the time integrals

$$\int_{-\infty}^0 \sin\Omega\tau\cos\Omega\tau\exp\left(-i\omega\tau + K_s\cos\Omega\tau\right)d\tau, \tag{3.124}$$

$$\int_{-\infty}^0 \sin\Omega\tau\cos\Omega\tau\exp(-i\omega\tau + A_s\cos(\Omega\tau - \alpha))d\tau, \tag{3.125}$$

and

$$\int_{-\infty}^0 \sin\Omega\tau\cos\Omega\tau\exp(-i\omega\tau + A_s\cos(\Omega\tau + \alpha))d\tau \tag{3.126}$$

which drop out due to positive and negative factors outside the integrals. The integrals (3.125) and (3.126) are also present within the fourth and fifth terms of Equation (3.117), but with different factors in front of the integrals than in the first and second terms. These integrals also drop out.

The expression for $n_{1s,in}$ then becomes

$$
\begin{aligned}
n_{1s,in} \quad = \quad & n_{1s,a} + \frac{q_s}{m_s} n_{0s} \exp\left[\frac{\beta_s m_s}{2} u_{xs}^2 - K_s\right] \\
& \times \left[\frac{i}{C}\omega\beta_s m_s u_{xs} \bar{A}_{1y} \int_{-\infty}^{0} \exp[-i\omega\tau + K_s \cos\Omega_{ys}\tau]d\tau \right. \\
& - \bar{A}_{1x} \frac{\omega k}{\Omega_{ys}}\left(\frac{1}{C} + b\right) \int_{-\infty}^{0} \sin\Omega_{ys}\tau \exp[-i\omega\tau + K_s \cos\Omega_{ys}\tau]d\tau \\
& - \frac{\bar{A}_{1x}}{4}[(\omega - iku_{xs})\cos T + (i\omega + ku_{xs})\sin T] \\
& \times \left(\frac{k}{\Omega_{ys}} \int_{-\infty}^{0} \sin\Omega_{ys}\tau \exp(-i\omega\tau + A_s \cos(\Omega_{ys}\tau - \alpha_s))d\tau \right. \\
& \left. + \beta_s m_s u_{xs} \int_{-\infty}^{0} \cos\Omega_{ys}\tau \exp(-i\omega\tau + A_s \cos(\Omega_{ys}\tau - \alpha_s))d\tau \right) \\
& - \frac{\bar{A}_{1x}}{4}[(\omega + iku_{xs})\cos T + (-i\omega + ku_{xs})\sin T] \\
& \times \left(\frac{k}{\Omega_{ys}} \int_{-\infty}^{0} \sin\Omega_{ys}\tau \exp(-i\omega\tau + A_s \cos(\Omega_{ys}\tau + \alpha_s))d\tau \right. \\
& \left. \left. - \beta_s m_s u_{xs} \int_{-\infty}^{0} \cos\Omega_{ys}\tau \exp(-i\omega\tau + A_s \cos(\Omega_{ys}\tau + \alpha_s))d\tau \right)\right], \qquad (3.127)
\end{aligned}
$$

where it should be noted that some more velocity integrals vanish since they have an odd integrand.

The time integrations can be carried out by using some of the integrals from Appendix F, which gives

$$
\begin{aligned}
n_{1s,in} \quad = \quad & n_{1s,a} + \frac{q_s}{m_s} n_{0s} \exp\left[\frac{\beta_s m_s}{2} u_{xs}^2 - K_s\right]\left[\frac{\beta_s m_s u_{xs}\omega \bar{A}_{1y}}{C} \sum_{m=-\infty}^{\infty} \frac{I_m(K_s)}{m\Omega_{ys} - \omega}\right. \\
& + \frac{\bar{A}_{1x}}{2}\frac{\omega k}{\Omega_{ys}}\left(\frac{1}{C} + b\right) \\
& \times \sum_{m=-\infty}^{\infty}\left[\frac{1}{(m+1)\Omega_{ys} - \omega} - \frac{1}{(m-1)\Omega_{ys} - \omega}\right]I_m(K_s) \\
& + \frac{\bar{A}_{1x}}{4}[(\omega - iku_{xs})\cos T + (i\omega + ku_{xs})\sin T] \\
& \left(\frac{k}{2\Omega_{ys}} \sum_{m=-\infty}^{\infty} I_m(A_s)\exp(-im\alpha_s)\left[\frac{1}{(m+1)\Omega_{ys} - \omega} - \frac{1}{(m-1)\Omega_{ys} - \omega}\right]\right. \\
& + \frac{i}{2}\beta_s m_s u_{xs} \\
& \left.\left. \times \sum_{m=-\infty}^{\infty} I_m(A_s)\exp(-im\alpha_s)\left[\frac{1}{(m+1)\Omega_{ys} - \omega} + \frac{1}{(m-1)\Omega_{ys} - \omega}\right]\right)\right.
\end{aligned}
$$

$$
+\frac{\bar{A}_{1x}}{4}[(\omega + iku_{xs})\cos T + (-i\omega + ku_{xs})\sin T]
$$

$$
\left(\frac{k}{2\Omega_{ys}}\sum_{m=-\infty}^{\infty} I_m(A_s)\exp(im\alpha_s)\left[\frac{1}{(m+1)\Omega_{ys}-\omega} - \frac{1}{(m-1)\Omega_{ys}-\omega}\right]\right.
$$

$$
-\frac{i}{2}\beta_s m_s u_{xs}
$$

$$
\left.\times\sum_{m=-\infty}^{\infty} I_m(A_s)\exp(im\alpha_s)\left[\frac{1}{(m+1)\Omega_{ys}-\omega} + \frac{1}{(m-1)\Omega_{ys}-\omega}\right]\right)\Bigg].
$$

$$(3.128)$$

In Appendix G, it is shown that the second sum in Equation (3.128) can be written as

$$
\sum_{m=-\infty}^{\infty} I_m(K_s)\left[\frac{1}{(m+1)\Omega_{ys}-\omega} - \frac{1}{(m-1)\Omega_{ys}-\omega}\right] = \frac{2}{K_s}\sum_{m=-\infty}^{\infty}\frac{mI_m(K_s)}{m\Omega_{ys}-\omega}. \quad (3.129)
$$

Using this result, together with the trigonometric expressions

$$
[(\omega - iku_{xs})\cos T + (i\omega + ku_{xs})\sin T]\exp(-im\alpha_s)
$$
$$
+[(\omega + iku_{xs})\cos T + (-i\omega + ku_{xs})\sin T]\exp(im\alpha_s)
$$
$$
= 2[\omega\cos(T - m\alpha_s) + ku_{xs}\sin(T - m\alpha_s)], \quad (3.130)
$$

and

$$
[(\omega - iku_{xs})\cos T + (i\omega + ku_{xs})\sin T]\exp(-im\alpha_s)
$$
$$
-[(\omega + iku_{xs})\cos T + (-i\omega + ku_{xs})\sin T]\exp(im\alpha_s)
$$
$$
= -2i[ku_{xs}\cos(T - m\alpha_s) - \omega\sin(T - m\alpha_s)], \quad (3.131)
$$

gives $n_{1s,in}$, finally, as

$$
n_{1s,in} = n_{1s,a} + q_s\beta_s n_{0s}\exp\left(\frac{\beta_s m_s}{2}u_{xs}^2 - K_s\right)\left[\frac{\omega\bar{A}_{1y}u_{xs}}{C}\sum_{m=-\infty}^{\infty}\frac{I_m(K_s)}{m\Omega_{ys}-\omega}\right.
$$

$$
+\bar{A}_{1x}\frac{\omega\Omega_{ys}}{k}\left(\frac{1}{C}+b\right)\sum_{m=-\infty}^{\infty}\frac{mI_m(K_s)}{m\Omega_{ys}-\omega}
$$

$$
+\frac{1}{4}\frac{\bar{A}_{1x}}{\beta_s m_s}\frac{k}{\Omega_{ys}}\sum_{m=-\infty}^{\infty}(\omega\cos(T - m\alpha_s) + ku_{xs}\sin(T - m\alpha_s))
$$

$$
\times\left[\frac{1}{(m+1)\Omega_{ys}-\omega} - \frac{1}{(m-1)\Omega_{ys}-\omega}\right]I_m(A_s)
$$

$$
+\frac{1}{4}u_{xs}\bar{A}_{1x}\sum_{m=-\infty}^{\infty}(ku_{xs}\cos(T - m\alpha_s) - \omega\sin(T - m\alpha_s))
$$

$$\times \left[\frac{1}{(m+1)\Omega_{ys} - \omega} + \frac{1}{(m-1)\Omega_{ys} - \omega} \right] I_m(A_s) \right]. \tag{3.132}$$

Note that the other Bessel function sum expressions cannot be simplified in a straightforward way, since the sum index, m, appears in the sine and cosine terms.

3.4.3.2 Perturbed Density Outside the Sheet

For the region outside the current sheet, the particle orbits are given by Equation (3.110), which gives the time integral (3.86) as

$$\int_{-\infty}^{0} [v_x \bar{A}_{1x} + (v_y \cos \Omega_{xs}\tau + v_z \sin \Omega_{xs}\tau)\bar{A}_{1y}] \exp[-i\omega\tau + ikv_x\tau]d\tau. \tag{3.133}$$

The perturbed density outside the sheet, $n_{1s,out}$, can then be calculated from the definition (3.111), and is given by

$$
\begin{aligned}
n_{1s,out} \;=\; & n_{1s,a} + q_s\beta_s \Bigg[i\omega \int f_{0s} d^3v \\
& \times \int_{-\infty}^{0} [v_x \bar{A}_{1x} + (v_y \cos \Omega_{xs}\tau + v_z \sin \Omega_{xs}\tau)\bar{A}_{1y}] \exp(-i\omega\tau + ikv_x\tau)d\tau \\
& + \frac{ik}{2} \frac{u_{xs}n_{0s}}{(\sqrt{2\pi}v_{th,s})^3} \exp(\beta_s m_s u_{xs}^2) \\
& \times \int \exp\left[-\frac{\beta_s m_s}{2}(v_x^2 + v_y^2 + v_z^2) \right] \sin(\beta_s m_s u_{xs}v_x + T)d^3v \\
& \times \int_{-\infty}^{0} [v_x \bar{A}_{1x} + (v_y \cos \Omega_{xs}\tau + v_z \sin \Omega_{xs}\tau)\bar{A}_{1y}] \exp(-i\omega\tau + ikv_x\tau)d\tau.
\end{aligned}
\tag{3.134}
$$

As in the calculation of the perturbed density inside the sheet (Section 3.4.3.1), the time and velocity integrations can be interchanged, since v_x, v_y and v_z do not depend on time. This gives

$$
\begin{aligned}
n_{1s,out} = q_s\beta_s \Bigg[& i\omega \bar{A}_{1x} \int_{-\infty}^{0} \exp(-i\omega\tau)d\tau \int v_x f_{0s} \exp(ikv_x\tau)d^3v \\
& + i\omega \bar{A}_{1y} \int_{-\infty}^{0} \cos \Omega_{xs}\tau \exp(-i\omega\tau)d\tau \int v_y f_{0s} \exp(ikv_x\tau)d^3v \\
& + \frac{ik}{2} \frac{u_{xs}n_{0s}}{(\sqrt{2\pi}v_{th,s})^3} \exp(\beta_s m_s u_{xs}^2)\bar{A}_{1x} \int_{-\infty}^{0} \exp(-i\omega\tau)d\tau \\
\times \int v_x \exp\Big[-\frac{\beta_s m_s}{2}(v_x^2 + v_y^2 + v_z^2) & + ikv_x\tau \Big] \sin(\beta_s m_s u_{xs}v_x + T)d^3v \Bigg] \\
& + n_{1s,a},
\end{aligned}
\tag{3.135}
$$

where it should be noted that the velocity integrals

$$\int_{-\infty}^{\infty} v_z f_{0s} \exp(ikv_x\tau) d^3v, \tag{3.136}$$

and

$$\int_{-\infty}^{\infty} v_y \exp\left[-\frac{\beta_s m_s}{2}\left(v_x^2 + v_y^2 + v_z^2\right) + ikv_x\tau\right] \sin(\beta_s m_s u_{xs} v_x + T) d^3v, \tag{3.137}$$

vanish as a result of the v_z- and v_y-integrations, respectively.

Carrying out the velocity integrations by using some of the integrals in Appendix E then gives

$$
\begin{aligned}
n_{1s,out} \quad &= n_{1s,a} - q_s\beta_s n_{0s} \exp\left(\frac{\beta_s m_s}{2} u_{xs}^2\right)\left[\frac{\omega k \bar{A}_{1x}}{\beta_s m_s}\left(\frac{1}{C} + b\right)\right. \\
&\times \int_{-\infty}^{0} \tau \exp\left(-i\omega\tau - \frac{k^2\tau^2}{2\beta_s m_s}\right) d\tau \\
&- \frac{i\omega u_{xs}\bar{A}_{1y}}{C}\int_{-\infty}^{0}\cos\Omega_{xs}\tau \exp\left(-i\omega\tau - \frac{k^2\tau^2}{2\beta_s m_s}\right) d\tau \\
&+ \frac{\bar{A}_{1x}k}{4\beta_s m_s}[(\omega - iku_{xs})\cos T + (i\omega + ku_{xs})\sin T] \\
&\times \int_{-\infty}^{0} \tau \exp\left(-i\omega\tau - ku_{xs}\tau - \frac{k^2\tau^2}{2\beta_s m_s}\right) d\tau \\
&+ \frac{\bar{A}_{1x}u_{xs}}{4}[(\omega - iku_{xs})\cos T + (i\omega + ku_{xs})\sin T] \\
&\times \int_{-\infty}^{0} \exp\left(-i\omega\tau - ku_{xs}\tau - \frac{k^2\tau^2}{2\beta_s m_s}\right) d\tau \\
&+ \frac{\bar{A}_{1x}k}{4\beta_s m_s}[(\omega + iku_{xs})\cos T + (-i\omega + ku_{xs})\sin T] \\
&\times \int_{-\infty}^{0} \tau \exp\left(-i\omega\tau + ku_{xs}\tau - \frac{k^2\tau^2}{2\beta_s m_s}\right) d\tau \\
&- \frac{\bar{A}_{1x}u_{xs}}{4}[(\omega + iku_{xs})\cos T + (-i\omega + ku_{xs})\sin T] \\
&\times \left.\int_{-\infty}^{0} \exp\left(-i\omega\tau + ku_{xs}\tau - \frac{k^2\tau^2}{2\beta_s m_s}\right) d\tau\right], \tag{3.138}
\end{aligned}
$$

where it should also be noted that some more velocity integrals vanish since they have an odd integrand.

The time integrals can be carried out by using some of the integrals from Appendix F, which gives the final expression for $n_{1s,out}$ as

$$n_{1s,out} \quad = \quad n_{1s,a} - q_s\beta_s n_{0s} \exp\left(\frac{\beta_s m_s}{2} u_{xs}^2\right)$$

$$\times \left[\frac{\omega}{2k} \bar{A}_{1x} \left(\frac{1}{C} + b \right) Z' \left(\frac{\omega}{\sqrt{2}|k|v_{th,s}} \right) \right.$$

$$+ \frac{\bar{A}_{1x}}{8k} \left[(\omega - iku_{xs}) \cos T + (i\omega + ku_{xs}) \sin T \right] Z' \left(\frac{\omega - iku_{xs}}{\sqrt{2}|k|v_{th,s}} \right)$$

$$+ \frac{\bar{A}_{1x}}{8k} \left[(\omega + iku_{xs}) \cos T + (-i\omega + ku_{xs}) \sin T \right] Z' \left(\frac{\omega + iku_{xs}}{\sqrt{2}|k|v_{th,s}} \right)$$

$$- \frac{i}{4} \frac{\bar{A}_{1x}u_{xs}}{\sqrt{2}|k|v_{th,s}} \left[(\omega - iku_{xs}) \cos T + (i\omega + ku_{xs}) \sin T \right]$$

$$\times Z \left(\frac{\omega - iku_{xs}}{\sqrt{2}|k|v_{th,s}} \right)$$

$$+ \frac{i}{4} \frac{\bar{A}_{1x}u_{xs}}{\sqrt{2}|k|v_{th,s}} \left[(\omega + iku_{xs}) \cos T + (-i\omega + ku_{xs}) \sin T \right]$$

$$\times Z \left(\frac{\omega + iku_{xs}}{\sqrt{2}|k|v_{th,s}} \right)$$

$$\left. - \frac{1}{2} \frac{\omega}{\sqrt{2}|k|v_{th,s}} \frac{\bar{A}_{1y}u_{xs}}{C} \left[Z \left(\frac{\omega - \Omega_{xs}}{\sqrt{2}|k|v_{th,s}} \right) + Z \left(\frac{\omega + \Omega_{xs}}{\sqrt{2}|k|v_{th,s}} \right) \right] \right], \qquad (3.139)$$

where Z is the plasma dispersion function, the properties of which are discussed further in Appendix D.

3.4.4 The Adiabatic Part of the Perturbed Current Density

Knowledge of the perturbed current density, $\mathbf{j}_1$, is essential for the stability analysis, since it can be substituted into the linearised form of Ampère's law (Equation (3.21)) to determine the perturbed fields, in addition to a dispersion relation for the instability. The perturbed current density can be obtained from the perturbed distribution function (3.87) by using the definition (3.33).

The adiabatic part of the perturbed current density, $\mathbf{j}_{1,a}$, is the part of $\mathbf{j}_1$ that does not contain the time integral (3.86). The x-component of $\mathbf{j}_{1,a}$ is given by

$$
\begin{aligned}
j_{1x,a} &= -\frac{1}{2} \sum_s q_s^2 \beta_s \frac{u_{xs}n_{0s}}{(\sqrt{2\pi}v_{th,s})^3} \exp(\beta_s m_s u_{xs}^2) \bar{A}_{1x} \\
&\quad \times \int v_x \exp \left[-\frac{\beta_s m_s}{2} (v_x^2 + v_y^2 + v_z^2) \right] \sin(\beta_s m_s u_{xs} v_x + T) d^3v \\
&= \frac{1}{2} \sum_s n_{0s} \beta_s q_s^2 u_{xs}^2 \exp \left(\frac{\beta_s m_s}{2} u_{xs}^2 \right) \left(\frac{2}{\cosh^2(z/L)} - 1 \right) \bar{A}_{1x}, \qquad (3.140)
\end{aligned}
$$

where Equation (E.13) from Appendix E has been used, together with the identity

$$\cos(4\tan^{-1} e^{z/L}) = 1 - \frac{2}{\cosh^2(z/L)}, \tag{3.141}$$

which is derived in Appendix A.

The y-component of $\mathbf{j}_{1,a}$ is given by

$$
\begin{aligned}
j_{1y,a} &= \sum_s q_s^2 \beta_s \frac{u_{xs} n_{0s}}{(\sqrt{2\pi} v_{th,s})^3} \frac{\bar{A}_{1y}}{C} \int v_y \exp\left[-\frac{\beta_s m_s}{2}(v_x^2 + v_y^2 + v_z^2) + \beta_s m_s u_{xs} v_y \right] d^3v \\
&= \sum_s n_{0s} q_s^2 u_{xs}^2 \beta_s \exp\left(\frac{\beta_s m_s}{2} u_{xs}^2 \right) \frac{\bar{A}_{1y}}{C}, \tag{3.142}
\end{aligned}
$$

where Equation (E.5) from Appendix E has been used. Note that the adiabatic current density is the same for the regions inside and outside of the sheet, since it does not depend upon the particle orbits.

As described by Schindler (2007), the adiabatic current density can be written in terms of the equilibrium current density, $\mathbf{j}_0$, as

$$\mathbf{j}_{1,a} = \frac{\partial \mathbf{j}_0}{\partial \mathbf{A}_0} \cdot \mathbf{A}_1, \tag{3.143}$$

where $\mathbf{A}_0$ and $\mathbf{A}_1$ are the equilibrium and perturbed vector potentials, respectively. It was stated in Section 1.4.2 that the components of $\mathbf{j}_0$ can be written in terms of the pressure function, P_{zz}, as

$$j_{0x} = \frac{\partial P_{zz}}{\partial A_{0x}}, \tag{3.144}$$

$$j_{0y} = \frac{\partial P_{zz}}{\partial A_{0y}}. \tag{3.145}$$

Using Equations (3.144) and (3.145) then gives the adiabatic current density as

$$\mathbf{j}_{1,a} = \left(\frac{\partial^2 P_{zz}}{\partial A_{0x}^2} \bar{A}_{1x}, \frac{\partial^2 P_{zz}}{\partial A_{0y}^2} \bar{A}_{1y}, 0 \right). \tag{3.146}$$

A simple consistency check can be carried out by checking that Equation (3.146) gives the same expressions for $j_{1x,a}$ and $j_{1y,a}$ as the ones given above in Equations (3.140) and (3.142). Starting with the force-free Harris sheet distribution function (2.59) and substituting into Equation (1.82) gives P_{zz} in terms of the microscopic parameters of the equilibrium as

$$P_{zz}(A_x, A_y) = \sum_s \frac{n_{0s}}{\beta_s} \exp\left(\frac{\beta_s m_s}{2} u_{xs}^2 \right)$$

$$\times \left[\exp(\beta_s u_{xs} q_s A_y) + \frac{1}{2} \cos(\beta_s u_{xs} q_s A_x) + b \right]. \tag{3.147}$$

The second partial derivatives of P_{zz} with respect to A_x and A_y are then given by

$$\frac{\partial^2 P_{zz}}{\partial A_x^2} = \frac{1}{2} \sum_s n_{0s} \beta_s u_{xs}^2 q_s^2 \exp\left(\frac{\beta_s m_s}{2} u_{xs}^2 \right) \left(\frac{2}{\cosh^2(z/L)} - 1 \right), \tag{3.148}$$

$$\frac{\partial^2 P_{zz}}{\partial A_y^2} = \sum_s n_{0s} \beta_s u_{xs}^2 q_s^2 \exp\left(\frac{\beta_s m_s}{2} u_{xs}^2 \right) \frac{1}{\cosh^2(z/L)}. \tag{3.149}$$

It is clear, therefore, that the expressions (3.140) and (3.142) calculated for $j_{1x,a}$ and $j_{1y,a}$ are the correct ones.

The adiabatic part of the perturbed current density can also be written in terms of the macroscopic parameters of the equilibrium as

$$j_{1x,a} = -\frac{1}{\mu_0 L^2} \left(1 - \frac{2}{\cosh^2(z/L)} \right) \bar{A}_{1x}, \tag{3.150}$$

$$j_{1y,a} = \frac{2}{\mu_0 L^2} \frac{1}{\cosh^2(z/L)} \bar{A}_{1y}, \tag{3.151}$$

by starting with the macroscopic form of P_{zz}, given by Equation (2.50). To show that everything is consistent, these expressions for $j_{1x,a}$ and $j_{1y,a}$ can be shown to be equivalent to the expressions in terms of microscopic parameters. The expressions (3.140) and (3.142) were calculated directly from the perturbed distribution function, and were shown to be equivalent to those obtained by starting with the microscopic form of P_{zz}, given by Equation (3.147). As was shown in Section 2.4, however, this expression can be simplified by using the assumption of strict charge neutrality (as used by Channell, 1976). Listed again for reference, an expression for P_{zz}, which is symmetric in electron and ion parameters, is given by

$$P_{zz} = n_0 \frac{\beta_e + \beta_i}{\beta_e \beta_i} \left[\frac{1}{2} \cos\left(\frac{2A_x}{A_0} \right) + \exp\left(\frac{2A_y}{A_0} \right) + b \right], \tag{3.152}$$

where A_0 and L are given by

$$A_0 = \frac{2(\beta_e + \beta_i)}{e \beta_e \beta_i |u_{yi} - u_{ye}|}, \tag{3.153}$$

$$L = \left[\frac{2(\beta_e + \beta_i)}{\mu_0 e^2 \beta_e \beta_i n_0 (u_{yi} - u_{ye})^2} \right]^{1/2}. \tag{3.154}$$

respectively.

Differentiating Equation (3.152) twice with respect to A_x, and using the fact that $\cos(2A_x/A_0) =$

$1 - 2/\cosh^2(z/L)$, gives

$$\frac{\partial^2 P_{zz}}{\partial A_x^2} = -n_0 \frac{\beta_e + \beta_i}{\beta_e \beta_i} \frac{2}{A_0^2} \left(1 - \frac{2}{\cosh^2(z/L)}\right) \tag{3.155}$$

$$= -\frac{n_0 e^2 \beta_e \beta_i (u_{yi} - u_{ye})^2}{2(\beta_e + \beta_i)} \left(1 - \frac{2}{\cosh^2(z/L)}\right) \tag{3.156}$$

$$= -\frac{1}{\mu_0 L^2} \left(1 - \frac{2}{\cosh^2(z/L)}\right), \tag{3.157}$$

which shows that the macroscopic expression (3.150) for $j_{1x,a}$ is equivalent to the microscopic expressions given by Equation (3.140), in addition to the x-component of Equation (3.146).

Differentiating Equation (3.152) twice with respect to A_y, and using the fact that $\exp(2A_y/A_0) = 1/\cosh^2(z/L)$, gives

$$\frac{\partial^2 P_{zz}}{\partial A_y^2} = n_0 \frac{\beta_e + \beta_i}{\beta_e \beta_i} \frac{4}{A_0^2 \cosh^2(z/L)} \tag{3.158}$$

$$= \frac{n_0 e^2 \beta_e \beta_i (u_{yi} - u_{ye})^2}{\beta_e + \beta_i} \tag{3.159}$$

$$= \frac{2}{\mu_0 L^2} \frac{1}{\cosh^2(z/L)}, \tag{3.160}$$

which shows that the macroscopic expression (3.151) for $j_{1y,a}$ is equivalent to the microscopic expressions given by Equation (3.142), in addition to the y-component of Equation (3.146).

3.4.5   The Perturbed Current Density Inside the Sheet

3.4.5.1 x-component of the Perturbed Current Density Inside the Sheet

The x-component of the perturbed current density inside the sheet is given by

$$j_{1x,in} = \sum_s q_s \int v_x \bar{f}_{1s} d^3 v, \tag{3.161}$$

using the appropriate expressions for the particle orbits (Equations (3.104) and (3.105)). As in the calculation of the density inside the sheet, the time integral in the perturbed distribution function is given by Equation (3.114). Swapping the velocity and time integrations as before, and using the fact that the velocity integral

$$\int_{-\infty}^{\infty} v_x v_y \exp\left[-\frac{\beta_s m_s}{2}\left(v_x^2 + v_y^2 + v_z^2\right) + X(v_x, v_z, \tau)\right] \sin(\beta_s m_s u_{xs} v_x + T) d^3 v, \tag{3.162}$$

vanishes, gives

$$
j_{1x,in} = -\sum_s q_s^2 \beta_s \left[i\omega \bar{A}_{1x} \int_{-\infty}^0 \sin \Omega_{ys}\tau d\tau \int v_x v_z f_{0s} \exp(X(v_x, v_z, \tau)) d^3v \right.
$$

$$
-i\omega \bar{A}_{1x} \int_{-\infty}^0 \cos \Omega_{ys}\tau d\tau \int v_x^2 f_{0s} \exp(X(v_x, v_z, \tau)) d^3v
$$

$$
-i\omega \bar{A}_{1y} \int_{-\infty}^0 d\tau \int v_x v_y f_{0s} \exp(X(v_x, v_z, \tau)) d^3v
$$

$$
+\frac{ik}{2} \frac{u_{xs} n_{0s}}{(\sqrt{2\pi} v_{th,s})^3} \exp(\beta_s m_s u_{xs}^2) \bar{A}_{1x} \int_{-\infty}^0 \sin \Omega_{ys}\tau d\tau
$$

$$
\times \int v_x v_z \exp\left[-\frac{\beta_s m_s}{2} (v_x^2 + v_y^2 + v_z^2) \right] \sin(\beta_s m_s u_{xs} v_x + T) \exp(X(v_x, v_z, \tau)) d^3v
$$

$$
-\frac{ik}{2} \frac{u_{xs} n_{0s}}{(\sqrt{2\pi} v_{th,s})^3} \exp(\beta_s m_s u_{xs}^2) \bar{A}_{1x} \int_{-\infty}^0 \cos \Omega_{ys}\tau d\tau
$$

$$
\left. \times \int v_x^2 \exp\left[-\frac{\beta_s m_s}{2} (v_x^2 + v_y^2 + v_z^2) \right] \sin(\beta_s m_s u_{xs} v_x + T) \exp(X(v_x, v_z, \tau)) d^3v \right]
$$

$$
+j_{1x,a}, \quad (3.163)
$$

where $j_{1x,a}$ is the x-component of the adiabatic part of the perturbed density, given in terms of microscopic parameters by Equation (3.140), or in terms of macroscopic parameters by Equation (3.150).

The velocity integrations can be carried out by using some of the integrals from Appendix E. Equation (3.163) contains six separate terms. After carrying out the velocity integrations, it can be seen that the first and second terms both contain the time integral

$$
\int_{-\infty}^0 \sin^2 \Omega_{ys}\tau \cos \Omega_{ys}\tau \exp[-i\omega\tau + K_s \cos \Omega_{ys}\tau] d\tau, \quad (3.164)
$$

which drops out due to the respective factors outside of the integrals (noting the definition (3.121) of K_s). Combining like terms and using Equations (3.119) and (3.120) then gives $j_{1x,in}$ as

$$
j_{1x,in} = \sum_s \frac{q_s^2}{m_s} n_{0s} \exp\left(\frac{\beta_s m_s}{2} u_{xs}^2 - K_s \right) \left[-\frac{i\omega \bar{A}_{1x}}{\beta_s m_s} \frac{k^2}{\Omega_{ys}^2} \left(\frac{1}{C(z)} + b \right) \right.
$$

$$
\times \int_{-\infty}^0 \sin^2 \Omega_{ys}\tau \exp(-i\omega\tau + K_s \cos \Omega_{ys}\tau) d\tau.
$$

$$
+\frac{i}{4} \frac{\bar{A}_{1x}}{\beta_s m_s} \frac{k}{\Omega_{ys}} [(\omega - iku_{xs}) \cos T + (i\omega + ku_{xs}) \sin T]
$$

$$
\times \int_{-\infty}^0 \sin \Omega_{ys}\tau (\cos \Omega_{ys}\tau - 1) \left(\frac{k}{\Omega_{ys}} \sin \Omega_{ys}\tau + \beta_s m_s u_{xs} \right)
$$

$$
\times \exp[-i\omega\tau + A_s \cos(\Omega_{ys}\tau - \alpha_s)] d\tau
$$

$$
+\frac{i}{4}\frac{\bar{A}_{1x}}{\beta_s m_s}\frac{k}{\Omega_{ys}}[(\omega+iku_{xs})\cos T+(-i\omega+ku_{xs})\sin T]
$$

$$
\times\int_{-\infty}^{0}\sin\Omega_{ys}\tau(\cos\Omega_{ys}\tau-1)\left(\frac{k}{\Omega_{ys}}\sin\Omega_{ys}\tau-\beta_s m_s u_{xs}\right)
$$

$$
\times\exp[-i\omega\tau+A_s\cos(\Omega_{ys}\tau+\alpha_s)]d\tau
$$

$$
+i\omega\bar{A}_{1x}\left(\frac{1}{C(z)}+b\right)\int_{-\infty}^{0}\cos\Omega_{ys}\tau\exp[-i\omega\tau+K_s\cos\Omega_{ys}\tau]d\tau
$$

$$
-\frac{\omega\bar{A}_{1y}}{C(z)}\frac{ku_{xs}}{\Omega_{ys}}\int_{-\infty}^{0}\sin\Omega_{ys}\tau\exp[-i\omega\tau+K_s\cos\Omega_{ys}\tau]d\tau
$$

$$
+\frac{i\bar{A}_{1x}}{4}[(\omega-iku_{xs})\cos T+(i\omega+ku_{xs})\sin T]
$$

$$
\times\int_{-\infty}^{0}\cos\Omega_{ys}\tau\left[1-\frac{1}{\beta_s m_s}\left(\frac{k}{\Omega_{ys}}\sin\Omega_{ys}\tau+\beta_s m_s u_{xs}\right)^2\right]
$$

$$
\times\exp[-i\omega\tau+A_s\cos(\Omega_{ys}\tau-\alpha_s)]d\tau
$$

$$
+\frac{i\bar{A}_{1x}}{4}[(\omega+iku_{xs})\cos T+(-i\omega+ku_{xs})\sin T]
$$

$$
\times\int_{-\infty}^{0}\cos\Omega_{ys}\tau\left[1-\frac{1}{\beta_s m_s}\left(\frac{k}{\Omega_{ys}}\sin\Omega_{ys}\tau-\beta_s m_s u_{xs}\right)^2\right]
$$

$$
\times\exp[-i\omega\tau+A_s\cos(\Omega_{ys}\tau+\alpha_s)]d\tau\Bigg]
$$

$$
+j_{1x,a}, \tag{3.165}
$$

where it should be noted that some more velocity integrals vanish since they have an odd integrand. Equation (3.165) contains eight different terms. There are some integrals which cancel between these terms. The second and sixth terms, when expanded out, both contain the integral

$$
\int_{-\infty}^{0}\sin^2\Omega_{ys}\tau\cos\Omega_{ys}\tau\exp[-i\omega\tau+A_s\cos(\Omega_{ys}\tau-\alpha_s)]d\tau, \tag{3.166}
$$

which drops out between the two terms, which can be seen by using the definition (3.121) of K_s. Additionally, the third and seventh terms in Equation (3.165) both contain the integral

$$
\int_{-\infty}^{0}\sin^2\Omega_{ys}\tau\cos\Omega_{ys}\tau\exp[-i\omega\tau+A_s\cos(\Omega_{ys}\tau+\alpha_s)]d\tau, \tag{3.167}
$$

which also drops out between the two terms. After these extra simplifications, $j_{1x,in}$ is given by

$$
j_{1x,in} = -\sum_s q_s^2\beta_s n_{0s}\exp\left[\frac{\beta_s m_s}{2}u_{xs}^2-K_s\right]\left[\frac{i\omega\bar{A}_{1x}}{\beta_s m_s}\left(\frac{1}{C}+b\right)\right.
$$

$$
\times\left(K_s\int_{-\infty}^{0}\sin^2\Omega_{ys}\tau\exp(-i\omega\tau+K_s\cos\Omega_{ys}\tau)d\tau\right.
$$

$$- \int_{-\infty}^{0} \cos \Omega_{ys}\tau \exp(-i\omega\tau + K_s \cos \Omega_{ys}\tau)d\tau \Bigg)$$

$$+ \frac{\bar{A}_{1y}u_{xs}}{\beta_s m_s C} \frac{\omega k}{\Omega_{ys}} \int_{-\infty}^{0} \sin \Omega_{ys}\tau \exp(-i\omega\tau + K_s \cos \Omega_{ys}\tau)d\tau$$

$$- \frac{i\bar{A}_{1x}}{4\beta_s^2 m_s^2} \frac{k}{\Omega_{ys}} ((\omega - iku_{xs})\cos T + (i\omega + ku_{xs})\sin T)$$

$$\times \Bigg(-\frac{k}{\Omega_{ys}} \int_{-\infty}^{0} \sin^2 \Omega_{ys}\tau \exp[-i\omega\tau + A\cos(\Omega_{ys}\tau - \alpha_s)]d\tau$$

$$+ \beta_s m_s u_{xs} \int_{-\infty}^{0} \sin \Omega_{ys}\tau \cos \Omega_{ys}\tau \exp[-i\omega\tau + A\cos(\Omega_{ys}\tau - \alpha_s)]d\tau$$

$$- \beta_s m_s u_{xs} \int_{-\infty}^{0} \sin \Omega_{ys}\tau \exp[-i\omega\tau + A\cos(\Omega_{ys}\tau - \alpha_s)]d\tau \Bigg)$$

$$- \frac{i\bar{A}_{1x}}{4\beta_s^2 m_s^2} \frac{k}{\Omega_{ys}} ((\omega + iku_{xs})\cos T + (-i\omega + ku_{xs})\sin T)$$

$$\times \Bigg(-\frac{k}{\Omega_{ys}} \int_{-\infty}^{0} \sin^2 \Omega_{ys}\tau \exp[-i\omega\tau + A\cos(\Omega_{ys}\tau + \alpha_s)]d\tau$$

$$- \beta_s m_s u_{xs} \int_{-\infty}^{0} \sin \Omega_{ys}\tau \cos \Omega_{ys}\tau \exp[-i\omega\tau + A\cos(\Omega_{ys}\tau + \alpha)]d\tau$$

$$+ \beta_s m_s u_{xs} \int_{-\infty}^{0} \sin \Omega_{ys}\tau \exp[-i\omega\tau + A\cos(\Omega_{ys}\tau + \alpha_s)]d\tau \Bigg)$$

$$- \frac{i\bar{A}_{1x}}{4\beta_s m_s} ((\omega - iku_{xs})\cos T + (i\omega + ku_{xs})\sin T)$$

$$\times \Bigg((1 - \beta_s m_s u_{xs}^2) \int_{-\infty}^{0} \cos \Omega_{ys}\tau \exp[-i\omega\tau + A\cos(\Omega_{ys}\tau - \alpha_s)]d\tau$$

$$- \frac{2ku_{xs}}{\Omega_{ys}} \int_{-\infty}^{0} \cos \Omega_{ys}\tau \sin \Omega_{ys}\tau \exp[-i\omega\tau + A\cos(\Omega_{ys}\tau - \alpha_s)]d\tau \Bigg)$$

$$- \frac{i\bar{A}_{1x}}{4\beta_s m_s} ((\omega + iku_{xs})\cos T + (-i\omega + ku_{xs})\sin T)$$

$$\times \Bigg((1 - \beta_s m_s u_{xs}^2) \int_{-\infty}^{0} \cos \Omega_{ys}\tau \exp[-i\omega\tau + A\cos(\Omega_{ys}\tau + \alpha_s)]d\tau$$

$$+ \frac{2ku_{xs}}{\Omega_{ys}} \int_{-\infty}^{0} \cos \Omega_{ys}\tau \sin \Omega_{ys}\tau \exp[-i\omega\tau + A\cos(\Omega_{ys}\tau + \alpha_s)]d\tau \Bigg) \Bigg]$$

$$+ j_{1x,a}. \tag{3.168}$$

The time integrations can then be carried out by using some of the integrals from Appendix F. Equations (G.7), (G.10) and (G.28) from Appendix G can also be used to simplify some of the

resulting sums over Bessel functions. In particular, the following time integrals

$$\int_{-\infty}^{0} \sin^2 \Omega_{ys}\tau \exp[-iw\tau + K_s \cos \Omega_{ys}\tau]d\tau, \tag{3.169}$$

and

$$\int_{-\infty}^{0} \cos \Omega_{ys}\tau \exp[-iw\tau + K_s \cos \Omega_{ys}\tau]d\tau, \tag{3.170}$$

in Equation (3.168) both give rise to the Bessel function sum

$$\sum_{m=-\infty}^{\infty} \frac{I'_m(K_s)}{m\Omega_{ys} - \omega}, \tag{3.171}$$

which drops out (note, however, that the integral (3.169) contains additional terms which do not cancel). After noting these simplifications, $j_{1x,in}$ is given by

$$
\begin{aligned}
j_{1x,in} \;=\; & j_{1x,a} + \sum_s q_s^2 \beta_s n_{0s} \exp\left(\frac{\beta_s m_s}{2} u_{xs}^2 - K_s\right)\left[\frac{\omega \bar{A}_{1y} u_{xs}}{C}\frac{\Omega_{ys}}{k}\sum_{m=-\infty}^{\infty}\frac{m I_m(K_s)}{m\Omega_{ys}-\omega}\right.\\
& + \omega \bar{A}_{1x}\frac{\Omega_{ys}^2}{k^2}\left(\frac{1}{C}+b\right)\sum_{m=-\infty}^{\infty}\frac{m^2 I_m(K_s)}{m\Omega_{ys}-\omega}\\
& - \frac{\bar{A}_{1x}}{4\beta_s m_s}\left(-\frac{K_s}{2}\right.\\
& \times \sum_{m=-\infty}^{\infty} I_m(A)\left[\frac{1}{(m+2)\Omega_{ys}-\omega}+\frac{1}{(m-2)\Omega_{ys}-\omega}-\frac{2}{m\Omega_{ys}-\omega}\right]\\
& \times [\omega\cos(T-m\alpha_s)+ku_{xs}\sin(T-m\alpha_s)]\\
& + \frac{ku_{xs}}{\Omega_{ys}}\sum_{m=-\infty}^{\infty} I_m(A)\left[\frac{1}{(m+1)\Omega_{ys}-\omega}-\frac{1}{(m-1)\Omega_{ys}-\omega}\right]\\
& \times [\omega\sin(T-m\alpha_s)-ku_{xs}\cos(T-m\alpha_s)]\\
& + (\beta_s m_s u_{xs}^2 - 1)\sum_{m=-\infty}^{\infty} I_m(A)\left[\frac{1}{(m+1)\Omega_{ys}-\omega}+\frac{1}{(m-1)\Omega_{ys}-\omega}\right]\\
& \times [\omega\cos(T-m\alpha_s)+ku_{xs}\sin(T-m\alpha_s)]\\
& + \frac{ku_{xs}}{2\Omega_{ys}}\sum_{m=-\infty}^{\infty} I_m(A)\left[\frac{1}{(m+2)\Omega_{ys}-\omega}-\frac{1}{(m-2)\Omega_{ys}-\omega}\right]\\
& \left.\left.\times [\omega\sin(T-m\alpha_s)-ku_{xs}\cos(T-m\alpha_s)]\right)\right],
\end{aligned}
\tag{3.172}
$$

where Equations (3.130) and (3.131) have also been used. Note that there is not an obvious way to simplify the terms with a dependence on $\cos(T-m\alpha)$ and $\sin(T-m\alpha)$, and so the sums above are left as they are.

Finally, the expression for $j_{1x,in}$ can be written in the form

$$j_{1x,in} = C_1(z, \omega, k)\bar{A}_{1x} + C_2(z, \omega, k)\bar{A}_{1y}, \tag{3.173}$$

where the coefficients $C_1(z, \omega, k)$ and $C_2(z, \omega, k)$ are given by

$$
\begin{aligned}
C_1(z, \omega, k) =\ & \frac{1}{2}\sum_s n_{0s}\beta_s u_{xs}^2 q_s^2 \exp\left(\frac{\beta_s m_s}{2}u_{xs}^2\right)\left(\frac{2}{\cosh^2(z/L)} - 1\right) \\
& + \sum_s q_s^2 \beta_s n_{0s}\exp\left(\frac{\beta_s m_s}{2}u_{xs}^2 - K_s\right) \\
& \times\left[\frac{\omega\Omega_{ys}^2}{k^2}\left(\frac{1}{C(z)} + b\right)\sum_{m=-\infty}^{\infty}\frac{m^2 I_m(K_s)}{m\Omega_{ys} - \omega}\right. \\
& - \frac{1}{4\beta_s m_s}\left(-\frac{1}{2}K_s(\omega\cos T + ku_{xs}\sin T)\right. \\
& \times\sum_{m=-\infty}^{\infty}\left[\frac{1}{(m+2)\Omega_{ys} - \omega} + \frac{1}{(m-2)\Omega_{ys} - \omega} - \frac{2}{m\Omega_{ys} - \omega}\right] \\
& \times I_m(A_s)\cos(m\alpha_s) \\
& -\frac{1}{2}K_s(\omega\sin T - ku_{xs}\cos T) \\
& \times\sum_{m=-\infty}^{\infty}\left[\frac{1}{(m+2)\Omega_{ys} - \omega} + \frac{1}{(m-2)\Omega_{ys} - \omega} - \frac{2}{m\Omega_{ys} - \omega}\right] \\
& \times I_m(A_s)\sin(m\alpha_s) \\
& +\frac{ku_{xs}}{\Omega_{ys}}(\omega\sin T - ku_{xs}\cos T) \\
& \times\sum_{m=-\infty}^{\infty}\left[\frac{1}{(m+1)\Omega_{ys} - \omega} - \frac{1}{(m-1)\Omega_{ys} - \omega}\right] I_m(A_s)\cos(m\alpha_s) \\
& -\frac{ku_{xs}}{\Omega_{ys}}(\omega\cos T + ku_{xs}\sin T) \\
& \times\sum_{m=-\infty}^{\infty}\left[\frac{1}{(m+1)\Omega_{ys} - \omega} - \frac{1}{(m-1)\Omega_{ys} - \omega}\right] I_m(A_s)\sin(m\alpha_s) \\
& +(\beta_s m_s u_{xs}^2 - 1)(\omega\cos T + ku_{xs}\sin T) \\
& \times\sum_{m=-\infty}^{\infty}\left[\frac{1}{(m+1)\Omega_{ys} - \omega} + \frac{1}{(m-1)\Omega_{ys} - \omega}\right] I_m(A_s)\cos(m\alpha_s) \\
& +(\beta_s m_s u_{xs}^2 - 1)(\omega\sin T - ku_{xs}\cos T) \\
& \times\sum_{m=-\infty}^{\infty}\left[\frac{1}{(m+1)\Omega_{ys} - \omega} + \frac{1}{(m-1)\Omega_{ys} - \omega}\right] I_m(A_s)\sin(m\alpha_s) \\
& +\frac{ku_{xs}}{2\Omega_{ys}}(\omega\sin T - ku_{xs}\cos T)
\end{aligned}
$$

$$\times \sum_{m=-\infty}^{\infty} \left[\frac{1}{(m+2)\Omega_{ys} - \omega} - \frac{1}{(m-2)\Omega_{ys} - \omega} \right] I_m(A_s) \cos(m\alpha_s)$$

$$- \frac{ku_{xs}}{2\Omega_{ys}} (\omega \cos T + ku_{xs} \sin T)$$

$$\times \left. \sum_{m=-\infty}^{\infty} \left[\frac{1}{(m+2)\Omega_{ys} - \omega} - \frac{1}{(m-2)\Omega_{ys} - \omega} \right] I_m(A_s) \sin(m\alpha_s) \right) \right],$$

$$(3.174)$$

$$C_2(z, \omega, k) = \sum_s q_s^2 \beta_s n_{0s} \exp\left(\frac{\beta_s m_s}{2} u_{xs}^2 - K_s \right) \frac{\omega u_{xs} \Omega_{ys}}{C(z)k} \sum_{m=-\infty}^{\infty} \frac{m I_m(K_s)}{m\Omega_{ys} - \omega}. \qquad (3.175)$$

The expression (3.173) is linear in $\bar{A}_{1x}$ and $\bar{A}_{1y}$, but the coefficients C_1 and C_2 depend on z, ω and k in a nonlinear fashion. This form of $j_{1x,in}$ will be used in Chaper 4, where Ampère's law is solved numerically.

3.4.5.2 y-component of the Perturbed Current Density Inside the Sheet

The y-component of the perturbed current density inside the sheet is given by

$$j_{1y,in} = \sum_s q_s \int v_y \bar{f}_{1s} d^3 v, \qquad (3.176)$$

where again Equations (3.104) and (3.105) must be used for the particle orbits inside the sheet. Swapping the velocity and time integrations, and using the fact that the velocity integrals (3.162) and

$$\int_{-\infty}^{\infty} v_y v_z \exp\left[-\frac{\beta_s m_s}{2} \left(v_x^2 + v_y^2 + v_z^2 \right) + X(v_x, v_z, \tau) \right] \sin(\beta_s m_s u_{xs} v_x + T) d^3 v, \quad (3.177)$$

vanish, gives

$$j_{1y,in} = j_{1y,a} - \sum_s q_s^2 \beta_s \left[i\omega \bar{A}_{1x} \int_{-\infty}^{0} \sin \Omega_{ys}\tau d\tau \int v_y v_z f_{0s} \exp(X(v_x, v_z, \tau)) d^3 v \right.$$

$$- i\omega \bar{A}_{1x} \int_{-\infty}^{0} \cos \Omega_{ys}\tau d\tau \int v_x v_y f_{0s} \exp(X(v_x, v_z, \tau)) d^3 v$$

$$- i\omega \bar{A}_{1y} \int_{-\infty}^{0} d\tau \int v_y^2 f_{0s} \exp(X(v_x, v_z, \tau)) d^3 v$$

$$- \frac{ik}{2} \frac{u_{xs} n_{0s}}{(\sqrt{2\pi} v_{th,s})^3} \exp(\beta_s m_s u_{xs}^2) \bar{A}_{1y} \int_{-\infty}^{0} d\tau$$

$$\times \int v_y^2 \exp\left[-\frac{\beta_s m_s}{2} (v_x^2 + v_y^2 + v_z^2) \right] \sin(\beta_s m_s u_{xs} v_x + T) \exp(X(v_x, v_z, \tau)) d^3 v \right], \quad (3.178)$$

where $j_{1y,a}$ is the y-component of the adiabatic part of the perturbed density, given in terms of microscopic parameters by Equation (3.142), or in terms of macroscopic parameters by Equation (3.151).

Carrying out the velocity integrations by using some of the integrals from Appendix E, simplifying by using Equation (3.119), and combining like terms then gives

$$
\begin{aligned}
j_{1y,in} \; = \; & j_{1y,a} + \sum_s \frac{q_s^2}{m_s} n_{0s} \exp\left[\frac{\beta_s m_s}{2} u_{xs}^2 - K_s\right] \\
& \times \left[-\frac{\bar{A}_{1x} u_{xs}}{C} \frac{\omega k}{\Omega_{ys}} \int_{-\infty}^0 \sin\Omega_{ys}\tau \exp(-i\omega\tau + K_s \cos\Omega_{ys}\tau)d\tau \right. \\
& + i\omega \bar{A}_{1y}\left(\frac{1}{C}\left(\beta_s m_s u_{xs}^2 + 1\right) + b\right) \\
& \times \int_{-\infty}^0 \exp(-i\omega\tau + K_s \cos\Omega_{ys}\tau)d\tau \\
& + \frac{i\bar{A}_{1y}}{4}\left((\omega - iku_{xs})\cos T + (i\omega + ku_{xs})\sin T\right) \\
& \times \int_{-\infty}^0 \exp\left(-i\omega\tau + K_s\cos\Omega_{ys}\tau - \frac{ku_{xs}}{\Omega_{ys}}\sin\Omega_{ys}\tau\right)d\tau \\
& + \frac{i\bar{A}_{1y}}{4}\left((\omega + iku_{xs})\cos T + (-i\omega + ku_{xs})\sin T\right) \\
& \left. \times \int_{-\infty}^0 \exp\left(-i\omega\tau + K_s\cos\Omega_{ys}\tau + \frac{ku_{xs}}{\Omega_{ys}}\sin\Omega_{ys}\tau\right)d\tau, \right. \qquad (3.179)
\end{aligned}
$$

where it should be noted that some more velocity integrals vanish since they have an odd integrand.

The time integrals can be evaluated by using some of the integrals from Appendix F, which gives j_{1ys} as

$$
\begin{aligned}
j_{1y,in} = \sum_s \frac{q_s^2}{m_s} n_{0s} \exp\left(\frac{\beta_s m_s}{2} u_{xs}^2 - K_s\right) & \left[\frac{\bar{A}_{1x}\beta_s m_s u_{xs}}{C} \frac{\omega\Omega_{ys}}{k} \sum_{m=-\infty}^{\infty} \frac{m I_m(K_s)}{m\Omega_{ys} - \omega} \right. \\
+ \omega \bar{A}_{1y}&\left(\frac{1}{C}\left(\beta_s m_s u_{xs}^2 + 1\right) + b\right) \sum_{m=-\infty}^{\infty} \frac{I_m(K_s)}{m\Omega_{ys} - \omega} \\
+ \frac{1}{2}\bar{A}_{1y} \sum_{m=-\infty}^{\infty} \left(\omega\cos(T - m\alpha_s) \right. & \left. + ku_{xs}\sin(T - m\alpha_s)\right)\frac{I_m(A)}{m\Omega_{ys} - \omega} \bigg] \\
& \qquad\qquad\qquad\qquad\qquad + j_{1y,a}, \quad (3.180)
\end{aligned}
$$

where Equation (G.7) from Appendix G has been used to simplify one of the resulting sums over Bessel functions, and Equations (3.120), (3.130) and (3.131) have also been used to simplify the expression.

Finally, the expression for $j_{1y,in}$ can be written as

$$j_{1y,in} = C_3(z, \omega, k)\bar{A}_{1x} + C_4(z, \omega, k)\bar{A}_{1y}, \tag{3.181}$$

where the coefficients $C_3(z, \omega, k)$ and $C_4(z, \omega, k)$ are given by

$$C_3(z, \omega, k) = \sum_s q_s^2 \beta_s n_{0s} \exp\left(\frac{\beta_s m_s}{2}u_{xs}^2 - K_s\right) \frac{u_{xs}\omega\Omega_{ys}}{kC(z)} \sum_{m=-\infty}^{\infty} \frac{mI_m(K_s)}{m\Omega_{ys} - \omega}, \tag{3.182}$$

$$
\begin{aligned}
C_4(z, \omega, k) = &\sum_s \frac{n_{0s}q_s^2 u_{xs}^2 \beta_s}{C(z)} \exp\left(\frac{\beta_s m_s}{2}u_{xs}^2\right) \\
&+ \sum_s \frac{q_s^2}{m_s}n_{0s}\exp\left(\frac{\beta_s m_s}{2}u_{xs}^2 - K_s\right) \\
&\times \left[\omega\left(\frac{1}{C(z)}(\beta_s m_s u_{xs}^2 + 1) + b\right) \sum_{m=-\infty}^{\infty} \frac{I_m(K_s)}{m\Omega_{ys} - \omega}\right. \\
&+ \frac{1}{2}[\omega\cos T(z) + ku_{xs}\sin T(z)] \sum_{m=-\infty}^{\infty} \frac{I_m(A)\cos m\alpha_s}{m\Omega_{ys} - \omega} \\
&\left.+ \frac{1}{2}[\omega\sin T(z) - ku_{xs}\cos T(z)] \sum_{m=-\infty}^{\infty} \frac{I_m(A)\sin m\alpha_s}{m\Omega_{ys} - \omega}\right]. \tag{3.183}
\end{aligned}
$$

Note that the coefficient $C_3(z, \omega, k)$ is equal to the coefficient $C_2(z, \omega, k)$ from $j_{1x,in}$, given by Equation (3.175).

As with the expression (3.173) for the x-component of the perturbed current density inside the sheet, the expression (3.181) is linear in $\bar{A}_{1x}$ and $\bar{A}_{1y}$, but the coefficients C_3 and C_4 are nonlinear in z, ω and k. This expression will also be used in the numerical solution of Ampère's law, discussed in Chapter 4.

3.4.6 The Perturbed Current Density Outside the Sheet

3.4.6.1 x-component of the Perturbed Current Density Outside the Sheet

For the region $z > L$ outside the current sheet, the particle orbits are given by the expressions in Equation (3.110). Swapping the velocity and time integrations, and using the fact that the velocity integrals

$$\int_{-\infty}^{\infty} v_x v_y \exp\left[ikv_x\tau - \frac{\beta_s m_s}{2}(v_x^2 + v_y^2 + v_z^2)\right]\sin(\beta_s m_s u_{xs}v_x + T)d^3v, \tag{3.184}$$

$$\int_{-\infty}^{\infty} v_x v_z \exp\left[ikv_x\tau - \frac{\beta_s m_s}{2}(v_x^2 + v_y^2 + v_z^2)\right] \sin(\beta_s m_s u_{xs} v_x + T) d^3 v, \tag{3.185}$$

and

$$\int_{-\infty}^{\infty} v_x v_z f_{0s} \exp(ikv_x\tau) d^3 v, \tag{3.186}$$

vanish, gives

$$
\begin{aligned}
j_{1x,out} &= j_{1x,a} + \sum_s q_s^2 \beta_s \int_{-\infty}^0 \exp(-i\omega\tau) d\tau \\
&\times \Bigg[i\omega \bar{A}_{1x} \int v_x^2 f_{0s} \exp(ikv_x\tau) d^3 v \\
&\quad + i\omega \bar{A}_{1y} \cos(\Omega_{xs}\tau) \int v_x v_y f_{0s} \exp(ikv_x\tau) d^3 v \\
&\quad + \frac{ik\bar{A}_{1x}}{2} \frac{u_{xs} n_{0s}}{(\sqrt{2\pi} v_{th,s})^3} \exp(\beta_s m_s u_{xs}^2) \\
&\quad \times \int v_x^2 \exp\left(ikv_x\tau - \frac{\beta_s m_s}{2}(v_x^2 + v_y^2 + v_z^2)\right) \sin(\beta_s m_s u_{xs} v_x + T(z)) d^3 v \Bigg].
\end{aligned}
\tag{3.187}
$$

The velocity integrals can be carried out by using some of the integrals listed in Appendix E, which gives

$$
\begin{aligned}
j_{1x,out} &= j_{1x,a} + \sum_s \frac{q_s^2}{m_s} n_{0s} \exp\left(\frac{\beta_s m_s}{2} u_{xs}^2\right) \\
&\times \Bigg[i\omega \bar{A}_{1x}\left(\frac{1}{C} + b\right) \int_{-\infty}^0 \left(1 - \frac{k^2\tau^2}{\beta_s m_s}\right) \exp\left(-i\omega\tau - \frac{k^2\tau^2}{2\beta_s m_s}\right) d\tau \\
&\quad - \frac{\omega k u_{xs} \bar{A}_{1y}}{C} \int_{-\infty}^0 \tau \cos(\Omega_{xs}\tau) \exp\left(-i\omega\tau - \frac{k^2\tau^2}{2\beta_s m_s}\right) d\tau \\
&\quad + \frac{i\bar{A}_{1x}}{4} \exp\left(\frac{\beta_s m_s}{2} u_{xs}^2\right) \\
&\quad \times [(\omega - iku_{xs})\cos T + (i\omega + ku_{xs})\sin T] \\
&\quad \times \int_{-\infty}^0 \left[1 - \frac{(k\tau + \beta_s m_s u_{xs})^2}{\beta_s m_s}\right] \exp\left[-i\omega\tau - \frac{(k\tau + \beta_s m_s u_{xs})^2}{2\beta_s m_s}\right] d\tau \\
&\quad + \frac{i\bar{A}_{1x}}{4} \exp\left(\frac{\beta_s m_s}{2} u_{xs}^2\right) \\
&\quad \times [(\omega + iku_{xs})\cos T + (-i\omega + ku_{xs})\sin T]
\end{aligned}
$$

$$\times \int_{-\infty}^{0} \left[1 - \frac{(k\tau - \beta_s m_s u_{xs})^2}{\beta_s m_s} \right] \exp\left[-i\omega\tau - \frac{(k\tau - \beta_s m_s u_{xs})^2}{2\beta_s m_s} \right] d\tau \Bigg],$$

(3.188)

where it should be noted that some more velocity integrals vanish since they have an odd integrand.

Carrying out the time integrals by using some of the integrals in Appendix F then gives

$$
\begin{aligned}
j_{1x,out} = \; & j_{1x,a} + \sum_s \frac{q_s^2}{m_s} n_{0s} \exp\left(\frac{\beta_s m_s}{2} u_{xs}^2 \right) \\
& \times \left[\frac{\omega \bar{A}_{1x}}{\sqrt{2}|k|v_{th,s}} \left(\frac{1}{C} + b \right) \left[Z\left(\frac{\omega}{\sqrt{2}|k|v_{th,s}} \right) + \frac{1}{2} Z''\left(\frac{\omega}{\sqrt{2}|k|v_{th,s}} \right) \right] \right. \\
& - \frac{\omega \bar{A}_{1y} u_{xs}}{4kC v_{th,s}^2} \\
& \times \left[Z'\left(\frac{\omega - \Omega_{xs}}{\sqrt{2}|k|v_{th,s}} \right) + Z'\left(\frac{\omega + \Omega_{xs}}{\sqrt{2}|k|v_{th,s}} \right) \right] \\
& + \frac{i\bar{A}_{1x}}{4} [(\omega - iku_{xs})\cos T + (i\omega + ku_{xs})\sin T] \\
& \times \left(\frac{i(\beta_s m_s u_{xs}^2 - 1)}{\sqrt{2}|k|v_{th,s}} Z\left(\frac{\omega - iku_{xs}}{\sqrt{2}|k|v_{th,s}} \right) - \frac{u_{xs}}{kv_{th,s}^2} Z'\left(\frac{\omega - iku_{xs}}{\sqrt{2}|k|v_{th,s}} \right) \right. \\
& \left. - \frac{i}{2} \frac{1}{\sqrt{2}|k|v_{th,s}} Z''\left(\frac{\omega - iku_{xs}}{\sqrt{2}|k|v_{th,s}} \right) \right) \\
& + \frac{i\bar{A}_{1x}}{4} [(\omega + iku_{xs})\cos T + (-i\omega + ku_{xs})\sin T] \\
& \times \left(\frac{i(\beta_s m_s u_{xs}^2 - 1)}{\sqrt{2}|k|v_{th,s}} Z\left(\frac{\omega + iku_{xs}}{\sqrt{2}|k|v_{th,s}} \right) + \frac{u_{xs}}{kv_{th,s}^2} Z'\left(\frac{\omega + iku_{xs}}{\sqrt{2}|k|v_{th,s}} \right) \right. \\
& \left. \left. - \frac{i}{2} \frac{1}{\sqrt{2}|k|v_{th,s}} Z''\left(\frac{\omega + iku_{xs}}{\sqrt{2}|k|v_{th,s}} \right) \right) \right],
\end{aligned}
$$

(3.189)

where Z is the plasma dispersion function (see Appendix D). This expression can be further simplified, through the use of Equation (D.3) from Appendix D, which can be differentiated to give

$$Z(\zeta) + \frac{1}{2} Z''(\zeta) = -\zeta Z'(\zeta),$$

(3.190)

giving rise to the expressions

$$Z\left(\frac{\omega}{\sqrt{2}|k|v_{th,s}} \right) + \frac{1}{2} Z''\left(\frac{\omega}{\sqrt{2}|k|v_{th,s}} \right) = -\frac{\omega}{\sqrt{2}|k|v_{th,s}} Z'\left(\frac{\omega}{\sqrt{2}|k|v_{th,s}} \right),$$

(3.191)

and

$$
\frac{i(\beta_s m_s u_{xs}^2 - 1)}{\sqrt{2}|k|v_{th,s}} Z\left(\frac{\omega \mp iku_{xs}}{\sqrt{2}|k|v_{th,s}}\right) \mp \frac{u_{xs}}{kv_{th,s}^2} Z'\left(\frac{\omega \mp iku_{xs}}{\sqrt{2}|k|v_{th,s}}\right)
$$

$$
- \frac{i}{2}\frac{1}{\sqrt{2}|k|v_{th,s}} Z''\left(\frac{\omega \mp iku_{xs}}{\sqrt{2}|k|v_{th,s}}\right)
$$

$$
= \frac{i}{\sqrt{2}|k|v_{th,s}}\left[\frac{u_{xs}^2}{v_{th,s}^2}Z\left(\frac{\omega \mp iku_{xs}}{\sqrt{2}|k|v_{th,s}}\right) + \frac{\omega \pm iku_{xs}}{\sqrt{2}|k|v_{th,s}}Z'\left(\frac{\omega \mp iku_{xs}}{\sqrt{2}|k|v_{th,s}}\right)\right]. \tag{3.192}
$$

This then gives

$$
j_{1x,out} = D_1(z,\omega,k)\bar{A}_{1x} + D_2(z,\omega,k)\bar{A}_{1y}, \tag{3.193}
$$

where the coefficients $D_1(z,\omega,k)$ and $D_2(z,\omega,k)$ are given by

$$
\begin{aligned}
D_1(z,\omega,k) &= \frac{1}{2}\sum_s q_s^2\beta_s n_{0s}u_{xs}^2\exp\left(\frac{\beta_s m_s}{2}u_{xs}^2\right)\left(\frac{2}{C}-1\right)\\
&\quad - \sum_s q_s^2\beta_s n_{0s}\exp\left(\frac{\beta_s m_s}{2}u_{xs}^2\right)\left[\frac{\omega^2}{2k^2}\left(\frac{1}{C}+b\right)Z'\left(\frac{\omega}{\sqrt{2}|k|v_{th,s}}\right)\right.\\
&\quad + \frac{v_{th,s}}{4\sqrt{2}|k|}[(\omega - iku_{xs})\cos T + (i\omega + ku_{xs})\sin T]\\
&\quad \times\left[\frac{u_{xs}^2}{v_{th,s}^2}Z\left(\frac{\omega - iku_{xs}}{\sqrt{2}|k|v_{th,s}}\right) + \frac{\omega + iku_{xs}}{\sqrt{2}|k|v_{th,s}}Z'\left(\frac{\omega - iku_{xs}}{\sqrt{2}|k|v_{th,s}}\right)\right]\\
&\quad + \frac{v_{th,s}}{4\sqrt{2}|k|}[(\omega - iku_{xs})\cos T + (-i\omega + ku_{xs})\sin T]\\
&\quad \left.\times\left[\frac{u_{xs}^2}{v_{th,s}^2}Z\left(\frac{\omega + iku_{xs}}{\sqrt{2}|k|v_{th,s}}\right) + \frac{\omega - iku_{xs}}{\sqrt{2}|k|v_{th,s}}Z'\left(\frac{\omega + iku_{xs}}{\sqrt{2}|k|v_{th,s}}\right)\right]\right], \tag{3.194}
\end{aligned}
$$

$$
\begin{aligned}
D_2(z,\omega,k) &= -\frac{\omega}{4kC(z)}\sum_s q_s^2\beta_s n_{0s}u_{xs}\exp\left(\frac{\beta_s m_s}{2}u_{xs}^2\right)\\
&\quad \times\left[Z'\left(\frac{\omega - \Omega_{xs}}{\sqrt{2}|k|v_{th,s}}\right) + Z'\left(\frac{\omega + \Omega_{xs}}{\sqrt{2}|k|v_{th,s}}\right)\right]. \tag{3.195}
\end{aligned}
$$

3.4.6.2 y-component of the Perturbed Current Density Outside Sheet

The relevant particle orbits are again given by the expressions in Equation (3.110). Swapping the velocity and time integrations, and using the fact that the velocity integrals (3.184),

$$
\int_{-\infty}^{\infty} v_y v_z f_{0s}\exp(ikv_x\tau)d^3v, \tag{3.196}
$$

and

$$\int_{-\infty}^{\infty} v_y v_z \exp\left[ikv_x\tau - \frac{\beta_s m_s}{2}(v_x^2 + v_y^2 + v_z^2)\right] \sin(\beta_s m_s u_{xs} v_x + T)d^3v, \tag{3.197}$$

vanish, gives the y-component of $\mathbf{j}_1$ outside the sheet as

$$
\begin{aligned}
j_{1y,out} \;=\;& j_{1y,a} + \sum_s q_s^2 \beta_s \int_{-\infty}^0 \exp(-i\omega\tau)d\tau \\
& \times \Bigg[i\omega\bar{A}_{1x}\int v_x v_y f_{0s}\exp(ikv_x\tau)d^3v \\
& + i\omega\cos(\Omega_{xs}\tau)\bar{A}_{1y}\int v_y^2 f_{0s}\exp(ikv_x\tau)d^3v \\
& + \frac{ik}{2}\frac{u_{xs}n_{0s}}{(\sqrt{2\pi}v_{th,s})^3}\exp\left(\beta_s m_s u_{xs}^2\right)\cos(\Omega_{xs}\tau)\bar{A}_{1y} \\
& \times \int v_y^2 \exp\left(-\frac{\beta_s m_s}{2}(v_x^2 + v_y^2 + v_z^2) + ikv_x\tau\right)\sin(\beta_s m_s u_{xs}v_x + T)d^3v\Bigg].
\end{aligned}
\tag{3.198}
$$

After carrying out the velocity integrations, again by using some of the integrals from Appendix E, the expression becomes

$$
\begin{aligned}
j_{1y,out} \;=\;& j_{1y,a} + \sum_s \frac{q_s^2}{m_s}n_{0s}\exp\left(\frac{\beta_s m_s}{2}u_{xs}^2\right) \times \\
& \Bigg[-\frac{\omega k u_{xs}\bar{A}_{1x}}{C}\int_{-\infty}^0 \tau\exp\left(-i\omega\tau - \frac{k^2\tau^2}{2\beta_s m_s}\right)d\tau \\
& + i\omega\bar{A}_{1y}\left[\frac{1}{C}\left(\beta_s m_s u_{xs}^2 + 1\right) + b\right] \\
& \times \int_{-\infty}^0 \cos(\Omega_{xs}\tau)\exp\left(-i\omega\tau - \frac{k^2\tau^2}{2\beta_s m_s}\right)d\tau \\
& + \frac{i\bar{A}_{1y}}{4}\exp\left(\frac{\beta_s m_s}{2}u_{xs}^2\right) \\
& \times [(\omega - ik u_{xs})\cos T + (i\omega + k u_{xs})\sin T] \\
& \times \int_{-\infty}^0 \cos(\Omega_{xs}\tau)\exp\left(-i\omega\tau - \frac{(k\tau + \beta_s m_s u_{xs})^2}{2\beta_s m_s}\right)d\tau \\
& + \frac{i\bar{A}_{1y}}{4}\exp\left(\frac{\beta_s m_s}{2}u_{xs}^2\right) \\
& \times [(\omega + ik u_{xs})\cos T + (-i\omega + k u_{xs})\sin T]] \\
& \times \int_{-\infty}^0 \cos(\Omega_{xs}\tau)\exp\left(-i\omega\tau - \frac{(k\tau - \beta_s m_s u_{xs})^2}{2\beta_s m_s}\right)d\tau\Bigg],
\end{aligned}
\tag{3.199}
$$

where it should be noted that some more velocity integrals vanish since they have an odd integrand.

The time integrals can then be evaluated by using some of the integrals from Appendix F, which gives $j_{1y,out}$ as

$$j_{1y,out} = D_3(z, \omega, k)\bar{A}_{1x} + D_4(z, \omega, k)\bar{A}_{1y}, \tag{3.200}$$

where the coefficients $D_3(z, \omega, k)$ and $D_4(z, \omega, k)$ are given by

$$D_3(z, \omega, k) = -\frac{\omega}{2kC} \sum_s q_s^2 \beta_s n_{0s} u_{xs} \exp\left(\frac{\beta_s m_s}{2} u_{xs}^2\right) Z'\left(\frac{\omega}{\sqrt{2}|k|v_{th,s}}\right), \tag{3.201}$$

$$
\begin{aligned}
D_4(z, \omega, k) = {} & \frac{1}{C} \sum_s n_{0s} q_s^2 u_{xs}^2 \beta_s \exp\left(\frac{\beta_s m_s}{2} u_{xs}^2\right) \\
& + \sum_s q_s^2 \beta_s n_{0s} \exp\left(\frac{\beta_s m_s}{2} u_{xs}^2\right) \\
& \times \left[\frac{\omega v_{th,s}}{2\sqrt{2}|k|} \left(\frac{1}{C}(\beta_s m_s u_{xs}^2 + 1) + b \right) \right. \\
& \times \left[Z\left(\frac{\omega + \Omega_{xs}}{\sqrt{2}|k|v_{th,s}}\right) + Z\left(\frac{\omega - \Omega_{xs}}{\sqrt{2}|k|v_{th,s}}\right) \right] \\
& + \frac{v_{th,s}}{8\sqrt{2}|k|} \left[(\omega - iku_{xs})\cos T + (i\omega + ku_{xs})\sin T \right] \\
& \times \left[Z\left(\frac{\omega - \Omega_{xs} - iku_{xs}}{\sqrt{2}|k|v_{th,s}}\right) + Z\left(\frac{\omega + \Omega_{xs} - iku_{xs}}{\sqrt{2}|k|v_{th,s}}\right) \right] \\
& + \frac{v_{th,s}}{8\sqrt{2}|k|} \left[(\omega + iku_{xs})\cos T + (-i\omega + ku_{xs})\sin T \right] \\
& \left. \times \left[Z\left(\frac{\omega - \Omega_{xs} + iku_{xs}}{\sqrt{2}|k|v_{th,s}}\right) + Z\left(\frac{\omega + \Omega_{xs} + iku_{xs}}{\sqrt{2}|k|v_{th,s}}\right) \right] \right],
\end{aligned}
\tag{3.202}
$$

where Z is the plasma dispersion function (see Appendix D).

3.5 Summary

The present chapter has focused on Vlasov stability. The initial steps have been carried out for a linear stability analysis of the equilibrium found by Harrison and Neukirch (2009b) for the force-free Harris sheet. After linearising the Vlasov-Maxwell equations, the perturbed distribution function was calculated by integrating the linearised Vlasov equation over the unperturbed particle orbits, since these are the characteristic curves of the Vlasov equation. All quantities were assumed to be independent of the y-coordinate, and to have a harmonic dependence on the x-coordinate and time.

In the calculation of the perturbed distribution function, the explicit expressions for the particle orbits were not given, although the expression contains a time integral depending upon them. The reasons for not giving the explicit expressions initially were twofold. Firstly, when calculating the perturbed density and current density later in the chapter, it was convenient to swap the order of integration and carry out the velocity integration first, thus the explicit particle orbits were used at this particular stage. The second reason was to keep things general since, in order to calculate the expressions for the particle orbits, it was necessary to use an approximation for the force-free Harris sheet field. The straight-line approximation, which has been used by various authors for the Harris sheet (e.g. Dobrowolny, 1968; Lapenta and Brackbill, 1997; Silin et al., 2002), is not appropriate for the force-free Harris sheet, due to the presence of the shear field $B_{y,ffhs}$. Another approximation was required, therefore, and the force-free Harris sheet field was approximated by two separate regions of constant magnetic field: an inner region, where the field is in the y-direction only, and an outer region, where the field is in the x-direction only. Although not ideal, this is a reasonable approximation to use, due to the fact that $B_{y,ffhs} = B_0/\cosh(z/L)$ tends to zero as z gets larger, and $B_{x,ffhs} = B_0 \tanh(z/L)$ heads to a constant value, and as z approaches zero from the positive and negative directions, $B_{y,ffhs}$ becomes more significant, reaching its maximum value at $z = 0$, whereas $B_{x,ffhs}$ gets less significant, vanishing at $z = 0$. It was then straightforward to calculate approximate particle orbits.

The perturbed distribution function was then used together with the approximate particle orbit expressions to calculate the perturbed density and current density. The perturbed density is not required for the stability investigation, but was calculated for completeness, and also because its calculation served as a good exercise to prepare for the longer calculation of the perturbed current density. For the region inside the current sheet, the perturbed density and perturbed current density expressions contain infinite sums of Bessel functions, which also include the eigenvalue ω (though not in the arguments of the Bessel functions). In the region outside the sheet, the expressions contain plasma dispersion functions, with the eigenvalue ω appearing in the arguments of the functions.

In Chapter 4, an approximate numerical solution of Ampère's law is given, in which it is assumed that the perturbation wavelength is large compared with the current sheet thickness, such that the current density can be approximated by a delta function (as used by Silin et al., 2002). The current density then only needs to be evaluated at $z = 0$ (so only the expressions for $j_{1x,in}$ and $j_{1y,in}$ will be needed), and Ampère's law can be reduced to a set of coupled algebraic equations, which can be solved to give various dispersion plots for the collisionless tearing mode.

Chapter 4

Numerical Investigation of Stability

4.1 Introduction

In Chapter 3, the calculations of the perturbed distribution function and, hence, the perturbed current density, were carried out for the Harrison and Neukirch (2009b) equilibrium for the force-free Harris sheet. In the present chapter, an approximate solution of Ampère's law is discussed, in which it is assumed that the perturbation wavelength is large compared with the current sheet thickness, such that the current density can be approximated by a delta function (as used by Silin et al., 2002). This simplifying approximation allows Ampère's law, in the form of two coupled second order ODEs, to be reduced to two coupled algebraic equations, which can be solved numerically via the Newton-Raphson method, for example, to give various dispersion plots for the instability. In Section 4.2, the full form of Ampère's law is given, and the approximate form is discussed in Section 4.3. In Section 4.4, the results of the numerical investigation are discussed, and several dispersion plots for the instability are given.

In Section 4.5, analytical solutions of Ampère's law in the outer region are discussed, which can be obtained by neglecting the plasma dispersion functions in Equations (3.193) and (3.200), and therefore assuming that the perturbed current density in the outer region consists only of the adiabatic part, given by Equations (3.140) and (3.142). Such solutions could be used when solving Ampère's law without the delta function approximation.

4.2 Ampère's Law

After calculating the perturbed current density components, the next stage in the stability analysis is to solve Ampère's Law,

$$\nabla \times \mathbf{B}_1 = \mu_0 \mathbf{j}_1, \tag{4.1}$$

to obtain dispersion plots for the instability. It was shown in Section 3.2 that Ampère's law can be written as

$$\nabla^2 \mathbf{A}_1 = -\mu_0 \mathbf{j}_1, \tag{4.2}$$

which can be written (using Equation (3.78)) as the following pair of coupled second order ODEs:

$$\frac{d^2 \bar{A}_{1x}}{dz^2} - k^2 \bar{A}_{1x} = -\mu_0 j_{1xs}(\bar{A}_{1x}, \bar{A}_{1y}, z), \tag{4.3}$$

$$\frac{d^2 \bar{A}_{1y}}{dz^2} - k^2 \bar{A}_{1y} = -\mu_0 j_{1ys}(\bar{A}_{1x}, \bar{A}_{1y}, z), \tag{4.4}$$

where

$$j_{1x} = \begin{cases} C_1(z, \omega, k)\bar{A}_{1x} + C_2(z, \omega, k)\bar{A}_{1y} & \text{if } z \leq L \text{ (inside sheet)} \\ D_1(z, \omega, k)\bar{A}_{1x} + D_2(z, \omega, k)\bar{A}_{1x} & \text{if } z > L \text{ (outside sheet)} \end{cases}, \tag{4.5}$$

$$j_{1y} = \begin{cases} C_2(z, \omega)\bar{A}_{1x} + C_4(z, \omega)\bar{A}_{1y} & \text{if } z \leq L \text{ (inside sheet)} \\ D_3(z, \omega, k)\bar{A}_{1x} + D_4(z, \omega, k)\bar{A}_{1x} & \text{if } z > L \text{ (outside sheet)} \end{cases}, \tag{4.6}$$

with the coefficients C_1, C_2, C_4, D_1, D_2, D_3 and D_4 given by Equations (3.174), (3.175), (3.183), (3.194), (3.195), (3.201) and (3.202), respectively. The coefficients depend on z, the eigenvalue ω, and wavenumber k. To solve Equations (4.3) and (4.4), a numerical method such as the shooting method (e.g. Stoer and Bulirsch, 1980; Press et al., 1992) is required to find the eigenvalues. This would involve writing Ampère's law as a set of ten coupled first order ODEs, since two additional ODEs would be required to determine the eigenvalues (Stoer and Bulirsch, 1980). The shooting method approach is beyond the scope of this thesis, however, and, in the next section, an alternative method for approximating Ampère's law is discussed.

4.3   Approximating Ampère's Law

An approximate solution of Ampère's law can be obtained via a method which has previously been used by Silin et al. (2002) for the Harris sheet (see Section 3.3). The method involves assuming that the perturbation wavelength is large compared with the sheet thickness, such that the current density can be approximated by a delta function, which is only non-zero at $z = 0$. As discussed previously in Section 3.3, the components of Ampère's law become

$$\left(\frac{d^2}{dz^2} - k^2 \right) \bar{A} = U(z)\delta(z), \tag{4.7}$$

where $\bar{A}$ represents either $\bar{A}_{1x}$ or $\bar{A}_{1y}$, and $U(z)$ represents the right-hand side expressions from Equations (4.3) and (4.4) for the inner region, multiplied by an additional factor of the length

scale L, in order to keep the delta function dimensionless (the dimension of the delta function is the inverse dimension of its argument z, which is $1/L$). Ampère's law at $z = 0$ can be then written as the following normalised system of algebraic equations,

$$-2\bar{k}\bar{A}_{1x}(0) = -\delta_i^2\mu_0 C_1(0,\omega,k)\bar{A}_{1x}(0) - \delta_i^2\mu_0 C_2(0,\omega,k)\bar{A}_{1y}(0), \tag{4.8}$$

$$-2\bar{k}\bar{A}_{1y}(0) = -\delta_i^2\mu_0 C_2(0,\omega,k)\bar{A}_{1x}(0) - \delta_i^2\mu_0 C_4(0,\omega,k)\bar{A}_{1y}(0), \tag{4.9}$$

where δ_i is the ion skin depth, to which all lengths are normalised, defined as

$$\delta_i = \frac{c}{\omega_{pi}}, \tag{4.10}$$

where ω_{pi} is the ion plasma frequency, given by

$$\omega_{pi} = \left(\frac{e^2 n_i}{\epsilon_0 m_i}\right)^{1/2}, \tag{4.11}$$

(n_i is given by Equation (2.77)) and c is the speed of light, which appears in the normalisation from the definition

$$\epsilon_0\mu_0 = \frac{1}{c^2}. \tag{4.12}$$

The ion skin depth is the distance over which electromagnetic radiation can penetrate the plasma.

Altogether, the normalisation is as follows: all frequencies are normalised to the ion gyrofrequency, Ω_{yi}, velocities to the ion thermal velocity, $v_{th,i}$, and lengths to the ion skin depth, δ_i, such that

$$\omega = \Omega_{yi}\bar{\omega}, \tag{4.13}$$

$$\Omega_{ye} = \frac{m_i}{m_e}\Omega_{yi}, \tag{4.14}$$

$$u_{xs} = v_{th,i}\bar{u}_{xs}, \tag{4.15}$$

$$k = \frac{\bar{k}}{\delta_i}, \tag{4.16}$$

The coefficients of $\bar{A}_{1x}$ and $\bar{A}_{1y}$ in Equations (4.8) and (4.9) are then given by

$$\delta_i^2\mu_0 C_1(0,\omega,k) = C_{1R} + iC_{1I}, \tag{4.17}$$

$$\delta_i^2\mu_0 C_2(0,\omega,k) = C_{2R} + iC_{2I}, \tag{4.18}$$

$$\delta_i^2\mu_0 C_4(0,\omega,k) = C_{4R} + iC_{4I}, \tag{4.19}$$

where

$$
\begin{aligned}
C_{1R} &= \frac{\bar{u}_{xi}^2}{4T_{ei}^2} + \frac{2e^{-K_i}}{1+2b}\left[\frac{1}{T_{ei}^2}\frac{1+b}{\bar{k}^2}[\omega_r S_{2R,i} - \gamma S_{2I,i}] - \frac{1}{8}K_i[\omega_r S_{3R,i} - \gamma S_{3I,i}]\right.\\
&\quad +\frac{1}{8}K_i T_{ei}\bar{k}\bar{u}_{xi}S_{4R,i} - \frac{1}{4}T_{ei}^2\bar{k}^2\bar{u}_{xi}^2 S_{5R,i} - \frac{1}{4}T_{ei}\bar{k}\bar{u}_{xi}[\omega_r S_{6R,i} - \gamma S_{6I,i}]\\
&\quad +\frac{1}{4}(\bar{u}_{xi}^2-1)[\omega_r S_{7R,i} - \gamma S_{7I,i}] - \frac{1}{4}T_{ei}\bar{k}\bar{u}_{xi}(\bar{u}_{xi}^2-1)S_{8R,i} - \frac{1}{8}T_{ei}^2\bar{k}^2\bar{u}_{xi}^2 S_{9R,i}\\
&\quad \left.-\frac{1}{8}T_{ei}\bar{k}\bar{u}_{xi}[\omega_r S_{10R,i} - \gamma S_{10I,i}]\right]\\
&\quad +\frac{2e^{-K_e}}{1+2b}\frac{m_i}{m_e}\left[\frac{1}{T_{ei}^2}\frac{T_i}{T_e}\frac{m_i}{m_e}\frac{1+b}{\bar{k}^2}[\omega_r S_{2R,e} - \gamma S_{2I,e}]\right.\\
&\quad -\frac{1}{8}K_e[\omega_r S_{3R,e} - \gamma S_{3I,e}] + \frac{1}{8}K_e T_{ei}\bar{k}\bar{u}_{xe}S_{4R,e} - \frac{1}{4}\frac{m_e}{m_i}T_{ei}^2\bar{k}^2\bar{u}_{xe}^2 S_{5R,e}\\
&\quad -\frac{1}{4}\frac{m_e}{m_i}T_{ei}\bar{k}\bar{u}_{xe}[\omega_r S_{6R,e} - \gamma S_{6I,e}] + \frac{1}{4}\left(\frac{T_i}{T_e}\frac{m_e}{m_i}\bar{u}_{xe}^2 - 1\right)[\omega_r S_{7R,e} - \gamma S_{7I,e}]\\
&\quad -\frac{1}{4}T_{ei}\bar{k}\bar{u}_{xe}\left(\frac{T_i}{T_e}\frac{m_e}{m_i}\bar{u}_{xe}^2 - 1\right)S_{8R,e} - \frac{1}{8}\frac{m_e}{m_i}T_{ei}^2\bar{k}^2\bar{u}_{xe}^2 S_{9R,e}\\
&\quad \left.-\frac{1}{8}\frac{m_e}{m_i}T_{ei}\bar{k}\bar{u}_{xe}[\omega_r S_{10R,e} - \gamma S_{10I,e}]\right], && (4.20)\\
C_{1I} &= \frac{2e^{-K_i}}{1+2b}\left[\frac{1}{T_{ei}^2}\frac{1+b}{\bar{k}^2}[\gamma S_{2R,i} + \omega_r S_{2I,i}] - \frac{1}{8}K_i[\gamma S_{3R,i} + \omega_r S_{3I,i}]\right.\\
&\quad +\frac{1}{8}K_i T_{ei}\bar{k}\bar{u}_{xi}S_{4I,i} - \frac{1}{4}T_{ei}^2\bar{k}^2\bar{u}_{xi}^2 S_{5I,i} - \frac{1}{4}T_{ei}\bar{k}\bar{u}_{xi}[\gamma S_{6R,i} + \omega_r S_{6I,i}]\\
&\quad +\frac{1}{4}(\bar{u}_{xi}^2-1)[\gamma S_{7R,i} + \omega_r S_{7I,i}] - \frac{1}{4}T_{ei}\bar{k}\bar{u}_{xi}(\bar{u}_{xi}^2-1)S_{8I,i} - \frac{1}{8}T_{ei}^2\bar{k}^2\bar{u}_{xi}^2 S_{9I,i}\\
&\quad \left.-\frac{1}{8}T_{ei}\bar{k}\bar{u}_{xi}[\gamma S_{10R,i} + \omega_r S_{10I,i}]\right]\\
&\quad +\frac{2e^{-K_e}}{1+2b}\frac{m_i}{m_e}\left[\frac{1}{T_{ei}^2}\frac{T_i}{T_e}\frac{m_i}{m_e}\frac{1+b}{\bar{k}^2}[\gamma S_{2R,e} + \omega_r S_{2I,e}]\right.\\
&\quad -\frac{1}{8}K_e[\gamma S_{3R,e} + \omega_r S_{3I,e}] + \frac{1}{8}K_e T_{ei}\bar{k}\bar{u}_{xe}S_{4I,e} - \frac{1}{4}\frac{m_e}{m_i}T_{ei}^2\bar{k}^2\bar{u}_{xe}^2 S_{5I,e}\\
&\quad -\frac{1}{4}\frac{m_e}{m_i}T_{ei}\bar{k}\bar{u}_{xe}[\gamma S_{6R,e} + \omega_r S_{6I,e}] + \frac{1}{4}\left(\frac{T_i}{T_e}\frac{m_e}{m_i}\bar{u}_{xe}^2 - 1\right)[\gamma S_{7R,e} + \omega_r S_{7I,e}]\\
&\quad -\frac{1}{4}T_{ei}\bar{k}\bar{u}_{xe}\left(\frac{T_i}{T_e}\frac{m_e}{m_i}\bar{u}_{xe}^2 - 1\right)S_{8I,e} - \frac{1}{8}\frac{m_e}{m_i}T_{ei}^2\bar{k}^2\bar{u}_{xe}^2 S_{9I,e}\\
&\quad \left.-\frac{1}{8}\frac{m_e}{m_i}T_{ei}\bar{k}\bar{u}_{xe}[\gamma S_{10R,e} + \omega_r S_{10I,e}]\right], && (4.21)\\
C_{2R} &= \frac{2e^{-K_i}}{1+2b}\frac{1}{T_{ei}}\frac{\bar{u}_{xi}}{\bar{k}}[\omega_r S_{1R,i} - \gamma S_{1I,i}]
\end{aligned}
$$

$$+\frac{2e^{-K_e}}{1+2b}\frac{1}{T_{ei}}\frac{m_i}{m_e}\frac{T_i}{T_e}\frac{\bar{u}_{xe}}{\bar{k}}[\omega_r S_{1R,e}-\gamma S_{1I,e}], \tag{4.22}$$

$$C_{2I} = \frac{2e^{-K_i}}{1+2b}\frac{1}{T_{ei}}\frac{\bar{u}_{xi}}{\bar{k}}[\gamma S_{1R,i}+\omega_r S_{1I,i}]$$
$$+\frac{2e^{-K_e}}{1+2b}\frac{1}{T_{ei}}\frac{T_i}{T_e}\frac{m_i}{m_e}\frac{\bar{u}_{xe}}{\bar{k}}[\gamma S_{1R,e}+\omega_r S_{1I,e}], \tag{4.23}$$

$$C_{4R} = \frac{\bar{u}_{xi}^2}{2T_{ei}^2}+\frac{2e^{-K_i}}{1+2b}\Big[(\bar{u}_{xi}^2+b+1)(\omega_r S_{11R,i}-\gamma S_{11I,i})$$
$$-\frac{1}{2}(\omega_r S_{12R,i}-\gamma S_{12I,i})+\frac{1}{2}T_{ei}\bar{k}\bar{u}_{xi}S_{13R,i}\Big]$$
$$+\frac{2e^{-K_e}}{1+2b}\frac{m_i}{m_e}\Bigg[\left(\frac{T_i}{T_e}\frac{m_e}{m_i}\bar{u}_{xe}^2+b+1\right)(\omega_r S_{11R,e}-\gamma S_{11I,e})$$
$$-\frac{1}{2}(\omega_r S_{12R,e}-\gamma S_{12I,e})+\frac{1}{2}T_{ei}\bar{k}\bar{u}_{xe}S_{13R,e}\Bigg], \tag{4.24}$$

$$C_{4I} = \frac{2e^{-K_i}}{1+2b}\Big[(\bar{u}_{xi}^2+b+1)(\gamma S_{11R,i}+\omega_r S_{11I,i})$$
$$-\frac{1}{2}(\gamma S_{12R,i}+\omega_r S_{12I,i})+\frac{1}{2}T_{ei}\bar{k}\bar{u}_{xi}S_{13I,i}\Big]$$
$$+\frac{2e^{-K_e}}{1+2b}\frac{m_i}{m_e}\Bigg[\left(\frac{T_i}{T_e}\frac{m_e}{m_i}\bar{u}_{xe}^2+b+1\right)(\gamma S_{11R,e}+\omega_r S_{11I,e})$$
$$-\frac{1}{2}(\gamma S_{12R,e}+\omega_r S_{12I,e})+\frac{1}{2}T_{ei}\bar{k}\bar{u}_{xe}S_{13I,e}\Bigg]. \tag{4.25}$$

where the terms $S_{1R,s}$, etc, are the real and imaginary parts of the various sums over Bessel functions, which are given in Appendix G, T_i/T_e is the ratio of ion and electron temperatures, and the term T_{ei} is given by

$$T_{ei} = \frac{1}{2}\left(\frac{1+2b}{1+T_e/T_i}\right)^{1/2}. \tag{4.26}$$

There are a number of important points to note at this stage. Firstly, assuming that the length scale is of the order of the ion skin depth, δ_i, introduces a factor of δ_i^2/δ_e^2 in the electron terms, where δ_e is the electron skin depth, given by

$$\delta_e = \frac{c}{\omega_{pe}}, \tag{4.27}$$

where ω_{pe} is the electron plasma frequency, given by Equation (1.2). Since the plasma is quasineutral ($n_i = n_e$), the ratio δ_i^2/δ_e^2 is given by the ion-electron mass ratio:

$$\frac{\delta_i^2}{\delta_e^2} = \frac{m_i}{m_e}. \tag{4.28}$$

A second point to note is that the term T_{ei} given by Equation (4.26) results from the factor

$$\frac{v_{th,i}}{\Omega_{yi}\delta_i},\tag{4.29}$$

which appears frequently in the expressions. This expression can be simplified by using the formula

$$\frac{u_{ys}^2}{v_{th,s}^2} = 4\frac{r_{g,s}^2}{L^2},\tag{4.30}$$

from Section 2.5.2. In Equation (4.30), $r_{g,s}$ is the gyroradius of particle species s, given by

$$r_{g,s} = \frac{v_{th,s}}{\Omega_{ys}},\tag{4.31}$$

and L is the current sheet thickness, given by

$$L = \left[\frac{2(\beta_e + \beta_i)}{\mu_0 e^2 \beta_e \beta_i n_0 (u_{yi} - u_{ye})^2}\right]^{1/2}.\tag{4.32}$$

Using Equation (4.15) and the assumption that $u_{xs} = u_{ys}$, Equation (4.30) can be rearranged to give

$$\frac{v_{th,i}}{\Omega_{yi}L} = \frac{\bar{u}_{xi}}{2},\tag{4.33}$$

where it has also been assumed that $\bar{u}_{xi} > 0$.

The current sheet width L normalised to the ion skin depth is given by

$$\frac{L}{\delta_i} = \left(2\left(1 + \frac{T_e}{T_i}\right)\frac{n_i}{n_0}\right)^{1/2}\frac{v_{th,i}}{u_{xi} - u_{xe}},\tag{4.34}$$

and upon using the relation

$$u_{xe} = -\frac{T_e}{T_i}u_{xi},\tag{4.35}$$

(obtained from Equation (2.71)), together with Equation (2.77), this becomes

$$\frac{L}{\delta_i} = \frac{1}{\bar{u}_{xi}}\left(\frac{1 + 2b}{1 + T_e/T_i}\right)^{1/2}.\tag{4.36}$$

The term $v_{th,i}/\Omega_{yi}\delta_i$ can then be rewritten, using Equations (4.33) and (4.36), as

$$\frac{v_{th,i}}{\Omega_{yi}\delta_i} = \frac{v_{th,i}}{\Omega_{yi}L}\frac{L}{\delta_i},\tag{4.37}$$

$$
= \frac{1}{2}\left(\frac{1+2b}{1+T_e/T_i}\right)^{1/2}, \tag{4.38}
$$

$$
= T_{ei}. \tag{4.39}
$$

The parameters K_i, K_e, A_i, A_e, α_i and α_e, which appear within the sums in the coefficients (4.20)-(4.25), can be written, under the current normalisation, as

$$
K_i = T_{ei}^2 \bar{k}^2, \tag{4.40}
$$

$$
K_e = \frac{T_e}{T_i}\frac{m_e}{m_i}T_{ei}^2 \bar{k}^2, \tag{4.41}
$$

$$
A_i = T_{ei}\bar{k}\sqrt{\bar{u}_{xi}^2 + K_i}, \tag{4.42}
$$

$$
A_e = \frac{m_e}{m_i}T_{ei}\bar{k}\sqrt{\bar{u}_{xe}^2 + \frac{T_e}{T_i}\frac{m_i}{m_e}K_e}, \tag{4.43}
$$

$$
\alpha_i = \tan^{-1}\left(-T_{ei}\frac{\bar{k}}{\bar{u}_{xi}}\right), \tag{4.44}
$$

$$
\alpha_e = \tan^{-1}\left(-T_{ei}\frac{T_e}{T_i}\frac{\bar{k}}{\bar{u}_{xe}}\right). \tag{4.45}
$$

Returning to the original problem, Equations (4.8) and (4.9) can be written as

$$
M\bar{\mathbf{A}}_1 = 0, \tag{4.46}
$$

where M is the following 2x2 matrix

$$
M = \begin{pmatrix} \delta_i^2\mu_0 C_1(0,\omega,k) - 2\bar{k} & \delta_i^2\mu_0 C_2(0,\omega,k) \\ \delta_i^2\mu_0 C_2(0,\omega,k) & \delta_i^2\mu_0 C_4(0,\omega,k) - 2\bar{k} \end{pmatrix}. \tag{4.47}
$$

To ensure a non-trivial solution to the equations, the determinant of the matrix M must vanish. Due to the fact that the coefficients C_1-C_4 are complex, this condition leads to the two equations

$$
\det(M)_{real} = C_{1R}C_{4R} - C_{1I}C_{4I} - 2\bar{k}(C_{1R} + C_{4R}) + 4\bar{k}^2 - C_{2R}^2 + C_{2I}^2 = 0, \tag{4.48}
$$

$$
\det(M)_{imag} = C_{1I}C_{4R} + C_{1R}C_{4I} - 2\bar{k}(C_{1I} + C_{4I}) - 2C_{2R}C_{2I} = 0, \tag{4.49}
$$

Equations (4.48) and (4.49) can be solved numerically. This will be discussed in the next section.

4.4 Results

To solve the approximate form of Ampère's law given by Equations (4.48) and (4.49), the multi-dimensional Newton-Raphson method was used. A Fortran 90 code was taken from Press et al.

(1992). The Bessel function sums in the coefficients (4.20)-(4.25) converge quickly due to the fact that $I_m \to 0$ as $m \to \infty$, and so they are straightforward to calculate numerically. This has been tested, and the majority of the sums converge after less than ten terms. In the Fortran code used, however, the first fifty terms were included in the sums to make sure of convergence.

The set of parameters from Figure 2.3 in Section 2.5.1 will be considered, for which the distribution function (2.59) has a single maximum. In Figure 2.3, $|u_{xs}| = v_{th,s}$ and $b_s = 2.85$, for either ions or electrons (both ions and electrons cannot have the same values). Choosing $\bar{u}_{xi} = 1$ and $b_i = 2.85$ gives $b = 2.85 \exp(-1/2)$ (using Equation (2.63)). In this case, b_i and $\bar{u}_{xi}$ satisfy the appropriate conditions such that the ion distribution function has a single maximum in both the v_x- and v_y-directions. Note that the electron parameters b_e and u_{xe} are related to b_i and u_{xi} through Equations (2.63) and (4.35). This means, therefore, that fixing the ion parameters also fixes the electron parameters for a given temperature ratio and mass ratio. Note, however, that it should also be ensured that the electron distribution function has a single maximum in both directions. For a realistic mass ratio, this will be the case unless the temperature ratio becomes unrealistic.

Ensuring a single maximum of both the ion and electron distribution functions in the velocity directions is important for the stability analysis presented in this chapter, since it is beyond the remit of the method to enter the parameter regime where the distribution functions become multi-peaked. Investigating the stability of the equilibrium under these conditions would require an investigation into the velocity space instabilities, which will not be considered in this thesis.

For the single maximum case described above, Figure 4.1 shows a surface plot of $\det(M)_{imag}$, from Equation (4.49), plotted over the ω_r-γ plane, for the ranges $-0.4 \leq \omega_r \leq 0.4$, $-0.4 \leq \gamma \leq 0.4$, with a realistic mass ratio $m_i/m_e \approx 1836$, a temperature ratio $T_i/T_e = 0.5$, and wavenumber $\bar{k} = 0.1$. Figure 4.2 shows the surface plotted over the ranges $0 \leq \omega_r \leq 0.4$, $0 \leq \gamma \leq 0.4$, for the same parameter values as in Figure 4.1. Figure 4.2 reveals that Equation (4.49) is identically satisfied when either $\omega_r = 0$ or $\gamma = 0$. On closer inspection of the coefficients in the equation, it can be seen, as expected, that each product contains a factor of $\omega_r\gamma$. The important equation to consider, therefore, is Equation (4.48). A surface plot of $\det(M)_{real}$ is given in Figure 4.3, for the same parameter values as used in Figure 4.2, but plotted over the ranges $-0.4 \leq \omega_r \leq 0.4$, $-0.4 \leq \gamma \leq 0.4$. It is clear from this figure that $\omega_r = 0$ is not a solution of Equation (4.48), and so γ must vanish, giving no instability. A plot of the real frequency ω_r against $\bar{k}$ is given in Figure 4.4, for the range $0.01 \leq \bar{k} \leq 0.5$, with the starting values for the Newton-Raphson method taken as $\omega_r = \gamma = 0.1$. Note that it is not possible to put $\bar{k} = 0$ into the numerical code, since some of the coefficients (4.20)-(4.25) are singular at this point. Note also that, although the range $0.01 \leq \bar{k} \leq 0.5$ has been used, the results for the higher values in this range may not be accurate since the long wavelength (small $\bar{k}$) approximation has been used. Figure 4.4 shows an increase of ω_r as $\bar{k}$ is increased.
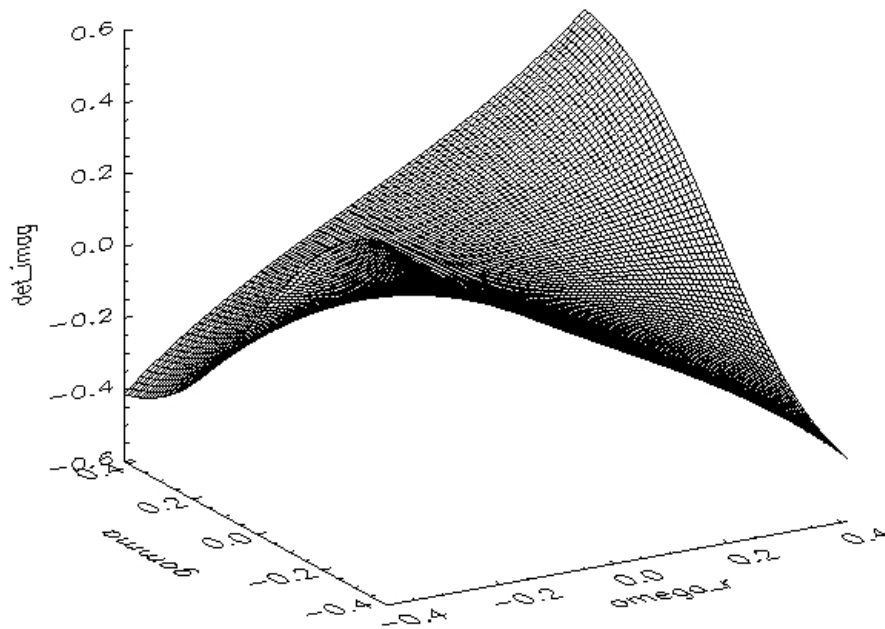
Figure 4.1: Surface plot of $\det(M)_{imag}$, plotted over the ranges $-0.4 \leq \omega_r \leq 0.4$, $-0.4 \leq \gamma \leq 0.4$, for $\bar{u}_{xi} = 1$, $b = 2.85 \exp(-1/2)$, $m_i/m_e \approx 1836$, $T_i/T_e = 0.5$ and $\bar{k} = 0.1$.
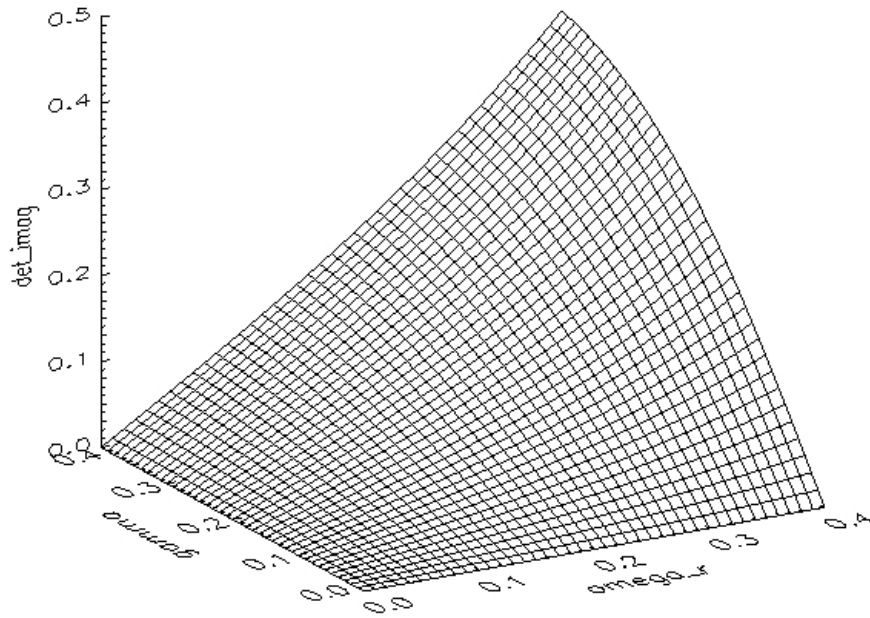
Figure 4.2: Surface plot of $\det(M)_{imag}$, plotted over the ranges $0 \leq \omega_r \leq 0.4$, $0 \leq \gamma \leq 0.4$, for $\bar{u}_{xi} = 1$, $b = 2.85 \exp(-1/2)$, $m_i/m_e \approx 1836$, $T_i/T_e = 0.5$ and $\bar{k} = 0.1$.
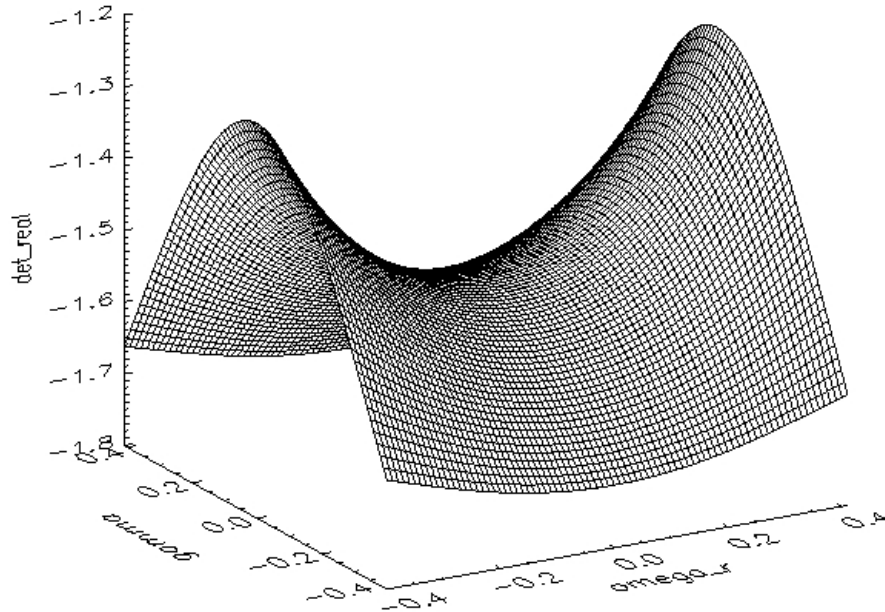
Figure 4.3: Surface plot of $\det(M)_{real}$, plotted over the ranges $-0.4 \leq \omega_r \leq 0.4$, $-0.4 \leq \gamma \leq 0.4$, for $\bar{u}_{xi} = 1$, $b = 2.85 \exp(-1/2)$, $m_i/m_e \approx 1836$, $T_i/T_e = 0.5$ and $\bar{k} = 0.1$.
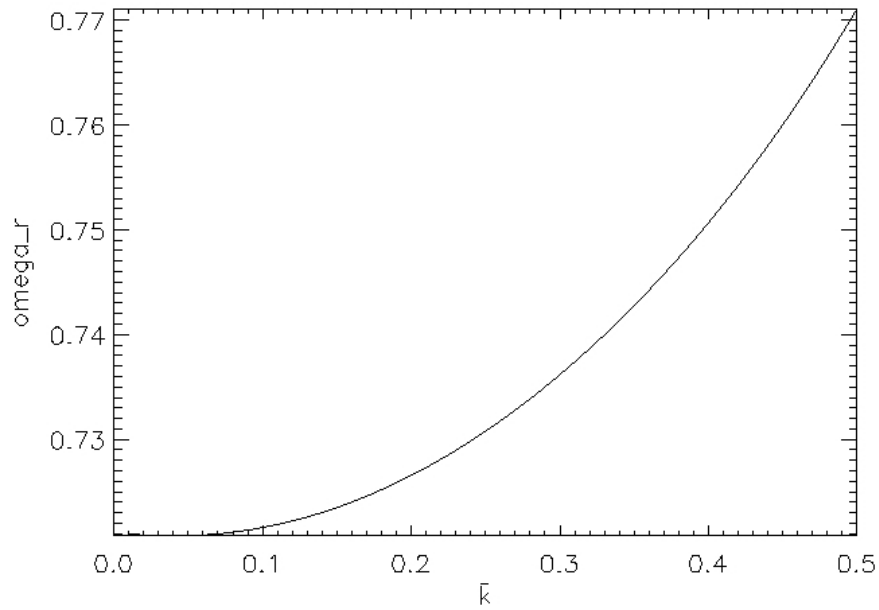
Figure 4.4: Plot of ω_r against $\bar{k}$, for $\bar{u}_{xi} = 1$, $b = 2.85 \exp(-1/2)$, $m_i/m_e \approx 1836$, $T_i/T_e = 0.5$ and starting with the initial values $\omega_r = 0.1$, $\gamma = 0.1$.

To find an instability, a parameter set must be chosen for which the surface $\det(M)_{real}$ moves up, so that the centre part is above the $\det(M)_{real} = 0$ plane, such that $\omega_r = 0$ is a solution of Equation (4.48). Such a case can be obtained, for example, by choosing the temperature ratio $T_i/T_e = 0.1$. A plot of $\det(M)_{real}$ for this case is shown in Figure 4.5, where all other parameters have the same values as in Figure 4.3. It can now be seen that $\omega_r = 0$ is a solution, since the centre
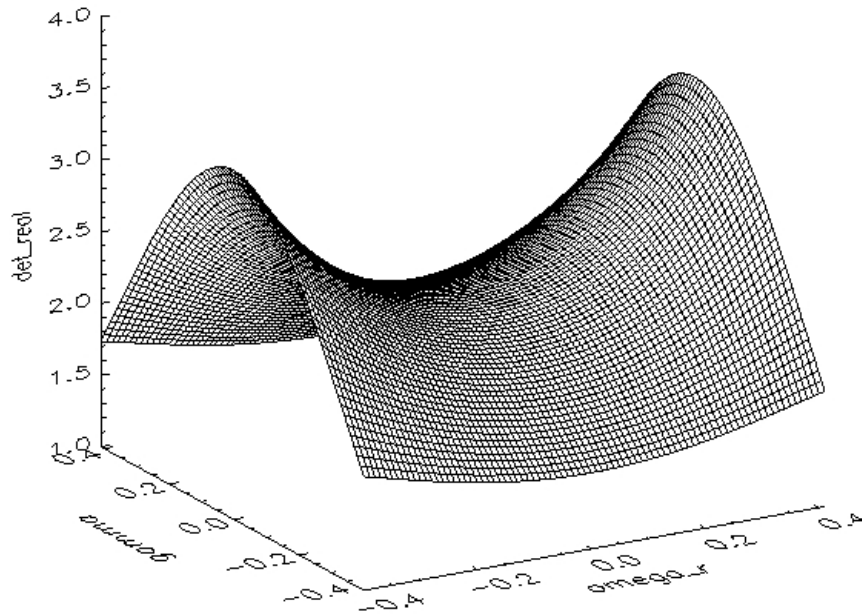
Figure 4.5: Surface plot of $\det(M)_{real}$, plotted over the ranges $-0.4 \leq \omega_r \leq 0.4$, $-0.4 \leq \gamma \leq 0.4$, for $\bar{u}_{xi} = 1$, $b = 2.85 \exp(-1/2)$, $m_i/m_e \approx 1836$, $T_i/T_e = 0.1$ and $\bar{k} = 0.1$.

part of the surface has now moved up and crossed over the $\det(M)_{real} = 0$ plane. For $\omega_r = 0$, the surface crosses the $\det(M)_{real} = 0$ plane for two values of γ, one positive and one negative. A dispersion plot showing how the positive growth rate varies with $\bar{k}$ is shown in Figure 4.6. For this figure, starting values of $\omega_r = \gamma = 0.1$ were chosen for the Newton-Raphson method, in order to pick out the positive γ. The negative γ solution can be obtained by starting with the initial values $\omega_r = 0.1$, $\gamma = -0.1$. A dispersion plot for this case is shown in Figure 4.7. These growth rates are just the negatives of the growth rates calculated for Figure 4.6, which reflects the fact that the surface is symmetrical about the line $\gamma = 0$. Negative growth rates correspond to damping.

It has been found that, for the single case considered, decreasing the ion-electron temperature ratio from 0.5 to 0.1 gives instability. Figure 4.8 shows a plot of how the growth rate changes as the temperature ratio is changed, for $\bar{k} = 0.1$, and the same parameters as before, and starting at $\omega_r = 0.1$, $\gamma = 0.1$. Figure 4.9 shows the region of non-zero γ values. These figures can
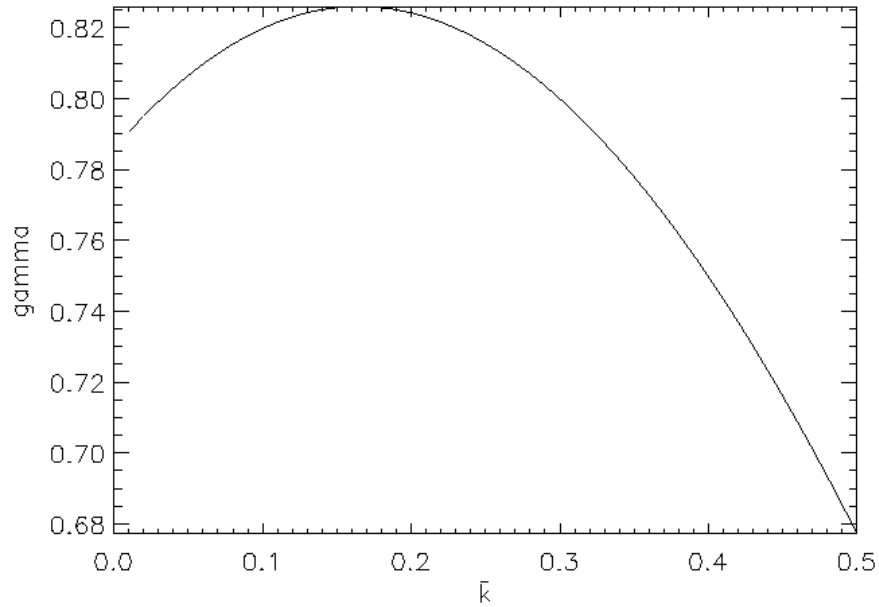
Figure 4.6: Plot of γ against $\bar{k}$, for $\bar{u}_{xi} = 1$, $b = 2.85 \exp(-1/2)$, $m_i/m_e \approx 1836$ and $T_i/T_e = 0.1$, starting with the initial values $\omega_r = 0.1$, $\gamma = 0.1$.
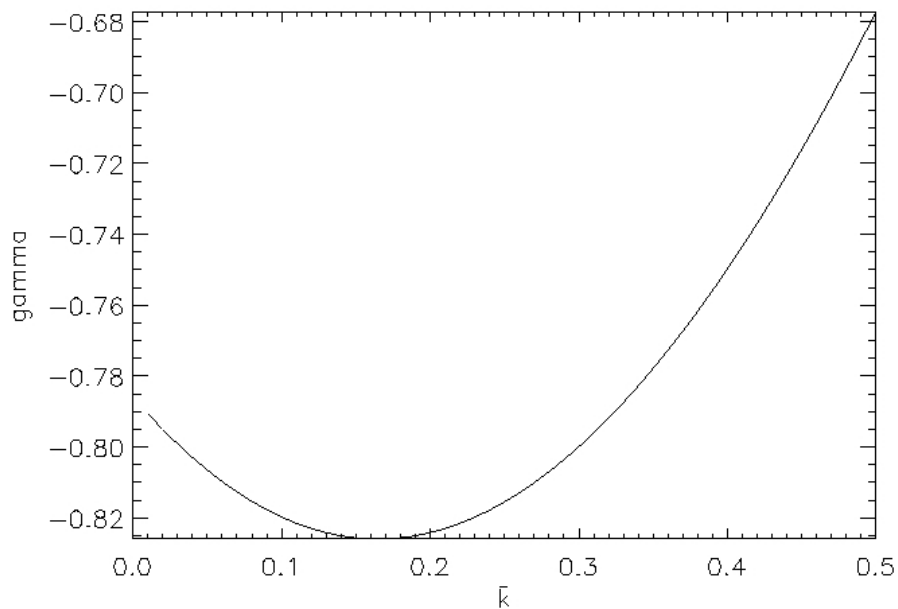
Figure 4.7: Plot of γ against $\bar{k}$, for $\bar{u}_{xi} = 1$, $b = 2.85 \exp(-1/2)$, $m_i/m_e \approx 1836$ and $T_i/T_e = 0.1$, starting with the initial values $\omega_r = 0.1$, $\gamma = -0.1$.
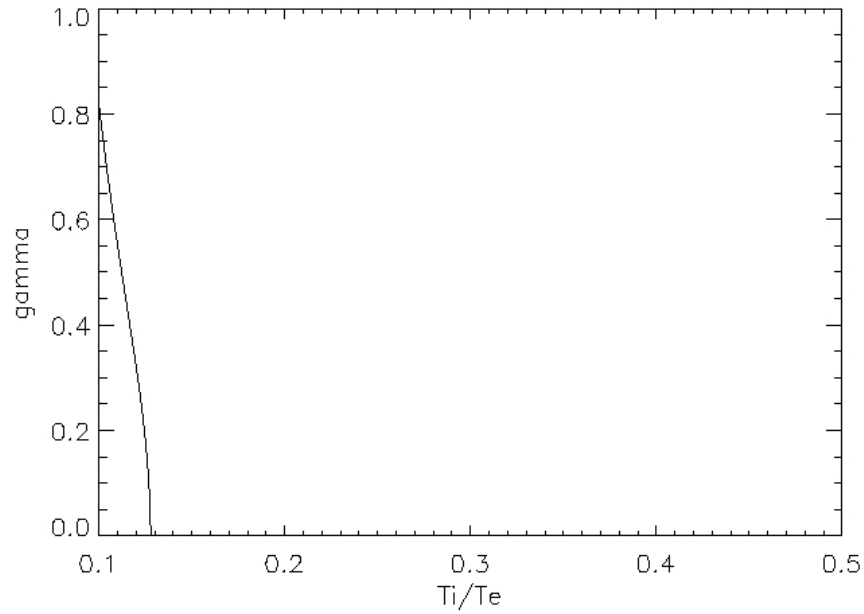
Figure 4.8: Plot of γ against T_i/T_e, for $\bar{u}_{xi} = 1$, $b = 2.85 \exp(-1/2)$, $m_i/m_e \approx 1836$ and $\bar{k} = 0.1$, starting with the initial values $\omega_r = 0.1$, $\gamma = 0.1$.
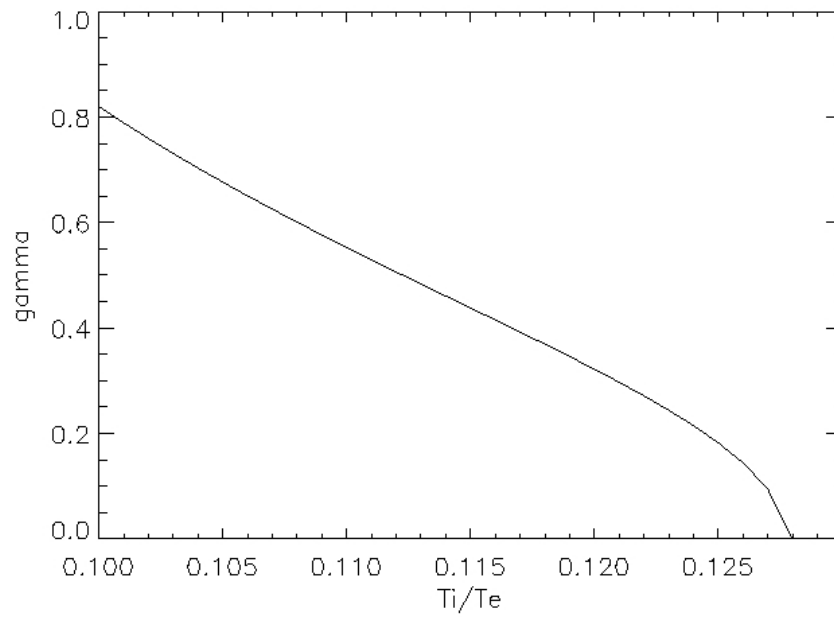
Figure 4.9: Plot of γ against T_i/T_e over a smaller range of values, for $\bar{u}_{xi} = 1$, $b = 2.85 \exp(-1/2)$, $m_i/m_e \approx 1836$ and $\bar{k} = 0.1$, starting with the initial values $\omega_r = 0.1$, $\gamma = 0.1$.

also be viewed as fixing the ion drift speed, $\bar{u}_{xi}$, and decreasing the electron drift speed, $\bar{u}_{xe}$, through Equation (4.35). It can be seen that, beyond an ion-electron temperature ratio of 0.128, the growth rate vanishes, meaning that the configuration is stable for temperature ratios above this value, for the particular value of $\bar{k}$ chosen. Figure 4.10 shows the corresponding variation of ω_r with temperature ratio. This figure reveals that ω_r is non-zero for temperature ratios above
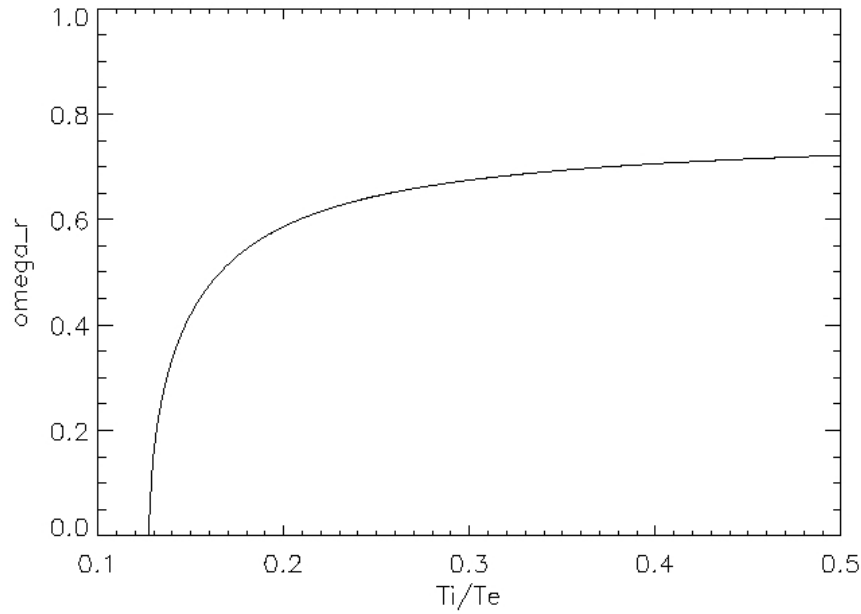
Figure 4.10: Plot of ω_r against T_i/T_e, for $\bar{u}_{xi} = 1$, $b = 2.85 \exp(-1/2)$, $m_i/m_e \approx 1836$ and $\bar{k} = 0.1$, starting with the initial values $\omega_r = 0.1$, $\gamma = 0.1$.

approximately 0.13. This fits with the conclusion from Figure 4.9 that the growth rate is only non-zero if T_i/T_e is less than 0.128 (since either γ or ω_r must vanish). This conclusion of course only applies to the case where $\bar{k} = 0.1$.

Another parameter which can be varied is the ion-electron mass ratio, m_i/m_e. In the cases discussed thus far, the mass ratio has always been chosen to be the realistic value of $m_i/m_e \approx 1836$. Figure 4.11 shows how the growth rate varies with increasing mass ratio, for $\bar{k} = 0.1$, $T_i/T_e = 0.1$, and all the same parameter values as before. It can be seen that the value of γ remains roughly constant for all mass ratios beyond $m_i/m_e = 100$. This can be explained by looking again at the coefficients (4.20)-(4.25). Firstly, some of the terms in the electron parts of these coefficients contain the ratio m_e/m_i, which, as m_i/m_e gets larger, will of course get smaller. Secondly, the electron sums in the coefficients, given in Appendix G, will become negligible rather quickly, since they all contain a factor of $(m_i/m_e)^4$ in their denominators, and no more than a factor of $(m_i/m_e)^2$ in their numerators. Thirdly, the arguments of the Bessel functions in the electron sums, K_e and A_e, both contain factors of m_e/m_i and so will get smaller as the mass ratio is increased.
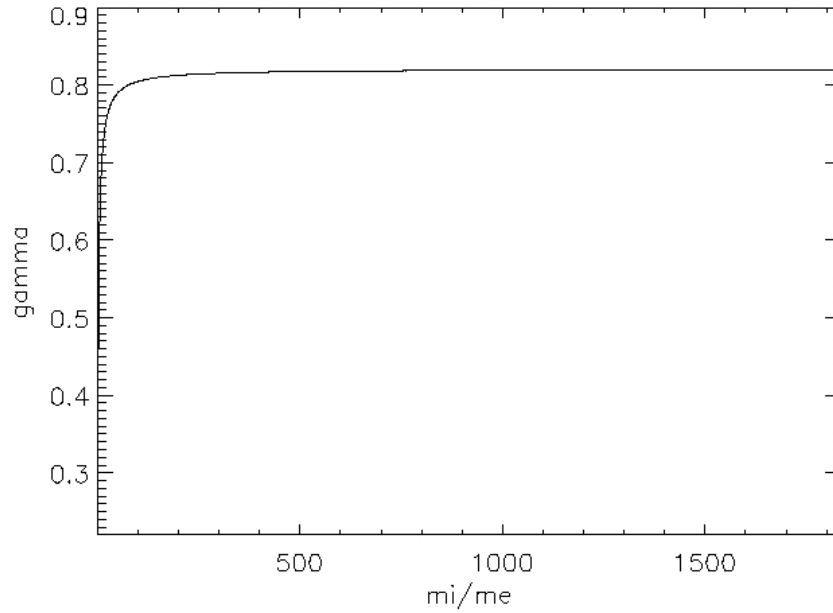
Figure 4.11: Plot of γ against m_i/m_e, for $\bar{u}_{xi} = 1$, $b = 2.85 \exp(-1/2)$, $T_i/T_e = 0.1$ and $\bar{k} = 0.1$, starting with the initial values $\omega_r = 0.1$, $\gamma = 0.1$.

A point will be reached where the electron terms are negligible compared with the ion terms, so that increasing the mass ratio further has no noticeable effect on the values of the coefficients (4.20)-(4.25).

The current sheet thickness, given by Equation (4.32), can be written, using Equation (4.35), as

$$L = \left[\frac{2(\beta_e + \beta_i)}{\mu_0 e^2 \beta_e \beta_i n_0} \right] \frac{1}{(1 + T_e/T_i)\, u_{xi}}. \tag{4.50}$$

It can be seen that decreasing the ion drift velocity u_{xi} gives rise to a thicker current sheet. This means that the maximum current density will be decreased, and so the configuration will be more stable. This is illustrated in Figure 4.12, which shows a plot of γ against $\bar{k}$ for the case $\bar{u}_{xi} = 0.96$, $T_i/T_e = 0.1$, and a realistic mass ratio as before. It can be seen that the maximum growth rate is significantly smaller for $\bar{u}_{xi} = 0.96$ than for $\bar{u}_{xi} = 1$ (see Figure 4.6). Note also that a decrease of $\bar{u}_{xi}$ for a given b_i will still give a single maximum case, since the lower limit on b_i given in condition (2.115) will decrease, and so there is no danger of going into the regime of multi-peaked distribution functions.

It is also clear from Equation (4.50) that increasing u_{xi} will result in the current sheet becoming progressively thinner. In Section 2.5, it was mentioned that, through Equation (2.140), decreasing the current sheet thickness will eventually result in a multi-peaked distribution function, firstly in the v_x-direction, by violating the condition (2.89), and then in the v_y-direction as the sheet
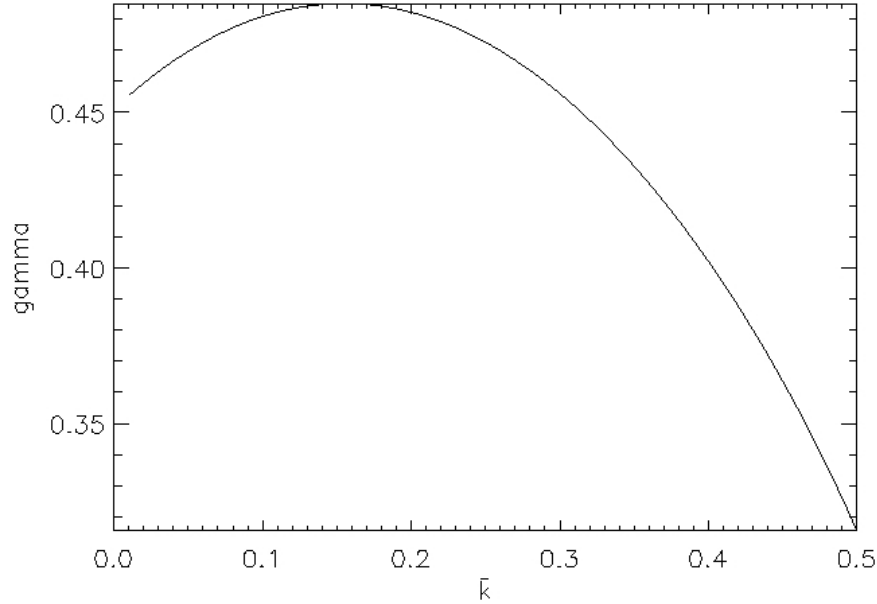
Figure 4.12: Plot of γ against $\bar{k}$, for $\bar{u}_{xi} = 0.96$, $b = 2.85 \exp(-1/2)$, $T_i/T_e = 0.1$ and $m_i/m_e \approx$ 1836, starting with the initial values $\omega_r = 0.1$, $\gamma = 0.1$.

thickness is decreased further. As previously stated, it is beyond the scope of this work to consider the effect of multi-peaked distribution functions on the stability of the equilibrium, since an investigation into such effects would require a different method.

4.5 Analytical Solutions in the Outer Region

As discussed previously, a full solution of Ampère's law in the form of Equations (4.3) and (4.4) would involve using a numerical method such as the shooting method (e.g. Press et al., 1992) to find the eigenvalues. It is, however, possible to find analytical solutions in the outer region, by assuming that the time integral (3.86) in this region is negligible, so that the perturbed current density consists only of the adiabatic part, given by Equations (3.140) and (3.142) in terms of the macroscopic parameters, or Equations (3.150) and (3.151) in terms of the microscopic parameters. The perturbed current density in the outer region is, therefore, assumed to be given by

$$j_{1x,out} \;=\; j_{1x,a} = D_{1,adi}\bar{A}_{1x}, \tag{4.51}$$

$$j_{1y,out} \;=\; j_{1y,a} = D_{2,adi}\bar{A}_{1y}, \tag{4.52}$$

where, using the macroscopic parameters,

$$D_{1,adi} = -\frac{1}{\mu_0 L^2}\left(1 - \frac{2}{\cosh^2(z/L)}\right), \tag{4.53}$$

$$D_{2,adi} = \frac{2}{\mu_0 L^2}\frac{1}{\cosh^2(z/L)}. \tag{4.54}$$

Ampère's law then has the form

$$\frac{d^2\bar{A}_{1x}}{dz^2} - k^2\bar{A}_{1x} = -\mu_0 j_{1xs}(\bar{A}_{1x}, \bar{A}_{1y}, z, \omega, k), \tag{4.55}$$

$$\frac{d^2\bar{A}_{1y}}{dz^2} - k^2\bar{A}_{1y} = -\mu_0 j_{1ys}(\bar{A}_{1x}, \bar{A}_{1y}, z, \omega, k), \tag{4.56}$$

where

$$j_{1x} = \begin{cases} C_1(z,\omega,k)\bar{A}_{1x} + C_2(z,\omega,k)\bar{A}_{1y} & \text{if } z \leq L \text{ (inside sheet)} \\ D_{1,adi}\bar{A}_{1x} & \text{if } z > L \text{ (outside sheet)} \end{cases}, \tag{4.57}$$

$$j_{1y} = \begin{cases} C_2(z,\omega,k)\bar{A}_{1x} + C_4(z,\omega,k)\bar{A}_{1y} & \text{if } z \leq L \text{ (inside sheet)} \\ D_{2,adi}\bar{A}_{1y} & \text{if } z > L \text{ (outside sheet)} \end{cases}, \tag{4.58}$$

with the coefficients C_1, C_2 and C_4 given by Equations (3.174), (3.175) and (3.183), respectively.

In the outer region, Ampère's law now consists of two uncoupled second order ODEs, one for $\bar{A}_{1x}$ and one for $\bar{A}_{1y}$. The equation for $\bar{A}_{1y}$ is given, after normalising both z and k to the current sheet width L, by

$$\frac{d^2\bar{A}_{1y}}{d\bar{z}^2} + \left(\frac{2}{\cosh^2\bar{z}} - \bar{k}^2\right)\bar{A}_{1y} = 0, \tag{4.59}$$

where the dimension of $\bar{A}_{1y}$ cancels out between the two sides and so there is no need to normalise as such. Equation (4.59) is the same as that described by Schindler (2007) in Section 10.4 on the resistive tearing instability, where a Harris sheet field profile is used. This similarity of the equations is to be expected, since the x-component of the force-free Harris sheet field and, hence, the y-component of the vector potential, are the same as the respective components for the Harris sheet. Equation (4.59) has the general solution,

$$\bar{A}_{1y} = K_1 e^{-\bar{k}\bar{z}}(\tanh\bar{z} + \bar{k}) + K_2 e^{\bar{k}\bar{z}}(\tanh\bar{z} - \bar{k}), \tag{4.60}$$

where K_1 and K_2 are arbitrary constants. This can be seen by substituting the function $\bar{A}_{1y} = e^{\lambda\bar{z}}U(\bar{z})$, where U is an arbitrary function of $\bar{z}$, into Equation (4.59), which gives

$$U''(\bar{z}) + 2\lambda U'(\bar{z}) + \left(\frac{2}{\cosh^2\bar{z}} + \lambda^2 - \bar{k}^2\right)U(\bar{z}) = 0, \tag{4.61}$$

which, on using the substitution $\mu = \tanh \bar{z}$ and assuming that $\lambda = \pm \bar{k}$, becomes

$$(1 - \mu^2)\frac{d^2 U}{d\mu^2} - 2(\mu - \lambda)\frac{dU}{d\mu} + 2U = 0. \tag{4.62}$$

The solution to Equation (4.62) can be found by trying a solution of the form $U(\mu) = c_1 \mu + c_2$, which gives the solution as $U(\mu) = c_1(\mu - \lambda)$, where $\lambda = \pm \bar{k}$. This then gives two linearly independent solutions of Equation (4.59) as

$$\bar{A}_{1y} = c_1(\tanh \bar{z} \mp \bar{k})e^{\pm \bar{k}\bar{z}}, \tag{4.63}$$

and so the general solution (4.60) is given by adding up the two linearly independent solutions. The condition that $\bar{A}_{1y} \to 0$ as $z \to \infty$ means, however, that the constant K_2 must vanish, which then gives the solution of Equation (4.59) as

$$\bar{A}_{1y} = K_1 e^{-\bar{k}\bar{z}}(\tanh \bar{z} + \bar{k}). \tag{4.64}$$

The constant K_1 would be determined by the boundary condition at $z = \pm L$, obtained from the inner solution (which would be found numerically).

Returning to Ampère's law, the equation for $\bar{A}_{1x}$ outside of the sheet is given, again after normalisation, by

$$\frac{d^2 \bar{A}_{1x}}{d\bar{z}^2} + \left(\frac{2}{\cosh^2 \bar{z}} - (\bar{k}^2 + 1)\right)\bar{A}_{1x} = 0. \tag{4.65}$$

This equation can be solved in the same way as Equation (4.59), by letting $\bar{k} = \sqrt{\bar{k}^2 + 1}$. This gives the general solution as

$$\bar{A}_{1x} = K_3 e^{-\sqrt{(\bar{k}^2+1)}\bar{z}}(\tanh \bar{z} + \sqrt{\bar{k}^2 + 1}) + K_4 e^{\sqrt{(\bar{k}^2+1)}\bar{z}}(\tanh \bar{z} - \sqrt{\bar{k}^2 + 1}), \tag{4.66}$$

and, using the boundary condition $\bar{A}_{1x} \to 0$ as $z \to \infty$, the constant K_4 must vanish, which gives the solution as

$$\bar{A}_{1x} = K_3 e^{-\sqrt{(\bar{k}^2+1)}\bar{z}}(\tanh \bar{z} + \sqrt{\bar{k}^2 + 1}), \tag{4.67}$$

where the constant K_3 would be determined by the boundary condition at $z = \pm L$, again obtained from the inner solution, which would be found numerically.

4.6   Summary

In this chapter, an approximate numerical solution of Ampère's law has been given for Harrison and Neukirch's equilibrium for the force-free Harris sheet (Harrison and Neukirch, 2009b), to investigate the occurrence of the collisionless tearing mode. The simplifying approximation discussed by Silin et al. (2002) for the Harris sheet was used, in which it was assumed that the perturbation wavalength is large compared with the current sheet thickness, such that the current density can be approximated by a delta function. Ampère's law was then reduced to a system of two algebraic equations, which were solved numerically by using the multidimensional Newton-Raphson method in Fortran 90 (Press et al., 1992). It was found that solutions exist only if either ω_r or γ vanishes. A set of parameters were chosen such that both the ion and electron distribution functions for the equilibrium have a single maximum. The single maximum case from Figure 2.3 was considered. Note that it is beyond the scope of the work in this thesis to consider parameter regimes for which the distribution functions can become multi-peaked, since this would require an investigation into the microinstabilities, using a numerical method such as that developed by Camporeale et al. (2006).

An important parameter in the stability analysis is the ion-electron temperature ratio, T_i/T_e. It was found that, for a temperature ratio $T_i/T_e = 0.5$, the only solution to the problem is $\gamma = 0$, and so the configuration is stable. The real frequency, ω_r, was found to increase with increasing wavenumber $\bar{k}$.

For a temperature ratio of $T_i/T_e = 0.1$, it was found that $\omega_r = 0$, meaning that γ is non-zero. Two solutions were found to exist, one with a positive growth rate, corresponding to instability, and one with a negative growth rate, corresponding to damping. The solution found by the numerical method depends on the chosen initial value of γ. When looking for an instability, it of course makes sense to start with a positive value, as starting with a negative value is more likely to pick out the damped solution. A plot of γ against $\bar{k}$ for this temperature ratio revealed that a maximum is reached at a wavenumber of approximately $\bar{k} = 0.16$, and then after this the growth rate decreases as $\bar{k}$ is increased further. It should be noted that it was not possible to set $\bar{k} = 0$ in the numerical code, since there are $\bar{k}$ terms in the denominators of the coefficients.

A plot of the growth rate against the ion-electron temperature ratio for $\bar{k} = 0.1$ revealed that, beyond a certain temperature ratio ($T_i/T_e \approx 0.13$), no instability was found, as the only solution is for $\gamma = 0$ and ω_r non-zero.

Another parameter which occurs frequently is the ion-electron mass ratio, m_i/m_e. Of course, in reality this parameter has a fixed value (≈ 1836), but in plasma physics research it is often taken to have a much smaller value (for example in PIC simulations of collisionless reconnection). A plot of the growth rate against mass ratio revealed that, for m_i/m_e beyond a value of around 100,

there was only a very small change in the growth rate. This can be explained by the fact that, beyond a certain value of m_i/m_e, the electron terms become negligible in comparison to the ion terms, due to factors of at least $(m_i/m_e)^2$ in the denominators.

Analytical solutions of Ampère's law were obtained for the region outside the sheet, which would be useful for solving the full problem without the delta function approximation, since a numerical method would then only be required for the region inside the sheet. These analytical solutions were found by making the simplifying assumption that the perturbed current density in the outer region is given by the adiabatic part only, given by Equations (3.140) and (3.142), so that the plasma dispersion functions in the coefficients (3.194), (3.195), (3.201) and (3.202) can be neglected. The solution for $\bar{A}_{1y}$ was found to be the same as that obtained in studies of the resistive tearing mode, starting with a Harris sheet equilibrium (Schindler, 2007). This is because the Harris sheet and force-free Harris sheet fields have the same x-component. The solution for $\bar{A}_{1x}$ was found to have a similar form as the $\bar{A}_{1y}$ solution, but with $\bar{k}$ from the $\bar{A}_{1y}$ solution replaced by $\sqrt{\bar{k}^2 + 1}$.

To conclude, the single maximum case considered in Section 4.4 has given an illustration of the fact that the Harrison and Neukirch (2009b) equilibrium is unstable to the collisionless tearing mode under certain conditions, with the growth rate of the instability depending crucially upon the ion-electron temperature ratio. It should be noted, however, that the delta function approximation is a hugely simplifying one, and so a definite conclusion cannot be given about the stability of the equilibrium at this stage. Instead of using the approximation to solve Ampère's law, a shooting method (e.g. Press et al., 1992), for example, could be used to solve the ODEs, and the results could then be compared with those from Section 4.4 in order to assess the validity of the approximation.

Chapter 5

Summary and Further Work

The work in this thesis has focused primarily on equilibrium and stability properties of collision-less current sheet models, in particular of the force-free Harris sheet model. In Chapter 2, the focus was on one-dimensional force-free Vlasov-Maxwell equilibria. Conditions on the existence of such equilibria have been given by Harrison and Neukirch (2009a). Of particular importance is the fact that the Vlasov-Maxwell equilibrium problem corresponds to the problem of solving the equations of motion of a particle moving in a two-dimensional conservative potential. A necessary condition for having a force-free equilibrium solution is that the pressure must have at least one contour that corresponds to a trajectory in the A_x-A_y-plane, where A_x and A_y are the x- and y-components of the vector potential, respectively. Such a condition is satisfied for the force-free Harris sheet equilibrium solution found by Harrison and Neukirch (2009b). The derivation of the distribution function was given, which relies crucially on the assumption that the pressure P_{zz} is a sum of two terms, one depending on A_x, and the other depending on A_y. The density and bulk flow velocity have been calculated by taking velocity moments of the distribution function. The current density was then obtained in terms of the microscopic parameters. A number of conditions have been given between the microscopic and macroscopic parameters of the equilibrium, and these can be used to show the consistency between the current density expression obtained from the distribution functions, and that obtained from the magnetic field profile through Ampère's law.

An important property of the distribution function found by Harrison and Neukirch (2009b) is that it can be multi-peaked in both the v_x- and v_y-directions, which may give rise to microinstabilities. Part of the distribution function has a cosine dependence on v_x, and so multiple maxima can arise if this term is significant enough. In the v_y-direction, the distribution function contains a drifting Maxwellian part, together with a part which is Maxwellian at rest. Multiple maxima can arise in this direction for parameter values such that the drifting part moves far enough away from the part which is at rest. Conditions on the parameters of the distribution function have been derived, which show when it can be single or multi-peaked for some value of z.

Some examples were given of attempts to find equilibria for nonlinear force-free magnetic field profiles other than that of the force-free Harris sheet. The method of Harrison and Neukirch (2009b) was used, but it was found that, even for seemingly simple magnetic field profiles, it was

not possible to find additional Vlasov-Maxwell equilibria by this method. The problem occurred mainly in the final step of the method, which involves using the Fourier transform method by Channell (1976) to solve an integral equation for the unknown part of the distribution function. In future work, it would be interesting to further investigate the possibility of finding equilibrium solutions, either analytically or numerically. Hermite functions could potentially be used, as suggested by Channell (1976). It would also be interesting to investigate whether it is possible to find equilibrium solutions for a P_{zz} of a different form, for example a multiplicative P_{zz} of the form $P_{zz} = P_1(A_x)P_2(A_y)$, instead of the additive P_{zz} used by Harrison and Neukirch (2009b).

A family of distribution functions for the force-free Harris sheet has been found, which includes the previously known distribution function found by Harrison and Neukirch (2009b), in addition to distribution functions with a different dependence upon the particle energy. The method employed to calculate this family uses the fact that Ampère's law can be written in terms of derivatives of the pressure function P_{zz} with respect to the components of the vector potential. An obvious consequence of this result is that two distribution functions giving rise to the same pressure function will automatically satisfy the Vlasov-Maxwell equations for the same magnetic field profile. Conditions on the parameters of the new distribution functions, such that they give rise to the P_{zz} found by Harrison and Neukirch (2009b), have been stated explicitly. Three examples of distribution functions from the new family have been given, in order to illustrate the use of the general method. Although there are currently no known nonlinear force-free Vlasov-Maxwell equilibria for magnetic field profiles other than the force-free Harris sheet, if such a solution were found then the method could potentially be used to extend that solution to a family of solutions. This would be interesting to investigate in future work, if another solution could be found for a different magnetic field profile.

The final part of the work in Chapter 2 involved an attempt to extend the general theory of one-dimensional force-free Vlasov-Maxwell equilibria to cylindrical coordinates, by considering the case where all quantities depend only upon the radial coordinate, r. An example was given of an attempt to find a linear force-free solution, by starting with a distribution function similar to that used by Channell (1976) and Attico and Pegoraro (1999) in Cartesian coordinates, which is known to give rise to a linear force-free equilibrium. It was found, however, that in cylindrical coordinates, this form of distribution function does not give rise to a force-free field. Another aim for future work, therefore, is to further investigate whether it is at all possible to find force-free cylindrical equilibria.

In Chapters 3 and 4, a linear stability analysis of the equilibrium found by Harrison and Neukirch (2009b) for the force-free Harris sheet was carried out, in order to investigate the occurrence of the collisionless tearing mode. In Chapter 3, the initial calculations were given. After linearising the Vlasov-Maxwell equations, the perturbed distribution function was calculated, in which the perturbed quantities were assumed to be independent of the y-coordinate, and to have a har-

monic dependence on x and t. A central difficulty in the Vlasov approach is the integration over unperturbed orbits, since an expression for the orbits themselves is required which, in general, cannot be found analytically without an approximation. The straight line orbit approximation, used by a number of authors for the Harris sheet (e.g. Dobrowolny, 1968; Lapenta and Brackbill, 1997; Silin et al., 2002) is not valid for the force-free Harris sheet, due to the y-component of the magnetic field. Another approximation was required, therefore, and so the force-free Harris sheet field was approximated by two separate regions of constant magnetic field: an inner region, where the field is in the y-direction only, and an outer region, where the field is in the x-direction only. Although not ideal, such an approximation is reasonable given the structure of the force-free Harris sheet field profile, and allowed for a straightforward calculation of the particle orbits. These expressions were then used with the perturbed distribution function expression to calculate the perturbed density and perturbed current density, by taking velocity moments of the perturbed distribution function, and integrating over both velocity space and time. As this stage, it was assumed that the perturbed vector potential remains constant along the particle orbits. Note that the perturbed density is not required for the stability analysis, but was calculated for completeness, and also because its calculation served as a good exercise to prepare for the longer calculation of the perturbed current density. For both the inner and outer regions, the perturbed current density components depend linearly on the components of the perturbed vector potential, but it was found that the coefficients of these terms depend upon z, the eigenvalue ω, and also the wavenumber k, in a nonlinear fashion. For the inner region, the coefficients include infinite sums over Bessel functions and, for the outer region, they include plasma dispersion functions.

An approximate numerical solution of Ampère's law was given in Chapter 4. The perturbation wavelength was assumed to be large compared with the current sheet thickness, such that the perturbed current density could then be approximated by a delta function. This method has been used by Silin et al. (2002) for the Harris sheet, and allows Ampère's law to be reduced to a pair of algebraic equations. The approximate form of Ampère's law was solved numerically using a Fortran 90 code to implement the multi-dimensional Newton-Raphson method. It was found that solutions to the problem exist only if either the growth rate or real frequency vanishes.

A crucial parameter in determining the stability of the configuration is the ion-electron temperature ratio, T_i/T_e. For the case considered (the case from Figure 2.3 for which the distribution functions have a single maximum), it was found that instability results for $T_i/T_e = 0.1$. For a given value of the wavenumber k, it was found that there will exist a threshold value of the temperature ratio, beyond which no instability occurs, and the real frequency is non-zero (which is consistent with the earlier statement that solutions to the problem exist only when either ω_r or γ vanishes).

The effect of the ion-electron mass ratio on the growth rate of the instability was also discussed, and it was found that, beyond a mass ratio of approximately 100, the growth rate did not change too much, due to the electron terms becoming negligible in comparison to the ion terms.

Analytical solutions of Ampère's law were obtained for the region outside the sheet, which would be useful if the problem were to be solved without the delta function approximation, since a numerical method would then only be required for the region inside the sheet. These analytical solutions were found by making the simplifying assumption that the perturbed current density in the outer region is given by the adiabatic part only, so that the plasma dispersion functions in the coefficients can be neglected. The solution for $\bar{A}_{1y}$ was found to be the same as that obtained in studies of the resistive tearing mode, starting with a Harris sheet equilibrium (Schindler, 2007). This is because the Harris sheet and force-free Harris sheet fields have the same x-component. The solution for $\bar{A}_{1x}$ was found to have a similar form as the $\bar{A}_{1y}$ solution, but with $\bar{k}$ from the $\bar{A}_{1y}$ solution replaced by $\sqrt{\bar{k}^2 + 1}$.

The approximate solution of Ampère's law has given an illustration of the fact that Harrison and Neukirch's equilibrium for the force-free Harris sheet (Harrison and Neukirch, 2009b) is unstable to the collisionless tearing mode under certain conditions, with the growth rate of the instability depending crucially upon the ion-electron temperature ratio. It should be noted, however, that the long wavelength assumption is a hugely simplifying one, and so a definite conclusion cannot be given about the stability of the equilibrium at this stage. An immediate aim for future work, therefore, is to solve Ampère's law numerically by, for example, using a shooting method (e.g. Press et al., 1992). These results could then be compared with those of Section 4.4, in order to assess the validity of the delta function approximation. The ODEs could be solved by using the analytical solutions from Section 4.5 for the outer region, and obtaining a numerical solution for the inner region, or by including the plasma dispersion functions in the perturbed current expression for the outer region, and solving the problem numerically in both regions.

Another possibility for approximating the particle orbits is to firstly approximate $B_{x,ffhs}$ by the piecewise linear function

$$B_{x,approx} = \begin{cases} B_0 \bar{z}, & \text{if } |\bar{z}| \leq 1 \text{ (inside sheet)} \\ B_0 \text{sign}(\bar{z}), & \text{if } |\bar{z}| > 1 \text{ (outside sheet)} \end{cases}, \tag{5.1}$$

as illustrated in Figure 5.1. Such an approximation on B_x has been used before for the Harris sheet (e.g. Hoh, 1966; Yamanaka, 1978) and gives rise to elliptic functions. For the field to remain force-free, it must satisfy the condition $B_{x,approx}^2 + B_{y,approx}^2 = B_0^2$, which would give

$$B_{y,approx} = \begin{cases} 0, & \text{if } \bar{z} < -1 \\ B_0 \sqrt{1 - \bar{z}^2}, & \text{if } -1 \leq \bar{z} \leq 0 \\ 0, & \text{if } \bar{z} > 1 \end{cases}, \tag{5.2}$$

where $\bar{z} = z/L$, as illustrated in Figure 5.2. This is not a particularly good approximation to $B_{y,ffhs}$. Although it is better than the approximation used in this thesis for the force-free Harris sheet field, calculating the orbits for such a field would present considerable difficulty. A piecewise
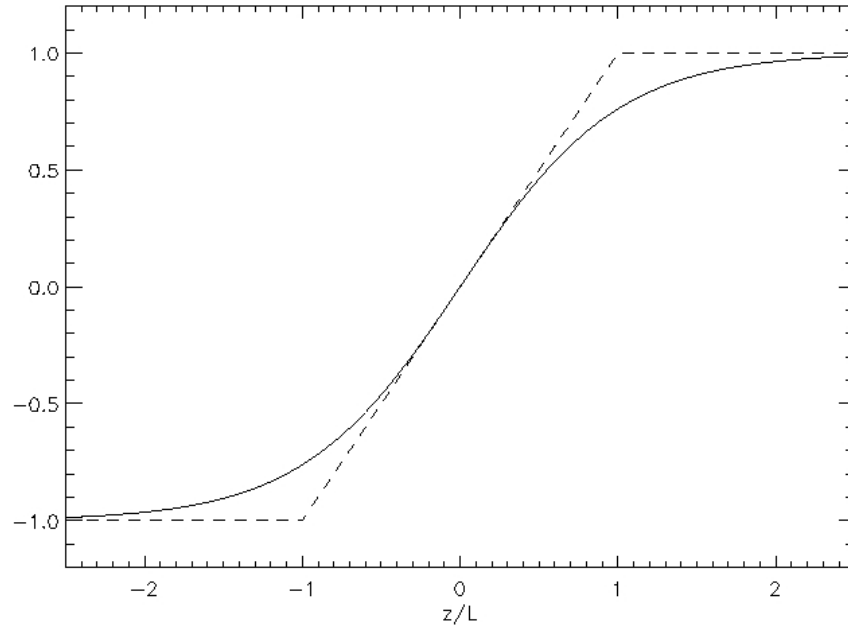
Figure 5.1: Plot of a possible approximation to $B_{x,ffhs}$ (dashed line) and $B_{x,ffhs}$ (solid line) against $z/L = \bar{z}$, for $B_0 = 1$.
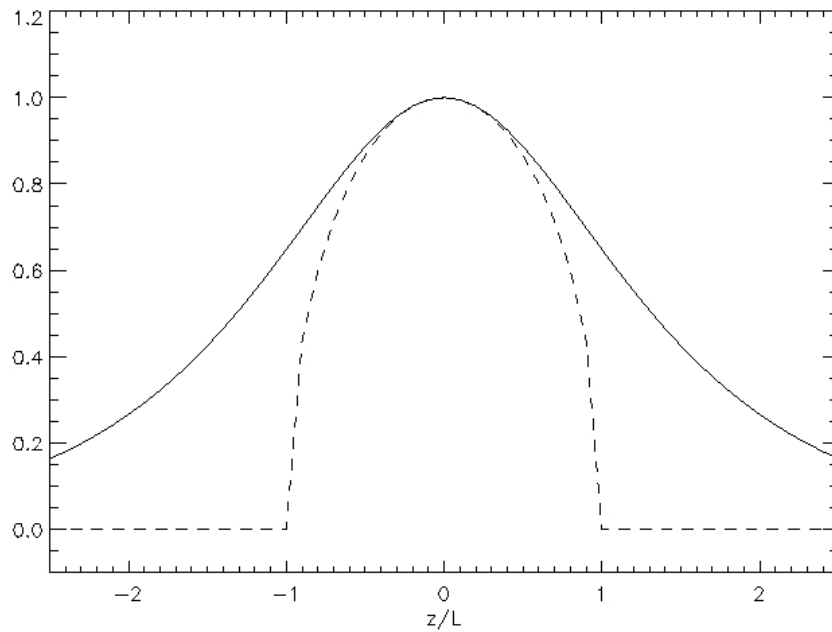
Figure 5.2: Plot of a possible approximation to $B_{y,ffhs}$ (dashed line) and $B_{y,ffhs}$ (solid line) against $z/L = \bar{z}$, for $B_0 = 1$.

linear function may be more appropriate for approximating $B_{y,ffhs}$, but this would violate the force-free condition. Instead of looking for another analytical approximation, therefore, it would make more sense to calculate the orbits numerically to achieve more accurate results in future work.

An investigation into the occurrence of microinstabilites, which may arise from the multi-peaked behaviour of the distribution function (2.59), is beyond the scope of this thesis, but would also be interesting to investigate in future work. Such a stability analysis would have to be carried out in three dimensions, using a numerical method such as that developed by Camporeale et al. (2006). It may also be interesting to consider the effect that three-dimensional perturbations have on the occurrence of macroinstabilities.

In the PhD thesis by Harrison (2009), 2.5D particle-in-cell simulations of collisionless reconnection were carried out for the force-free Harris sheet, using the Harrison and Neukirch (2009b) equilibrium as initial conditions. This was done for mass ratios $m_i/m_e = 1$ and $m_i/m_e = 9$. It would be interesting to investigate the effect of increasing the mass ratio, and to carry out 3D PIC simulations. These simulations could also potentially be carried out using some of the other force-free Harris sheet equilibria from Section 2.8 as initial conditions, to see what effect different equilibria have on the collisionless reconnection process.

Appendix A

Some Useful Trigonometric Identities

In the calculations from Chapters 2 and 3 for the force-free Harris sheet, the terms $\sin[4\tan^{-1}(e^{z/L})]$ and $\cos[4\tan^{-1}(e^{z/L})]$ appear on a number of occasions. These can be rewritten in terms of hyperbolic functions as

$$
\sin[4\tan^{-1}(e^{z/L})] \;=\; -2\frac{\sinh(z/L)}{\cosh^2(z/L)}, \tag{A.1}
$$

$$
\cos[4\tan^{-1}(e^{z/L})] \;=\; 1 - \frac{2}{\cosh^2(z/L)}, \tag{A.2}
$$

Equation (A.1) can be proved, firstly, by expressing the right hand side in terms of $e^{z/L}$, which gives

$$
-2\frac{\sinh\bar{z}}{\cosh^2\bar{z}} = -4\frac{(e^{z/L} - e^{-z/L})}{(e^{z/L} + e^{-z/L})^2}, \tag{A.3}
$$

which can be written in terms of $\bar{A}_{x,ffhs}$, the x-component of the vector potential for the force-free Harris sheet (normalised to $B_0 L$), as

$$
-2\frac{\sinh(z/L)}{\cosh^2(z/L)} = -4\frac{\left(\tan(\bar{A}_x/2) - 1/(\tan(\bar{A}_x/2))\right)}{\left(\tan(\bar{A}_x/2) + 1/\tan(\bar{A}_x/2)\right)^2}, \tag{A.4}
$$

since

$$
\bar{A}_{x,ffhs} = 2\tan^{-1}(e^{z/L}), \tag{A.5}
$$

which gives

$$
e^{z/L} = \tan\left(\frac{\bar{A}_x}{2}\right). \tag{A.6}
$$

Equation (A.4) can be written as

$$
-2\frac{\sinh(z/L)}{\cosh^2(z/L)} = -4\frac{\left(\sin(\bar{A}_x/2)/\cos(\bar{A}_x/2) - \cos(\bar{A}_x/2)/\sin(\bar{A}_x/2)\right)}{\left(\sin(\bar{A}_x/2)/\cos(\bar{A}_x/2) - \cos(\bar{A}_x/2)/\sin(\bar{A}_x/2)\right)^2}, \tag{A.7}
$$

which, on multiplying through by $\cos^2(\bar{A}_x/2)\sin^2(\bar{A}_x/2)$ and simplifying, becomes

$$-2\frac{\sinh(z/L)}{\cosh^2(z/L)} = -4\cos(\bar{A}_x/2)\sin(\bar{A}_x/2)\left[\sin^2(\bar{A}_x/2) - \cos^2(\bar{A}_x/2)\right]. \tag{A.8}$$

Using the trigonometric identities

$$\sin(2X) = 2\sin X\cos X, \tag{A.9}$$

$$\cos 2X = \cos^2 X - \sin^2 X, \tag{A.10}$$

then gives

$$-2\frac{\sinh(z/L)}{\cosh^2(z/L)} = \sin(2\bar{A}_x). \tag{A.11}$$

Finally, substituting in the definition (A.5) of $\bar{A}_{x,fhhs}$ gives Equation (A.1), as required.

Equation (A.2) can be obtained from Equation (A.1), since $\cos X = (1 - \sin^2 X)^{1/2}$, which gives

$$\cos^2[4\tan^{-1}(e^{z/L})] = 1 - \sin^2[4\tan^{-1}(e^{z/L})] \tag{A.12}$$

$$= 1 - 4\frac{\sinh^2(z/L)}{\cosh^4(z/L)} \tag{A.13}$$

$$= 1 - 4\frac{\cosh^2(z/L) - 1}{\cosh^4(z/L)} \tag{A.14}$$

$$= 1 - \frac{4}{\cosh^2(z/L)} + \frac{4}{\cosh^4(z/L)} \tag{A.15}$$

$$= \left(1 - \frac{2}{\cosh^2(z/L)}\right)^2, \tag{A.16}$$

and taking the square root gives Equation (A.2), as required.

Appendix B

Evaluation of Integrals From Section 2.8

In each of the three examples in Section 2.8, after changing to a cylindrical coordinate system (r, θ), the θ-integrations can be carried out by using the formulae

$$\int_0^{2\pi} \cos(a \cos \theta) d\theta = 2\pi J_0(a), \tag{B.1}$$

$$\int_0^{2\pi} \exp(a \sin \theta) d\theta = 2\pi I_0(a), \tag{B.2}$$

where J_0 is a Bessel function of the first kind, and I_0 is a modified Bessel function of the first kind. Using the fact that the cosine function is symmetric, the result (B.1) can be proved by firstly writing

$$\int_0^{2\pi} \cos(a \cos \theta) d\theta = 2 \int_0^{\pi} \cos(a \cos \theta) d\theta, \tag{B.3}$$

and then by using the formula (Abramowitz and Stegun, 1964)

$$J_0(a) = \frac{1}{\pi} \int_0^{\pi} \cos(a \cos \theta) d\theta. \tag{B.4}$$

The result (B.2) can be proved by firstly writing

$$\int_0^{2\pi} \exp(a \sin \theta) d\theta = \int_0^{\pi} \exp(a \sin \theta) d\theta + \int_{\pi}^{2\pi} \exp(a \sin \theta) d\theta. \tag{B.5}$$

which, upon using the substitution $\bar{\theta} = \theta - \pi$ in the second integral on the right-hand side, together with the identity $\sin(\bar{\theta} + \pi) = -\sin \bar{\theta}$, gives

$$\int_0^{2\pi} \exp(a \sin \theta) d\theta = \int_0^{\pi} \exp(a \sin \theta) d\theta + \int_0^{\pi} \exp(-a \sin \bar{\theta}) d\bar{\theta}. \tag{B.6}$$

Using the identity $\sin x = \cos(\pi/2 - x)$, together with the substitution $\phi = \theta - \pi/2$ for the first integral on the right-hand side, and the substitution $\phi = \bar{\theta} - \pi/2$ for the second integral, gives

$$\int_0^{2\pi} \exp(a \sin \theta) d\theta = \int_{-\pi/2}^{0} \left(\exp(a \cos \phi) + \exp(-a \cos \phi) \right) d\phi$$

$$+ \int_0^{\pi/2} \left(\exp(a \cos \phi) + \exp(-a \cos \phi) \right) d\phi. \tag{B.7}$$

Using the further substitutions $\psi = \phi + \pi$ in the first integral on the right-hand side, and $\psi = \phi$ in the second integral, together with the identity $\cos(x - \pi) = -\cos x$, allows both integrals to be combined to give

$$\int_0^{2\pi} \exp(a \sin \theta) d\theta = \int_0^{\pi} \left(\exp(a \cos \psi) + \exp(-a \cos \psi) \right) d\psi$$
$$= 2 \int_0^{\pi} \cosh(a \cos \psi) d\psi. \tag{B.8}$$

Finally, using the formula

$$I_0(a) = \frac{1}{\pi} \int_0^{\pi} \cosh(a \cos \psi) d\psi, \tag{B.9}$$

(Abramowitz and Stegun, 1964) then gives the result (B.2), as required.

After evaluating the θ-integrals, the r-integrals in Section 2.8 then take the form

$$\int_0^1 r(1 - r^2)^\lambda J_0(ar) dr, \tag{B.10}$$

$$\int_0^1 r(1 - r^2)^\lambda I_0(ar) dr. \tag{B.11}$$

Integrals of the form (B.10) can be evaluated firstly by using the substitution $r = \sin t$, and then by using the formula

$$\int_0^{\pi/2} J_\mu(z \sin t) \sin^{\mu+1} t \cos^{2\nu+1} t dt = \frac{2^\nu \Gamma(\nu + 1)}{z^{\nu+1}} J_{\mu+\nu+1}(z), \tag{B.12}$$

which is valid for $\Re\mu, \Re\nu > -1$ (Abramowitz and Stegun, 1964). This gives

$$\int_0^1 r(1 - r^2)^\lambda J_0(ar) dr = \frac{2^\lambda \Gamma(\lambda + 1)}{a^{\lambda+1}} J_{\lambda+1}(a). \tag{B.13}$$

Integrals of the form (B.11) can be evaluated by firstly using the identity

$$I_0(a) = J_0(ia), \tag{B.14}$$

and then by using the same steps that were used to evaluate the integrals of the form (B.10). This gives

$$\int_0^1 r(1 - r^2)^\lambda I_0(ar) dr = \frac{2^\lambda \Gamma(\lambda + 1)}{(ia)^{\lambda+1}} J_{\lambda+1}(ia). \tag{B.15}$$

Details of Results From Section 2.10 in Cylindrical Coordinates

The relations (1.76)-(1.80), from Section 1.4.2, have the following corresponding form in cylindrical coordinates

$$\frac{\partial \sigma}{\partial A_\theta} + \frac{\partial j_\theta}{\partial \phi} = 0, \tag{C.1}$$

$$\frac{\partial \sigma}{\partial A_z} + \frac{\partial j_z}{\partial \phi} = 0, \tag{C.2}$$

$$\frac{\partial j_\theta}{\partial A_z} - \frac{\partial j_z}{\partial A_\theta} = 0, \tag{C.3}$$

$$j_\theta = \frac{\partial P_{rr}}{\partial A_\theta}, \tag{C.4}$$

$$j_z = \frac{\partial P_{rr}}{\partial A_z}, \tag{C.5}$$

$$\frac{\partial P_{rr}}{\partial \phi} = -\sigma. \tag{C.6}$$

$$\tag{C.7}$$

where σ is the charge density, ϕ is the electric potential, P_{rr} is the rr-component of the pressure tensor, j_θ and j_z are the θ- and z-components of the current density, and A_θ and A_z are the θ- and z-components of the vector potential.

The calculation of the results (C.1)-(C.6) are similar to those in Cartesian coordinates (see Appendix A of Harrison and Neukirch, 2009a). Starting with the left-hand-side of Equation (C.1) gives

$$\frac{\partial \sigma}{\partial A_\theta} + \frac{\partial j_\theta}{\partial \phi} = \sum_s q_s r \left(\frac{\partial}{\partial A_\theta} \int_{-\infty}^{\infty} f_s d\mathbf{v} + r \frac{\partial}{\partial \phi} \int_{-\infty}^{\infty} \dot{\theta} f_s d\mathbf{v} \right) \tag{C.8}$$

$$= \sum_s q_s r \int_{-\infty}^{\infty} \left(\frac{\partial f_s}{\partial p_\theta} \frac{\partial p_\theta}{\partial A_\theta} + r\dot{\theta} \frac{\partial f_s}{\partial H_s} \frac{\partial H_s}{\partial \phi} \right) d\mathbf{v} \tag{C.9}$$

$$= \sum_s (q_s r)^2 \int_{-\infty}^{\infty} \left(\frac{\partial f_s}{\partial p_\theta} + \dot{\theta} \frac{\partial f_s}{\partial H_s} \right) d\mathbf{v} \tag{C.10}$$

$$= \sum_s \frac{q_s}{m}(mr^2) \int_{-\infty}^{\infty} \left(\frac{\partial f_s}{\partial p_\theta} + \dot{\theta}\frac{\partial f_s}{\partial H_s} \right) d\mathbf{v} \tag{C.11}$$

$$= \sum_s \frac{q_s}{m} \int_{-\infty}^{\infty} \frac{\partial f_s}{\partial \dot{\theta}} d\mathbf{v} \tag{C.12}$$

$$= 0, \tag{C.13}$$

where $d\mathbf{v} = d\dot{r}d\dot{\theta}d\dot{z}$, and the last step comes from using integration by parts as follows,

$$\int_{-\infty}^{\infty} \frac{\partial f_s}{\partial \dot{\theta}} d\mathbf{v} = \int_{-\infty}^{\infty}\int_{-\infty}^{\infty} \left(\int_{-\infty}^{\infty} \frac{\partial f_s}{\partial \dot{\theta}} d\dot{\theta} \right) d\dot{r}d\dot{z} \tag{C.14}$$

$$= \int_{-\infty}^{\infty}\int_{-\infty}^{\infty} \left([f_s]_{-\infty}^{\infty} - \int_{-\infty}^{\infty} (0 \times f_s) d\dot{\theta} \right) d\dot{r}d\dot{z} \tag{C.15}$$

$$= 0. \tag{C.16}$$

The relation (C.2) can then be proved in exactly the same way by replacing A_θ by A_z and j_θ by j_z.

The first term on the left-hand-side of the Equation (C.3), $\partial j_\theta / \partial A_z$, can be written in the following way

$$\frac{\partial j_\theta}{\partial A_z} = \sum_s q_s r^2 \int_{-\infty}^{\infty} \dot{\theta}\frac{\partial f_s}{\partial p_z}\frac{\partial p_z}{\partial A_z} d\mathbf{v} \tag{C.17}$$

$$= \sum_s (q_s r)^2 \int_{-\infty}^{\infty} \dot{\theta}\frac{\partial f_s}{\partial p_z} d\mathbf{v} \tag{C.18}$$

$$= \sum_s (q_s r)^2 \int_{-\infty}^{\infty} \left(\frac{1}{m_s}\frac{\partial}{\partial \dot{z}}(\dot{\theta}f_s) - \dot{\theta}\dot{z}\frac{\partial f_s}{\partial H_s} \right) d\mathbf{v} \tag{C.19}$$

$$= -\sum_s (q_s r)^2 \int_{-\infty}^{\infty} \dot{\theta}\dot{z}\frac{\partial f_s}{\partial H_s} d\mathbf{v}. \tag{C.20}$$

In the third step above, the p_z derivative has been expressed as follows

$$\frac{\partial f_s}{\partial \dot{z}} = \frac{\partial f_s}{\partial H_s}\frac{\partial H_s}{\partial \dot{z}} + \frac{\partial f_s}{\partial p_z}\frac{\partial p_z}{\partial \dot{z}} = m_s \left(\dot{z}\frac{\partial f_s}{\partial H_s} + \frac{\partial f_s}{\partial p_z} \right). \tag{C.21}$$

The term $\partial j_z / \partial A_\theta$ on the left-hand-side of Equation (C.3) can be written as

$$\frac{\partial j_z}{\partial A_\theta} = \sum_s q_s r \int_{-\infty}^{\infty} \dot{z}\frac{\partial f_s}{\partial p_\theta}\frac{\partial p_\theta}{\partial A_\theta} d\mathbf{v} \tag{C.22}$$

$$= \sum_s (q_s r)^2 \int_{-\infty}^{\infty} \dot{z}\frac{\partial f_s}{\partial p_\theta} d\mathbf{v} \tag{C.23}$$

$$= \sum_s (q_s r)^2 \int_{-\infty}^{\infty} \left(\frac{1}{m_s r^2}\frac{\partial}{\partial \dot{\theta}}(\dot{z}f_s) - \dot{\theta}\dot{z}\frac{\partial f_s}{\partial H_s} \right) d\mathbf{v} \tag{C.24}$$

$$= -\sum_s (q_s r)^2 \int_{-\infty}^{\infty} \dot{\theta} \dot{z} \frac{\partial f_s}{\partial H_s} d\mathbf{v} \tag{C.25}$$

$$= \frac{\partial j_\theta}{\partial A_z}, \tag{C.26}$$

where, in the third step, the p_θ derivative has been expressed as

$$\frac{\partial f_s}{\partial \dot{\theta}} = \frac{\partial f_s}{\partial H_s} \frac{\partial H_s}{\partial \dot{\theta}} + \frac{\partial f_s}{\partial p_\theta} \frac{\partial p_\theta}{\partial \dot{\theta}} = m_s r^2 \left(\dot{\theta} \frac{\partial f_s}{\partial H_s} + \frac{\partial f_s}{\partial p_\theta} \right). \tag{C.27}$$

This proves the result (C.3).

The relation (C.6) can be proved as follows

$$\frac{\partial P_{rr}}{\partial \phi} = \sum_s m_s r \int_{-\infty}^{\infty} \dot{r}^2 \frac{\partial f_s}{\partial H_s} \frac{\partial H_s}{\partial \phi} d\mathbf{v} \tag{C.28}$$

$$= \sum_s m_s q_s r \int_{-\infty}^{\infty} \dot{r}^2 \frac{\partial f_s}{\partial H_s} d\mathbf{v} \tag{C.29}$$

$$= \sum_s m_s q_s r \int_{-\infty}^{\infty} \dot{r}^2 \left(\frac{1}{m_s \dot{r}} \frac{\partial f_s}{\partial \dot{r}} \right) d\mathbf{v} \tag{C.30}$$

$$= \sum_s q_s r \int_{-\infty}^{\infty} \dot{r} \frac{\partial f_s}{\partial \dot{r}} d\mathbf{v} \tag{C.31}$$

$$= -\sum_s q_s r \int_{-\infty}^{\infty} f_s d\mathbf{v} \tag{C.32}$$

$$= -\sigma, \tag{C.33}$$

where in the third step above, the derivative $\partial f_s / \partial \dot{r}$ can be written as

$$\frac{\partial f_s}{\partial \dot{r}} = \frac{\partial f_s}{\partial H_s} \frac{\partial H_s}{\partial \dot{r}}, \tag{C.34}$$

so that

$$\frac{\partial f_s}{\partial H_s} = \frac{\partial f_s / \partial \dot{r}}{\partial H_s / \partial \dot{r}} = \frac{1}{m_s \dot{r}} \frac{\partial f_s}{\partial \dot{r}}. \tag{C.35}$$

In addition, in the fifth step above, integration by parts can be used as follows,

$$\int_{-\infty}^{\infty} \dot{r} \frac{\partial f_s}{\partial \dot{r}} d\mathbf{v} = \left[\dot{r} f_s \right]_{-\infty}^{\infty} - \int_{-\infty}^{\infty} f_s d\mathbf{v} = -\int_{-\infty}^{\infty} f_s d\mathbf{v}, \tag{C.36}$$

where $\left[\dot{r} f_s \right]_{-\infty}^{\infty}$ vanishes since $f_s \to 0$ as $(\dot{r}, \dot{\theta}, \dot{z}) \to \pm\infty$.

The right-hand-side of relation (C.4) can be expressed as

$$\frac{\partial P_{rr}}{\partial A_\theta} = \sum_s m_s r \int_{-\infty}^{\infty} \dot{r}^2 \frac{\partial f_s}{\partial p_\theta} \frac{\partial p_\theta}{\partial A_\theta} d\mathbf{v} \tag{C.37}$$

$$= \sum_s q_s m_s r^2 \int_{-\infty}^{\infty} \dot{r}^2 \frac{\partial f_s}{\partial p_\theta} d\mathbf{v}. \tag{C.38}$$

Then, using the fact that

$$\frac{\partial f_s}{\partial \dot{\theta}} = \frac{\partial f_s}{\partial H_s} \frac{\partial H_s}{\partial \dot{\theta}} + \frac{\partial f_s}{\partial p_\theta} \frac{\partial p_\theta}{\partial \dot{\theta}} = m_s r^2 \left(\dot{\theta} \frac{\partial f_s}{\partial H_s} + \frac{\partial f_s}{\partial p_\theta} \right), \tag{C.39}$$

gives,

$$\frac{\partial P_{rr}}{\partial A_\theta} = \sum_s q_s \int_{-\infty}^{\infty} \left(\dot{r}^2 \frac{\partial f_s}{\partial \dot{\theta}} - m_s r^2 \dot{r}^2 \dot{\theta} \frac{\partial f_s}{\partial H_s} \right) d\mathbf{v} \tag{C.40}$$

$$= \sum_s q_s \int_{-\infty}^{\infty} \left(\dot{r}^2 \frac{\partial f_s}{\partial \dot{\theta}} - r^2 \dot{\theta} \dot{r} \frac{\partial f_s}{\partial \dot{r}} \right) d\mathbf{v} \tag{C.41}$$

$$= -\sum_s q_s r^2 \int_{-\infty}^{\infty} \dot{\theta} \dot{r} \frac{\partial f_s}{\partial \dot{r}} d\mathbf{v} \tag{C.42}$$

$$= -\sum_s q_s r^2 \left(\left[\dot{\theta} \dot{r} f_s \right]_{-\infty}^{\infty} - \int_{-\infty}^{\infty} \dot{\theta} f_s d\mathbf{v} \right) \tag{C.43}$$

$$= \sum_s q_s r^2 \int_{-\infty}^{\infty} \dot{\theta} f_s d\mathbf{v} \tag{C.44}$$

$$= j_\theta, \tag{C.45}$$

which proves the relation (C.4). Note that Equation (C.35) was used in the second step above, and integration by parts was used in the fourth step. The result (C.5) can be obtained in a similar way, by direct differentiation of P_{rr} with respect to A_z.

Appendix D

The Plasma Dispersion Function

Whenever a distribution function with a Maxwellian part is present, the plasma dispersion function (e.g. Fried and Conte, 1961) can be used, which is defined as

$$Z(\zeta) = \frac{1}{\sqrt{\pi}} \int_{-\infty}^{\infty} \frac{e^{-x^2}}{x - \zeta} dx, \tag{D.1}$$

where ζ is, in general, a complex variable, and so the integration is carried out in the complex plane, which involves integrating around the pole at $x = \zeta$. This function is related to the complex error function through the representation

$$\begin{aligned} Z(\zeta) &= 2ie^{-\zeta^2} \int_{-\infty}^{i\zeta} e^{-x^2} dx \\ &= i\sqrt{\pi}e^{-\zeta^2} \text{erfc}(-i\zeta) \end{aligned} \tag{D.2}$$

The plasma dispersion function satisfies the differential equation

$$Z'(\zeta) = -2[1 + \zeta Z(\zeta)], \tag{D.3}$$

since

$$Z'(\zeta) = \frac{1}{\sqrt{\pi}} \int_{-\infty}^{\infty} \frac{e^{-x^2}}{(x - \zeta)^2} dx. \tag{D.4}$$

The second derivative of Z can then be obtained from Equation (D.3) as

$$\begin{aligned} Z''(\zeta) &= -2[Z(\zeta) + \zeta Z'(\zeta)] \tag{D.5} \\ &= -2[Z(\zeta) - 2\zeta(1 + \zeta Z(\zeta))] \tag{D.6} \\ &= -2[(1 - 2\zeta^2)Z(\zeta) - 2\zeta]. \tag{D.7} \end{aligned}$$

The following integrals occur in Section 3.3 in the Vlasov stability calculation for the Harris sheet.

$$\int_{-\infty}^{\infty} \frac{xe^{-x^2}}{x - \zeta} dx = -\frac{\sqrt{\pi}}{2} Z'(\zeta), \tag{D.8}$$

$$\int_{-\infty}^{\infty} \frac{x^2 e^{-x^2}}{x - \zeta} dx = -\frac{\sqrt{\pi}}{2} \zeta Z'(\zeta). \tag{D.9}$$

Equation (D.8) can be proved by firstly using integration by parts, and then by using the definition (D.1), which gives

$$\int_{-\infty}^{\infty} \frac{x e^{-x^2}}{x - \zeta} dx = -\frac{1}{2} \int_{-\infty}^{\infty} \frac{e^{-x^2}}{(x - \zeta)^2} dx \tag{D.10}$$

$$= -\frac{1}{2} \frac{d}{d\zeta} \int_{-\infty}^{\infty} \frac{e^{-x^2}}{x - \zeta} dx \tag{D.11}$$

$$= -\frac{\sqrt{\pi}}{2} Z'(\zeta). \tag{D.12}$$

Equation (D.9) can be proved by firstly considering the integral

$$\int_{-\infty}^{\infty} \frac{x^2 e^{-ax^2}}{x - \zeta} dx = -\frac{d}{da} \int_{-\infty}^{\infty} \frac{e^{-ax^2}}{x - \zeta} dx, \tag{D.13}$$

and then by using the substitution $\bar{x} = \sqrt{a}x$, which gives

$$\int_{-\infty}^{\infty} \frac{x^2 e^{-ax^2}}{x - \zeta} dx = -\frac{d}{da} \int_{-\infty}^{\infty} \frac{e^{-\bar{x}^2}}{\bar{x} - \sqrt{a}\zeta} d\bar{x} \tag{D.14}$$

$$= -\sqrt{\pi} \frac{d}{da} \left[Z\left(\sqrt{a}\zeta\right) \right] \tag{D.15}$$

$$= -\frac{1}{2} \sqrt{\frac{\pi}{a}} \zeta Z'\left(\sqrt{a}\zeta\right). \tag{D.16}$$

Finally, taking the limit $a \to 1$ gives,

$$\int_{-\infty}^{\infty} \frac{x^2 e^{-x^2}}{x - \zeta} dx = -\frac{\sqrt{\pi}}{2} \zeta Z'(\xi). \tag{D.17}$$

The plasma dispersion function also appears through a number of integrals in the force-free Harris sheet stability analysis of Section 3.4. These are detailed in Appendix F.

Velocity Integrals

E.1   Summary of Velocity Integrals

The following integrals are needed in the velocity integrations for the calculations of the perturbed density and perturbed current density inside and outside the sheet.

$$\int_{-\infty}^{\infty} \exp(-ax^2)dx = \sqrt{\frac{\pi}{a}}, \tag{E.1}$$

$$\int_{-\infty}^{\infty} x^2 \exp(-ax^2)dx = \frac{1}{2a}\sqrt{\frac{\pi}{a}}, \tag{E.2}$$

$$\int_{-\infty}^{\infty} x \exp(-a(x-b)^2)dx = b\sqrt{\frac{\pi}{a}}, \tag{E.3}$$

$$\int_{-\infty}^{\infty} \exp(-ax^2 + bx)dx = \sqrt{\frac{\pi}{a}}\exp\left(\frac{b^2}{4a}\right), \tag{E.4}$$

$$\int_{-\infty}^{\infty} x \exp(-ax^2 + bx)dx = \sqrt{\frac{\pi}{a}}\frac{b}{2a}\exp\left(\frac{b^2}{4a}\right), \tag{E.5}$$

$$\int_{-\infty}^{\infty} x^2 \exp(-ax^2 + bx)dx = \frac{1}{2a}\sqrt{\frac{\pi}{a}}\left(1+\frac{b^2}{2a}\right)\exp\left(\frac{b^2}{4a}\right), \tag{E.6}$$

$$\int_{-\infty}^{\infty} \exp(-ax^2 \pm ibx)dx = \sqrt{\frac{\pi}{a}}\exp\left(-\frac{b^2}{4a}\right), \tag{E.7}$$

$$\int_{-\infty}^{\infty} x \exp(-ax^2 \pm ibx)dx = \pm\frac{ib}{2a}\sqrt{\frac{\pi}{a}}\exp\left(-\frac{b^2}{4a}\right), \tag{E.8}$$

$$\int_{-\infty}^{\infty} x^2 \exp(-ax^2 \pm ibx)dx = \frac{1}{2a}\sqrt{\frac{\pi}{a}}\left(1-\frac{b^2}{2a}\right)\exp\left(-\frac{b^2}{4a}\right), \tag{E.9}$$

$$\int_{-\infty}^{\infty} \exp(-ax^2)\cos[b(x+\lambda)]dx = \sqrt{\frac{\pi}{a}}\exp\left(-\frac{b^2}{4a}\right)\cos b\lambda, \tag{E.10}$$

$$\int_{-\infty}^{\infty} \exp(-ax^2)\sin[b(x+\lambda)]dx = \sqrt{\frac{\pi}{a}}\exp\left(-\frac{b^2}{4a}\right)\sin b\lambda, \tag{E.11}$$

$$\int_{-\infty}^{\infty} x \exp(-ax^2)\cos[b(x+\lambda)]dx = -\frac{b}{2a}\sqrt{\frac{\pi}{a}}\exp\left(-\frac{b^2}{4a}\right)\sin b\lambda, \tag{E.12}$$

$$\int_{-\infty}^{\infty} x \exp(-ax^2) \sin[b(x + \lambda)]dx = \frac{b}{2a}\sqrt{\frac{\pi}{a}} \exp\left(-\frac{b^2}{4a}\right) \cos b\lambda, \quad (E.13)$$

$$\int_{-\infty}^{\infty} \exp(-ax^2 + ibx) \cos(cx + d)dx = \frac{1}{2}\sqrt{\frac{\pi}{a}}[\cos d + i \sin d]$$
$$\times \exp\left(-\frac{(b+c)^2}{4a}\right)$$
$$+\frac{1}{2}\sqrt{\frac{\pi}{a}}[\cos d - i \sin d]$$
$$\times \exp\left(-\frac{(b-c)^2}{4a}\right), \quad (E.14)$$

$$\int_{-\infty}^{\infty} x \exp(-ax^2 + ibx) \cos(cx + d)dx = \frac{i}{4a}\sqrt{\frac{\pi}{a}}[\cos d + i \sin d](b + c)$$
$$\times \exp\left(-\frac{(b+c)^2}{4a}\right)$$
$$+\frac{i}{4a}\sqrt{\frac{\pi}{a}}[\cos d - i \sin d](b - c)$$
$$\times \exp\left(-\frac{(b-c)^2}{4a}\right), \quad (E.15)$$

$$\int_{-\infty}^{\infty} x^2 \exp(-ax^2 + ibx) \cos(cx + d)dx = \frac{1}{4a}\sqrt{\frac{\pi}{a}}[\cos d + i \sin d]\left(1 - \frac{(b+c)^2}{2a}\right)$$
$$\times \exp\left(-\frac{(b+c)^2}{4a}\right)$$
$$+\frac{1}{4a}\sqrt{\frac{\pi}{a}}[\cos d - i \sin d]\left(1 - \frac{(b-c)^2}{2a}\right)$$
$$\times \exp\left(-\frac{(b-c)^2}{4a}\right), \quad (E.16)$$

$$\int_{-\infty}^{\infty} \exp(-ax^2 + ibx) \sin(cx + d)dx = \frac{1}{2}\sqrt{\frac{\pi}{a}}[\sin d - i \cos d]$$
$$\times \exp\left(-\frac{(b+c)^2}{4a}\right)$$
$$+\frac{1}{2}\sqrt{\frac{\pi}{a}}[\sin d + i \cos d]$$
$$\times \exp\left(-\frac{(b-c)^2}{4a}\right), \quad (E.17)$$

$$\int_{-\infty}^{\infty} x \exp(-ax^2 + ibx) \sin(cx + d)dx = \frac{i}{4a}\sqrt{\frac{\pi}{a}}[\sin d - i \cos d](b + c)$$
$$\times \exp\left(-\frac{(b+c)^2}{4a}\right)$$
$$+\frac{i}{4a}\sqrt{\frac{\pi}{a}}[\sin d + i \cos d](b - c)$$

$$\times \exp\left(-\frac{(b-c)^2}{4a}\right), \tag{E.18}$$

$$\int_{-\infty}^{\infty} x^2 \exp(-ax^2 + ibx)\sin(cx+d)dx = \frac{1}{4a}\sqrt{\frac{\pi}{a}}[\sin d - i\cos d]\left(1 - \frac{(b+c)^2}{2a}\right)$$

$$\times \exp\left(-\frac{(b+c)^2}{4a}\right)$$

$$+\frac{1}{4a}\sqrt{\frac{\pi}{a}}[\sin d + i\cos d]\left(1 - \frac{(b-c)^2}{2a}\right)$$

$$\times \exp\left(-\frac{(b-c)^2}{4a}\right). \tag{E.19}$$

E.2 Evaluation of Velocity Integrals

The integral (E.1) is a standard integral. The integral (E.2) can be evaluated by taking $-d/da$ of Equation (E.1), which gives

$$\int_{-\infty}^{\infty} x^2 \exp(-ax^2)dx = -\frac{d}{da}\int_{-\infty}^{\infty}\exp(-ax^2)dx$$

$$= -\frac{d}{da}\left(\sqrt{\frac{\pi}{a}}\right)$$

$$= \frac{1}{2a}\sqrt{\frac{\pi}{a}}. \tag{E.20}$$

The integral (E.3) can be evaluated by using the substitution $w = x - b$ along with Equation (E.1), which gives

$$\int_{-\infty}^{\infty} x \exp(-a(x-b)^2)dx = \int_{-\infty}^{\infty}(w+b)\exp(-aw^2)dw$$

$$= b\int_{-\infty}^{\infty}\exp(-aw^2)dw + \int_{-\infty}^{\infty} w\exp(-aw^2)dw$$

$$= b\sqrt{\frac{\pi}{a}}, \tag{E.21}$$

since the second integral on the right-hand side of the second line vanishes.

The integral (E.4) can be evaluated firstly by completing the square in the argument of the exponential, and then by using the substitution $w = x - b/2a$, along with Equation (E.1), which gives

$$\int_{-\infty}^{\infty}\exp(-ax^2 + bx)dx = \exp\left(\frac{b^2}{4a}\right)\int_{-\infty}^{\infty}\exp\left(-a\left(x - \frac{b}{2a}\right)^2\right)dx$$

$$= \exp\left(\frac{b^2}{4a}\right) \int_{-\infty}^{\infty} \exp\left(-aw^2\right) dw$$

$$= \sqrt{\frac{\pi}{a}} \exp\left(\frac{b^2}{4a}\right). \tag{E.22}$$

The integral (E.5) can be evaluated by again completing the square in the argument of the exponential, then by using Equation (E.3), which gives

$$\int_{-\infty}^{\infty} x \exp(-ax^2 + bx) dx = \exp\left(\frac{b^2}{4a}\right) \int_{-\infty}^{\infty} x \exp\left(-a\left(x - \frac{b}{2a}\right)^2\right) dx$$

$$= \sqrt{\frac{\pi}{a}} \frac{b}{2a} \exp\left(\frac{b^2}{4a}\right). \tag{E.23}$$

The integral (E.6) can be evaluated by taking $-d/da$ of Equation (E.4), which gives

$$\int_{-\infty}^{\infty} x^2 \exp(-ax^2 + bx) dx = -\frac{d}{da} \int_{-\infty}^{\infty} \exp(-ax^2 + bx) dx$$

$$= -\frac{d}{da}\left(\sqrt{\frac{\pi}{a}} \exp\left(\frac{b^2}{4a}\right)\right)$$

$$= \frac{1}{2a} \sqrt{\frac{\pi}{a}} \left(1 + \frac{b^2}{2a}\right) \exp\left(\frac{b^2}{4a}\right). \tag{E.24}$$

The integral (E.7) is listed in Appendix C of Gary (2005), but could also be obtained from (E.4), by letting $b = \pm ib$. Likewise, the integrals (E.8) and (E.9) can be evaluated by letting $b = \pm ib$ in Equations (E.5) and (E.6), respectively.

The integrals (E.10) and (E.11) are listed in Gradshteyn and Ryzhik (1966). The integral (E.12) can then be evaluated by firstly taking d/db of Equation (E.11), which gives

$$\frac{d}{db} \int_{-\infty}^{\infty} \exp(-ax^2) \sin[b(x + \lambda)] dx = \int_{-\infty}^{\infty} (x + \lambda) \exp(-ax^2) \cos[b(x + \lambda)] dx, \tag{E.25}$$

so that

$$\int_{-\infty}^{\infty} x \exp(-ax^2) \cos[b(x + \lambda)] dx = \frac{d}{db} \int_{-\infty}^{\infty} \exp(-ax^2) \sin[b(x + \lambda)] dx$$

$$- \lambda \int_{-\infty}^{\infty} x \exp(-ax^2) \cos[b(x + \lambda)] dx. \tag{E.26}$$

Using Equations (E.10) and (E.11) and cancelling terms then gives

$$\int_{-\infty}^{\infty} x \exp(-ax^2) \cos[b(x + \lambda)] dx = \sqrt{\frac{\pi}{a}} \frac{d}{db} \left(\exp\left(-\frac{b^2}{4a}\right) \sin b\lambda\right)$$

$$-\lambda\sqrt{\frac{\pi}{a}}\exp\left(-\frac{b^2}{4a}\right)\cos b\lambda$$
$$=\quad-\frac{b}{2a}\sqrt{\frac{\pi}{a}}\exp\left(-\frac{b^2}{4a}\right)\sin b\lambda. \tag{E.27}$$

The integral (E.13) can be evaluated by firstly taking $-d/db$ of Equation (E.10), which gives

$$-\frac{d}{db}\int_{-\infty}^{\infty}\exp(-ax^2)\cos[b(x+\lambda)]dx \quad=\quad \int_{-\infty}^{\infty}(x+\lambda)\exp(-ax^2)\sin[b(x+\lambda)]dx, \tag{E.28}$$

so that

$$\int_{-\infty}^{\infty}x\exp(-ax^2)\sin[b(x+\lambda)]dx \quad=\quad -\frac{d}{db}\int_{-\infty}^{\infty}\exp(-ax^2)\cos[b(x+\lambda)]dx$$
$$-\lambda\int_{-\infty}^{\infty}\exp(-ax^2)\sin[b(x+\lambda)]dx, \tag{E.29}$$

Using Equations (E.10) and (E.11) and cancelling terms then gives

$$\int_{-\infty}^{\infty}x\exp(-ax^2)\sin[b(x+\lambda)]dx \quad=\quad -\sqrt{\frac{\pi}{a}}\frac{d}{db}\left(\exp\left(-\frac{b^2}{4a}\right)\cos b\lambda\right)$$
$$-\lambda\sqrt{\frac{\pi}{a}}\exp\left(-\frac{b^2}{4a}\right)\sin b\lambda$$
$$=\quad \frac{b}{2a}\sqrt{\frac{\pi}{a}}\exp\left(-\frac{b^2}{4a}\right)\cos b\lambda. \tag{E.30}$$

The integral (E.14) can be evaluated firstly by using the identity $\cos x=\cosh ix$, which gives

$$\cos(cx+d) \quad=\quad \cosh[i(cx+d)]$$
$$=\quad \frac{1}{2}\left(\exp[i(cx+d)]+\exp[-i(cx+d)]\right), \tag{E.31}$$

which then gives

$$\int_{-\infty}^{\infty}\exp(-ax^2+ibx)\cos(cx+d)dx \quad=\quad \frac{1}{2}\exp(id)\int_{-\infty}^{\infty}\exp\left(-ax^2+i(b+c)x\right)dx$$
$$+\frac{1}{2}\exp(-id)\int_{-\infty}^{\infty}\exp\left(-ax^2+i(b-c)x\right)dx$$
$$=\quad \frac{1}{2}\sqrt{\frac{\pi}{a}}[\cos d+i\sin d]\exp\left(-\frac{(b+c)^2}{4a}\right)$$
$$+\frac{1}{2}\sqrt{\frac{\pi}{a}}[\cos d-i\sin d]\exp\left(-\frac{(b-c)^2}{4a}\right), \tag{E.32}$$

where Equation (E.7) has also been used.

The integral (E.15) can be evaluated by taking d/db of Equation (E.14) and multiplying by $-i$, which gives

$$
\begin{aligned}
\int_{-\infty}^{\infty} x \exp(-ax^2 + ibx)\cos(cx+d)dx &= -i\frac{d}{db}\int_{-\infty}^{\infty}\exp(-ax^2+ibx)\cos(cx+d)dx\\
&= -i\frac{d}{db}\left[\frac{1}{2}\sqrt{\frac{\pi}{a}}[\cos d + i\sin d]\right.\\
&\quad\times\exp\left(-\frac{(b+c)^2}{4a}\right)\\
&\quad\left.+\frac{1}{2}\sqrt{\frac{\pi}{a}}[\cos d - i\sin d]\exp\left(-\frac{(b-c)^2}{4a}\right)\right]\\
&= \frac{i}{4a}\sqrt{\frac{\pi}{a}}[\cos d + i\sin d](b+c)\\
&\quad\times\exp\left(-\frac{(b+c)^2}{4a}\right)\\
&\quad+\frac{i}{4a}\sqrt{\frac{\pi}{a}}[\cos d - i\sin d](b-c)\\
&\quad\times\exp\left(-\frac{(b-c)^2}{4a}\right).
\end{aligned}
\tag{E.33}
$$

The integral (E.16) can be evaluated by taking $-d/da$ of Equation (E.14), which gives

$$
\begin{aligned}
\int_{-\infty}^{\infty} x^2 \exp(-ax^2 + ibx)\cos(cx+d)dx &= -\frac{d}{da}\int_{-\infty}^{\infty}\exp(-ax^2+ibx)\cos(cx+d)dx\\
&= -\frac{d}{da}\left[\frac{1}{2}\sqrt{\frac{\pi}{a}}[\cos d + i\sin d]\right.\\
&\quad\times\exp\left(-\frac{(b+c)^2}{4a}\right)\\
&\quad\left.+\frac{1}{2}\sqrt{\frac{\pi}{a}}[\cos d - i\sin d]\exp\left(-\frac{(b-c)^2}{4a}\right)\right]\\
&= \frac{1}{4a}\sqrt{\frac{\pi}{a}}[\cos d + i\sin d]\\
&\quad\times\left(1 - \frac{(b+c)^2}{2a}\right)\exp\left(-\frac{(b+c)^2}{4a}\right)\\
&\quad+\frac{1}{4a}\sqrt{\frac{\pi}{a}}[\cos d - i\sin d]\\
&\quad\times\left(1 - \frac{(b-c)^2}{2a}\right)\exp\left(-\frac{(b-c)^2}{4a}\right).
\end{aligned}
\tag{E.34}
$$

The integral (E.17) can be evaluated by using the identity $\sin x = -i \sinh ix$, which gives

$$
\begin{aligned}
\sin(cx + d) &= -i \sinh[i(cx + d)] \\
&= -\frac{i}{2} \left[\exp[i(cx + d)] - \exp[-i(cx + d)] \right],
\end{aligned}
\tag{E.35}
$$

which then gives

$$
\begin{aligned}
\int_{-\infty}^{\infty} \exp(-ax^2 + ibx) \sin(cx + d) dx &= -\frac{i}{2} \exp(id) \int_{-\infty}^{\infty} \exp\left(-ax^2 + i(b + c)x\right) dx \\
&\quad + \frac{i}{2} \exp(-id) \int_{-\infty}^{\infty} \exp\left(-ax^2 + i(b - c)x\right) dx \\
&= \frac{1}{2}\sqrt{\frac{\pi}{a}}[\sin d - i \cos d] \exp\left(-\frac{(b + c)^2}{4a}\right) \\
&\quad + \frac{1}{2}\sqrt{\frac{\pi}{a}}[\sin d + i \cos d] \exp\left(-\frac{(b - c)^2}{4a}\right),
\end{aligned}
\tag{E.36}
$$

where Equation (E.7) has also been used.

The integral (E.18) can be evaluated by taking d/db of Equation (E.17) and multiplying by $-i$, which gives

$$
\begin{aligned}
\int_{-\infty}^{\infty} x \exp(-ax^2 + ibx) \sin(cx + d) dx &= -i\frac{d}{db} \int_{-\infty}^{\infty} \exp(-ax^2 + ibx) \sin(cx + d) dx \\
&= -i\frac{d}{db}\left(\frac{1}{2}\sqrt{\frac{\pi}{a}}[\sin d - i \cos d] \right. \\
&\quad \times \exp\left(-\frac{(b + c)^2}{4a}\right) \\
&\quad \left. + \frac{1}{2}\sqrt{\frac{\pi}{a}}[\sin d + i \cos d] \exp\left(-\frac{(b - c)^2}{4a}\right) \right) \\
&= \frac{i}{4a}\sqrt{\frac{\pi}{a}}[\sin d - i \cos d](b + c) \\
&\quad \times \exp\left(-\frac{(b + c)^2}{4a}\right) \\
&\quad + \frac{i}{4a}\sqrt{\frac{\pi}{a}}[\sin d + i \cos d](b - c) \\
&\quad \times \exp\left(-\frac{(b - c)^2}{4a}\right).
\end{aligned}
\tag{E.37}
$$

Finally, the integral (E.19) can be evaluated by taking $-d/da$ of Equation (E.17), which gives

$$
\begin{aligned}
\int_{-\infty}^{\infty} x^2 \exp(-ax^2 + ibx) \sin(cx + d) dx &= -\frac{d}{da} \int_{-\infty}^{\infty} \exp(-ax^2 + ibx) \sin(cx + d) dx \\
&= -\frac{d}{da} \left(\frac{1}{2} \sqrt{\frac{\pi}{a}} [\sin d - i \cos d] \right. \\
&\quad \times \exp\left(-\frac{(b+c)^2}{4a} \right) \\
&\quad \left. + \frac{1}{2} \sqrt{\frac{\pi}{a}} [\sin d + i \cos d] \exp\left(-\frac{(b-c)^2}{4a} \right) \right) \\
&= \frac{1}{4a} \sqrt{\frac{\pi}{a}} [\sin d - i \cos d] \\
&\quad \times \left(1 - \frac{(b+c)^2}{2a} \right) \exp\left(-\frac{(b+c)^2}{4a} \right) \\
&\quad + \frac{1}{4a} \sqrt{\frac{\pi}{a}} [\sin d + i \cos d] \\
&\quad \times \left(1 - \frac{(b-c)^2}{2a} \right) \exp\left(-\frac{(b-c)^2}{4a} \right).
\end{aligned}
$$

$$(E.38)$$

Time Integrals

F.1 Summary of Time Integrals

In Chapter 3, the calculation of the perturbed density and perturbed current density inside the current sheet involve time integrals of the form

$$\int_{-\infty}^{0} \exp\left(-i\omega t + A\cos(\Omega t \pm \alpha)\right) dt = -i \sum_{m=-\infty}^{\infty} \frac{I_m(A)\exp(\pm im\alpha)}{m\Omega - \omega}, \qquad \text{(F.1)}$$

$$\int_{-\infty}^{0} \cos(\Omega t)\exp\left(-i\omega t + A\cos(\Omega t \pm \alpha)\right) dt = -\frac{i}{2} \sum_{m=-\infty}^{\infty} I_m(A)\exp(\pm im\alpha) \qquad \text{(F.2)}$$
$$\times \left[\frac{1}{(m+1)\Omega - \omega} + \frac{1}{(m-1)\Omega - \omega}\right],$$

$$\int_{-\infty}^{0} \sin(\Omega t)\exp\left(-i\omega t + A\cos(\Omega t \pm \alpha)\right) dt = -\frac{1}{2} \sum_{m=-\infty}^{\infty} I_m(A)\exp(\pm im\alpha) \qquad \text{(F.3)}$$
$$\times \left[\frac{1}{(m+1)\Omega - \omega} - \frac{1}{(m-1)\Omega - \omega}\right],$$

$$\int_{-\infty}^{0} \cos(\Omega t)\sin(\Omega t)$$
$$\times \exp\left(-i\omega t + A\cos(\Omega t \pm \alpha)\right) dt = -\frac{1}{4} \sum_{m=-\infty}^{\infty} I_m(A_s)\exp(\pm im\alpha) \qquad \text{(F.4)}$$
$$\times \left[\frac{1}{(m+2)\Omega - \omega} - \frac{1}{(m-2)\Omega - \omega}\right],$$

$$\int_{-\infty}^{0} \sin^2(\Omega t)\exp\left(-i\omega t + A\cos(\Omega t \pm \alpha)\right) dt = \frac{i}{4} \sum_{m=-\infty}^{\infty} I_m(A)\exp(\pm im\alpha)$$
$$\times \left[\frac{1}{(m+2)\Omega - \omega} + \frac{1}{(m-2)\Omega - \omega}\right.$$
$$\left. - \frac{2}{m\Omega - \omega}\right]. \qquad \text{(F.5)}$$

The calculations for the region outside the current sheet involve the following time integrals,

$$\int_{-\infty}^{0} \exp(-a^2t^2 \mp ibt)dt = -\frac{i}{2|a|}Z\left(\pm\frac{b}{2|a|}\right), \tag{F.6}$$

$$\int_{-\infty}^{0} t\exp(-a^2t^2 \mp ibt)dt = \frac{1}{4a^2}Z'\left(\pm\frac{b}{2|a|}\right), \tag{F.7}$$

$$\int_{-\infty}^{0} t^2\exp(-a^2t^2 \mp ibt)dt = \frac{i}{8|a|^3}Z''\left(\pm\frac{b}{2|a|}\right), \tag{F.8}$$

$$\int_{-\infty}^{0} \exp(-a^2t^2 \mp ibt)\cos(ct)dt = -\frac{i}{4|a|}\left[Z\left(\frac{\pm b - c}{2|a|}\right) + Z\left(\frac{\pm b + c}{2|a|}\right)\right], \tag{F.9}$$

$$\int_{-\infty}^{0} t\exp(-a^2t^2 \mp ibt)\cos(ct)dt = \frac{1}{8a^2}\left[Z'\left(\frac{\pm b - c}{2|a|}\right) + Z'\left(\frac{\pm b + c}{2|a|}\right)\right]. \tag{F.10}$$

where Z is the plasma dispersion function (see Appendix D).

F.2 Evaluation of Time Integrals

The integrals (F.1)-(F.5) for the region inside the sheet can all be carried out by using the formula

$$\exp(z\cos\theta) = \sum_{m=-\infty}^{\infty} I_m(z)\exp(im\theta), \tag{F.11}$$

(from Appendix C of Gary, 2005) where I_m is a modified Bessel function of the first kind (e.g. Abramowitz and Stegun, 1964). For illustration, the integral (F.1) is given by

$$
\begin{aligned}
\int_{-\infty}^{0} \exp\left(-i\omega t + A\cos(\Omega t \pm \alpha)\right) dt &= \int_{-\infty}^{0} \exp(-i\omega t) \\
&\quad \times \sum_{m=-\infty}^{\infty} I_m(A)\exp(im(\Omega t \pm \alpha))dt \\
&= \sum_{m=-\infty}^{\infty} I_m(A)\exp(\pm im\alpha) \\
&\quad \times \int_{-\infty}^{0} \exp[i(m\Omega - \omega)t]dt \\
&= -i\sum_{m=-\infty}^{\infty} \frac{I_m(A)\exp(\pm im\alpha)}{m\Omega - \omega} \\
&\quad \times \left[\exp(i(m\Omega - \omega)t)\right]_{-\infty}^{0} \\
&= -i\sum_{m=-\infty}^{\infty} \frac{I_m(A)\exp(\pm im\alpha)}{m\Omega - \omega}, \tag{F.12}
\end{aligned}
$$

where it is assumed that $\exp(i(m\Omega - \omega)t)$ vanishes as $t \to -\infty$, which implies that the imaginary part of the harmonic frequency $\omega = \omega_r + i\gamma$ must be positive, since

$$
\begin{aligned}
\exp(i(m\Omega - \omega)t) &= \exp[i(m\Omega - \omega_r - i\gamma)t] \\
&= \exp[(i[m\Omega - \omega_r] + \gamma)t].
\end{aligned}
\tag{F.13}
$$

The integrals (F.3)-(F.5) can be evaluated in a similar way to the integral (F.1), by using the additional identities $\cos x = \cosh(ix)$ and $\sin x = -i \sinh ix$.

The integrals (F.6)-(F.8) are all obtained from equation (A.2) in Appendix A of Gary (2005), which is

$$
\int_0^\infty \exp(-a^2 t^2 \pm ibt) dt = -\frac{i}{2|a|} Z\left(\pm\frac{b}{2|a|}\right).
\tag{F.14}
$$

This integral can be rewritten to obtain the integral (F.6), by changing the integration variable from t to $-t$, and then by swapping the limits of integration. The integral (F.7) can then be evaluated by taking d/db of Equation (F.6) and multiplying by $\pm i$, which gives

$$
\begin{aligned}
\int_{-\infty}^0 t \exp(-a^2 t^2 \mp ibt) dt &= \pm i \frac{d}{db} \int_{-\infty}^0 \exp(-a^2 t^2 \mp ibt) dt \\
&= \pm \frac{d}{db}\left[\frac{1}{2|a|} Z\left(\pm\frac{b}{2|a|}\right)\right] \\
&= \frac{1}{4a^2} Z'\left(\pm\frac{b}{2|a|}\right).
\end{aligned}
\tag{F.15}
$$

The integral (F.8) can be evaluated by taking d/db of Equation (F.7), then multiplying by $\pm i$, which gives

$$
\begin{aligned}
\int_{-\infty}^0 t^2 \exp(-a^2 t^2 \mp ibt) dt &= \pm i \frac{d}{db} \int_{-\infty}^0 t \exp(-a^2 t^2 \mp ibt) dt \\
&= \pm \frac{i}{4a^2} \frac{d}{db}\left(Z'\left(\pm\frac{b}{2|a|}\right)\right) \\
&= \frac{i}{8|a|^3} Z''\left(\pm\frac{b}{2|a|}\right).
\end{aligned}
\tag{F.16}
$$

The integral (F.9) can be evaluated by using the identity $\cos x = \cosh(ix)$, together with Equation (F.6), which gives

$$
\begin{aligned}
\int_{-\infty}^0 \exp(-a^2 t^2 \mp ibt) \cos(ct) dt &= \frac{1}{2} \int_{-\infty}^\infty \exp\left(-a^2 t^2 \pm i(b \pm c)t\right) dt \\
&\quad + \frac{1}{2} \int_{-\infty}^\infty \exp\left(-a^2 t^2 \pm i(b \mp c)t\right) dt
\end{aligned}
$$

$$= -\frac{i}{4|a|}\left[Z\left(\frac{\pm b - c}{2|a|}\right) + Z\left(\frac{\pm b + c}{2|a|}\right)\right]. \qquad \text{(F.17)}$$

The integral (F.10) can be evaluated by taking d/db of Equation (F.9), and by multiplying by $\pm i$, which gives

$$
\begin{aligned}
\int_{-\infty}^{0} t \exp(-a^2 t^2 \mp ibt)\cos(ct)dt &= \pm i\frac{d}{db}\int_{-\infty}^{0} \exp(-a^2 t^2 \mp ibt)\cos(ct)dt \\
&= \pm\frac{1}{4|a|}\frac{d}{db}\left[Z\left(\frac{\pm b - c}{2|a|}\right) + Z\left(\frac{\pm b + c}{2|a|}\right)\right] \\
&= \frac{1}{8a^2}\left[Z'\left(\frac{\pm b - c}{2|a|}\right) + Z'\left(\frac{\pm b + c}{2|a|}\right)\right]. \qquad \text{(F.18)}
\end{aligned}
$$

Appendix G

Sums of Bessel Functions

In the stability calculation of Section 3.4, the following recurrence relations (from Abramowitz and Stegun, 1964)

$$I_{m-1}(z) + I_{m+1}(z) = 2I'_m(z), \tag{G.1}$$

$$I_{m-1}(z) - I_{m+1}(z) = \frac{2m}{z}I_m(z), \tag{G.2}$$

$$I'_m(z) = I_{m-1}(z) - \frac{m}{z}I_m(z), \tag{G.3}$$

$$I'_m(z) = I_{m+1}(z) + \frac{m}{z}I_m(z), \tag{G.4}$$

where I_m is a modified Bessel function of the first kind, can be used to simplify various infinite sums involving I_m. Firstly, the sum

$$\sum_{m=-\infty}^{\infty} I_m(A) \left[\frac{1}{(m+1)\Omega_y - \omega} - \frac{1}{(m-1)\Omega_y - \omega} \right], \tag{G.5}$$

can be simplified by writing

$$\sum_{m=-\infty}^{\infty} I_m(A) \frac{1}{(m+1)\Omega_y - \omega}$$
$$- \sum_{m=-\infty}^{\infty} I_m(A) \frac{1}{(m-1)\Omega_y - \omega} = \sum_{m=-\infty}^{\infty} \frac{I_{n-1}(A) - I_{n+1}(A)}{n\Omega_y - \omega}, \tag{G.6}$$

upon letting $n = m + 1$ in the first sum and $n = m - 1$ in the second sum. Then, using the recurrence relation (G.2) and using m instead of n gives

$$\sum_{m=-\infty}^{\infty} I_m(A) \left[\frac{1}{(m+1)\Omega_y - \omega} - \frac{1}{(m-1)\Omega_y - \omega} \right] = \frac{2}{A} \sum_{m=-\infty}^{\infty} \frac{mI_m(A)}{m\Omega_y - \omega}. \tag{G.7}$$

The sum

$$\sum_{m=-\infty}^{\infty} I_m(A) \left[\frac{1}{(m+1)\Omega_y - \omega} + \frac{1}{(m-1)\Omega_y - \omega} \right], \tag{G.8}$$

can also be simplified, by writing

$$\sum_{m=-\infty}^{\infty} I_m(A)\frac{1}{(m+1)\Omega_y - \omega}$$
$$+ \sum_{m=-\infty}^{\infty} I_m(A)\frac{1}{(m-1)\Omega_y - \omega} = \sum_{m=-\infty}^{\infty} \frac{I_{n-1}(A) + I_{n+1}(A)}{n\Omega_y - \omega}, \tag{G.9}$$

again by letting $n = m+1$ in the first sum and $n = m-1$ in the second sum. Using the recurrence relation (G.1), and using m instead of n, then gives

$$\sum_{m=-\infty}^{\infty} I_m(A)\left[\frac{1}{(m+1)\Omega_y - \omega} + \frac{1}{(m-1)\Omega_y - \omega}\right] = 2\sum_{m=-\infty}^{\infty} \frac{I'_m(A)}{m\Omega_y - \omega}. \tag{G.10}$$

Now, a simpler expression is required for the sums

$$\sum_{m=-\infty}^{\infty} I_m(A)\left[\frac{1}{(m+2)\Omega_y - \omega} - \frac{1}{(m-2)\Omega_y - \omega}\right], \tag{G.11}$$

and

$$\sum_{m=-\infty}^{\infty} I_m(A)\left[\frac{1}{(m+2)\Omega_y - \omega} + \frac{1}{(m-2)\Omega_y - \omega} - \frac{2}{m\Omega_y - \omega}\right]. \tag{G.12}$$

The sum (G.11) can be written as

$$\sum_{m=-\infty}^{\infty} \frac{I_m(A)}{(m+2)\Omega_y - \omega}$$
$$- \sum_{m=-\infty}^{\infty} \frac{I_m(A)}{(m-2)\Omega_y - \omega} = \sum_{n=-\infty}^{\infty} \frac{1}{n\Omega_y - \omega}[I_{n-2}(A) - I_{n+2}(A)], \tag{G.13}$$

by letting $n = m+2$ in the first sum and $n = m-2$ in the second sum. Setting $m = n-1$ in the recurrence relation (G.2) then gives,

$$I_{n-2}(z) - I_n(z) = \frac{2(n-1)}{z}I_{n-1}(z), \tag{G.14}$$

and setting $m = n+1$ in the relation (G.1) gives

$$I_n(z) + I_{n+2}(z) = 2I'_{n+1}(z). \tag{G.15}$$

Subtracting Equation (G.15) from Equation (G.14) then gives

$$I_{n-2} - I_{n+2} = 2I_n + \frac{2(n-1)}{z}I_{n-1}(z) - 2I'_{n+1}(z). \tag{G.16}$$

Equation (G.3) can be used to give

$$I'_{n+1}(z) = I_n(z) - \frac{n+1}{z} I_{n+1}(z), \tag{G.17}$$

(by setting $m = n + 1$) so that Equation (G.16) becomes

$$I_{n-2}(z) - I_{n+2}(z) = \frac{2n}{z}(I_{n-1}(z) + I_{n+1}(z)) + \frac{2}{z}(I_{n+1}(z) - I_{n-1}(z)). \tag{G.18}$$

Finally, using Equations (G.1) and (G.2) gives

$$I_{n-2}(z) - I_{n+2}(z) = \frac{4n}{z}\left[I'_n(z) - \frac{1}{z} I_n(z) \right], \tag{G.19}$$

and so the sum (G.11) can be expressed (using m instead of n) as

$$\sum_{m=-\infty}^{\infty} I_m(A) \left[\frac{1}{(m+2)\Omega_y - \omega} - \frac{1}{(m-2)\Omega_y - \omega} \right] = \frac{4}{A} \sum_{m=-\infty}^{\infty} \frac{m}{m\Omega_y - \omega}$$
$$\times \left[I'_m(A) - \frac{1}{A} I_m(A) \right]. \tag{G.20}$$

The sum (G.12) can be written as

$$\sum_{m=-\infty}^{\infty} \frac{I_m(A)}{(m+2)\Omega_y - \omega} + \sum_{m=-\infty}^{\infty} \frac{I_m(A)}{(m-2)\Omega_y - \omega} - 2 \sum_{m=-\infty}^{\infty} \frac{I_m(A)}{m\Omega_y - \omega}$$
$$= \sum_{n=-\infty}^{\infty} \frac{I_{n-2}(A)}{n\Omega_y - \omega} + \sum_{n=-\infty}^{\infty} \frac{I_{n+2}(A)}{n\Omega_y - \omega} - 2 \sum_{m=-\infty}^{\infty} \frac{I_m(A)}{m\Omega_y - \omega}$$
$$= \sum_{n=-\infty}^{\infty} \frac{1}{n\Omega_y - \omega} [I_{n-2}(A) + I_{n+2}(A)] - 2 \sum_{m=-\infty}^{\infty} \frac{I_m(A)}{m\Omega_y - \omega}, \tag{G.21}$$

by letting $n = m + 2$ in the first sum and $n = m - 2$ in the second sum. This time, an expression for $I_{n-2}(z) + I_{n+2}(z)$ is required. Firstly, setting $m = n + 1$ in the recurrence relation (G.2) gives

$$I_n(z) - I_{n+2}(z) = \frac{2(n+1)}{z} I_{n+1}(z), \tag{G.22}$$

and setting $m = n - 1$ in the recurrence relation (G.1) gives

$$I_{n-2}(z) + I_n(z) = 2I'_{n-1}(z). \tag{G.23}$$

Subtracting Equation (G.22) from Equation (G.23) then gives

$$I_{n-2}(z) + I_{n+2}(z) = 2I'_{n-1}(z) - \frac{2(n+1)}{z} I_{n+1}(z). \tag{G.24}$$

Equation (G.4) can be used to give

$$I'_{n-1}(z) = I_n(z) + \frac{n-1}{z}I_{n-1}(z), \tag{G.25}$$

(by setting $m = n - 1$) so that Equation (G.24) then becomes

$$I_{n-2}(z) + I_{n+2}(z) = 2I_n(z) + \frac{2n}{z}[I_{n-1}(z) - I_{n+1}(z)] - \frac{2}{z}[I_{n-1}(z) + I_{n+1}(z)]. \tag{G.26}$$

Finally, using the recurrence relations (G.1) and (G.2) gives

$$I_{n-2}(z) + I_{n+2}(z) = 2I_n(z) + \frac{4}{z}\left[\frac{n^2}{z}I_n(z) - I'_n(z)\right], \tag{G.27}$$

and so the sum (G.12) can be written (upon writing m instead of n) as

$$\sum_{m=-\infty}^{\infty} \frac{I_m(A)}{(m+2)\Omega_y - \omega} + \sum_{m=-\infty}^{\infty} \frac{I_m(A)}{(m-2)\Omega_y - \omega} - 2\sum_{m=-\infty}^{\infty} \frac{I_m(A)}{m\Omega_y - \omega}$$

$$= \frac{4}{A}\sum_{m=-\infty}^{\infty} \left[\frac{m^2}{A}I_m(A) - I'_m(A)\right]\frac{1}{m\Omega_y - \omega}. \tag{G.28}$$

G.1   Bessel Sums For Fortran Code

The following infinite sums of Bessel functions appear in the expressions for the perturbed current density inside the sheet. For the purpose of using these sums in a Fortran 90 code, it is convenient to write the summation from $m = 0$ to $m = \infty$ instead of from $m = -\infty$ to ∞. The sums all contain the normalised eigenvalue $\bar{\omega}$, which is complex, and so the expressions must be split into real and imaginary parts. In the expressions below, $X_i = 1$ (for ions) and $X_e = m_i/m_e$ (for electrons), with the latter expression arising from the normalisation in Chapter 4 (all frequencies are normalised to the ion gyrofrequency). The sums can be written as follows:

$$\sum_{m=-\infty}^{\infty} \frac{mI_m(K_s)}{X_s m - \bar{\omega}} = 2X_s\sum_{m=0}^{\infty} \frac{m^2 I_m(K_s)(X_s^2 m^2 - \omega_r^2 + \gamma^2)}{(X_s^2 m^2 - \omega_r^2 + \gamma^2)^2 + 4\gamma^2\omega_r^2}$$

$$+4iX_s\gamma\omega_r\sum_{m=0}^{\infty} \frac{m^2 I_m(K_s)}{(X_s^2 m^2 - \omega_r^2 + \gamma^2)^2 + 4\gamma^2\omega_r^2}$$

$$= S_{1R,s} + iS_{1I,s}. \tag{G.29}$$

$$\sum_{m=-\infty}^{\infty} \frac{m^2 I_m(K_s)}{X_s m - \bar{\omega}} = 2 \sum_{m=0}^{\infty} \frac{m^2 I_m(K_s)(\omega_r(X_s^2 m^2 - \omega_r^2) - \gamma^2 \omega_r)}{(X_s^2 m^2 - \omega_r^2 + \gamma^2)^2 + 4\gamma^2 \omega_r^2}$$

$$+2i \sum_{m=-\infty}^{\infty} \frac{m^2 I_m(K_s)(\gamma(X_s^2 m^2 + \gamma^2) + \gamma \omega_r^2)}{(X_s^2 m^2 - \omega_r^2 + \gamma^2)^2 + 4\gamma^2 \omega_r^2}$$

$$= S_{2R,s} + iS_{2I,s}. \tag{G.30}$$

$$\sum_{m=-\infty}^{\infty} \left[\frac{1}{X_s(m+2) - \bar{\omega}} + \frac{1}{X_s(m-2) - \bar{\omega}} - \frac{2}{X_s m - \bar{\omega}} \right] I_m(A_s) \cos(m\alpha_s)$$

$$= 2 \sum_{m=1}^{\infty} \left[\frac{\omega_r(X_s^2(m-2)^2 - \omega_r^2) - \gamma^2 \omega_r}{[X_s^2(m-2)^2 - \omega_r^2 + \gamma^2]^2 + 4\gamma^2 \omega_r^2} + \frac{\omega_r(X_s^2(m+2)^2 - \omega_r^2) - \gamma^2 \omega_r}{[X_s^2(m+2)^2 - \omega_r^2 + \gamma^2]^2 + 4\gamma^2 \omega_r^2} \right.$$

$$\left. -2 \frac{\omega_r(X_s^2 m^2 - \omega_r^2) - \gamma^2 \omega_r}{[X_s^2 m^2 - \omega_r^2 + \gamma^2]^2 + 4\gamma^2 \omega_r^2} \right] I_m(A_s) \cos(m\alpha_s)$$

$$+2 \left[\frac{\omega_r}{\omega_r^2 + \gamma^2} + \frac{\omega_r(4X_s^2 - \omega_r^2) - \gamma^2 \omega_r}{[4X_s^2 - \omega_r^2 + \gamma^2]^2 + 4\gamma^2 \omega_r^2} \right] I_0(A_s)$$

$$+2i \sum_{m=1}^{\infty} \left[\frac{\gamma(X_s^2(m-2)^2 + \gamma^2) + \gamma \omega_r^2}{(X_s^2(m-2)^2 - \omega_r^2 + \gamma^2)^2 + 4\gamma^2 \omega_r^2} \right.$$

$$+\frac{\gamma(X_s^2(m+2)^2 + \gamma^2) + \gamma \omega_r^2}{(X_s^2(m+2)^2 - \omega_r^2 + \gamma^2)^2 + 4\gamma^2 \omega_r^2}$$

$$\left. -2 \frac{\gamma(X_s^2 m^2 + \gamma^2) + \gamma \omega_r^2}{(X_s^2 m^2 - \omega_r^2 + \gamma^2)^2 + 4\gamma^2 \omega_r^2} \right] I_m(A_s) \cos(m\alpha_s)$$

$$+2i \left[\frac{\gamma(4X_s^2 + \gamma^2) + \gamma \omega_r^2}{(4X_s^2 - \omega_r^2 + \gamma^2)^2 + 4\gamma^2 \omega_r^2} - \frac{\gamma}{\omega_r^2 + \gamma^2} \right] I_0(A_s)$$

$$= S_{3R,s} + iS_{3I,s}. \tag{G.31}$$

$$\sum_{m=-\infty}^{\infty} \left[\frac{1}{X_s(m+2) - \bar{\omega}} + \frac{1}{X_s(m-2) - \bar{\omega}} - \frac{2}{X_s m - \bar{\omega}} \right] I_m(A_s) \sin(m\alpha_s)$$

$$= 2X_s \sum_{m=1}^{\infty} \left[\frac{(m-2)[X_s^2(m-2)^2 - \omega_r^2 + \gamma^2]}{[X_s^2(m-2)^2 - \omega_r^2 + \gamma^2]^2 + 4\omega_r^2 \gamma^2} + \frac{(m+2)[X_s^2(m+2)^2 - \omega_r^2 + \gamma^2]}{[X_s^2(m+2)^2 - \omega_r^2 + \gamma^2]^2 + 4\omega_r^2 \gamma^2} \right.$$

$$\left. -2 \frac{m[X_s^2 m^2 - \omega_r^2 + \gamma^2]}{[X_s^2 m^2 - \omega_r^2 + \gamma^2]^2 + 4\omega_r^2 \gamma^2} \right] I_m(A_s) \sin(m\alpha_s)$$

$$+4iX_s \sum_{m=1}^{\infty} \left[\frac{(m-2)\omega_r\gamma}{[X_s^2(m-2)^2 - \omega_r^2 + \gamma^2]^2 + 4\omega_r^2\gamma^2} \right.$$

$$+ \frac{(m+2)\omega_r\gamma}{[X_s^2(m+2)^2 - \omega_r^2 + \gamma^2]^2 + 4\omega_r^2\gamma^2}$$

$$\left. -2\frac{m\omega_r\gamma}{[X_s^2 m^2 - \omega_r^2 + \gamma^2]^2 + 4\omega_r^2\gamma^2} \right] I_m(A_s)\sin(m\alpha_s)$$

$$= S_{4R,s} + iS_{4I,s}. \tag{G.32}$$

$$\sum_{m=-\infty}^{\infty} \left[\frac{1}{X_s(m+1) - \bar{\omega}} - \frac{1}{X_s(m-1) - \bar{\omega}} \right] I_m(A_s)\cos(m\alpha_s)$$

$$= 2X_s \sum_{m=1}^{\infty} \left[-\frac{(m-1)[X_s^2(m-1)^2 - \omega_r^2 + \gamma^2]}{[X_s^2(m-1)^2 - \omega_r^2 + \gamma^2]^2 + 4\omega_r^2\gamma^2} \right.$$

$$\left. + \frac{(m+1)[X_s^2(m+1)^2 - \omega_r^2 + \gamma^2]}{[X_s^2(m+1)^2 - \omega_r^2 + \gamma^2]^2 + 4\omega_r^2\gamma^2} \right] I_m(A_s)\cos(m\alpha_s)$$

$$+ \frac{2X_s[X_s^2 - \omega_r^2 + \gamma^2]}{[X_s^2 - \omega_r^2 + \gamma^2]^2 + 4\omega_r^2\gamma^2} I_0(A_s)$$

$$+4X_s i \sum_{m=1}^{\infty} \left[-\frac{(m-1)\omega_r\gamma}{[X_s^2(m-1)^2 - \omega_r^2 + \gamma^2]^2 + 4\omega_r^2\gamma^2} \right.$$

$$\left. + \frac{(m+1)\omega_r\gamma}{[X_s^2(m+1)^2 - \omega_r^2 + \gamma^2]^2 + 4\omega_r^2\gamma^2} \right] I_m(A_s)\cos(m\alpha_s)$$

$$+ \frac{4X_s i\omega_r\gamma}{[X_s^2 - \omega_r^2 + \gamma^2]^2 + 4\omega_r^2\gamma^2} I_0(A_s)$$

$$= S_{5R,s} + iS_{5I,s}. \tag{G.33}$$

$$\sum_{m=-\infty}^{\infty} \left[\frac{1}{X_s(m+1) - \bar{\omega}} - \frac{1}{X_s(m-1) - \bar{\omega}} \right] I_m(A_s)\sin(m\alpha_s)$$

$$= 2 \sum_{m=1}^{\infty} \left[-\frac{\omega_r(X_s^2(m-1)^2 - \omega_r^2) - \gamma^2\omega_r}{[X_s^2(m-1)^2 - \omega_r^2 + \gamma^2]^2 + 4\gamma^2\omega_r^2} \right.$$

$$\left. + \frac{\omega_r(X_s^2(m+1)^2 - \omega_r^2) - \gamma^2\omega_r}{[X_s^2(m+1)^2 - \omega_r^2 + \gamma^2]^2 + 4\gamma^2\omega_r^2} \right] I_m(A_s)\sin(m\alpha_s)$$

$$+2i \sum_{m=1}^{\infty} \left[-\frac{\gamma(X_s^2(m-1)^2 + \gamma^2) + \gamma\omega_r^2}{(X_s^2(m-1)^2 - \omega_r^2 + \gamma^2)^2 + 4\gamma^2\omega_r^2} \right.$$

$$+ \frac{\gamma(X_s^2(m+1)^2 + \gamma^2) + \gamma\omega_r^2}{(X_s^2(m+1)^2 - \omega_r^2 + \gamma^2)^2 + 4\gamma^2\omega_r^2}\Bigg] I_m(A_s)\sin(m\alpha_s)$$

$$= S_{6R,s} + iS_{6I,s}. \tag{G.34}$$

$$\sum_{m=-\infty}^{\infty} \left[\frac{1}{X_s(m+1) - \bar\omega} + \frac{1}{X_s(m-1) - \bar\omega} \right] I_m(A_s)\cos(m\alpha_s)$$

$$= 2\sum_{m=1}^{\infty} \left[\frac{\omega_r(X_s^2(m-1)^2 - \omega_r^2) - \gamma^2\omega_r}{[X_s^2(m-1)^2 - \omega_r^2 + \gamma^2]^2 + 4\gamma^2\omega_r^2} + \frac{\omega_r(X_s^2(m+1)^2 - \omega_r^2) - \gamma^2\omega_r}{[X_s^2(m+1)^2 - \omega_r^2 + \gamma^2]^2 + 4\gamma^2\omega_r^2} \right]$$

$$\times I_m(A_s)\cos(m\alpha_s)$$

$$+ \frac{2(\omega_r(X_s^2 - \omega_r^2) - \gamma^2\omega_r)}{(X_s^2 - \omega_r^2 + \gamma^2)^2 + 4\gamma^2\omega_r^2} I_0(A_s)$$

$$+ 2i\sum_{m=1}^{\infty} \left[\frac{\gamma(X_s^2(m-1)^2 + \gamma^2) + \gamma\omega_r^2}{(X_s^2(m-1)^2 - \omega_r^2 + \gamma^2)^2 + 4\gamma^2\omega_r^2} \right.$$

$$\left. + \frac{\gamma(X_s^2(m+1)^2 + \gamma^2) + \gamma\omega_r^2}{(X_s^2(m+1)^2 - \omega_r^2 + \gamma^2)^2 + 4\gamma^2\omega_r^2} \right] I_m(A_s)\cos(m\alpha_s)$$

$$+ 2\frac{\gamma(X_s^2 + \gamma^2) + \gamma\omega_r^2}{(X_s^2 - \omega_r^2 + \gamma^2)^2 + 4\gamma^2\omega_r^2} I_0(A_s)$$

$$= S_{7R,s} + iS_{7I,s}. \tag{G.35}$$

$$\sum_{m=-\infty}^{\infty} \left[\frac{1}{X_s(m+1) - \bar\omega} + \frac{1}{X_s(m-1) - \bar\omega} \right] I_m(A_s)\sin(m\alpha_s)$$

$$= 2X_s\sum_{m=1}^{\infty} \left[\frac{(m-1)[X_s^2(m-1)^2 - \omega_r^2 + \gamma^2]}{[X_s^2(m-1)^2 - \omega_r^2 + \gamma^2]^2 + 4\omega_r^2\gamma^2} + \frac{(m+1)[X_s^2(m+1)^2 - \omega_r^2 + \gamma^2]}{[X_s^2(m+1)^2 - \omega_r^2 + \gamma^2]^2 + 4\omega_r^2\gamma^2} \right]$$

$$\times I_m(A_s)\sin(m\alpha_s)$$

$$+ 4X_si\sum_{m=1}^{\infty} \left[\frac{(m-1)\omega_r\gamma}{[X_s^2(m-1)^2 - \omega_r^2 + \gamma^2]^2 + 4\omega_r^2\gamma^2} \right.$$

$$\left. + \frac{(m+1)\omega_r\gamma}{[X_s^2(m+1)^2 - \omega_r^2 + \gamma^2]^2 + 4\omega_r^2\gamma^2} \right] I_m(A_s)\sin(m\alpha_s)$$

$$= S_{8R,s} + iS_{8I,s}. \tag{G.36}$$

$$\sum_{m=-\infty}^{\infty} \left[\frac{1}{X_s(m+2)-\bar{\omega}} - \frac{1}{X_s(m-2)-\bar{\omega}} \right] I_m(A_s)\cos(m\alpha_s)$$

$$= 2X_s \sum_{m=1}^{\infty} \left[- \frac{(m-2)[X_s^2(m-2)^2-\omega_r^2+\gamma^2]}{[X_s^2(m-2)^2-\omega_r^2+\gamma^2]^2+4\omega_r^2\gamma^2} \right.$$

$$\left. + \frac{(m+2)[X_s^2(m+2)^2-\omega_r^2+\gamma^2]}{[X_s^2(m+2)^2-\omega_r^2+\gamma^2]^2+4\omega_r^2\gamma^2} \right] I_m(A_s)\cos(m\alpha_s)$$

$$+ \frac{4X_s[4X_s^2-\omega_r^2+\gamma^2]}{[4X_s^2-\omega_r^2+\gamma^2]^2+4\omega_r^2\gamma^2} I_0(A_s)$$

$$+4X_s i \sum_{m=1}^{\infty} \left[- \frac{(m-2)\omega_r\gamma}{[X_s^2(m-2)^2-\omega_r^2+\gamma^2]^2+4\omega_r^2\gamma^2} \right.$$

$$\left. + \frac{(m+2)\omega_r\gamma}{[X_s^2(m+2)^2-\omega_r^2+\gamma^2]^2+4\omega_r^2\gamma^2} \right] I_m(A_s)\cos(m\alpha_s)$$

$$+ \frac{8X_s i\omega_r\gamma}{[4X_s^2-\omega_r^2+\gamma^2]^2+4\omega_r^2\gamma^2} I_0(A_s)$$

$$= S_{9R,s} + iS_{9I,s}. \tag{G.37}$$

$$\sum_{m=-\infty}^{\infty} \left[\frac{1}{X_s(m+2)-\bar{\omega}} - \frac{1}{X_s(m-2)-\bar{\omega}} \right] I_m(A_s)\sin(m\alpha_s)$$

$$= 2 \sum_{m=1}^{\infty} \left[- \frac{\omega_r(X_s^2(m-2)^2-\omega_r^2)-\gamma^2\omega_r}{[X_s^2(m-2)^2-\omega_r^2+\gamma^2]^2+4\gamma^2\omega_r^2} \right.$$

$$\left. + \frac{\omega_r(X_s^2(m+2)^2-\omega_r^2)-\gamma^2\omega_r}{[X_s^2(m+2)^2-\omega_r^2+\gamma^2]^2+4\gamma^2\omega_r^2} \right] I_m(A_s)\sin(m\alpha_s)$$

$$+ 2i \sum_{m=1}^{\infty} \left[- \frac{\gamma(X_s^2(m-2)^2+\gamma^2)+\gamma\omega_r^2}{(X_s^2(m-2)^2-\omega_r^2+\gamma^2)^2+4\gamma^2\omega_r^2} \right.$$

$$\left. + \frac{\gamma(X_s^2(m+2)^2+\gamma^2)+\gamma\omega_r^2}{(X_s^2(m+2)^2-\omega_r^2+\gamma^2)^2+4\gamma^2\omega_r^2} \right] I_m(A_s)\sin(m\alpha_s)$$

$$= S_{10R,s} + iS_{10I,s}. \tag{G.38}$$

$$\sum_{m=-\infty}^{\infty} \frac{I_m(K_s)}{X_s m-\bar{\omega}} = 2 \sum_{m=1}^{\infty} \frac{\omega_r(X_s^2 m^2-\omega_r^2)-\gamma^2\omega_r}{[X_s^2 m^2-\omega_r^2+\gamma^2]^2+4\gamma^2\omega_r^2} I_m(K_s) - \frac{\omega_r I_0(K_s)}{\omega_r^2+\gamma^2}$$

$$+2i \sum_{m=1}^{\infty} \frac{\gamma(X_s^2 m^2 + \gamma^2) + \gamma \omega_r^2}{[X_s^2 m^2 - \omega_r^2 + \gamma^2]^2 + 4\gamma^2 \omega_r^2} I_m(K_s) + i\frac{\gamma I_0(K_s)}{\omega_r^2 + \gamma^2}$$

$$= S_{11R,s} + iS_{11I,s}. \tag{G.39}$$

$$\sum_{m=-\infty}^{\infty} \frac{I_m(A_s)\cos(m\alpha_s)}{X_s m - \bar{\omega}} = 2\sum_{m=1}^{\infty} \frac{\omega_r(X_s^2 m^2 - \omega_r^2) - \gamma^2 \omega_r}{[X_s^2 m^2 - \omega_r^2 + \gamma^2]^2 + 4\gamma^2 \omega_r^2} I_m(A_s)\cos(m\alpha_s)$$

$$- \frac{\omega_r I_0(A_s)}{\omega_r^2 + \gamma^2}$$

$$+ 2i\sum_{m=1}^{\infty} \frac{\gamma(X_s^2 m^2 + \gamma^2) + \gamma \omega_r^2}{[X_s^2 m^2 - \omega_r^2 + \gamma^2]^2 + 4\gamma^2 \omega_r^2} I_m(A_s)\cos(m\alpha_s)$$

$$+ i\frac{\gamma I_0(A_s)}{\omega_r^2 + \gamma^2}$$

$$= S_{12R,s} + iS_{12I,s}. \tag{G.40}$$

$$\sum_{m=-\infty}^{\infty} \frac{I_m(A_s)\sin(m\alpha_s)}{X_s m - \bar{\omega}} = 2X_s\sum_{m=1}^{\infty} \frac{m(X_s^2 m^2 - \omega_r^2 + \gamma^2)}{[X_s^2 m^2 - \omega_r^2 + \gamma^2]^2 + 4\gamma^2 \omega_r^2} I_m(A_s)\sin(m\alpha_s)$$

$$+ 4iX_s\sum_{m=1}^{\infty} \frac{m\gamma\omega_r}{[X_s^2 m^2 - \omega_r^2 + \gamma^2]^2 + 4\gamma^2 \omega_r^2} I_m(A_s)\sin(m\alpha_s)$$

$$= S_{13R,s} + iS_{13I,s}, \tag{G.41}$$

Bibliography

M. Abramowitz and I. A Stegun. *Handbook of Mathematical Functions*. National Bureau of Standards, Washington DC, 1964.

H. Alfvén. Existence of Electromagnetic-Hydrodynamic Waves. *Nature*, 150:405–406, October 1942. doi: 10.1038/150405d0.

W. Alpers. Steady State Charge Neutral Models of the Magnetopause. *Astrophysics and Space Science*, 5:425–437, December 1969. doi: 10.1007/BF00652391.

N. Attico and F. Pegoraro. Periodic equilibria of the Vlasov-Maxwell system. *Physics of Plasmas*, 6:767–770, March 1999. doi: 10.1063/1.873315.

B. Bertotti. Fine structure in current sheaths. *Annals of Physics*, 25:271–289, December 1963.

D. Biskamp. *Nonlinear Magnetohydrodynamics (Cambridge Monographs on Plasma Physics)*. Cambridge University Press, 1993. ISBN 0521402069.

J. A. Bittencourt. *Fundamentals of Plasma Physics*. Pergamon Pr, 1986. ISBN 0080339239.

N. A. Bobrova and S. I. Syrovatskiĭ. Violent instability of one-dimensional forceless magnetic field in a rarefied plasma. *Soviet Journal of Experimental and Theoretical Physics Letters*, 30: 535–+, November 1979.

N. A. Bobrova, S. V. Bulanov, J. I. Sakai, and D. Sugiyama. Force-free equilibria and reconnection of the magnetic field lines in collisionless plasma configurations. *Physics of Plasmas*, 8:759–768, March 2001. doi: 10.1063/1.1344196.

T. J. M. Boyd and J. J. Sanderson. *Plasma Dynamics (Applications of Mathematics)*. Thomas Nelson & Sons Ltd, 1969. ISBN 017771610X.

T. J. M. Boyd and J. J. Sanderson. *The Physics of Plasmas*. Cambridge University Press, 2003. ISBN 0521459125.

E. Camporeale, G. L. Delzanno, G. Lapenta, and W. Daughton. New approach for the study of linear Vlasov stability of inhomogeneous systems. *Physics of Plasmas*, 13(9):092110–+, September 2006. doi: 10.1063/1.2345358.

P. J. Channell. Exact Vlasov-Maxwell equilibria with sheared magnetic fields. *Physics of Fluids*, 19:1541–1545, October 1976.

F. F. Chen. *Introduction to Plasma Physics*. Springer, 1995. ISBN 0306307553.

B. Coppi, G. Laval, and R. Pellat. Dynamics of the Geomagnetic Tail. *Physical Review Letters*, 16:1207–1210, June 1966. doi: 10.1103/PhysRevLett.16.1207.

W. Daughton. Kinetic theory of the drift kink instability in a current sheet. *Journal of Geophysical*

Research, 1032:29429–29444, December 1998. doi: 10.1029/1998JA900028.

W. Daughton. The unstable eigenmodes of a neutral sheet. *Physics of Plasmas*, 6:1329–1343, April 1999. doi: 10.1063/1.873374.

C. M. Davies. The boundary layer between a cold plasma and a confined magnetic field when the plasma is not normally incident on the boundary. *Planetary and Space Science*, 16:1249–+, October 1968.

R. O. Dendy. *Plasma Physics: An Introductory Course*. Cambridge University Press, 1994. ISBN 0521433096.

M. Dobrowolny. Instability of a neutral sheet. *Nuovo Cimento B Serie*, 55:427–442, June 1968. doi: 10.1007/BF02711653.

D. Fleisch. *A Student's Guide to Maxwell's Equations*. Cambridge University Press, 2008. ISBN 0521701473.

J. P. Freidberg. *Ideal Magnetohydrodynamics (Modern Perspectives in Energy)*. Springer, 1987. ISBN 0306425122.

B. D. Fried and S. P. Conte. *The Plasma Dispersion Function*. Academic Press, 1961.

W.-Z. Fu and L.-N. Hau. Vlasov-Maxwell equilibrium solutions for Harris sheet magnetic field with Kappa velocity distribution. *Physics of Plasmas*, 12(7):070701–+, July 2005. doi: 10.1063/1.1941047.

G. A. Gary. Plasma Beta above a Solar Active Region: Rethinking the Paradigm. *Solar Physics*, 203:71–86, October 2001.

S. Peter Gary. *Theory of Space Plasma Microinstabilities (Cambridge Atmospheric and Space Science Series)*. Cambridge University Press, 2005. ISBN 0521437482.

J. P. Hans Goedbloed and Stefaan Poedts. *Principles of Magnetohydrodynamics: With Applications to Laboratory and Astrophysical Plasmas*. Cambridge University Press, 2004. ISBN 0521626072.

H. Grad. Boundary Layer between a Plasma and a Magnetic Field. *Physics of Fluids*, 4:1366–1375, November 1961.

I.S. Gradshteyn and I.M. Ryzhik. *Tables of Integrals, Series and Products*. Academic Press Inc.,U.S., 1966. ISBN 0122947509.

J. M. Greene. One-dimensional Vlasov-Maxwell equilibria. *Physics of Fluids B*, 5:1715–1722, June 1993.

E. G. Harris. On a plasma sheath separating regions of oppositely directed magnetic field. *Nuovo Cimento*, 23:115, 1962.

M. G. Harrison. *Equilibrium and Dynamics of Collisionless Current Sheets*. PhD Thesis, University of St Andrews, 2009.

M. G. Harrison and T. Neukirch. Some remarks on one-dimensional force-free Vlasov-Maxwell equilibria. *Physics of Plasmas*, 16(2):022106–+, February 2009a. doi: 10.1063/1.3077307.

M. G. Harrison and T. Neukirch. One-Dimensional Vlasov-Maxwell Equilibrium for the Force-Free Harris Sheet. *Physical Review Letters*, 102(13):135003–+, April 2009b. doi: 10.1103/

PhysRevLett.102.135003.

F. C. Hoh. Stability of Sheet Pinch. *Physics of Fluids*, 9:277–284, February 1966. doi: 10.1063/1.1761670.

J. Hurley. Analysis of the Transition Region between a Plasma and its Confining Magnetic Field. *Physical Review*, 124:1307–1308, December 1961. doi: 10.1103/PhysRev.124.1307.

J. Hurley. Analysis of the Transition Region between a Uniform Plasma and its Confining Magnetic Field. II. *Physics of Fluids*, 6:83–88, January 1963.

J. R. Kan. Equilibrium configurations of Vlasov plasmas carrying a current component along an external magnetic field. *Journal of Plasma Physics*, 7:445–+, June 1972.

V. V. Kocharovsky, Vl. V. Kocharovsky, and V. Ju. Martyanov. Self-consistent current sheets and filaments in relativistic collisionless plasma with arbitrary energy distribution of particles. *Phys. Rev. Lett.*, 104(21):215002, May 2010. doi: 10.1103/PhysRevLett.104.215002.

N. A. Krall and A. W. Trivelpiece. *Principles of plasma physics*. International Student Edition - International Series in Pure and Applied Physics, Tokyo: McGraw-Hill Kogakusha, 1973, 1973.

S. H. Lam. One-Dimensional Static Pinch Solutions. *Physics of Fluids*, 10:2454–2457, November 1967.

G. Lapenta and J. U. Brackbill. A kinetic theory for the drift-kink instability. *Journal of Geophysical Research*, 1022:27099–27108, December 1997. doi: 10.1029/97JA02140.

L. C. Lee and J. R. Kan. Transition layer between two magnetized plasmas. *Journal of Plasma Physics*, 22:515–524, December 1979a.

L. C. Lee and J. R. Kan. A unified kinetic model of the tangential magnetopause structure. *Journal of Geophysical Research (Space Physics)*, 84:6417–6426, November 1979b.

J. Lemaire and L. F. Burlaga. Diamagnetic boundary layers - A kinetic theory. *Astrophysics and Space Science*, 45:303–325, December 1976.

I. Lerche. On the Boundary Layer between a Warm, Streaming Plasma and a Confined Magnetic Field. *Journal of Geophysical Research (Space Physics)*, 72:5295–+, November 1967.

B.L. Moiseiwitsch. *Integral Equations (Longman mathematical texts)*. Prentice Hall Press, 1977. ISBN 0582442885.

A. I. Morozov and L. S. Solov'ev. A kinetic examination of some equilibrium plasma configurations. *Soviet Physics JETP*, 13:927–932, 1961.

P. M. Morse and H. Feshbach. *Methods of Theoretical Physics, Part I*. McGraw-Hill Science/Engineering/Math, 1953. ISBN 007043316X.

F. Mottez. Exact nonlinear analytic Vlasov-Maxwell tangential equilibria with arbitrary density and temperature profiles. *Physics of Plasmas*, 10:2501–2508, June 2003. doi: 10.1063/1.1573639.

F. Mottez. The pressure tensor in tangential equilibria. *Annales Geophysicae*, 22:3033–3037, August 2004.

H. E. Mynick, W. M. Sharp, and A. N. Kaufman. Realistic Vlasov slab equilibria with magnetic

shear. *Physics of Fluids*, 22:1478–1484, August 1979.

T. Neukirch. *Introduction to the Theory of MHD Equilibria*. 1998. URL http://www-solar.mcs.st-andrews.ac.uk/~thomas.

T. Neukirch, F. Wilson, and M. G. Harrison. A detailed investigation of the properties of a Vlasov-Maxwell equilibrium for the force-free Harris sheet. *Physics of Plasmas*, 16(12):122102–+, December 2009. doi: 10.1063/1.3268771.

R. B. Nicholson. Solution of the Vlasov Equations for a Plasma in an Externally Uniform Magnetic Field. *Physics of Fluids*, 6:1581–1586, November 1963.

E. N. Parker. Confinement of a Magnetic Field by a Beam of Ions. *Journal of Geophysical Research (Space Physics)*, 72:2315–+, May 1967.

W. H. Press, S. A. Teukolsky, W. T. Vetterling, and B. P. Flannery. *Numerical recipes in FORTRAN. The art of scientific computing*. Cambridge: University Press, —c1992, 2nd ed., 1992.

M. Roth. The plasmapause as a plasma sheath: a minimum thickness. *Journal of Atmospheric and Terrestrial Physics*, 38:1065–1070, 1976.

M. Roth, J. de Keyser, and M. M. Kuznetsova. Vlasov Theory of the Equilibrium Structure of Tangential Discontinuities in Space Plasmas. *Space Science Reviews*, 76:251–317, May 1996. doi: 10.1007/BF00197842.

K. Schindler. *Physics of Space Plasma Activity*. Cambridge, 2007.

J. Schmid-Burgk. *Two-Dimensional Self Consistent Solutions of the Stationary Vlasov Equation for Two-Component Plasmas*. Master's Thesis, Ludwig-Maximilians-Universitat Munchen, 1965.

A. Sestero. Structure of Plasma Sheaths. *Physics of Fluids*, 7:44–51, January 1964.

A. Sestero. Vlasov Equation Study of Plasma Motion across Magnetic Fields. *Physics of Fluids*, 9:2006–2013, October 1966.

A. Sestero. Self-Consistent Description of a Warm Stationary Plasma in a Uniformly Sheared Magnetic Field. *Physics of Fluids*, 10:193–197, January 1967.

A. Sestero and M. Zannetti. Self-consistent astron e layer with spread in energy and angular momentum. *Phys. Rev. Lett.*, 19(24):1377–1379, Dec 1967. doi: 10.1103/PhysRevLett.19.1377.

I. Silin, J. Büchner, and L. Zelenyi. Instabilities of collisionless current sheets: Theory and simulations. *Physics of Plasmas*, 9:1104–1112, April 2002. doi: 10.1063/1.1459056.

J. Stoer and R. Bulirsch. *Introduction to Numerical Analysis*. Springer, 1980. ISBN 0387904204.

S.-Y. Su and B. U. Ö. Sonnerup. On the equilibrium of the magnetopause current layer. *Journal of Geophysical Research (Space Physics)*, 76:5181–5188, 1971.

L. Tonks. Trajectory-Wise Analysis of Cylindrical and Plane Plasmas in a Magnetic Field and Without Collisions. *Physical Review*, 113:400–407, January 1959. doi: 10.1103/PhysRev.113.400.

E. S. Weibel. On the Confinement of a Plasma by Magnetostatic Fields. *Physics of Fluids*, 2:52–56, January 1959.

F. Wilson and T. Neukirch. A Family of One-Dimensional Vlasov-Maxwell Equilibria for the Force-free Harris Sheet. *Physics of Plasmas*, 18:082108, August 2011. doi: 10.1063/1.3623740.

K. Yamanaka. Threshold of electromagnetic instability in a magnetic neutral sheet. *Physica Scripta*, 17:15–22, January 1978. doi: 10.1088/0031-8949/17/1/004.

P. H. Yoon, A. T. Y. Lui, and R. B. Sheldon. On the current sheet model with κ distribution. *Physics of Plasmas*, 13(10):102108–+, October 2006. doi: 10.1063/1.2357720.

List of Figures

List of Tables